Technische Universität München

Fakultät für Medizin

Lehrstuhl für Stoffwechselerkrankungen

Polypharmacological strategies to reverse obesity and improve multiple aspects of the metabolic syndrome in mice

Sigrid Hedwig Jall

Vollständiger Abdruck der von der Fakultät für Medizin der Technischen Universität München zur Erlangung des akademischen Grades eines

Doktors der Naturwissenschaften

genehmigten Dissertation.

Vorsitzender: Prof. Dr. Percy A. Knolle

Prüfer der Dissertation: 1. Prof. Dr. Matthias Tschöp
                            2. Prof. Dr. Johannes Beckers

Die Dissertation wurde am 17.01.2019 bei der Technischen Universität München eingereicht und durch die Fakultät der Medizin am 13.08.2019 angenommen.

Table of Contents

Glossary of Terms

α-MSH	α-melanocyte-stimulating hormone
Abca1	ATP binding cassette subfamily A member 1
Abcg5	ATP binding cassette subfamily G member 5
ACh	Acetylcholine
ADP	Adenosine diphosphate
AgRP	Agouti-related peptide
AKT	Protein kinase B
AKT2	Protein kinase Akt-2
ALT	L-alanine:2-oxoglutarate aminotransferase/alanine aminotransferase
AMPK	Adenosine monophosphate-activated protein kinase
ANCOVA	Analysis of covariance
ANOVA	Analysis of variance
Apoe	Apolipoprotein E
AR	Adrenergic receptors
ARH	Arcuate nucleus
AST	Aspartate aminotransferase
Atf4	Activating transcription factor 4
ATP	Adenosine triphosphate
Atp5b	ATP synthase F1 subunit beta
AUC	Area under the curve
BAT	Brown adipose tissue
betaless	$\beta_1\beta_2\beta_3$-AR KO
BCA	Bicinchoninic acid
BMI	Body mass index
BPD	Biliopancreatic diversion
BSA	Bovine serum albumin
BW	Body weight
cAMP	Cyclic adenosine monophosphate
Cd68	CD68 molecule
cDNA	Complementary deoxyribonucleic acid
cFOS+	cFOS immunoreactive
CHO	Chinese hamster ovary
Chrn	Cholinergic receptor nicotinic subunit
Chrnb4	Cholinergic receptor nicotinic beta 4 subunit
CI	Confidence interval
Cidea	Cell death-inducing DFFA-like effector A
Ckmt1	Creatine Kinase, Mitochondrial 1B
Ckmt2	Creatine Kinase, Mitochondrial 2
CNS	Central nervous system
Cox2	Mitochondrially encoded cytochrome C oxidase II
Cox4	Cytochrome C oxidase subunit 4I1
Cyp3a11	Cytochrome P450, family 3, subfamily a, polypeptide 11
Cyp7b1	Cytochrome P450 family 7 subfamily B member 1
Cyp8b1	Cytochrome P450 family 8 subfamily B member 1
Cyp27a1	Cytochrome P450 family 27 subfamily A member 1
CytC	Cytochrome C
DAPI	4′,6-diamidino-2-phenylindole
dH$_2$O	Deionized water

DIO	Diet-induced obese
Dio2	Iodothyronine deiodinase 2
DMEM	Dulbecco's modified eagle medium
DMPP	Dimethylphenylpiperazinium
DMSO	Dimethyl sulfoxide
DNP	2,4-dinitrophenol
dNTP	Deoxynucleotide-triphosphate
DPP-IV	Dipeptidyl peptidase-IV
DRG	Dorsal root ganglion/ganglia
DTT	Dithiothreitol
EC_{50}	Half maximal effective concentration
EcD	Electrochemical detector
ECL^+	Enhanced chemiluminescence
EDTA	Ethylenediaminetetraacetic acid
EGFPf	Farnesylated enhanced green fluorescent protein
EMA	European Medicines Agency
Epac	Exchange protein activated by cyclic-adenosine monophosphate 2
Epi	Epinephrine
ER	Endoplasmic reticulum
ESC	Embryonic stem cells
eWAT	Epididymal white adipose tissue
FCCP	Carbonyl cyanide-p-trifluoromethoxyphenylhydrazone
FDA	Food and Drug Administration
FFA	Free fatty acids
FGF21	Fibroblast growth factor 21
FPLC	Fast-performance liquid chromatography
G6PC	Glucose-6-phosphatase
GABA	γ-aminobutyric acid
Gamt	Guanidinoacetate N-Methyltransferase
Gatm	Glycine Amidinotransferase
GcgR	Glucagon receptor
GcgR Li-KO	Liver-specific glucagon receptor KO
gDNA	Genomic deoxyribonucleic acid
GIP	Glucose-dependent insulinotropic polypeptide
GIPR	Glucose-dependent insulinotropic polypeptide receptor
GLP-1	Glucagon-like peptide 1
GLP-1R	Glucagon-like peptide 1 receptor
GLUT	Glucose transporter
GLUT4	Glucose transporter type 4
GTT	Glucose tolerance test
GYS2	Glycogen synthase 2 (Liver)
^{3}H-2-DG	^{3}H-labelled 2-deoxy-glucose
^{3}H-2-DG-6-P	Phosphorylated ^{3}H-2-DG
H&E	Hematoxylin and eosin
HbA1c	Glycated hemoglobin
HBSS	Hanks' Balanced Salt Solution
HDL	High-density lipoproteins
HEPES	4-(2-hydroxyethyl)-1-piperazineethanesulfonic acid
HFD	High-fat, high-sugar diet / High-fat, high sucrose diet
HFHS	High-fat, high-sugar
HI-FBS	Heat-inactivated fetal bovine serum

Hmgcr	3-Hydroxy-3-methylglutaryl-CoA reductase
HOMA-IR	Homeostatic model assessment of insulin resistance
HPLC	High performance liquid chromatography
Hprt	Hypoxanthine-guanine phosphoribosyltransferase
HRP	Horseradish peroxidase
Hspa5	Heat shock protein family A (Hsp70) member 5
IBMX	Isobutyl-methylxanthine
IGT	Impaired glucose tolerance
IHC	Immunohistochemistry
IL-1	Interleukin-1
i.p.	Intraperitoneal
ipGTT	Intraperitoneal glucose tolerance test
IRS	Insulin receptor substrate
ITT	Insulin tolerance test
iWAT	Inguinal white adipose tissue
JIB	Jejunoileal bypass
kg	Kilogram
KO	Knockout
Lcat	Lecithin-cholesterol acyltransferase
LDL	Low-density lipoproteins
Ldlr	Low density lipoprotein receptor
LepR	Leptin receptors
Lipc	Lipase C, hepatic type
Lrp1	LDL receptor related protein 1
m	Meter
MC4R	Melanocortin-4 receptor
ME	Median eminence
MSOT	Multi-Spectral Optoacoustic Tomography
nAChR	Nicotinic acetylcholine receptor
NAFLD	Non-alcoholic fatty liver disease
NAS	NAFLD activity score
NE	Norepinephrine
NEFA	Non-esterified fatty acids
NIH	U.S. National Institutes of Health
NPY	Neuropeptide Y
Nrf1	Nuclear respiratory factor 1
OCR	Oxygen consumption rate
OXPHOS	Oxidative phosphorylation
PAS	Phospho Akt substrate
PBS	Phosphate-buffered saline
PCR	Polymerase chain reaction
P-CREB	Phosphorylated cyclic adenosine monophosphate response element
PEPCK	Phosphoenolpyruvate carboxykinase
PFA	Paraformaldehyde
PGC1α	Peroxisome proliferator-activated receptor gamma, coactivator 1 alpha
PGM	Phosphoglucomutase 1
PI3-kinase	Phosphatidylinositol-4,5-bisphosphate 3-kinase
PIP$_2$	Phosphatidylinositol 4,5-bisphosphate
PIP$_3$	Phosphatidylinositol (3,4,5)-trisphosphate
Pirt	Phosphoinositide interacting regulator of TRPs

Pirt$^{-/-}$	Pirt deficient
PKA	Protein kinase A
PKC	Protein kinase C
POMC	Proopiomelanocortin
PPIB	Peptidylprolyl isomerase B
Prdm16	PR/SET domain 16
PTT	Pyruvate tolerance test
PVN	Paraventricular nucleus
PYGL	Glycogen phosphorylase L
PYY	Peptide YY
qPCR	Quantitative real-time PCR
RER	Respiratory exchange ratio
RNA	Ribonucleic acid
RPMI	Roswell Park Memorial Institute
s.c.	Subcutaneous
SDS-PAGE	Sodium dodecyl sulfate-polyacrylamide gel electrophoresis
s.e.m.	Standard error of the mean
Ser/Thr	Serine/Threonine
Slc6a8	Solute Carrier Family 6 Member 8
Sort1	Sortilin 1
Sqle	Squalene epoxidase
T2DM	Type 2 diabetes mellitus
T3	Tri-iodothyronine
TAE	Tris-acetate-EDTA
TBC1D1	TBC1 Domain Family Member 1
TBC1D4	TBC1 Domain Family Member 4
TBS	Tris-buffered saline
TCA	Tricarboxylic acid
TMB	Tetramethylbenzidine
TNF-α	Tumor necrosis factor-alpha
TORC2	CREB-regulated transcription coactivator 2
TRβ	Thyroid receptor β
TRP	Transient receptor potential
TRPM8	Transient receptor potential melastatin 8
TRPV1	Transient receptor potential vanilloid 1
UCP1	Uncoupling protein 1
VMH	Ventromedial hypothalamic nucleus
VSG	Vertical sleeve gastrectomy
WHO	World Health Organization
WHR	Waist-to-hip ratio
WT	Wild-type
$2^{-\Delta\Delta Ct}$	Threshold cycle method
2-DG	2-deoxy-glucose

Index of tables

Index of figures

Abstract

Obesity and its comorbidities, such as type 2 diabetes mellitus (T2DM), are major threats to worldwide health. Strategies to halt the obesity and T2DM pandemic include lifestyle modification, pharmacotherapy, and bariatric surgery. Currently, the latter most effectively induces body weight loss, but surgeries are costly, invasive, and only indicated in morbidly obese patients, precluding a large-scale use. Patients, on average, lose ~ 30% of their initial body weight following 4 years after Roux-en-Y gastric bypass, highlighting the potential that obesity therapy holds, but thus far has not been accomplished using pharmacology (up to ~ 10% body weight loss). Over the past years, the simultaneous activation of distinctly different mechanisms using polypharmacology has evolved. In this PhD thesis, the efficacy of two novel polypharmacological approaches to induce body weight loss and improve associated metabolic complications in diet-induced obese (DIO) mice was assessed.

In the first approach, the specific efficacy of a novel glucagon-like peptide 1 (GLP-1)/glucose-dependent insulinotropic polypeptide (GIP)/glucagon triagonist to ameliorate metabolic disturbances in female mice was investigated. Currently, female animals are largely neglected in the preclinical evaluation of newly developed drugs, which limits the translational value to humans. Following the call of the U.S. National Institutes of Health to include female mice in biology research, the GLP-1/GIP/glucagon triagonist as effectively lowered body weight in female DIO mice as in fat mass-matched male mice. In female mice, treatment with high-dose triagonist for 27 days was superior in the amelioration of non-alcoholic fatty liver disease (NAFLD) compared to male mice.

In the second approach, two major canonical modulators of human energy metabolism – tobacco smoking and cold exposure – were pharmacologically mimicked. Using a combinatorial small molecule strategy with icilin and dimethylphenylpiperazinium (DMPP) respectively, energy expenditure was induced by activating the cold receptor, transient receptor potential melastatin 8 (TRPM8) and at the same time food intake was inhibited by targeting the α3β4 nicotinic acetylcholine receptor (nAChR). Icilin monotherapy increased energy expenditure, while DMPP treatment reduced food intake and improved glucose tolerance in DIO mice. The concerted, chronic activation of cold and nicotinic receptors synergistically reduced body weight, improved diet-induced glucose tolerance and insulin sensitivity, and reversed NAFLD in male DIO mice.

Mechanistically, the signaling molecule phosphoinositide interacting regulator of TRPs (Pirt), which is an endogenous regulator of TRPM8, showed to be dispensable for the induction of energy expenditure upon icilin-mediated TRPM8 activation. Assessing the mechanistic action

of DMPP on blood glucose regulation, acute DMPP induced the secretion of epinephrine and led to a pronounced hyperglycemia, while chronically, it enhanced peripheral insulin sensitivity in DIO mice.

The presented PhD thesis contributes to the preclinical evaluation of urgently needed novel pharmacological options to treat obesity and associated diseases.

Zusammenfassung

Adipositas und Begleiterkrankungen wie Typ-2-Diabetes mellitus (T2DM) stellen eine große gesundheitliche Bedrohung für die weltweite Bevölkerung dar. Strategien zur Behandlung der Pandemien umfassen die Änderung des Lebensstils, die Pharmakotherapie und die bariatrische Chirurgie. Gegenwärtig führt Letztere zur effektivsten Reduktion des Körpergewichts, aber die Interventionen sind teuer, invasiv und nur bei morbid adipösen Patienten indiziert, wodurch eine groß angelegte Anwendung ausgeschlossen ist. Patienten verlieren im Durchschnitt ~ 30% ihres ursprünglichen Körpergewichts in einem Zeitraum von 4 Jahren nach Roux-en-Y Magenbypass. Dies zeigt, dass eine erfolgreiche Adipositas-Therapie durchaus möglich ist, bisher jedoch pharmakologisch nicht erreicht wurde (bis zu ~ 10% Körpergewichtsverlust). In den letzten Jahren wurde die Idee der Polypharmakologie entwickelt, mit der gleichzeitig unterschiedliche Mechanismen aktiviert werden. Im Rahmen dieser Doktorarbeit wurde die Wirksamkeit zweier neuer polypharmakologischer Ansätze getestet und in Hinblick auf die Reduktion des Körpergewichts und der Verbesserung metabolischer Komplikationen in Diät-induzierten fettleibigen (DIO) Mäusen untersucht.

Im ersten Ansatz wurde spezifisch die Wirksamkeit eines neuartigen glucagon-like peptide 1 (GLP-1)/glucose-dependent insulinotropic polypeptide (GIP)/Glukagon Triagonisten zur Verbesserung von Stoffwechselstörungen bei weiblichen Mäusen untersucht. Gegenwärtig werden weibliche Tiere in der präklinischen Beurteilung neu entwickelter Arzneimittel weitgehend vernachlässigt, was den Tranlsationswert dieser Daten auf den Menschen einschränkt. Der Forderung der U.S. National Institutes of Health folgend, weibliche Mäuse in die biologische Forschung einzubeziehen, zeigte der GLP-1/GIP/Glukagon-Triagonist eine ebenso effektive Senkung des Körpergewichts bei weiblichen Mäusen wie bei männlichen Mäusen, welche den Weibchen in der Fettmasse glichen. Bei weiblichen Mäusen war die Behandlung mit hochdosiertem Triagonisten über 27 Tage bei der Verbesserung der nichtalkoholischen Fettleber (NAFLD) im Vergleich zu männlichen Mäusen sogar überlegen.

In einem zweiten Ansatz wurden zwei wichtige kanonische Modulatoren des menschlichen Energiestoffwechsels - Tabakrauchen und Kälteexposition - pharmakologisch nachgeahmt. Mit einer Kombinationsstrategie unter Verwendung von Icilin bzw. Dimethylphenylpiperazinium (DMPP), wurde der Energieverbrauch durch Aktivierung der Kälterezeptoren, transient receptor potential melastatin 8 (TRPM8), induziert und gleichzeitig wurde die Nahrungsaufnahme, durch Aktivierung von $\alpha3\beta4$ nikotinerge Acetylcholinrezeptoren (nAChR), gehemmt. Die Monotherapie mit Icilin erhöhte den Energieverbrauch, während die DMPP-Behandlung die Nahrungsaufnahme reduzierte und die

Glukosetoleranz bei DIO Mäusen verbesserte. Die gleichzeitige, chronische Aktivierung von Kälte- und Nikotinrezeptoren reduzierte das Körpergewicht synergistisch, verbesserte die Glukosetoleranz und Insulinsensitivität, und machte die NAFLD in männlichen DIO Mäusen rückgängig.

Mechanistisch wurde gezeigt, dass das Signalmolekül phosphoinositide interacting regulator of TRPs (Pirt), welches ein endogener Regulator von TRPM8 ist, für die Erhöhung des Energieverbrauchs nach Icilin-vermittelter TRPM8-Aktivierung nicht wesentlich ist. Außerdem zeigte sich bei der Beurteilung der mechanistischen Wirkung von DMPP auf die Blutzuckerregulation, dass DMPP akut eine Sekretion von Adrenalin induzierte und zu einer ausgeprägten Hyperglykämie führte, während es chronisch die periphere Insulinsensitivität in DIO-Mäusen verbesserte.

Mit der vorgestellten Doktorarbeit wurde zur präklinischen Evaluation dringend benötigter neuer pharmakologischer Optionen zur Behandlung von Fettleibigkeit und damit verbundenen metabolischen Erkrankungen beigetragen.

1 Introduction

1.1 The obesity and diabetes pandemic – an ever-growing problem for the 21st century

1.1.1 Obesity and type 2 diabetes mellitus

Disease occurrence varies. While some diseases, like breast cancer can occur sporadically, other endemic diseases, such as adiposity, have always been part of humanity (van der Groep et al., 2006). In times of famines, some excess fat depots were essential for survival, but in times of food abundance, obesity has turned into a preventable disease (Lev-Ran, 2001). Over the past decades, overweight and obesity have reached pandemic dimensions (Meldrum et al., 2017). In 2016, more than 1.9 billion adults worldwide were overweight. Of these, over 650 million were diagnosed as obese (WHO, 2018b). A chronic surplus in energy intake increases circulating fatty acids, which results in hyperplasia and –trophy of the adipose tissue (Schuster, 2010). The latter leads to local hypoxia due to a reduced blood flow and increased apoptosis, which induces a macrophage infiltration (Ye, 2009, Weisberg et al., 2003). All together, these conditions promote local and systemic proinflammatory cytokine secretion, such as interleukin (IL)-1, IL-6, and tumor necrosis factor-alpha (TNF-α) (Schuster, 2010, Samad et al., 1997, Fried et al., 1998). This chronic inflammation results in an increased prevalence of hypertension, coronary heart disease, sleep apnea, cancer, and type 2 diabetes mellitus (T2DM) (Poirier et al., 2006). Devastatingly, also childhood obesity has increased, with obese youngsters already suffering from metabolic complications like hypertension (Sahoo et al., 2015, Weiss and Caprio, 2005). Anthropometrically, obesity is classified according to the body mass index (BMI), which is calculated as the body weight in kilogram (kg) divided by the squared height in meters (m) (see **Table 1. 1**) (WHO, 2018a). The BMI classification dates back to 1842, when Adolphe Quetelet realized that in normal weighed individuals, the weight was proportional to the height squared (Quetelet A, 1968).

Table 1. 1 Classification of body weight according to World Health Organization (WHO)

Classification	BMI (kg/m^2)
Underweight	< 18.5
Normal weight	18.5 – 24.99
Overweight	**≥ 25**
Pre-obese	25 – 29.99
Obese	**≥ 30**
Obese class I	30 – 34.99
Obese class II	35-39.99
Obese class III	≥ 40

As BMI does not distinguish between fat and lean mass (Nuttall, 2015), a novel classification system has evolved, which is based on the measurement of the waist-to-hip ratio (WHR) and the waist circumference (Dalton et al., 2003, Prentice and Jebb, 2001). The WHR takes into account the differences between the lower-body (gynoid) and the upper-body (android) obesity. Superficial, subcutaneous adipose tissue that is metabolically less active makes up the majority of the lower-body adipose tissue (Sniderman et al., 2007, Bjorndal et al., 2011). Android obesity primarily consists of deep subcutaneous and visceral adipose tissue, which is lipolytically more active compared to subcutaneous adipose tissue (Morigny et al., 2016, Lafontan and Langin, 2009). From the visceral fat, free fatty acids (FFA) circulate directly, via the portal vein, to the liver and promote gluconeogenesis, lipid synthesis, and lipid accumulation in insulin-sensitive organs (Kahn et al., 2006b, Despres et al., 2001). In a meta-analysis, visceral adiposity showed the strongest positive correlation with a marker for β-cell function and insulin resistance, the homeostatic model assessment of insulin resistance (HOMA-IR) (Zhang et al., 2015, Matthews et al., 1985). In general, insulin resistance is the reduced ability of defined concentrations of insulin to dispose circulating plasma glucose (Reaven, 1988). A prolonged condition of insulin resistance is a clear risk factor for T2DM (Lillioja et al., 1993). In 2017, about 451 million adults worldwide were estimated to suffer from T2DM, which represents a quadrupling since 1980 (Cho et al., 2018). The World Health Organization (WHO) states that, annually, 1.6 million deaths can be directly attributed to T2DM (WHO, 2016). The criteria for the diagnosis of T2DM are displayed in **Table 1. 2** (American Diabetes, 2014).

Table 1. 2 Criteria for the diagnosis of T2DM

Criteria	Plasma glucose levels (mg/dl)
Glycated hemoglobin (HbA1c) ≥ 6.5%	/
or	
6-hours fasting plasma glucose	≥ 126
or	
2-hours plasma glucose during glucose tolerance test (GTT)	≥ 200
or	
ad libitum hyperglycemia	≥ 200

Besides the physiological and psychological consequences of obesity and its associated diseases like T2DM, also the economic burden is tremendously high. In Germany, annual direct costs of obesity are estimated to €29 billion with further €33 billion of indirect costs (Effertz et al., 2016).

1.1.2 Regulation of energy intake and energy expenditure

In a healthy state, the body weight of an individual is relatively stable over long periods of time. As reported in the Framingham Study, the average increase in body weight of an adult was 10% over 20 years (Belanger, 1988), which highlights the presence of continuous regulatory mechanisms for body weight homeostasis (Harris, 1990, Leibel, 1990, Leibel et al., 1995). Interpersonal differences in the propensity to gain body weight are most likely due to genetic (Bogardus et al., 1986, Herrera and Lindgren, 2010) and environmental factors (Brehm and D'Alessio, 2000). A critical role in the regulation of food intake has been attributed to the adipose tissue-derived hormone leptin, as mice that lack the gene for leptin or the leptin receptor are hyperphagic and severely obese (Chua et al., 1996, Zhang et al., 1994). Leptin receptors (LepR) are densely expressed in the hypothalamic arcuate nucleus (ARH), which is the main sensor of peripheral cues related to the energy state (Roh and Kim, 2016, Cowley et al., 2003). Leptin is secreted in proportion to the fat mass, passes the blood brain barrier and, in the ARH, activates anorexigenic proopiomelanocortin (POMC) neurons and simultaneously inhibits orexigenic agouti-related peptide (AgRP)/neuropeptide Y (NPY) neurons (Cowley et al., 2001, Balthasar et al., 2004). The binding of leptin to LepR initiates the processing of POMC to α-melanocyte-stimulating hormone (α-MSH), which binds melanocortin 4 receptors (MC4R) expressed in the paraventricular nucleus (PVN) resulting in the suppression of food intake (Varela and Horvath, 2012). Moreover, the binding of α-MSH to MC4R induces energy expenditure via the activation of the sympathetic nervous system, resulting in the secretion of norepinephrine (NE) that activates β_3-adrenergic receptors (AR) on the brown adipose tissue (BAT) (Commins et al., 2000). The consequent expression of uncoupling protein 1 (UCP1) induces BAT-dependent thermogenesis (Morrison et al., 2014). In obesity, leptin levels are constantly elevated but do not signal appropriately, which has led to the assumption of an obesity-induced leptin resistance (Maffei et al., 1995, Considine et al., 1996). The modulation of the central regulation of energy intake and expenditure has been subject of interest in the context of anti-obesity therapy – historically and also in the presented thesis.

1.2 Current treatment options

1.2.1 Lifestyle interventions

The first treatment option for obese and diabetic patients is lifestyle modification, including dietary-, exercise-, behavioral-, and if indicated also psychotherapy.

In general, nutritional therapy aims for an energy deficit by 500 kcal/day, which is achieved with different weight-reducing diets e.g. low-fat, low-carb, energy-reduced mixed, or

Mediterranean diet. Dietary interventions target a body weight reduction of 0.5 kg/week over 12 to maximally 24 weeks (Wirth et al., 2014). Obese patients with a BMI ≥ 30 kg/m² can substitute their food for a maximum of 12 weeks with formula products that contain 800 to 1200 kcal/day. Formula diets consist of high quality protein sources, only little fat, and the recommended portion of vitamins and minerals (2004, Wadden, 1995) and they represent the most effective dietary method to induce initial body weight loss (Anderson et al., 1992, Apfelbaum et al., 1987, Atkinson, 1989). In conjunction to dietary interventions, obese patients should work out > 150 minutes per week with an energy expenditure of 1200 to 1800 kcal/week (Wirth et al., 2014). Initially, interventions for the treatment of obesity can be successful and induce a loss in body weight of 7% and more (Look and Wing, 2010, Unick et al., 2013). At this efficacy, severely obese patients may remain in the obese class III BMI category, but metabolic benefits are nevertheless evident. Such benefits can involve the lowering of low-density lipoproteins (LDL)-cholesterol, plasma triglycerides, blood pressure, and cardiovascular disease risk factor values and the increase in high-density lipoproteins (HDL)-cholesterol (Unick et al., 2013). Moreover, meta-analyses and randomized controlled trials established associations of lifestyle interventions with improved obstructive sleep apnea (Araghi et al., 2013) and reduced symptoms of depression (Rubin et al., 2014, van Dammen et al., 2018). However, continual change in lifestyle habits is difficult and consequently, the long-term positive rates of these interventions are disappointingly low (Middleton et al., 2013). The efficacy of lifestyle interventions also depends on physiological, genetic, and epigenetic factors (Sparks, 2017). About 40-70% of the BMI is influenced by the individuals' genetic predisposition (Allison et al., 1994, Chagnon et al., 1997, Chung, 2012, Goran, 1997) and twin studies suggest that specific genes change the susceptibility to respond to weight loss therapies (Bouchard et al., 1990, Bouchard et al., 1994, Ukkola et al., 2004). Thus, it is important to carefully distinguish between patients that, upon the same lifestyle intervention, successfully lose body weight whereas others do not. Differentiations of patients to responders and non-responders hold the potential for precision medicine. As such, the National Institutes of Health (NIH) proposed to take advantage of the genomic information of patients to tailor weight loss interventions to maximize the health benefits (Bray et al., 2016). These attempts are cost-intensive. Moreover, lifestyle interventions only induce limited weight loss and often lead to weight cycling, which has been associated with higher mortality (Lissner et al., 1991, Mehta et al., 2014). Thus, there is a need for safe and effective pharmacotherapeutical options (Farag and Gaballa, 2011, Müller et al., 2018).

1.2.2 Pharmacological interventions

1.2.2.1 Pharmacological therapy for obesity

In the USA, President Franklin Roosevelt signed the first legal document to report the safety of drugs to the Food and Drug Administration (FDA) in 1938 (Colman, 2005). For Europe, the European Medicines Agency (EMA) is in charge for the legal supervision of the marketing and distribution of newly manufactured drugs. Currently, four distinct clinical phases of drug development exist (U.S. Food & Drug, 2018). Phase I involves the application of either the drug or placebo to healthy volunteers (20-80) and specifically focuses on tolerability, pharmacokinetics, and safety. In phase II, either drug or placebo are applied to a small group of well-informed patients (100-300) to investigate the effectiveness and tolerability. Phase II clinical trials are too small to assess the risks or benefits of the drugs. Thus, based on information obtained during this stage of development, research protocols for larger-scale phase III clinical trial are designed (U.S. Food & Drug, 2018). About 31% of the evaluated drugs progress to phase III where longer-term safety, efficacy, and differences to similar treatment options are tested in multicenter patient trials (1000-3000) (Patel et al., 2017). Upon successful completion of these three phases, the drugs can be officially registered. Prior to commercialization, phase IV studies confirm the effects in larger-scale, chronic studies (National Institutes of Health, 2017). Although the drug development process underlies these clear legal requirements, several approved drugs had to be withdrawn, because beneficial effects were outweighed by safety concerns (Müller et al., 2018). In the first half of the 20th century, pharmacological activation of energy metabolism was explored as an anti-obesity treatment. During the First World War, 2,4-dinitrophenol (DNP) together with picric acid was used in French munitions factories to produce explosives, but soon workers noticed a pronounced body weight loss upon exposure to DNP (Perkins, 1919). In 1933, Cutting *et al* published that 3.5 mg/kg orally administered DNP increased basal metabolic rate in men by 20 - 30% for 24 hours. Chronically, daily oral doses of 3 mg/kg for 80 days raised the basal metabolic rate to 40% and, on average, induced a weekly body weight loss of 0.9 kg in obese patients (Cutting et al., 1933). However, it became evident that the therapeutic window of DNP was small and it could induce lethal pyrexia. The consequences were high rates of fatalities that were directly caused by DNP (Grundlingh et al., 2011, Tainter et al., 1934). The severe side effects associated with DNP might have steered the anti-obesity field away from drugs that increase energy expenditure and towards appetite-suppressants (Bray and Greenway, 1976). In the 1950s, amphetamines were prescribed to induce body weight loss by increasing central nervous system (CNS) activity and decreasing appetite (Heal et al., 2013).

By 1977, amphetamine prescriptions were largely limited as the risk of addiction was too high (Colman, 2005). However, the amphetamine phentermine has been approved by the FDA in conjunction with the fructose derivate topiramate (Qsymia™, Vivus, Mountain View, USA) in 2012. Phentermine is a sympathomimetic and stimulates the release of primarily NE, but also dopamine and serotonin. Topiramate increases satiety most likely via enhanced γ-aminobutyric acid (GABA)-mediated appetite suppression (Lonneman et al., 2013). Simultaneously, topiramate antagonizes kainate/AMPA glutamate receptors (Kaminski et al., 2004). Activation of these receptors upon injection of glutamate to the lateral hypothalamus induced an immediate eating initiation in rats (Stanley et al., 1993). Another FDA-approved drug for the treatment of obesity is lorcaserin (Belviq™, Eisai, Woodcliff Lake, USA), which is a serotonin 2C agonist and acts centrally to suppress binge-related food intake (Gustafson et al., 2013).

According to the current S3-Leitlinie for the prevention and treatment of obesity, which was released from the *Deutsche Adipositas-Gesellschaft* e.V. in 2014 (Deutsche Adipositas Gesellschaft, 2014), the only EMA-approved anti-obesity drug was the gastrointestinal lipase inhibitor orlistat (Xenical®, CHEPLAPHARM Arzneimittel GmbH, Greifswald, Germany), which reduces the fatty acid absorption (Drent et al., 1995). Orlistat is indicated at a BMI > 28 kg/m^2 in the presence of comorbidities or a BMI ≥ 30 kg/m^2 and a failure of effective lifestyle modification (Götz, 2017, EMA, 2012a). Since the release of the S3-Leitlinie in 2014, two more substances had been approved for the treatment of obesity by the EMA. These are the glucagon-like peptide 1 (GLP-1) receptor agonist liraglutide, 3 mg (Saxenda®, Novo Nordisk, Bagsvaerd, Denmark) and the combination therapy of naltrexone/bupropion (Mysimba®, Orexigen Therapeutics, La Jolla, USA) (EMA, 2014c, EMA, 2015). The opioid antagonist naltrexone together with the dopamine- and NE-reuptake inhibitor bupropion synergistically activate POMC neurons to decrease food intake (Sherman et al., 2016). Unfortunately the body weight-lowering efficacy of these currently available pharmacological anti-obesity interventions is underwhelming and ranges typically between 5%-10% (Sjostrom et al., 1998). Nevertheless, this loss in excess fat can already be clinically important and it reduces the susceptibility of patients to develop comorbidities like T2DM.

1.2.2.2 Pharmacological therapy for T2DM

The oldest diabetes therapeutic is metformin (Aurobindo Pharma - Milpharm Ltd., Middlesex, Great Britain) (Rojas and Gomes, 2013, EMA, 2016). In 1957, a French physician named Jean Sterne discovered that metformin lowered blood glucose (Sterne, 1957). Meanwhile, it has been shown that metformin reduces hepatic gluconeogenesis and improves peripheral

insulin sensitivity (Hundal et al., 2000), while mechanistically, many questions remain unanswered (Hardie et al., 2012). Studies in mice suggest that metformin in the liver activates liver kinase B1, which phosphorylates and activates adenosine monophosphate-activated protein kinase (AMPK) (Shaw et al., 2005). Upon AMPK activation, CREB-regulated transcription coactivator 2 (TORC2) gets phosphorylated, inhibiting the transcription of gluconeogenic enzymes (Shaw et al., 2005, Cao et al., 2014). Moreover, metformin inhibits mitochondrial respiration, increasing the ADP/ATP or AMP/ATP ratio, which further activates AMPK (El-Mir et al., 2000, Hardie et al., 2012). Another class of T2DM medications are sulfonylureas, which close ATP-sensitive K^+-channels in the pancreatic β-cell leading to the depolarization of the cell membrane (Ashcroft, 1996). These changes trigger the opening of voltage-dependent Ca^{2+} channels leading to the influx of Ca^{2+} and enhancing Ca^{2+}-induced Ca^{2+} release from the endoplasmic reticulum, resulting in the secretion of insulin (Frohlich et al., 1978). Thiazolidinediones can also be used to treat T2DM to primarily improve peripheral insulin sensitivity and pancreatic β-cell function (Miyazaki et al., 2001, Hanley et al., 2010). The advanced progression of T2DM is associated with a marked failure of β-cells to secrete insulin (Cerf, 2013), a reduction in β-cell mass (Butler et al., 2003), and/or the dedifferentiation of β-cells respectively (Talchai et al., 2012), which necessitates the exogenous administration of insulin (Swinnen et al., 2009). According to the American Diabetes Association, metformin should be the first line pharmacological treatment option for T2DM (American Diabetes, 2015), as it holds many benefits, such as the ease of oral application, low risks of hypoglycemia, and if co-administered with sulfonylureas, thiazolidinediones, or insulin, it prevents a gain in body weight that is otherwise often associated with these anti-diabetic drugs (EMA, 2016, Kooy et al., 2009, Cheng and Kashyap, 2011, Garber et al., 2003, Kahn et al., 2006a, Rosenstock et al., 2008). In contrast, peptides that target the GLP-1 receptor (GLP-1R) favorably impact body weight loss and potently improve T2DM-associated complications (Cheng and Kashyap, 2011). GLP-1 is secreted from intestinal L-cells upon ingestion of a meal (Rask et al., 2001, Lim and Brubaker, 2006). Its receptors are expressed primarily in the brain, in the pancreatic β-cell, and the gastrointestinal tract (Tornehave et al., 2008, Campbell and Drucker, 2013). GLP-1 increases glucose-stimulated insulin secretion and inhibits the release of glucagon (Drucker et al., 1987, De Marinis et al., 2010). Preclinical rodent data suggest that GLP-1 promotes β-cell proliferation (Wang et al., 1999, Buteau et al., 2003), reduces the risk for cardiovascular diseases (Noyan-Ashraf et al., 2009), and suppresses hepatic gluconeogenesis (Ip et al., 2013). Human studies showed that GLP-1 reduces food intake (Gutzwiller et al., 1999) and improves

skeletal muscle insulin sensitivity (Zander et al., 2002). Based on these pleiotropic beneficial effects of GLP-1 on (glucose) metabolism, the therapeutic benefit of GLP-1 in the treatment of T2DM has garnered a lot of attention. The short half-life time of endogenous GLP-1 (between 1 and 2 min) necessitated the synthesis of GLP-1 analogs with an extended half-life time. Some of these have already been approved by the FDA and EMA for the treatment of T2DM, e.g. exenatide (Byetta®, Amylin Pharmaceuticals Inc., San Diego, USA) (EMA, 2012b), liraglutide (Victoza®, Novo Nordisk) (EMA, 2017b), lixisenatide (Lyxumia®, Sanofi, Paris, France) (EMA, 2012c), dulaglutide (Trulicity®, Eli Lilly & Co, Indianapolis, USA) (EMA, 2014b), albiglutide (Eperzan®, GlaxoSmithKline, Brentford, Great Britain) (EMA, 2014a), which was withdrawn from sale in 2017, and semaglutide (Ozempic®, Novo Nordisk) (EMA, 2017a). The preparations differ with respect to the mode of action, as some are short-acting (exenatide, administered twice daily; lixisenatide, administered once daily) and others are long-acting with once daily (liraglutide) or once weekly administration (dulaglutide, albiglutide, and semaglutide) (Abd El Aziz et al., 2017). Endogenously, GLP-1 is cleaved by dipeptidyl peptidase-IV (DPP-IV) (Mentlein et al., 1993). The inhibition of the cleavage activity of DPP-IV represents another treatment option that exerts most effective glycemic benefits in conjunction with metformin (Richter et al., 2008, Karagiannis et al., 2012).

Taken together, albeit a meta-analysis reported that anti-diabetes pharmacotherapies are superior in improving hyperglycemia compared to dietary interventions, they also showed that the beneficial effect deteriorates over time. Thus, bariatric surgery remains the most effective current treatment option (Schauer et al., 2017).

1.2.3 Bariatric surgery

Traditionally, bariatric surgeries are divided into three different categories with each group representing a distinct mechanism to induce body weight loss (**Figure 1. 1**). Bariatric surgeries have evolved over the past 66 years with some procedures disappearing and novel approaches appearing (Celio and Pories, 2016).
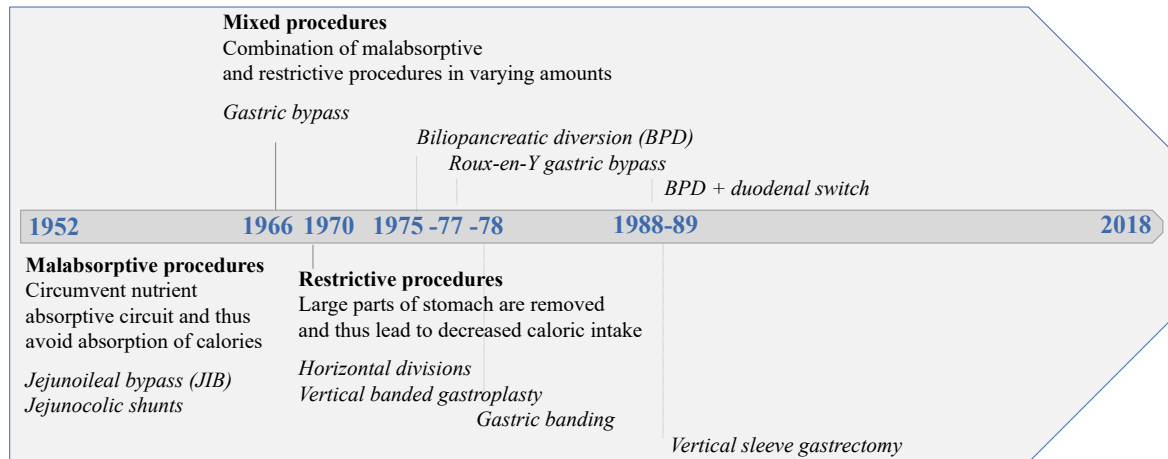
Figure 1. 1 Timeline of the evolution of different bariatric surgery procedures. Malabsorptive, restrictive, and mixed procedures at their chronological appearance from 1952 until 2018.

1.2.3.1 Malabsorptive procedures

The idea to treat obesity by malabsorptive invasive procedures arose as a Swedish surgeon, Dr Henrikson, realized in the early 1950s that small bowel resections were associated with side effects, such as loss in body weight and improvement in intestinal function (Henrikson, 1994). From 1953 on, U.S. surgeons performed and developed the intestinal bypass to treat severe obesity (Kremen et al., 1954, Buchwald and Rucker, 1987). The procedures ranged from jejunoileal bypass (JIB), where the proximal small intestine was joined to the distal ileum, to jejunocolic shunts, which involved anastomosing a segment of proximal jejunum to the transverse colon (**Figure 1. 1**). Especially the latter was associated with severe complications, but also for JIB, side effects like diarrhea and liver dysfunctions occurred. In a 25-year follow-up study, 28% of the 36 patients that underwent JIB have had the operation reversed, which resulted in a regain of body weight except for one case. Of the remaining patients, 23 people were still alive. Of those, pre-operative median BMI was 41, which was reduced to 30 at 25-year follow-up and none of the patients (median age of 56 years) suffered from T2DM (Vage et al., 2002). However, severe side effects persisted even 25 years after the surgeries (Vage et al., 2002). Since less morbid bariatric surgeries were on the forefront in the mid-1970s, JIB interventions became less popular (Griffen et al., 1977).

1.2.3.2 Mixed malabsorptive and restrictive procedures

One of these novel interventions was the biliopancreatic diversion (BPD), which was a Roux-en-Y version of the JIB (**Figure 1. 1**). The 2-year outcome of BPD in 1282 patients resulted in the loss of 70.12% (95% confidence interval (CI): 73.91%-66.34%) of excess body weight and an absolute weight loss of 46.39 kg (CI: 51.58 kg-41.20 kg) (Buchwald et al., 2004).

9

Additionally, T2DM in patients undergoing BPD was completely resolved in 98.9% (CI: 96.8%-100%) of the cases (Buchwald et al., 2004). However, severe side effects involved protein malnutrition, associated with anemia and bone demineralization (Scopinaro et al., 1996). In the late 1980s, BPD was modified adding a duodenal switch, but comorbidities still occurred (**Figure 1. 1**) (Hess and Hess, 1998). In 1966, the first gastric bypass surgery was performed and over the years, the intervention was favored over JIB and BPD. The procedure was refined until, in 1977, the Roux-en-Y configuration was introduced (**Figure 1. 1**), which involved minimizing the stomach to an egg-sized pouch physically restricting the patients from overeating (Griffen et al., 1977). As the jejunum got directly linked to the gastric pouch, nutrients were bypassing the absorptive capacity of the duodenum, thus leading to malabsorption and the loss of calories in feces (Celio and Pories, 2016). Body weight loss 4 years after Roux-en-Y gastric bypass was 27.5% (95% CI: 23.8%-31.2%) (Maciejewski et al., 2016) and generally, gastric bypass is associated with less severe side effects (Torgersen et al., 2014). Nevertheless, the intervention is invasive and patients need to supplement with calcium, iron, and vitamin B12 for the rest of their lives.

1.2.3.3 Restrictive procedures

Aiming to modify gastric anatomy and induce early satiety, gastroplasty interventions were performed in the 1970s. Techniques ranged from horizontal divisions of the upper stomach to vertical banded gastroplasty (**Figure 1. 1**). Overall gastroplasty was less prone to induce side effects, but, likely due to dehiscence of staple lines, the body weight-lowering efficacy was underwhelming (Balsiger et al., 2000). The least invasive bariatric surgery is gastric banding, where nonadjustable bands were used starting in 1978 (**Figure 1. 1**) (Wilkinson and Peloso, 1981). However slippage and erosion of the band occurred, leading to vomiting, food intolerances, and esophageal dilatation (Baker, 2011). Advancements lead to the usage of adjustable gastric bands, which were also less prone to dilatation because they were placed higher on the stomach (Fielding and Ren, 2005). Long-term studies suggest that gastric banding is less effective in body weight reduction compared to other bariatric surgeries and reoperations are frequent (annual rate of 5%) (Buchwald et al., 2004, Biertho et al., 2005). One of the proposed advantages of gastroplasty and gastric banding is reversibility. Vertical sleeve gastrectomy (VSG), however, is another purely restrictive procedure where ~ 80% of the stomach is irreversibly resected. Originally, surgeons started to perform sleeve gastrectomies in the late 1980s, often preceding gastric bypass surgeries for initial weight loss to limit the risk of complications (**Figure 1. 1**) (Silecchia et al., 2006, Johnston et al., 2003). Time revealed that VSG was associated with minimal morbidity and less long-term side

effects. Consequently, it has evolved as a stand-alone therapy and in a recent 5 year follow-up study, sleeve gastrectomy was not only superior in losing body weight and improving glycated hemoglobin (HbA1c) compared to medical therapy, but even comparably efficient to improve metabolic disturbances as Roux-en-Y gastric bypass. Body weight loss 5 years after gastric bypass, sleeve gastrectomy, and/or medical therapy was 23%, 19%, and 5% respectively, with a decrease in triglyceride levels of 40%, 29%, and 8%, an increase in HDL cholesterol of 32%, 30%, and 7%, and a discontinuation of insulin therapy in 35%, 34%, and 13% of the cases (Schauer et al., 2017). As VSG does not lead to malabsorption and only creates a portion of the restriction compared to Roux-en-Y gastric bypass (Colquitt et al., 2014), these observations fueled first hypotheses that restriction and malabsorption were not the exclusive causes of the weight-lowering effects of bariatric surgery.

1.2.3.4 Mechanical-independent effects of bariatric surgery

A reduced ingestion of nutrients results in lower levels of leptin and insulin, which leads to an increased feeling of hunger and a decrease in the metabolic rate (Schwartz et al., 2000). Upon bariatric surgery, the failure to absorb nutrients should render patients craving for food, but in fact they are less hungry (le Roux and Bueter, 2014). Stefater *et al* suggested that VSG leads to an alteration in the body weight set point (Stefater et al., 2010). In rats, sleeve gastrectomy induced a sustained body weight loss that persisted also after the initial anorectic post surgery phase. 50 days after surgery, the rats were challenged with a chronic food restriction protocol. Upon completion of the challenge, the rats had *ad libitum* access to food and although they physically could have eaten until reaching the pre-surgery obese state, they only ate until they regained pre-restriction body weight (Stefater et al., 2010, Makaronidis and Batterham, 2016). These results indicate that restriction is not the sole mediator of body weight loss and it has been shown that upon bariatric interventions, a variety of gut-secreted peptides, as well as bile acids, are increased or altered after ingestion of a meal (Patti et al., 2009, Clemmensen et al., 2017). For classical gut hormones, such as ghrelin and glucose-dependent insulinotropic polypeptide (GIP), the body of evidence is uncertain. Ghrelin, which is the typical orexigenic "hunger hormone", was reduced after VSG (Nosso et al., 2016, Pradhan et al., 2013). However, the intervention improved metabolism as effectively in ghrelin deficient mice as compared to WT mice, suggesting a ghrelin-independent mechanism (Chambers et al., 2013). GIP is secreted by enteroendocrine K-cells from the proximal gut and enhances the insulinotropic action of GLP-1 (Buffa et al., 1975, Buchan et al., 1978). Like GLP-1, also GIP is rapidly degraded by DPP-IV (Deacon, 2004). The effects of gastric bypass on GIP secretion are unclear, with studies reporting increases (Laferrere et al., 2007), no changes

(Korner et al., 2007), and even decreases (Wu et al., 2013) of GIP levels. Limitations in the interpretation of the data exist as they measured the DPP-IV degraded, non-active from of GIP at different post-surgical timepoints and surgical techniques varied between studies. However, for GLP-1 and the co-secreted peptide YY (PYY) the literature is not conflicting and clear associations suggest an increased secretion of both peptides upon bariatric surgery (Laferrere et al., 2008, Peterli et al., 2012). Humans that achieved an equivalent degree of weight loss by dieting did not have as high postprandial GLP-1 levels as patients undergoing bariatric surgery (Laferrere et al., 2008). These results highlight the potential contribution of GLP-1 on the outcomes of gastric bypass and VSG, however in mice that globally lack GLP-1R, VSG was as effective as in WT mice (Wilson-Perez et al., 2013). In humans following gastric bypass, inhibiting GLP-1 or PYY signaling did not affect food consumption, yet blocking the action of both peptides simultaneously increased food intake by ~ 20% (Svane et al., 2016). These studies suggest that the beneficial effects of bariatric surgery may be ascribed to GLP-1 acting in concert with other factors or hormones.

1.3 Polypharmacological approaches – Gut paves path forward

Others and we therefore aim to mimic bariatric surgery by modulating energy intake, energy expenditure, and peripheral insulin sensitivity using different polypharmacological strategies.

1.3.1 Novel peptide-based hormonal polyagonists

In a polypharmacological approach, tolerability can be improved because each component targets similar mechanisms, yet via different receptors allowing application of lower doses of the single entities. Ideally, with similar acting polyagonists, synergism can be achieved. With synergism, metabolic disturbances can be ameliorated to a degree, which is greater than the sum of each singular drug. Recently, polypharmacological approaches have centered on GLP-1. As discussed in 1.2.2.2, currently approved GLP-1R monoagonists lower body weight and improve glucose metabolism, but the effectiveness is limited by dose-dependent adverse gastrointestinal events (Bettge et al., 2017). In a combinatorial approach, GLP-1 co-administered with PYY exerted an additive anorectic action in mice and humans (Neary et al., 2005, De Silva et al., 2011). Moreover, exenatide with cholecystokinin (Trevaskis et al., 2015), exendin-4 with salmon calcitonin (Bello et al., 2010), and liraglutide with a MC4R agonist (Clemmensen et al., 2015) have been evaluated in preclinical rodent and/or nonhuman primate studies. However, drugs that are co-administered at a single formulation each have different pharmacokinetics and thus differ with respect to absorption, distribution, metabolic processing, and excretion (Müller et al., 2018). Hence, research has further progressed to the

development of singular unimolecular multiagonists. If balanced agonism at each of the receptors is achieved, synergistic efficacy increases. The team of Richard DiMarchi and Matthias Tschöp has excelled in the development of single-molecule hormone combinations. Provocatively, they combined the insulinotropic, anorectic effect of GLP-1 with glucagon (Day et al., 2009). Glucagon receptors (GcgR) are predominantly expressed in the liver and kidney and upon activation with glucagon, hepatic gluconeogenesis and glycogenolysis is induced (Stevenson et al., 1987). Thus, glucagon increases the availability of circulating plasma glucose and it further decreases glucose uptake into skeletal muscle (Chen et al., 2007). As GcgR expression in skeletal muscle tissue is sparse, the mechanism is presumably mediated indirectly (Authier and Desbuquois, 2008). In humans, glucagon acutely induces lipolysis (Carlson et al., 1993) and the resultant rise of non-esterified fatty acids (NEFAs) is assumed to impair non-hepatic insulin-mediated glucose disposal (Chen et al., 2007). These actions of glucagon led to previous attempts to antagonize GcgR for the therapy of T2DM (Kim et al., 2012, Mu et al., 2011, Okamoto et al., 2015, Eisenstein and Strack, 1968). However, glucagon also has multiple beneficial effects on metabolism. As such, it acts centrally to reduce appetite (de Castro et al., 1978, Geary et al., 1993, Geary et al., 1992, Weatherford and Ritter, 1988), increases energy expenditure by activating BAT-dependent thermogenesis (Billington et al., 1991), and induces fat mass loss by enhancing lipolysis (Salter, 1960, Paloyan and Harper, 1961). Thus, the GLP-1/glucagon co-agonist, in which GLP-1 would buffer against the hyperglycemic actions of glucagon, was conceptualized. The once weekly administration of the GLP-1/glucagon co-agonist for four weeks significantly reduced body fat mass, reversed hepatic steatosis, and most notably, improved glucose tolerance in diet-induced obese (DIO) mice (Day et al., 2009). Using modified co-agonists with different agonistic action for GcgR together with the testing of the stable co-agonist in GLP-1R knockout (KO) mice, the efficacy was confirmed to be based on both, GLP-1 as well as glucagon action (Day et al., 2009). Further studies showed that the GLP-1/glucagon co-agonist improved leptin sensitivity in DIO mice (Clemmensen et al., 2014). Following these promising preclinical data, the concept of GLP-1/glucagon co-agonism has been pursued by researchers and pharmaceutical companies and has been positively evaluated in nonhuman primates (Henderson et al., 2016, Elvert et al., 2018). Sir Steve Bloom *et al* moreover showed that co-infusion of GLP-1 and glucagon induces energy expenditure, reduces energy intake, and improves hyperglycemia in humans (Tan et al., 2013, Cegla et al., 2014). Consequently, the monomeric GLP-1/glucagon co-agonist has been evaluated in clinical phase I and currently T2DM patients are recruited for phase II studies (U.S. National Institutes of Health,

2018). The preclinical development of other GLP-1-based unimolecular multihormonal medicines has further progressed. To potentiate the insulinotropic action, GLP-1 has been conjugated with the incretin hormone GIP to create the GLP-1/GIP co-agonist (Finan et al., 2013). Besides the promotion of insulin secretion, GIP can act as a blood glucose-stabilizing hormone and as such can induce glucagon secretion when blood glucose levels are low (Pederson and Brown, 1978, Christensen et al., 2011). Although, several *in vitro* and *in vivo* studies suggest that GIP promotes de novo lipogenesis (Oben et al., 1991), it has also been shown that GIP increases adipose tissue lipoprotein lipase activity, which stimulates clearance of chylomicron triglycerides (Wasada et al., 1981, Ebert et al., 1991, Eckel et al., 1979). However, due to the assigned lipogenic effect of GIP, the administration of the GLP-1/GIP co-agonist may have seemed contentious, but it potently reduced body weight and improved glucose tolerance in DIO mice, rats, nonhuman primates, and humans (Finan et al., 2013). Based on the positive preclinical outcomes, safety, efficacy, and tolerability are being currently assessed in clinical trials (Tschöp et al., 2016). The consequence of the positive results achieved with the GLP-1/glucagon and the GLP-1/GIP co-agonists was the combination of all three hormones to the monomeric GLP-1/GIP/glucagon triagonist. GLP-1, GIP, and glucagon share a high degree of sequence homology and activate G protein-coupled receptors that are expressed on the cell surface. Finan *et al* confirmed with *in vitro* binding assays that the GLP-1/GIP/glucagon triagonist had balanced agonism at all three receptors (Finan et al., 2015). According to the hypothesis, GLP-1 and glucagon would synergize to reduce body weight by decreasing food intake and increasing energy expenditure, while GIP would potentiate the beneficial effects of GLP-1 on glucose metabolism and together, GLP-1 and GIP would override glucagon's hyperglycemic action. In several rodent models of diet-induced and genetic obesity, the triagonist was superior in reducing body weight and improving insulin sensitivity compared to the GLP-1/GIP co-agonist and the potency of the triagonist was comparable to results obtained upon bariatric surgery (Yin et al., 2011). However, in the preclinical evaluation of novel drugs, a sex-bias confounds the translation value to both, men and women. Especially in obesity and T2DM research, typically male rodents are assessed in pharmacological studies, as female C57Bl/6j mice are somewhat protected from weight gain and diet-induced glucose intolerance (Pettersson et al., 2012, Yang et al., 2014, Gallou-Kabani et al., 2007).

1.3.1.1 Aim of the thesis (Chapter 1): Efficacy of GLP-1/GIP/glucagon triple agonism to reverse DIO in male and female mice

Peptide-based hormone polypharmacology to treat obesity and type 2 diabetes in diet-induced obese female and male mice

Following the initiative of the NIH to also include female mice in preclinical studies (Clayton and Collins, 2014), the objective was to assess the efficacy of the GLP-1/GIP/glucagon triagonist to reverse DIO and improve multiple nodes of metabolic disorders in female mice compared to a cohort of male mice that were matched in fat content and a cohort of male mice that were matched to the duration of diet-exposure.

1.3.2 Novel small molecule-based polyagonists

Stimulated by the increasing polypharmacological success in treating obesity in rodents (Finan et al., 2012, Finan et al., 2013, Finan et al., 2015, Finan et al., 2016, Jall et al., 2017, Quarta et al., 2017, Clemmensen et al., 2014), the aim of the thesis was to develop different strategies for personalized treatment options. In a novel approach, the CNS-feeding circuits and the BAT-dependent thermogenesis pathways were simultaneously targeted using small molecule-based polypharmacology. The most well established mechanism to increase energy expenditure is cold exposure (Cannon and Nedergaard, 2004). Upon cold the sympathetic nervous system is activated and promotes secretion of NE, which induces the thermogenic activity of the brown fat via β_3-AR (see 1.1.2) (Ikeda et al., 2018, Rehnmark et al., 1990, van Marken Lichtenbelt et al., 2009). The BAT is a key metabolically active tissue and especially important in small mammals and newborn infants, because it dissipates large amounts of chemical energy as heat (Cannon and Nedergaard, 2004). The advances in laboratory techniques enabled detection of considerable amounts of active BAT in cold-exposed humans (van Marken Lichtenbelt et al., 2009). From then on, pharmacological activation of the BAT for the treatment of obesity has ignited keen interest. The acute oral administration of a β_3-AR agonist, mirabegron (Myrbetriq, Astellas Pharma, Inc.), induced BAT metabolic activity and increased resting metabolic rate by ~ 200 kcal/d at a dose of 200 mg in healthy human subjects (Cypess et al., 2015). However, at this dose, mirabegron activated β_1-AR, which was associated with tachycardia (Cypess et al., 2015). Due to these safety concerns, alternative pathways to induce BAT activity have evolved. Ma *et al* proposed a novel, β_3-AR-independent, mechanism as mice without functional β_3-adrenergic receptors maintained colonic temperature and normal brown adipose tissue hypertrophy upon chronic cold exposure (Ma et al., 2012, Susulic et al., 1995). They reported that the activation of cold receptors, transient receptor potential melastatin 8 (TRPM8) channels, induced BAT thermogenesis (Ma et al., 2012). The cold receptors TRPM8 are Ca^{2+}-permeable non-selective

cationic channels. Chinese hamster ovary (CHO) cells, stably overexpressing TRPM8, showed an increase in Ca^{2+} influx at temperatures between 26ºC to 8ºC (Peier et al., 2002, McKemy et al., 2002). Besides cold temperatures, TRPM8 can also be pharmacologically activated by chemical ligands such as menthol and the synthetic super-agonist icilin (McKemy et al., 2002). Using whole-cell patch clamp on *Xenopus* oocytes expressing TRPM8 channels, McKemy *et al* demonstrated that icilin had 2.5 higher efficacy and almost 200% increased potency to activate TRPM8 compared to menthol (McKemy et al., 2002). To counteract a compensatory hyperphagia, which is associated with the activation of the metabolic rate (Ravussin et al., 2014, Cottle and Carlson, 1954), the nicotinic acetylcholine receptor (nAChR) subtype α3β4 was chosen as promising target in conjunction with icilin (Audrain-McGovern and Benowitz, 2011). Recent evidence showed that POMC neurons have a cholinergic phenotype and pharmacological stimulation of hypothalamic α3β4 nAChRs with nicotine and cytisine, a more selective agonist for α3β4 nAChRs (Picciotto et al., 1995), suppressed appetite via the hypothalamic-melanocortin system (Mineur et al., 2011, Meister et al., 2006). The therapeutic applicability of the broad nAChRs-agonist nicotine is however limited as smoking in humans is associated with an increased risk to develop cancer (Walser et al., 2008), non-alcoholic fatty liver disease (NAFLD) (Sinha-Hikim et al., 2014), and peripheral insulin resistance (Bergman et al., 2009). Using the relatively selective agonist for α3β4 nAChRs, dimethylphenylpiperazinium (DMPP), the aim was to target nAChRs expressed in POMC neurons to reduce food intake in mice (Xiao and Kellar, 2004, Mineur et al., 2011).

1.3.2.1 Aim of the thesis (Chapter 2): Pharmacological mimicking of cold and nicotine exposure

Small molecule-based polypharmacology to treat obesity and type 2 diabetes in diet-induced obese mice

The scope of the PhD thesis was to pharmacologically mimic cold exposure *in vivo* by activating TRPM8 receptors using icilin. Striving for synergism, α3β4 nAChRs were selectively activated with DMPP and together a role of TRPM8 and α3β4 nAChR pharmacology in body weight homeostasis and glucose metabolism in DIO mice was unraveled.

1.3.2.2 Aim of the thesis (Chapter 3): Role of downstream signaling molecule in regulation of TRPM8 pharmacology

Role of downstream signaling molecule in body weight regulation, glucose metabolism, and cold receptor activation

Upon TRPM8 activation with menthol, the two-transmembrane domain protein, phosphoinositide interacting regulator of TRPs (Pirt) binds to TRPM8 (Tang et al., 2013).

Pirt, together with the canonical cellular signal molecule phosphatidylinositol 4,5-bisphosphate (PIP$_2$), enhances TRPM8 sensitivity to agonists like menthol (Tang et al., 2016). As part of the PhD thesis, the role of Pirt in body weight regulation, energy expenditure, and BAT thermogenesis was determined. Most importantly, it was assessed whether Pirt was required for the induction of energy expenditure after pharmacological activation of TRPM8.

1.3.2.3 Aim of the thesis (Chapter 4): Mechanistic evaluation of potent DMPP-mediated improvements in glucose tolerance

Mechanistic evaluation of opposing acute and chronic effects of nicotine receptor activation on blood glucose

Chronically, DMPP improves glucose tolerance, independent of body weight loss (see 1.3.2.1). However, a single, first DMPP administration in DIO mice induced pronounced hyperglycemia. The aim was to unravel the mechanism underlying the acute and chronic effects of DMPP on blood glucose in DIO mice.

2 Methodology

2.1 Animal studies

2.1.1 Diet-induced obese mice and diets

In general, six to eight-week old female or male C57Bl/6j mice (Charles River Laboratories, Wilmington, MA) or genetically modified mouse lines were fed a high-fat, high-sugar diet (HFD) comprising 58% kcal from fat and sucrose (D12331i; Research Diets, New Brunswick, NJ, USA, see **Figure 6. 1** (Appendix)). All mice were maintained at 23 ± 1ºC, constant humidity, and on a 12-h light-dark cycle with free access to food and water. For the thermoneutral study, DIO mice were housed at constant 30ºC ambient temperature for four to seven weeks before initiation of the study. Except for chapter I, mice at all temperatures were housed under specific-pathogen free conditions.

2.1.2 Genetically modified mouse lines

UCP1 KO, Lep[db] mice, and MC4R KO were originally provided from Jackson Laboratory (strain names: B6.129-Ucp1tm1Kz/J; BKS.Cg-Dock7m +/+ Leprdb/J; B6;129S4-Mc4rtm1Lowl/J, Maine, USA). TRPM8 KO mice were generated as described (Bautista et al., 2007) and provided from Jackson Laboratory (strain name: B6.129P2-$Trpm8$[tm1Jul]/J). The generation of the $\beta_1\beta_2\beta_3$-AR KO (betaless), cholinergic receptor nicotinic beta 4 subunit (Chrnb4) KO, fibroblast growth factor 21 (FGF21) KO, and Pirt deficient (Pirt^{-/-}) mice is described elsewhere (Kim et al., 2008, Bachman et al., 2002, Xu et al., 1999, Hotta et al., 2009) (see also **Appendix 6.1.1**). GcgR flox mice were bred with Alb cre mice to generate a colony of homozygous GcgR flox x Alb cre mice. For pharmacological and phenotyping studies, homozygous mice were used to generate the colony of homozygous WT and KO mice, except for the FGF21 KO cohort, which was generated using heterozygous breedings. Genotyping protocols for all transgenic mice are supplied under **Appendix 6.1.2**.

2.1.3 Phenotyping of Pirt^{-/-} mice

Phenotypic analysis of Pirt^{-/-} and WT mice was initiated at 8 weeks of age. Cohorts of eight WT and eight Pirt^{-/-} male and female mice were phenotypically monitored on a standard chow diet or switched from chow to HFD at the age of 8 weeks. Until the age of 25 weeks, body weight and food intake were assessed once per week.

2.1.4 Body composition and metabolic phenotyping

Body composition was analyzed using a nuclear magnetic resonance technology (Echo-MRI, Houston, USA). For registration of energy expenditure, respiratory exchange ratio (RER) and home-cage locomotor activity a combined indirect calorimetry system was used (TSE

PhenoMaster, TSE Systems, Bad Homburg, Germany). Mice were acclimatized for 24 hours and afterwards, O_2 consumption and CO_2 production were registered every five or ten minutes. Home-cage locomotor activity was determined based on multidimensional infrared light beams, which scan the bottom and top levels of the cage. Locomotor activity is determined and expressed as beam breaks.

2.1.5 Pharmacology

For pharmacological *in vivo* studies, mice were randomly assigned to treatment groups based on body weight and body fat. The GLP-1/GIP/glucagon triagonist (chapter I) was characterized previously and it was used without any chemical modification (Finan et al., 2015). DMPP (D5891, Sigma-Aldrich, Munich, Germany) and icilin (10137, Cayman Chemical, Michigan, USA) (chapter II) were dissolved in a vehicle of 0.01N NaOH and 1% Tween-80 in saline. For DMPP single-administration studies (chapter IV), the vehicle control group received 1% DMSO in saline. Subcutaneous (s.c.) injections of all compounds were performed before the beginning of the dark phase (0-2 hours) at the doses indicated in the figures at 5 µl per g body weight, unless stated otherwise. Icilin and DMPP were co-administered at single formulation. No blinding to the treatment groups was executed. The animal studies were approved and conducted in accordance to the Danish Animal Experimentation Inspectorate and Animal Ethics Committee of the government of Upper Bavaria, Germany.

2.1.6 Glucose metabolism studies

Glucose tolerance, insulin sensitivity, and pyruvate tolerance were analyzed approximately 20 hours after the last compound injections. For glucose and insulin tolerance tests, mice were fasted for 6 hours and challenged by an intraperitoneal (i.p.) injection of 1.5 g or 1.75 g glucose per kg body weight or 0.75 units insulin per kg body weight. Pyruvate tolerance was assessed in overnight fasted mice at an i.p. dose of 1 g pyruvate per kg body weight. Glucose levels in all tolerance tests were measured in the blood sampled from the tail veins before (0 minutes) and at 15, 30, 60, and 120 minutes post injection using a handheld glucometer (Abbott, Wiesbaden, Germany; Arseus Medical NV, Bornem, Belgium). For glucose-stimulated insulin secretion, blood was withdrawn from tail veins and collected into EDTA-coated microvette tubes (Sarstedt, Nümbrecht, Germany) at indicated time points. Glucose clearance was assessed by i.p. injection of glucose (1.75 g/kg body weight) at 10 µl per gram body weight together with ^{3}H-labelled 2-deoxy-glucose (^{3}H-2-DG) (60 µCi/ml) in mice fasted for six hours (chapter IV). ^{3}H-2-DG clearance was analyzed by assessing plasma ^{3}H activity at 10, 20, and 40 minutes after glucose injection in 5 µl of collected blood by scintillation

counting. The tissue accumulation of phosphorylated ^{3}H-2-DG (^{3}H-2-DG-6-P) was determined using the precipitation method (see 2.1.7) (Maarbjerg et al., 2009). The *in vivo* ^{3}H-2-DG clearance was assessed in collaboration with Dr. Christoffer Clemmensen from the NNF Center for Basic Metabolic Research at the University of Copenhagen and Dr. Annemarie Lundsgaard, Dr. Andreas Fritzen, Prof. Dr. Erik Richter, and Prof. Dr. Bente Kiens from the Department of Nutrition, Exercise and Sport at the University of Copenhagen.

2.1.7 Analysis of *in vivo* 2-deoxy-glucose clearance

For analysis of ^{3}H-2-DG clearance, 20-25 mg from each homogenized tissue sample was mixed with 200 µl 0.1 M NaOH and boiled at 96ºC for 30 minutes. Upon dissolution, 200 µl of 0.1 M HCl was added and vigorously mixed. For total ^{3}H-2-DG analysis, 150 µl of the tissue-NaOH-HCl-homogenate was added to 600 µl of 4.6% perchloric acid, mixed, and centrifuged at 17000 g for 4 minutes. 600 µl of the supernatant was added to 4 ml of scintillation fluid and radioactivity was measured (Packard TriCarb 2900TR; Perkin-Elmer, Boston, MA, USA). For dephosphorylated ^{3}H-2-DG analysis, 150 µl of the tissue-NaOH-HCl-homogenate was added to 300 µl of BaOH, vigorously mixed, and further neutralized with 300 µl of ZnSO$_4$. After mixing, the samples were centrifuged at 17000 g for 4 minutes. 600 µl of the supernatant was mixed with 4 ml of scintillation fluid and analyzed (Packard TriCarb 2900TR; Perkin-Elmer, Boston, MA, USA). Glucose clearance was calculated as the division of tissue ^{3}H-2-DG-6-P counts with systemic ^{3}H-2-DG exposure, which was assessed with the trapezoidal method.

2.1.8 Blood parameters

For tissue analysis, mice were injected with the respective treatment and immediately fasted for 2 to 4 hours prior to sample collection. Blood was stored on ice until centrifugation at 3000 g and 4ºC for 10 minutes. Plasma was aliquoted and immediately stored at -80°C. Plasma levels of insulin (ALPCO Diagnostics, Salem, USA), cholesterol (Thermo Fisher Scientific, Waltham, USA), NEFA, triglycerides (Wako Chemicals, Neuss, Germany), leptin (ALPCO Diagnostics), FGF21 (Merck Millipore, Darmstadt, Germany), alanine aminotransferase (ALT), and aspartate aminotransferase (AST) (Thermo Fisher Scientific) were measured with commercially available kits, which were used according to the kit descriptions. The HOMA-IR was calculated as: HOMA-IR = [fasting insulin (mU/l) * fasting glucose (mg/dl) / 405] (Matthews et al., 1985). For fast-performance liquid chromatography (FPLC) of cholesterol distribution in different lipoprotein fractions, plasma of the different treatment groups was pooled and measured on two Superose 6 columns connected in series (Hofmann et al., 2008). A high performance liquid chromatography (HPLC) system coupled

with an electrochemical detector (EcD) was used to assess plasma catecholamines as described previously (Nagler et al., 2018). The sample clean-up was performed as described in manufacturers' protocol (RECIPE, Munich, Germany). As plasma availability was limited, dilution of the plasma was necessary. Thus, 30 - 40 µl of plasma were mixed with 40 µl of water and 10 µl of internal standard was added. The diluted plasma was vigorously mixed and charged on the sample preparation column. After a 10 minutes shake of the column, the solvent was removed on a vacuum manifold. To remove interfering components, the column was washed three times using 1 ml washing solution. The column was dried and the elution reagent was added (140 µL). Using centrifugation force, the catecholamines were eluted from the extraction column via centrifugation and 20 µl of the eluate was injected as such into the HPLC-EcD system.

The FPLC analyses were performed by Sebastian Cucuruz and Prof. Dr. Susanna Hofmann from the Institute of Diabetes and Regeneration Research at the Helmholtz Zentrum München. The catecholamine analyses were performed by Dr. Meri De Angelis and Prof. Dr. Karl-Werner Schramm from the Molecular EXposomics at the Helmholtz Zentrum München.

2.1.9 Multi-spectral Optoacoustic Tomography

For Multi-Spectral Optoacoustic Tomography (MSOT), a 256-channel real-time imaging MSOT scanner was used (Dima et al., 2014) (inVision 256-TF, iThera Medical GmbH, Munich, Germany), which has a tunable (wavelength range: 680-960 nm) pulsed (pulse duration: <10 ns) optical parametric oscillator laser with a 10 Hz repetition rate. Homogeneous light along a line of illumination surrounding the animal body was delivered using a fiber bundle. The 256-element transducer array covered a solid angle of 270° around the imaged animal. The elements detected at a central frequency of 5 MHz. MSOT is based on the acquisition of cross-sectional (transverse) images of oxygenated and deoxygenated hemoglobin over time. These images result in estimations of total blood volume, tissue oxygen saturation, and of their transients. Different transverse planes are imaged with a moving stage, whereas illumination and ultrasound detection are static.

2.1.10 Mouse MSOT measurements *in vivo*

Anesthetization of C57Bl/6j mice was performed by i.p. injection of 139 mg/kg ketamine and 6.8 mg/kg xylazine. MSOT measurement was conducted as described earlier (Razansky et al., 2011). In brief, anesthetized mice were positioned onto a polyethylene membrane and placed in a water bath (34°C). The water was kept at controlled temperature, which allowed acoustic coupling and ensured maintenance of animal temperature while imaging. Vehicle, DMPP, icilin, or the combination of DMPP and icilin were injected i.p. 40 minutes prior to imaging

of the BAT. Six animals per compound treatment were used for the MSOT experiment. For the MSOT measurement, multiple images were recorded from a range of wavelengths spanning 700 nm to 900 nm with 20-nm steps. The commercial suite provided by the manufacturing company (ViewMSOT, Xvue Ltd, Greece) was used for preliminary data processing. Finally, application of a model-based image reconstruction method on the raw optoacoustic signals was followed by a spectral unmixing step in order to calculate the saturation maps over selected regions of interest. With eigenspectra optoacoustic tomography quantitative blood oxygenation imaging deep in tissues can be achieved (Tzoumas et al., 2016). MSOT measurement was performed by Stephan Sachs from the Institute for Diabetes and Obesity, Dr. Josefine Reber, Dr. Angelos Karlas, and Prof. Dr. Vasilis Ntziachristos from the Institute of Biological and Medical Imaging at the Helmholtz Zentrum München.

2.2 Molecular biological analyses

2.2.1 Biochemical analyses

Two hours prior to the sacrifice of mice, compounds were injected and food was removed. Mice were euthanized using CO_2 and tissue samples were dissected and immediately snap frozen in liquid nitrogen or kept on dry ice. RNA was isolated using RNeasy Kit (Qiagen, Hilden, Germany) according to the manufacturers' instructions to perform gene expression analysis. Using QuantiTect Reverse Transcription Kit (Qiagen, Hilden, Germany), which includes a gDNA elimination step, total RNA was reverse transcribed into cDNA. Gene expression in tissues was assessed with quantitative real-time PCR (qPCR) using either TaqMan single probes or SYBR green (Thermo Fisher Scientific, Erlangen, Germany). Relative expression of selected genes was normalized to the reference genes peptidylprolyl isomerase B (Ppib) or hypoxanthine-guanine phosphoribosyltransferase (Hprt). Hepatic glycogen was analyzed using a commercially available kit (Biovision, Milpitas, USA) following the manufacturers' instructions.

2.2.2 Western blot

Quadriceps muscle (25 mg) was homogenized (Tissue Lyzer II, Qiagen, Germany) in ice-cold buffer as described previously (Kleinert et al., 2017). After homogenization, lysates were rotated for one hour at 4ºC, centrifuged at 16000 g for 20 minutes at 4ºC, and the supernatant of each sample was collected. Protein concentrations of samples were analyzed using the bicinchoninic acid (BCA) method in triplicates (Pierce Biotechnology BCA, USA). Protein samples were heated in Laemmli buffer at 96 °C for 10 minutes and sodium dodecyl sulfate-polyacrylamide gel electrophoresis (SDS-PAGE) and semi-dry blotting were executed

subsequently. The primary antibodies are listed in **Table 6. 20**. Anti-TBC1D1 was kindly provided by Professor Grahame Hardie, University of Dundee, UK. Secondary antibodies were obtained from Dako Cymation (Denmark). Membranes were incubated with enhanced chemiluminescence (ECL$^+$; Amersham Biosciences, USA), and visualized using BioRad ChemiDoc™ MP Imaging System (Hercules, USA). Signals were quantified (Image Lab, Life Sciences, USA) and shown as arbitrary units. Western blot analyses were performed by Dr. Annemarie Lundsgaard and Dr. Andreas Fritzen from the Department of Nutrition, Exercise and Sport at the University of Copenhagen.

2.2.3 Immunohistochemistry

For cFOS immunohistochemistry, DIO WT mice or DIO Chrnb4 KO mice received daily s.c. injections of vehicle, DMPP, icilin or the combination of DMPP and icilin for two days. Two hours prior to perfusion, food was removed and mice were treated with the respective compound. For Pirt immunohistochemical evaluation, WT and Pirt$^{-/-}$ male mice were used. Mice were euthanized using CO_2 and transcardially perfused using saline (0.9% NaCl) and subsequently perfused with 4% paraformaldehyde (PFA) in phosphate-buffered saline (PBS) (pH=7.4). Brains were dissected and kept in 4% PFA at 4°C. After post-fixation with PFA, the brains were equilibrated for 48h with 30% sucrose in tris-buffered saline (TBS; pH 7.2). Brains were sectioned into 30 μm coronal slices using a cryostat, washed in TBS, blocked in 25% gelatin and 0.5% Triton X-100 in TBS for 1 hour and incubated overnight at 4°C with a primary antibody anti-cFOS (rabbit polyclonal SC-52, 1:1000, Santa Cruz Biotechnology, Inc, USA) or anti-Pirt (1:500, Biorbyt LLC, orb158159) in the blocking solution. Sections were washed in TBS, incubated with Alexa Fluor 568 donkey anti-rabbit (1:1000, Thermo Fisher Scientific, A10042) or Alexa Fluor 568 goat anti-rabbit (1:500, Thermo Fisher Scientific, A-11011) secondary antibody diluted in the blocking solution for 1 hour at room temperature and stained with 4′,6-diamidino-2-phenylindole (DAPI) solution (1:3000, Thermo Fisher Scientific, 62248) for 3 minutes. After a final wash series with TBS, sections were mounted on gelatin pre-coated glass slides with Slowfade Gold mounting medium (Thermo Fisher Scientific) and a coverslip was mounted onto the sections for image quantification. For Pirt evaluation, z-stacks of sections were collected at an interval of 2 μm using a Leica SP5 scanning confocal microscope (Leica Mikrosysteme GmbH, Wetzlar, Germany) with a 20x objective. Final images were obtained by maximum intensity projection of the z-stack using the ImageJ software. For cFOS immunoreactive (cFos+) cells, images of single focal planes were recorded at 20x magnification using a BZ-9000 fluorescence microscope (Keyence Coporation Itasca, USA). The number of cFos+ nuclei within the PVN

was assessed based on the Allen mouse brain atlas and cFos+ cells were quantified using ImageJ software. Morphometric experiments were analyzed without knowledge of the experimental group. The immunohistochemical stainings were performed in collaboration with Tim Gruber, Dr. Carmelo Quarta, and Dr. Gustav Collden from the Institute for Diabetes and Obesity at the Helmholtz Zentrum München.

2.2.4 Histopathology

Formalin fixed BAT, inguinal white adipose tissue (iWAT), and liver samples were paraffin-embedded using a vacuum infiltration processor TissueTEK VIP (Sakura, AV Alphen aan den Rijn, Netherland). Slides at a thickness of 3 to 4 µm were cut using a HMS35 (Zeiss, Jena, Germany) or HM340E (Thermo Fisher Scientific, Erlangen, Germany) rotatory microtome and hematoxylin and eosin (H&E) staining was performed. In brief, with decreasing ethanol series, rehydration of tissues was achieved. Samples were rinsed with tapwater, incubated with Mayers acid Hemalum for 2 minutes followed by blueing in tapwater and a final incubation with EosinY (both Sigma-Aldrich, USA) for 1 minute. With increasing ethanol series, samples were dehydrated, and mounted onto slides with Pertex® (Medite GmbH, Burgdorf, Germany) and coverslips (CarlRoth Chemicals, Karlsruhe, Germany). The slides were evaluated using a brightfield microscope (Axioplan; Zeiss, Jena, Germany). Morphological features were summarized in an activity score, which is used for diagnosis of steatohepatitis in NAFLD in humans (Kleiner et al., 2005). The definition of the NAFLD activity score (NAS) is the unweighted sum of the three individual scores for steatosis, lobular inflammation, and ballooning degeneration: Steatosis is categorized by the amount of fat vacuoles in liver cells according to the percentage of affected tissue (0: <5%; 1: 5-33%; 2: 33-66%; 3: >66%). Lobular inflammation is graded by the overall assessment of inflammatory foci per 200x field (0: no foci; 1: <2 foci; 2: 2-4 foci; 3: >4 foci). Ballooning degeneration can be scored as 0 (none), 1 (few cells), or 2 (many cells). Therefore, NAS is scored between 0 to 8 and a score < 2 is considered as non-steatohepatitis, a score from 3 to 4 is categorized as possible/borderline steatohepatitis, whereas a score ≥ 5 results in diagnosis of definite steatohepatitis.

For UCP1 immunoreactivity, iWAT and BAT samples at 3 µm sections were processed with a rabbit anti-UCP1 antibody (1:1500; ab 10983, Abcam, Cambridge, UK) on a Discovery XT automated stainer (Roche Diagnostics, Mannheim, Germany). Signal was detected with a biotinylated goat anti-rabbit secondary antibody (1:750, BA-1000, Vector Laboratories, Burlingame, USA) and Dako detection kit (K5001; Agilent, Waldbronn, Germany). Using an

AxioScan.Z1 digital slide scanner (Zeiss, Jena, Germany) with a 20x magnification objective, the stained tissue sections were scanned.

Image analysis was performed using the commercially available software Definiens Developer XD 2 (Definiens AG, Munich, Germany), where a specifically developed ruleset was applied to detect and quantify UCP1 stained tissue. This resulted in a parameter which was based on the ratio of UCP1 stained tissue. The histological evaluations were performed in collaboration with Dr. Frauke Neff from the Institute of Pathology and Dr. Annette Feuchtinger from the Research Unit Analytical Pathology at the Helmholtz Zentrum München.

2.3 Cell culture

2.3.1 Isolation of primary brown adipocytes

Isolation of primary brown adipocytes was performed from six- to eight-week-old male C57Bl/6j mice. After mincing of the BAT, the tissue was digested at 37ºC for 40 minutes (1 mg/ml Collagenase II (Thermo Fisher Scientific, Erlangen, Germany), 3 U/ml Dispase II (Sigma-Aldrich, Munich, Germany), 0.01 mM $CaCl_2$ in PBS), which was interrupted by vigorous vortex steps every five minutes. The suspension of cells was filtered through a 100 µm cell strainer, centrifuged at 300 g for 5 minutes, and resuspended in growth medium (DMEM/F12 1:1 plus Glutamax (Thermo Fisher Scientific, Erlangen, Germany) containing 1% Penicilin/Streptomycin (Thermo Fisher Scientific) and 10% heat-inactivated fetal bovine serum (HI-FBS)). Using a 40 µm cell strainer, the cell solution was filtered a second time, centrifuged at 300 g for 5 minutes, resuspended in the desired volume of growth medium for culturing of cells. Pre-adipocytes were plated into collagen-coated 12-well plates (VWR International GmbH, Darmstadt, Germany) and cultured to confluency at 37ºC and 5% CO_2. Upon confluency, differentiation was induced with dexamethasone (5 µM), isobutyl-methylxanthine (IBMX) (0.5 mM), rosiglitazone (1 µM), indomethacine (50 µM), T3 (1 nM), and insulin (0.5 µg/ml) in growth medium. Two days after induction of differentiation, adipocytes were cultured in growth medium supplemented with rosiglitazone, T3, and insulin. At day 4 of differentiation, culture medium was switched to contain growth medium with T3 and insulin.

Isolation and culturing of human brown adipocytes was performed as described previously (Broeders et al., 2015). In brief, the BAT stromal vascular fraction was dissected from an individual, who underwent deep neck surgery. Differentiation of human brown adipocytes was performed for 7 days using a differentiation medium containing biotin (33 mM),

pantothenate (17 mM), insulin (100 nM), dexamethasone (100 nM), IBMX (250 mM), rosiglitazone (5 mM), T3 (2 nM), and transferrin (10 mg/ml). For another five days, adipocytes were cultured in maintenance medium, which consisted of biotin (33 mM), pantothenate (17 mM), insulin (100 nM), dexamethasone (10 nM), T3 (2 nM), and transferrin (10 mg/ml). The human brown adipocyte experiments were performed by Dr. Emmani B.M. Nascimento and Prof. Dr. Patrick Schrauwen from the Department of Human Biology and Human Movement Sciences at the Maastricht University Medical Center.

2.3.2 Primary brown adipocytes, gene expression

Gene expression experiments were performed in differentiated primary brown adipocytes, where cells were treated with isoproterenol (Sigma-Aldrich, Munich, Germany, 1 µM), icilin (1 and 10 µM), or control (0.1% DMSO) at day six of differentiation in serum-free growth medium. Six hours after addition of the compounds, medium was quickly removed and the plates were snap-frozen at -80ºC until further processing.

2.3.3 Bioenergetics analyses

For bioenergetic experiments, primary brown adipocytes were seeded, cultured, and differentiated on a XF96^e well plate. Cells at day five of differentiation were washed and incubated in DMEM XF Assay medium (Seahorse Bioscience, Santa Clara, USA), supplemented with 25 mM glucose (Carl Roth, Karlsruhe, Germany) and 1.5% fatty acid free-bovine serum albumin (BSA) (Sigma-Aldrich, Munich, Germany) at 37ºC in a non-CO_2 incubator for ten minutes. Compounds at a ten-fold higher concentration were dissolved in DMEM XF Assay medium without supplements and loaded into the ports of a XF Assay Cartridge. Oxygen consumption rate (OCR) was assessed with an extracellular flux analyzer (XF96, Seahorse Bioscience). A description of the bioenergetic flux protocol is detailed in section 6.3 (**Table 6. 25**). In brief, basal OCR was recorded for nine minutes, followed by injection of oligomycin (2 µg/ml, 23 minutes), norepinephrine (1 µM, 27 minutes), icilin (1 µM, 27 minutes) or vehicle (0.1% DMSO, 27 minutes), carbonyl cyanide-p-trifluoromethoxyphenylhydrazone (FCCP) (1 µM, 14 minutes), rotenone (2.5 µM)/ antimycin A (2.5 µM)/2-deoxy-glucose (2-DG) (10 mM) (nine minutes). The cell plate was subsequently fixed with 4% PFA followed by a co-staining with DAPI and Nile red. The fluorescence signal was detected using a PheraStar plate reader and the bioenergetics measurements were corrected for cell number and differentiation, as evaluated by DAPI and Nile red signal respectively.

2.4 Statistics

Data analyses were performed using GraphPad Prism (version 6 and 8; GraphPad Software, San Diego, CA, USA). Normally distributed data were analyzed by t-test or one-, two- or three-way analysis of variance (ANOVA) with Bonferroni or Tukey (where applicable and when appropriate) post-hoc multiple comparison analysis to determine statistically significant differences. Statistically significant outliers were assessed using the maximum normed residual (Grubb's) test. No power calculation or similar was used to predetermine the necessary sample size for a specific significance for *in vivo* pharmacology studies. As previously suggested, mean energy expenditure was assessed using the analysis of covariance (ANCOVA) with body weight as covariate (Tschöp et al., 2011). P-values ≤ 0.05 were considered statistically significant. All results are presented as mean $\pm$ standard error of the mean (s.e.m.).

3 Publications and Manuscripts

Chapter 1 – Peptide-based hormone polypharmacology to treat obesity and type 2 diabetes in diet-induced obese female and male mice

"Monomeric GLP-1/GIP/glucagon triagonism corrects obesity, hepatosteatosis, and dyslipidemia in female mice"
Sigrid Jall, Stephan Sachs, Christoffer Clemmensen, Brian Finan, Frauke Neff, Richard D. DiMarchi, Matthias H. Tschöp, Timo D. Müller[#], Susanna M. Hofmann[#]
[#]*Co-corresponding authors*

Contribution: S.J. performed the experiments, evaluated the data, and drafted the manuscript.

Chapter 2 – Small molecule-based polypharmacology to treat obesity and type 2 diabetes in diet-induced obese mice

"Coordinated targeting of cold and nicotinic receptors synergistically improves obesity and type 2 diabetes"
Christoffer Clemmensen[*], Sigrid Jall[*], Maximilian Kleinert, Carmelo Quarta, Tim Gruber, Josefine Reber, Stephan Sachs, Katrin Fischer, Annette Feuchtinger, Angelos Karlas, Stephanie E. Simonds, Gerald Grandl, Daniela Loher, Eva Sanchez-Quant, Susanne Keipert, Martin Jastroch, Susanna M. Hofmann, Emmani B.M. Nascimento, Patrick Schrauwen, Vasilis Ntziachristos, Michael A. Cowley, Brian Finan[#], Timo D. Müller[#] and Matthias H. Tschöp[#]
[*]*Both authors contributed equally*, [#]*Co-corresponding authors*

Contribution: (…) S.J. (…) coconceptualized the project, designed and performed the experiments, analyzed and interpreted data, and co-wrote the manuscript

Chapter 3 – Role of downstream signaling molecule in body weight regulation, glucose metabolism, and cold receptor activation

"Pirt deficiency has subtle female-specific effects on energy and glucose metabolism in mice"
Sigrid Jall, Brian Finan, Katrin Fischer, Gustav Collden, Xinzhong Dong, Matthias H. Tschöp, Timo D. Müller[#], Christoffer Clemmensen[#]
[#]*Co-corresponding authors*

Manuscript in revision

Contribution: S.J. designed and performed the experiments, analyzed and interpreted data, and drafted the manuscript.

Chapter 4 – Mechanistic evaluation of opposing acute and chronic effects of nicotine receptor activation on blood glucose

"Pharmacological targeting of α3β4 nicotinic receptors improves peripheral insulin sensitivity in diet-induced obese mice"

Sigrid Jall, Meri De Angelis, Annemarie M. Lundsgaard, Andreas M. Fritzen, Aaron Novikoff, Erik A. Richter, Bente Kiens, Karl-Werner Schramm, Matthias H. Tschöp, Christoffer Clemmensen[#], Timo D. Müller[#], Maximilian Kleinert[#]

[#]*Co-corresponding authors*

Manuscript for submission

Contribution: S.J. designed and performed the experiments, analyzed and interpreted data, and wrote the manuscript.

_____

Dr. Timo Müller (Mentor and direct supervisor)
Acting director of Institute for Diabetes and Obesity
Helmholtz Zentrum München

Chapter 1 – *Peptide-based hormone polypharmacology to treat obesity and type 2 diabetes in diet-induced obese female and male mice*
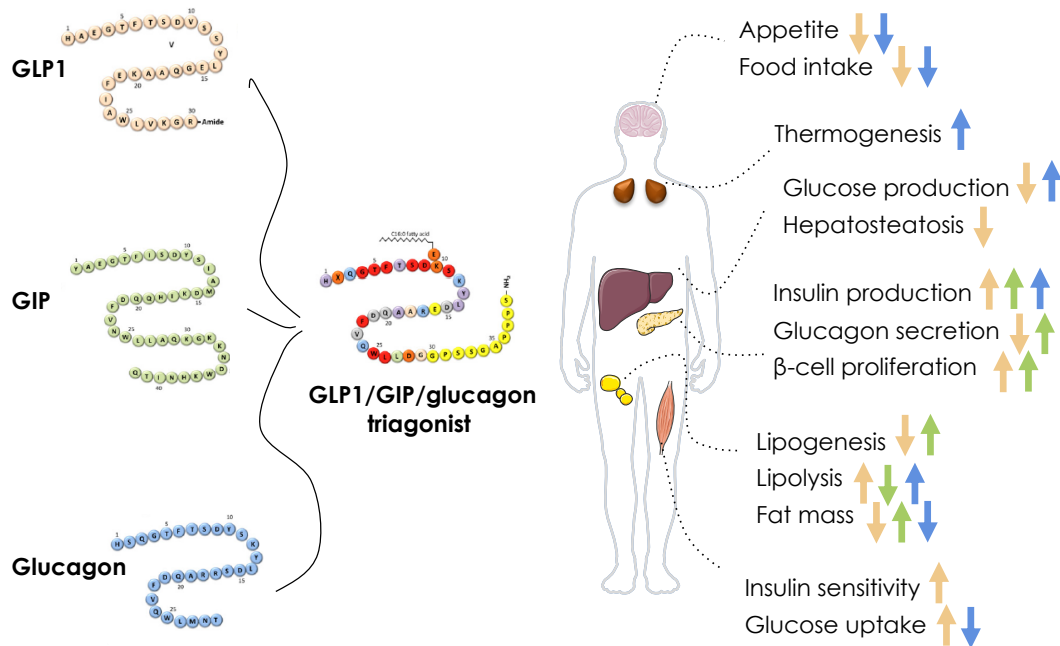
Figure ... **GLP-1, GIP, and glucagon on metabolism** of GLP-1 (orange), GIP (green), and/or glucagon (blue) on the brain, BAT, liver, pancreas, adipose tissue, and muscle. Combination of single hormones to the monomeric GLP-1/GIP/glucagon triagonist as suggested by Finan et al., 2015. Sequence homology between the three hormones is indicated in red in the illustrated triagonist. The figure was modified from Müller et al., 2018 and created using Sevier medical art.

Brief Communication

MOLECULAR METABOLISM

Monomeric GLP-1/GIP/glucagon triagonism corrects obesity, hepatosteatosis, and dyslipidemia in female mice

CrossMark

Sigrid Jall [1,2], Stephan Sachs [1,6], Christoffer Clemmensen [1,2,3], Brian Finan [1,2,3], Frauke Neff [7,8], Richard D. DiMarchi [4], Matthias H. Tschöp [1,2,3], Timo D. Müller [1,2,3,*], Susanna M. Hofmann [3,5,6,**]

ABSTRACT

Objective: Obesity is a major health threat that affects men and women equally. Despite this fact, weight-loss potential of pharmacotherapies is typically first evaluated in male mouse models of diet-induced obesity (DIO). To address this disparity we herein determined whether a monomeric peptide with agonism at the receptors for glucagon-like peptide 1 (GLP-1), glucose-dependent insulinotropic polypeptide (GIP), and glucagon is equally efficient in correcting DIO, dyslipidemia, and glucose metabolism in DIO female mice as it has been previously established for DIO male mice.

Methods: Female C57BL/6J mice and a cohort of fatmass-matched C57BL/6J male mice were treated for 27 days via subcutaneous injections with either the GLP-1/GIP/glucagon triagonist or PBS. A second cohort of C57BL/6J male mice was included to match the females in the duration of the high-fat, high-sugar diet (HFD) exposure.

Results: Our results show that GLP-1/GIP/glucagon triple agonism inhibits food intake and decreases body weight and body fat mass with comparable potency in male and female mice that have been matched for body fat mass. Treatment improved dyslipidemia in both sexes and reversed diet-induced steatohepatitis to a larger extent in female mice compared to male mice.

Conclusions: We herein show that a recently developed unimolecular peptide triagonist is equally efficient in both sexes, suggesting that this polypharmaceutical strategy might be a relevant alternative to bariatric surgery for the treatment of obesity and related metabolic disorders.

© 2017 The Authors. Published by Elsevier GmbH. This is an open access article under the CC BY-NC-ND license (http://creativecommons.org/licenses/by-nc-nd/4.0/).

Keywords Obesity; Sex differences; Diabetes; Glucose homeostasis; Dyslipidemia; Pharmacotherapy

1. INTRODUCTION

Obesity and its metabolic comorbidities like type 2 diabetes impose major threats to global public health and socioeconomic prosperity [1,2]. Lifestyle modification as a first intervention proves mostly ineffective to fight excess adiposity [3,4]. The acceptance for therapeutic or surgical intervention is considerably high, albeit constrained by substantial side effects [5]. Long-term studies clearly suggest bariatric surgery as the most effective, yet most cost-intensive therapy for sustained body weight normalization [6,7]. Approximately 80% of patients undergoing bariatric surgery are women, although no differences in eligibility criteria between sexes exist [8,9]. In sharp contrast to this, preclinical obesity studies largely neglect female rodents, because of a relative resistance to diet-induced obesity and glucose intolerance that is typically observed in most conventional strains [10,11]. A further concern is that sex hormones and fluctuations in the estrous cycle can have an impact on key metabolic endpoints and can increase the natural variance of drug effects, resulting in the necessity for larger group sizes to detect metabolic benefits [12,13]. Recent evidence shows that some pharmacological treatment strategies have differing effects in women and men, as well as higher rates of adverse drug reactions in women [14,15]. This signifies that detailed pre-clinical investigations of differences between the sexes are warranted to accurately assess the therapeutic utility of drug candidates. In line with this notion, an initiative of the U.S. National Institutes of Health (NIH) recently

suggested to expand preclinical studies to also include female rodents [16].

Whereas most previous weight-loss pharmacotherapies are hampered by limited efficacy or unacceptable adverse effects, there is hope resting on recent advances in the development of single molecules which promote their biological action through simultaneous agonism at multiple key metabolic receptors [17,18]. In this regard, a monomeric peptide with balanced agonism at the receptors for glucagon-like peptide 1 (GLP-1), glucose-dependent insulinotropic polypeptide (GIP), and glucagon has previously been shown to correct diet-induced obesity (DIO), dyslipidemia, and insulin resistance in male mice [19]. The principle underlying this molecule is that the anorectic action of central GLP-1 receptor (GLP-1R) agonism synergizes with the action of glucagon to increase energy expenditure, resulting in a net loss of body weight. The combined glycemic action of GLP-1R and GIP receptor (GIPR) agonism restrains the hyperglycemic effect of glucagon, improves insulin sensitivity, and results in body weight improvements. While the efficacy of this GLP-1/GIP/glucagon triagonist to correct the metabolic syndrome has been shown in male mice [19], its metabolic effects in female mice remain unknown. Accordingly, the aim of this study was to comparatively evaluate the metabolic efficacy of this triple agonist in female and male DIO mice.

2. MATERIALS AND METHODS

2.1. Animals and diet

Due to the fact that progression of obesity differs between both sexes, with male mice gaining body fat more rapidly compared to female mice [20], we determined metabolic effects of the triagonist in age-matched male and female mice with similar body fat mass as well as in female and male mice cohorts exposed for equal periods of time to high fat diet feeding. Eight-week old female and male C57BL/6J mice (Charles River Laboratories, Wilmington, MA) were fed a high-fat, high-sugar diet (HFD) comprising 58% kcal from fat (D12331; Research Diets, New Brunswick, NJ, USA). To match females in body fat mass, another cohort of male C57BL/6J mice was switched from a regular diet to HFD at 30 weeks of age. The mice were maintained at $23 \pm 1\,^{\circ}$C, constant humidity, and on a 12-h light—dark cycle with free access to food and water. At the age of 38 weeks, mice were randomized within the three cohorts and equally distributed according to body composition. All procedures were approved by the Animal Use and Care Committee of Bavaria, Germany in accordance with the Guide for the Care and Use of Laboratory Animals [21].

2.2. GLP-1/GIP/glucagon triple agonist

The synthesis, purification, and characterization of the GLP-1/GIP/ glucagon triagonist was described previously and was used without any further chemical modification or change in formulation [19].

2.3. Evaluation of GLP-1/GIP/glucagon triagonist in females and males *in vivo*

All female and male mice were treated daily via subcutaneous injections (5 μl/g body weight) at the indicated doses. Vehicle mice received an equivalent volume of PBS. Whole-body composition was analyzed using nuclear magnetic resonance technology (EchoMRI, Houston, TX, USA). In accordance with previous reports, glucose tolerance was analyzed in 6-h fasted mice that received an intraperitoneal injection of 1.5 g glucose per kg body weight [22]. For the tolerance test, glucose was measured in blood samples from the tail veins at the indicated time points using a handheld glucometer (Abbott GmbH & Co. KG, Wiesbaden, Germany).

2.4. Biochemical analysis

For tissue analysis, mice were injected with the respective treatment dose of the triagonist or vehicle and immediately fasted for 4 h prior to sample collection. Plasma levels of insulin (ALPCO Diagnostics, Salem, NH, USA), cholesterol (Thermo Fisher Scientific, Waltham, MA, USA), free fatty acids, triglycerides (Wako Chemicals, Neuss, Germany), leptin (ALPCO Diagnostics), fibroblast growth factor 21 (FGF21) (Merck Millipore, Darmstadt, Germany), L-alanine:2-oxoglutarate aminotransferase (ALT), and aspartate aminotransferase (AST) (Thermo Fisher Scientific) were measured with the respective kits according to the manufacturers' instructions. The homeostatic model assessment of insulin resistance (HOMA-IR) was calculated using the formula: HOMA-IR = [fasting insulin (mU/l) * fasting glucose (mg/dl)/405] [23]. For lipoprotein separation, samples from the different treatment groups were pooled and analyzed in a fast-performance liquid chromatography gel filtration on two Superose 6 columns connected in series [24]. For evaluation of steatosis, formalin fixed liver samples were embedded in paraffin. Tissue was cut in 4 μm sections and stained with hematoxylin and eosin. Morphological features were recorded and summarized in an activity score that is recommended for diagnosis of steatohepatitis in non-alcoholic fatty liver disease (NAFLD) in humans [25]. The NAFLD activity score (NAS) is defined as the unweighted sum of the three individual scores for steatosis, lobular inflammation, and ballooning degeneration. Steatosis is graded by the presence of fat vacuoles in liver cells according to the percentage of affected tissue (0: <5%; 1: 5—33%; 2: 33—66%; 3: >66%). Lobular inflammation is scored by overall assessment of inflammatory foci per 200× field (0: no foci; 1: <2 foci; 2: 2—4 foci; 3: >4 foci). The individual score for ballooning degeneration ranges from 0 (none), 1 (few cells) to 2 (many cells). Thus, NAS scores range from 0 to 8, with scores ≤2 considered as non-steatohepatitis, scores from 3 to 4 considered as possible/borderline steatohepatitis, scores ≥5 are diagnostic for definite steatohepatitis.

2.5. Statistics

Differences between treatment groups were assessed by two-way ANOVA followed by Tukey's *post hoc* analysis as appropriate or an unpaired two-tailed Student's *t*-test. All results are presented as mean $\pm$ s.e.m. $P < 0.05$ was considered statistically significant.

3. RESULTS

3.1. Triagonist treatment normalizes body weight with equal efficiency in DIO female and male mice matched for fat mass

Because of the well-known delay in diet-induced body weight gain in female mice, and in order to achieve a single cohort of mice matched for age and body composition, we delayed the introduction of HFD to male mice relative to female mice in this single cohort study. To achieve a comparable body fat mass of 16.05 ± 0.79 g and 15.10 ± 0.87 g ($p > 0.05$) in females and males respectively, the duration of HFD exposure before treatment initiation was 30 weeks for females and 8 weeks for males. Female and male DIO mice (age 38 weeks) were randomized by body fat mass and injected daily for 27 days with either vehicle or the triagonist at doses of 5 or 10 nmol/kg. Treatment with the triagonist resulted in a dose-dependent decrease in body weight with identical relative weight loss in both sexes (Figure 1A). The triagonist-induced weight loss was accompanied by a dose-dependent decrease in food intake (Figure 1B) and body fat mass (Figure 1C) with negligible inter-sexual variation at both doses tested. The weight loss induced by the triagonist slightly decreased lean tissue mass in male mice with no effect in females (Figure 1D). In line with the marked reduction in body weight and body fat mass, plasma levels of

Brief Communication

Legend:
- ● / ■ Female Vehicle   ● / ■ Female Triagonist 5 nmol/kg   ○ / ■ Female Triagonist 10 nmol/kg
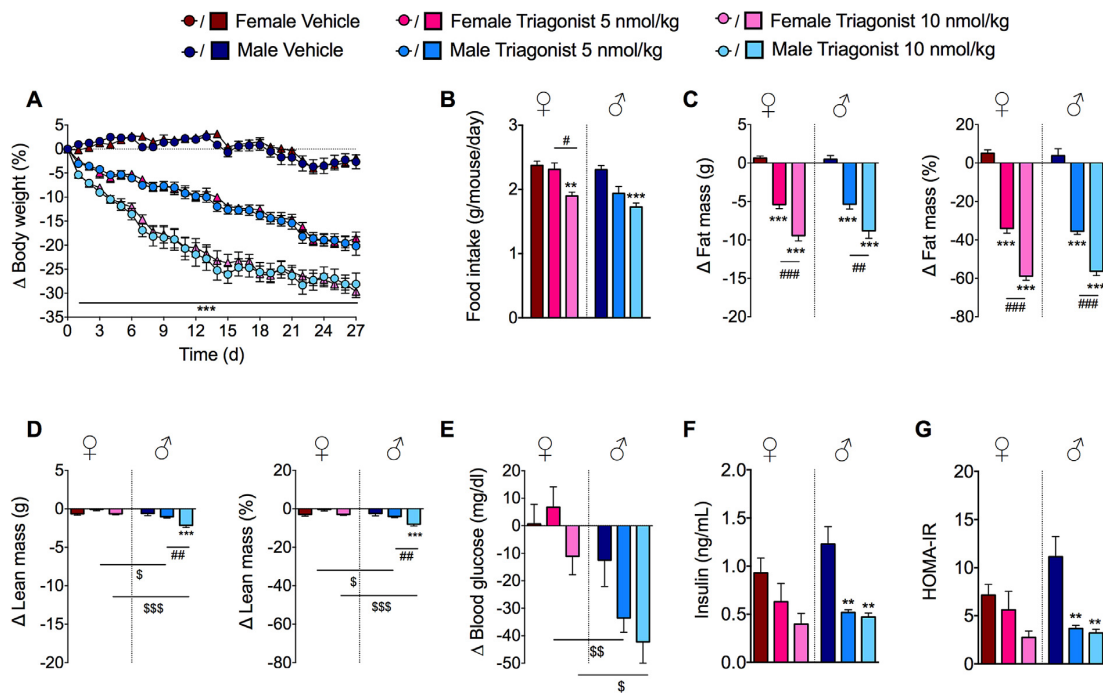- ● / ■ Male Vehicle   ● / ■ Male Triagonist 5 nmol/kg   ○ / ■ Male Triagonist 10 nmol/kg

Figure 1: Equal efficiency of the monomeric triagonist to normalize body weight in female and fat mass-matched male mice (A–G). Effects on body weight change (**A**), daily food intake (**B**), fat mass change in females and in males in gram and percent (**C**), and lean mass change in females and males in gram and percent (d0 - d20) (**D**). Effects of triagonist treatment on fasted blood glucose change (d0 - d22) in female and male mice (**E**), plasma insulin levels (d22) (**F**), HOMA-IR (d22) (**G**) of fat mass-matched female and male mice (age 9 months; ♀ $n = 6{-}10$; ♂ $n = 6{-}8$ per group) treated daily with vehicle and the GLP-1/GIP/glucagon triagonist at 5 nmol/kg or 10 nmol/kg. Data represent mean ± s.e.m. *$P < 0.05$, **$P < 0.01$, ***$P < 0.001$, determined by two-way ANOVA comparing vehicle with compound injections in both sexes. #$P < 0.05$, ##$P < 0.01$, ###$P < 0.001$ determined by two-way ANOVA comparing 5 nmol/kg and 10 nmol/kg doses of the triagonist in both sexes. $$P < 0.05$, $$$P < 0.01$, $$$$P < 0.001$ determined by two-way ANOVA comparing both sexes. ANOVA was followed by Tukey *post hoc* multiple comparison analysis to determine statistical significance.

leptin were dose-dependently decreased in both sexes (Suppl. Table 1). In female mice, but not male mice, we observed an increase in plasma levels of free fatty acids ($p < 0.001$) and FGF21 ($p < 0.05$) following treatment with 10 nmol/kg and 5 nmol/kg of the triagonist, while levels of triglycerides were unchanged (Suppl. Table 1).

3.2. Triagonist treatment does not further enhance normal glucose tolerance in DIO female mice in contrast to male mice matched for body fat mass

In line with previous findings (19), we observed a dose-dependent improvement in glucose metabolism, in particular in male mice, reflected by lower fasting levels of blood glucose (Figure 1E), decreased levels of fasting insulin (Figure 1F), an improved glucose tolerance (Suppl. Fig. 1A,C), and insulin sensitivity, as indicated by the HOMA-IR (Figure 1G). Triagonist treatment did not further enhance an already normal glucose tolerance in female mice (Suppl. Fig. 1B,C). Although female mice are known to be largely protected from the development of diet-induced glucose intolerance and insulin resistance [10,26], we still observed a mild improvement of diet-induced hyperinsulinemia in DIO females (Figure 1F,G).

3.3. Triagonist treatment improves diet-induced hypercholesterolemia in both sexes with a pronounced effect on steatohepatitis in female mice

As previously reported in obese male mice [19], treatment with the triagonist potently improves diet-induced dyslipidemia and NAFLD.

Thus, it was of great interest to investigate potential sex differences in changes of NAFLD and hypercholesterolemia following triagonist treatment. In females, plasma cholesterol levels were only significantly decreased in high-dose triagonist treated mice ($p < 0.05$), whereas in males, both doses significantly reduced plasma cholesterol ($p < 0.001$) (Figure 2A). This decrease in plasma cholesterol was attributed to a substantial reduction in LDL in the high-dose treated mice and a slight reduction in HDL (Figure 2B,C) in both sexes.

Histological analysis of the liver showed that 88.9% of the vehicle treated females and 62.5% of the vehicle treated males were diagnosed with a definite steatohepatitis (Figure 2D). Treatment with the triagonist dose-dependently improved steatohepatitis. The majority of mice that have been treated with 10 nmol/kg of the triagonist showed either a complete resolution of steatohepatitis (females) or only a borderline steatohepatitis (males) at the end of the study (Figure 2D–F). We observed a pronounced effect on lowering hepatic lipid content and hepatocellular vacuolation in females that have been treated with the higher dose of the triagonist (Figure 2D,E). Although hepatic lipid content was diminished also in males treated with the same dose of the triagonist, they displayed a greater variability in reactive changes like hepatocyte ballooning, polyploidy (red dotted arrow, Figure 2F), and sustained inflammatory process (black arrow, Figure 2F), resulting in mild periportal fibrosis (black dotted arrow, Figure 2F). Moreover, treatment with the highest dose of the triagonist lowered plasma levels of ALT to a larger extent in female mice than in males (Suppl. Table 1). Levels of AST in the plasma of
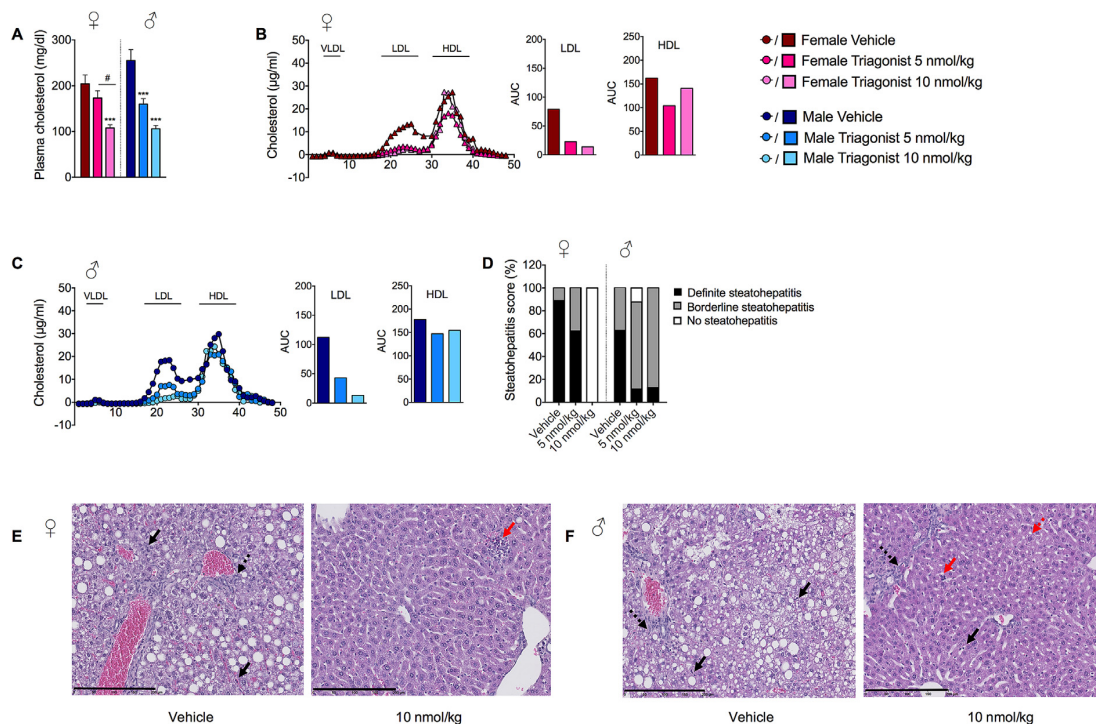
MOLECULAR
METABOLISM

Figure 2: GLP-1/GIP/glucagon triple agonism reverses dyslipidemia and NAFLD in female and fat mass-matched male mice (A-F). Plasma cholesterol (d22) (**A**), plasma lipoprotein fractions in females (**B**) and males (d27) (**C**). Hepatic steatosis score of liver samples (**D**), effects on hepatocellular vacuolation after 27 days of treatment in female (**E**) and male mice (**F**) (age 9 months; ♀ $n = 7-10$; ♂ $n = 7-8$ per group) treated daily with vehicle and the GLP-1/GIP/glucagon triagonist at 5 nmol/kg or 10 nmol/kg. Scale bars in **E** and **F**, 200 μm. Beginning fibrosis periportal (black, dotted arrow), inflammatory intraparenchymal cells (black arrow), microgranuloma (red arrow), focal hepatocyte ballooning and polyploidy (red, dotted arrow). Data represent mean ± s.e.m. *$P < 0.05$, **$P < 0.01$, ***$P < 0.001$, determined by two-way ANOVA comparing vehicle with compound injections in both sexes. #$P < 0.05$ determined by two-way ANOVA comparing 5 nmol/kg and 10 nmol/kg doses of the triagonist in both sexes. ANOVA was followed by Tukey *post hoc* multiple comparison analysis to determine statistical significance.

female and male mice remained unaltered by the treatment with the triagonist (Suppl. Table 1).

3.4. Triagonist treatment normalizes body weight without inducing excessive fat mass loss in male and female mice matched for the duration of HFD exposure

To evaluate whether the duration of HFD exposure affects the efficacy of the triagonist to improve metabolic disease, we also compared female mice to a cohort of age-matched male mice, which were kept on a HFD for the same duration as the female mice (30 weeks). Body weight and body fat mass substantially differed between these cohorts with female mice weighing 39.63 ± 0.92 g and having 16.05 ± 0.79 g body fat mass and male mice weighing 54.20 ± 0.59 g and having 22.44 ± 0.53 g body fat. Relative weight-loss induced by 5 nmol/kg of the triagonist was remarkably similar between both sexes (♀ −18.55± 1.28% and ♂ −25.33± 1.67% relative to baseline, Figure 3A). When treated with 10 nmol/kg of the triagonist, male mice had significantly greater relative weight-loss compared to female mice with females losing 29.64± 1.29% compared to baseline and males 42.82± 1.56% (Figure 3A). The enhanced relative weight loss in males was accompanied by a greater reduction in food intake compared to vehicle treated controls (Figure 3B) and was reflected by a greater absolute and relative loss of fat and lean mass (Figure 3C,D). As shown in Figure 3A, the slopes of body weight loss curves flattened

in both, male and female mice after 15 days of treatment with 10 nmol/kg indicating that normal healthy body composition was achieved and no excessive fat mass loss was observed. As stated earlier, due to the fact that female mice are protected against diet-induced insulin resistance [10], improvement in glucose metabolism relative to vehicle controls was evident only in male mice (Figure 3E,F).

4. DISCUSSION

Our data show that chronic treatment of DIO mice with the GLP-1/GIP/glucagon triagonist potently improves metabolic disease in both sexes with comparable efficiency in female and male mice when pre-treatment body composition is considered. Side by side comparisons between sexes, to determine the efficacy of a pharmacological compound to improve DIO in mouse models, are hampered by the fact that progression of obesity differs between females and males [20]. Herein, we thus opted first for a comparison at a time point when fat mass was similar between male and female mice. In our case, the duration of HFD exposure to achieve similar fat mass in both sexes was 8 weeks in males and 30 weeks in females. With this experimental design we were not able to determine whether the period of HFD feeding itself may alter pharmacological effects of the triagonist to improve metabolic disease. Thus, we included a group of DIO male mice that were fed a HFD for the same period of time (30 weeks) as the DIO female mice. Treatment with
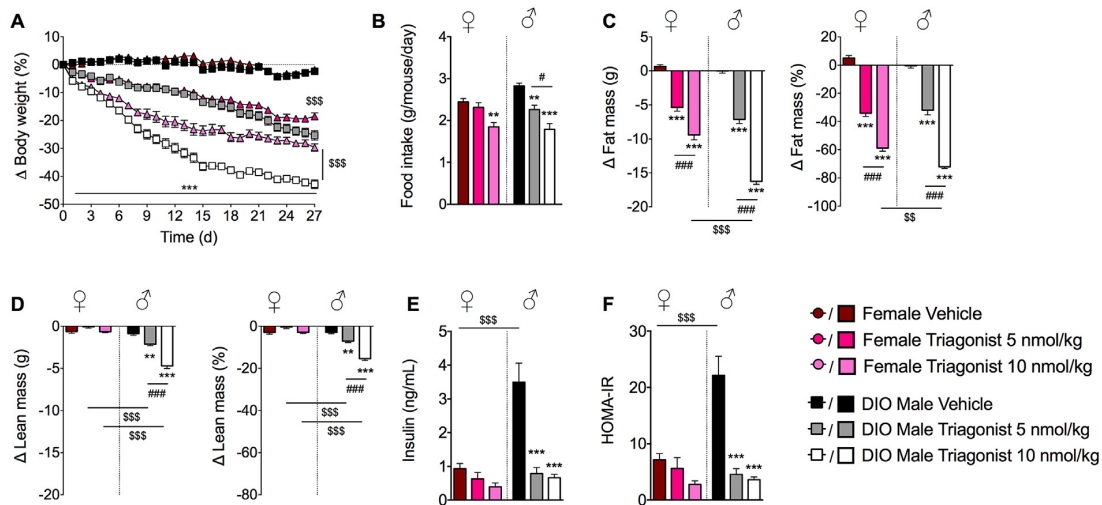
443

Brief Communication

Figure 3: Efficiency of the monomeric triagonist to normalize body weight and reverse hyperinsulinemia in HFD-matched DIO female and male mice (A-F). Effects on body weight change (**A**), average daily food intake (**B**), fat mass change (**C**), and lean mass change in HFD-matched DIO male compared to female mice (d0 - d20) (**D**), plasma insulin levels (d22) (**E**), and HOMA-IR (d22) (**F**) of male DIO mice compared to female mice (age 9 months; ♀ $n = 6-10$; ♂ $n = 6-8$ per group) treated daily with vehicle and the GLP-1/GIP/glucagon triagonist at 5 nmol/kg or 10 nmol/kg. Data represent mean $\pm$ s.e.m. **$P < 0.01$, ***$P < 0.001$, determined by two-way ANOVA comparing vehicle with compound injections in both sexes. #$P < 0.05$, ###$P < 0.001$ determined by two-way ANOVA comparing 5 nmol/kg and 10 nmol/kg doses of the triagonist in both sexes. $$P < 0.01$, $$$P < 0.001$ determined by two-way ANOVA comparing both sexes. ANOVA was followed by Tukey *post hoc* multiple comparison analysis to determine statistical significance.

10 nmol/kg of the triagonist normalized body weight in both sexes with a higher weight-lowering potency in the DIO male group due to the fact that this group had markedly more fat mass at study start than DIO female mice. DIO male mice lost significantly more body fat than male mice that matched females with respect to body fat, although food intake for both male cohorts did not differ. This strongly suggests a prominent role for the GLP-1/GIP/glucagon triagonist in directly targeting the fat mass in mice. Importantly, throughout our study, we did not observe excessive body weight or fat mass loss in the triagonist treated mice suggesting that triagonist treatment normalizes fat mass up to healthy conditions. These results imply that the triagonist may be a safe drug to use, because even at high dosages it does not lead to excessive body weight and fat mass loss.

Similarly to previous studies [19], triagonist treatment potently improved glycemic control in male DIO mice. Due to the evidence in literature and in this study showing that DIO female mice of the C57BL/6 strain do not become as hyperglycemic as male DIO mice and become only moderately hyperinsulinemic [10,26], triagonist treatment was not able to further improve glucose tolerance in female DIO mice. Female mice did develop a mild hyperinsulinemia under HFD feeding, which the triagonist treatment was able to reduce along with improving HOMA-IR. Based on the fact that one prominent and very early sign of metabolic disease in men and women is fasting hyperinsulinemia [27], we propose that the observed insulin lowering effect of the triagonist in both sexes presents a promising novel therapeutic option for men as well as for women even before onset of type 2 diabetes.

It has been previously reported that female C57BL/6J mice fed a diet rich in fructose are more susceptible to develop a NAFLD compared to male mice [28]. We here extend this finding to DIO female mice, as nearly 100% of vehicle treated female mice were diagnosed with a full-blown steatohepatitis after 30 weeks of HFD, while fat mass-matched male mice were not as severely affected. The male cohort

was on a HFD for 8 weeks to match females in fat mass content, which could also have an impact on the observed difference. Conversely, treatment with the GLP-1/GIP/glucagon triagonist for 27 days completely resolved NAFLD-associated complications in female mice. Interestingly, both sexes of the high-dose treated mice displayed a nearly total diminishment of hepatic lipid content, but, in males, sustained inflammatory processes resulted in mild periportal fibrosis. Our results are in line with previous findings by Ganz M. et al. reporting that obese female mice develop steatosis without inflammation in contrast to steatohepatitis found in obese male mice [29]. Based on a recent study showing that astaxanthin reversed advanced non-alcoholic steatohepatitis (NASH) in male mice after 12 weeks of treatment [30] we hypothesize that a comparable amelioration of NAFLD hallmarks may occur in males after an elongation of triagonist treatment duration. When we measured ALT and AST in plasma of triagonist treated male and female mice, we detected a significant reduction in ALT levels in female mice and a clear trend of reduced ALT levels in male mice. Plasma levels of AST were not significantly altered in neither sex. These findings are in line with the results published recently by Finan B. et al. [19] demonstrating a significant reduction in ALT but not AST in DIO obese male mice upon chronic triagonist treatment. Compared to AST, ALT is especially expressed in liver and thus the reduction of ALT plasma levels may reflect a reduction in diet-induced liver cell injury by the triagonist treatment [31]. Our histological findings of a significant improvement of NAFLD in triagonist treated female and male mice, together with the observed reduction of plasma ALT levels in both sexes, underscore the profound effect of the triagonist to resolve the HFD induced liver damage

5. CONCLUSION

For translational applicability, the inclusion of female mice in pharmacological research is indispensable. To this end, we here

MOLECULAR
METABOLISM

demonstrate equal efficiency of the GLP-1/GIP/glucagon triagonist in reversing DIO and liver steatosis in female and male rodent models of adiposity. Reports on body weight loss 4 weeks after bariatric surgery in comparably obese male and female mice show reductions of approximately 30% of the starting body weight mirroring the loss in body weight we observed in the high-dose triagonist treated mice [32,33]. In conclusion, our findings indicate that triagonist treatment may reduce body weight as efficiently as bariatric surgery highlighting the potential of the monomeric triagonist as an effective treatment option for severe obesity also in women.

AUTHOR CONTRIBUTIONS

S.J. performed the experiments, evaluated the data, and drafted the manuscript. S.S. performed the experiments, evaluated the data, and helped composing the manuscript. C.C. made substantial contributions in the study design, helped with the in vivo experiments, evaluated the data, and helped draft the manuscript. B.F. and R.D.D. designed, synthesized, and characterized compounds, made substantial contributions in the study design and interpretation of data, and helped edit the manuscript. F.N. interpreted histopathological hepatic data. M.H.T. made substantial contributions in the study design and interpretation of data and helped edit the manuscript. T.D.M. oversaw the in vivo experiments, evaluated the data, helped draft the manuscript, made substantial contributions in the study design and interpretation of data, and helped edit the manuscript. S.M.H. headed the lipoprotein profile measurements and analysis, oversaw S.S. in this project and mentored S.J. for the generation of this manuscript. T.D.M. and S.M.H. are the guarantors of this work and, as such, had full access to all the data in the study and take responsibility for the integrity of the data and the accuracy of the data analysis.

DUALITY OF INTEREST

No potential conflicts of interest relevant to this article were reported.

APPENDIX A. SUPPLEMENTARY DATA

Supplementary data related to this article can be found at http://dx.doi.org/10.1016/j.molmet.2017.02.002.

REFERENCES

[1] Ng, M., Fleming, T., Robinson, M., Thomson, B., Graetz, N., Margono, C., et al., 2014. Global, regional, and national prevalence of overweight and obesity in children and adults during 1980-2013: a systematic analysis for the Global Burden of Disease Study 2013. Lancet 384:766—781.

[2] Dee, A., Kearns, K., O'Neill, C., Sharp, L., Staines, A., O'Dwyer, V., et al., 2014. The direct and indirect costs of both overweight and obesity: a systematic review. BMC Research Notes 7:242.

[3] Tuomilehto, J., Lindstrom, J., Eriksson, J.G., Valle, T.T., Hamalainen, H., Ilanne-Parikka, P., et al., 2001. Prevention of type 2 diabetes mellitus by changes in lifestyle among subjects with impaired glucose tolerance. The New England Journal of Medicine 344:1343—1350.

[4] Wadden, T.A., Berkowitz, R.I., Womble, L.G., Sarwer, D.B., Phelan, S., Cato, R.K., et al., 2005. Randomized trial of lifestyle modification and pharmacotherapy for obesity. The New England Journal of Medicine 353:2111—2120.

[5] Krentz, A.J., Fujioka, K., Hompesch, M., 2016. Evolution of pharmacological obesity treatments: focus on adverse side-effect profiles. Diabetes, Obesity and Metabolism 18:558—570.

[6] Schauer, P.R., Bhatt, D.L., Kirwan, J.P., Wolski, K., Brethauer, S.A., Navaneethan, S.D., et al., 2014. Bariatric surgery versus intensive medical therapy for diabetes—3-year outcomes. The New England Journal of Medicine 370:2002—2013.

[7] Hoerger, T.J., Zhang, P., Segel, J.E., Kahn, H.S., Barker, L.E., Couper, S., 2010. Cost-effectiveness of bariatric surgery for severely obese adults with diabetes. Diabetes Care 33:1933—1939.

[8] Fuchs, H.F., Broderick, R.C., Harnsberger, C.R., Chang, D.C., Sandler, B.J., Jacobsen, G.R., et al., 2015. Benefits of bariatric surgery do not reach obese men. Journal of Laparoendoscopic & Advanced Surgical Techniques Part A 25:196—201.

[9] Nguyen, D.M., El-Serag, H.B., 2010. The epidemiology of obesity. Gastroenterology Clinics of North America 39:1—7.

[10] Pettersson, U.S., Walden, T.B., Carlsson, P.O., Jansson, L., Phillipson, M., 2012. Female mice are protected against high-fat diet induced metabolic syndrome and increase the regulatory T cell population in adipose tissue. PLoS One 7:e46057.

[11] Hong, J., Stubbins, R.E., Smith, R.R., Harvey, A.E., Nunez, N.P., 2009. Differential susceptibility to obesity between male, female and ovariectomized female mice. Nutrition Journal 8:11.

[12] Wizemann, T.M., Pardue, M.L., 2001. Exploring the biological contributions to human health: does sex matter?. Washington (DC): National Academies Press.

[13] Shi, H., Clegg, D.J., 2009. Sex differences in the regulation of body weight. Physiology& Behavior 97:199—204.

[14] Franconi, F., Brunelleschi, S., Steardo, L., Cuomo, V., 2007. Gender differences in drug responses. Pharmacological Research 55:81—95.

[15] Martin, R.M., Biswas, P.N., Freemantle, S.N., Pearce, G.L., Mann, R.D., 1998. Age and sex distribution of suspected adverse drug reactions to newly marketed drugs in general practice in England: analysis of 48 cohort studies. British Journal of Clinical Pharmacology 46:505—511.

[16] Clayton, J.A., Collins, F.S., 2014. Policy: NIH to balance sex in cell and animal studies. Nature 509:282—283.

[17] Tschöp, M.H., DiMarchi, R.D., 2012. Outstanding Scientific Achievement Award Lecture 2011: defeating diabesity: the case for personalized combinatorial therapies. Diabetes 61:1309—1314.

[18] Tschöp, M.H., Finan, B., Clemmensen, C., Gelfanov, V., Perez-Tilve, D., Müller, T.D., et al., 2016. Unimolecular polypharmacy for treatment of diabetes and obesity. Cell Metabolism 24:51—62.
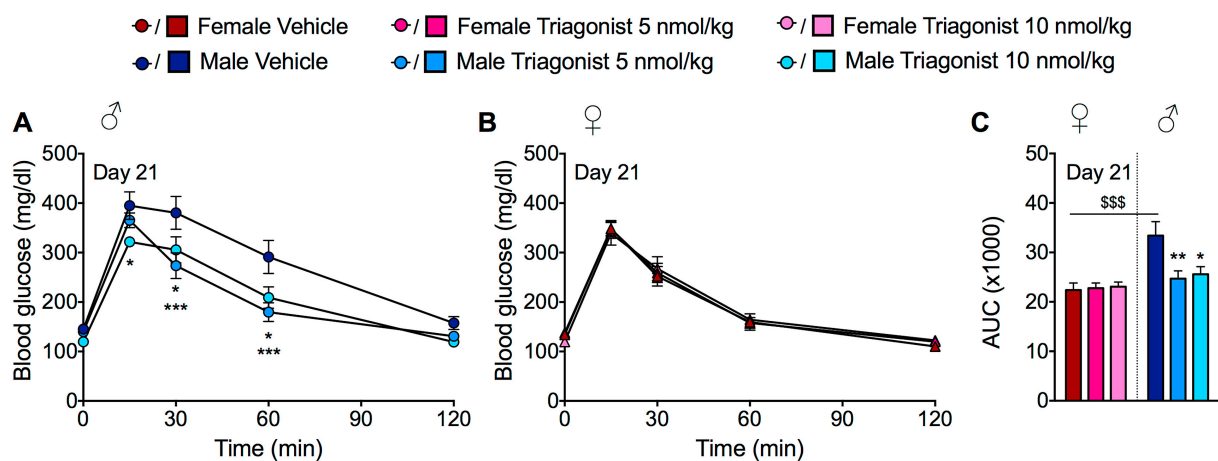
Brief Communication

[19] Finan, B., Yang, B., Ottaway, N., Smiley, D.L., Ma, T., Clemmensen, C., et al., 2015. A rationally designed monomeric peptide triagonist corrects obesity and diabetes in rodents. Nature Medicine 21:27—36.

[20] Yang, Y., Smith Jr., D.L., Keating, K.D., Allison, D.B., Nagy, T.R., 2014. Variations in body weight, food intake and body composition after long-term high-fat diet feeding in C57BL/6J mice. Obesity (Silver Spring) 22:2147—2155.

[21] National Institutes of Health, 2011. National research council (US) committee for the update of the Guide for the Care and use of laboratory Animals. Guide for the Care and use of laboratory Animals. http://dx.doi.org/10.17226/12910. Available from: https://www.ncbi.nlm.nih.gov/books/NBK54050/. Accessed 23 January 2017.

[22] Clemmensen, C., Chabenne, J., Finan, B., Sullivan, L., Fischer, K., Kuchler, D., et al., 2014. GLP-1/glucagon coagonism restores leptin responsiveness in obese mice chronically maintained on an obesogenic diet. Diabetes 63:1422—1427.

[23] Matthews, D.R., Hosker, J.P., Rudenski, A.S., Naylor, B.A., Treacher, D.F., Turner, R.C., 1985. Homeostasis model assessment: insulin resistance and beta-cell function from fasting plasma glucose and insulin concentrations in man. Diabetologia 28:412—419.

[24] Hofmann, S.M., Perez-Tilve, D., Greer, T.M., Coburn, B.A., Grant, E., Basford, J.E., et al., 2008. Defective lipid delivery modulates glucose tolerance and metabolic response to diet in apolipoprotein E-deficient mice. Diabetes 57: 5—12.

[25] Kleiner, D.E., Brunt, E.M., Van Natta, M., Behling, C., Contos, M.J., Cummings, O.W., et al., 2005. Design and validation of a histological scoring system for nonalcoholic fatty liver disease. Hepatology 41:1313—1321.

[26] Morselli, E., Fuente-Martin, E., Finan, B., Kim, M., Frank, A., Garcia-Caceres, C., et al., 2014. Hypothalamic PGC-1alpha protects against high-fat diet exposure by regulating ERalpha. Cell Reports 9:633—645.

[27] Lundgren, H., Bengtsson, C., Blohme, G., Lapidus, L., Waldenstrom, J., 1990. Fasting serum insulin concentration and early insulin response as risk determinants for developing diabetes. Diabetic Medicine 7:407—413.

[28] Spruss, A., Henkel, J., Kanuri, G., Blank, D., Puschel, G.P., Bischoff, S.C., et al., 2012. Female mice are more susceptible to nonalcoholic fatty liver disease: sex-specific regulation of the hepatic AMP-activated protein kinase-plasminogen activator inhibitor 1 cascade, but not the hepatic endotoxin response. Molecular Medicine 18:1346—1355.

[29] Ganz, M., Csak, T., Szabo, G., 2014. High fat diet feeding results in gender specific steatohepatitis and inflammasome activation. World Journal of Gastroenterology 20:8525—8534.

[30] Ni, Y., Nagashimada, M., Zhuge, F., Zhan, L., Nagata, N., Tsutsui, A., et al., 2015. Astaxanthin prevents and reverses diet-induced insulin resistance and steatohepatitis in mice: a comparison with vitamin E. Scientific Reports 5: 17192.

[31] Giannini, E.G., Testa, R., Savarino, V., 2005. Liver enzyme alteration: a guide for clinicians. CMAJ 172:367—379.

[32] Yin, D.P., Gao, Q., Ma, L.L., Yan, W., Williams, P.E., McGuinness, O.P., et al., 2011. Assessment of different bariatric surgeries in the treatment of obesity and insulin resistance in mice. Annals of Surgery 254:73—82.

[33] Frank, A.P., Zechner, J.F., Clegg, D.J., 2016. Gastric bypass surgery but not caloric restriction improves reproductive function in obese mice. Obesity Surgery 26:467—473.

Supplemental Table 1: Effect of GLP-1/GIP/glucagon triple agonism on circulating levels of selected markers in female and fat mass-matched male mice. Concentration of leptin, triglycerides, non-esterified free fatty acids (NEFAs), FGF21, L-alanine:2-oxoglutarate aminotransferase (ALT), and aspartate aminotransferase (AST) in plasma of 6 hours-fasted female and fat mass-matched male mice treated daily with vehicle, 5 nmol/kg or 10 nmol/kg of the triagonist (age 9 months; ♀ n = 5-10; ♂ n = 6-8 per group). Leptin, triglycerides, and NEFAs were measured at study day 22, FGF21, ALT, and AST at study day 27. Data represent mean ± s.e.m. *P < 0.05, **P < 0.01, ***P < 0.001, determined by two-way ANOVA comparing vehicle with compound injections in both sexes. $^{\$}P$ < 0.05 determined by two-way ANOVA comparing both sexes. ANOVA was followed by Tukey *post hoc* multiple comparison analysis to determine statistical significance.

	Females			Males		
Treatment	**Vehicle**	**5 nmol/kg**	**10 nmol/kg**	**Vehicle**	**5 nmol/kg**	**10 nmol/kg**
Leptin (ng/ml)	13.88 ± 1.96	4.75 ± 1.42*	3.76 ± 1.20**	12.78 ± 2.26	7.23 ± 2.03	3.55± 0.53*
Triglycerides (mg/dl)	96.27 ± 4.9	91.57 ± 6.4	105.74 ± 6.8	98.73 ± 4.8	87.09 ± 6.5	85.62 ± 6.6
NEFAs (mM)	1.01 ± 0.09$^{\$}$	1.34 ± 0.14	2.06 ± 0.17***	1.60 ± 0.11	1.42 ± 0.08	1.54 ± 0.18
FGF21 (pg/ml)	238.7 ± 44.4	637.3 ± 167.2*	429.4 ± 66.0	290.5 ± 64.4	427.0 ± 68.4	307.9 ± 45.8
ALT (U/l)	31.61 ± 9.08	12.21 ± 3.92	11.56 ± 3.65*	18.61 ± 4.56	9.50 ± 2.51	5.43 ± 0.99
AST (U/l)	33.92 ± 8.68	22.48 ± 6.00	17.65 ± 4.22	30.53 ± 8.98	35.95 ± 12.76	30.87 ± 6.47

Fig S1. Enhanced triagonist-mediated improvement of glycemic parameters in fat mass-matched male mice (A-C). Fasted blood glucose after an intraperitoneal glucose test in female mice (A) and in fat mass-matched male mice (B) with corresponding area under the curve (AUC) (C) in female and male mice at day 21 (age 9 months; ♀ n = 10; ♂ n = 8 per group) treated daily with vehicle and the GLP-1/GIP/glucagon triagonist at 5 nmol/kg or 10 nmol/kg. Data represent mean ± s.e.m. *P < 0.05, **P < 0.01, ***P < 0.001, determined by two-way ANOVA comparing vehicle with compound injections. $^{\$\$\$}$P < 0.001 determined by two-way ANOVA comparing both sexes. ANOVA was followed by Tukey post hoc multiple comparison analysis to determine statistical significance.

Chapter 2 – *Small molecule-based polypharmacology to treat obesity and type 2 diabetes in diet-induced obese mice*
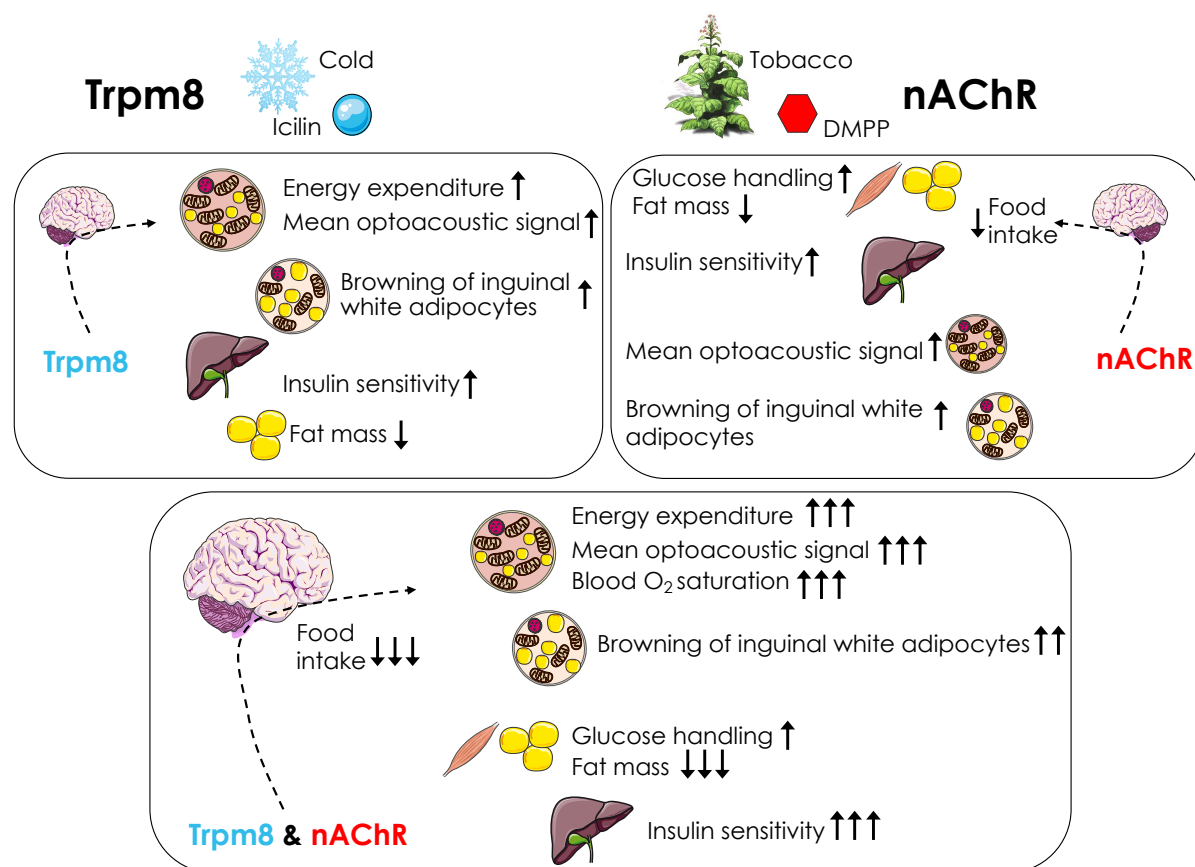
Figure 3. 2: Singular and combined effects of icilin and DMPP on metabolism. Effects of icilin-mediated TRPM8 activation on the BAT, iWAT, liver, and adipose tissue and DMPP-mediated nAChR activation on food intake, adipose tissue, muscle, liver, BAT, and iWAT. Synergistic effect of DMPP and icilin co-administration on metabolism. The figure was created using Sevier medical art and summarizes Clemmensen et al., 2018.
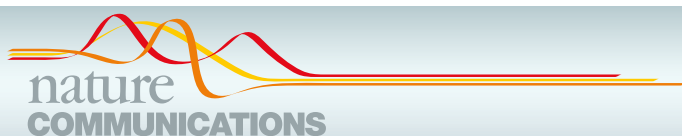
40

ARTICLE

Coordinated targeting of cold and nicotinic receptors synergistically improves obesity and type 2 diabetes

Christoffer Clemmensen ⬤ et al.[#]

Pharmacological stimulation of brown adipose tissue (BAT) thermogenesis to increase energy expenditure is progressively being pursued as a viable anti-obesity strategy. Here, we report that pharmacological activation of the cold receptor transient receptor potential cation channel subfamily M member 8 (TRPM8) with agonist icilin mimics the metabolic benefits of cold exposure. In diet-induced obese (DIO) mice, treatment with icilin enhances energy expenditure, and decreases body weight, without affecting food intake. To further potentiate the thermogenic action profile of icilin and add complementary anorexigenic mechanisms, we set out to identify pharmacological partners next to icilin. To that end, we specifically targeted nicotinic acetylcholine receptor (nAChR) subtype alpha3beta4 (α3β4), which we had recognized as a potential regulator of energy homeostasis and glucose metabolism. Combinatorial targeting of TRPM8 and nAChR α3β4 by icilin and dimethylphenylpiperazinium (DMPP) orchestrates synergistic anorexic and thermogenic pathways to reverse diet-induced obesity, dyslipidemia, and glucose intolerance in DIO mice.

ARTICLE

Successful management of the global obesity epidemic is required to halt the increasing prevalence of cardiometabolic diseases[1]. Pharmacological stimulation of metabolic rate was explored as a weight-lowering strategy in the first half of the 20th century. However, harmful side effects, such as excessive heat production and microvascular disease, following chronic administration of drugs such as 2,4-dinitrophenol (DNP) may have contributed to direct the anti-obesity field towards appetite-suppressants[2]. The now decade-old observation that humans possess recruitable brown adipose tissue (BAT) that generates heat in response to cold stress[3–5] reinvigorated substantial research on BAT thermogenesis and anti-obesity therapeutic strategies aimed to increase energy expenditure.

A family of thermoreceptors, the transient receptor potential (TRP) channels, are expressed in afferent dorsal root ganglion (DRG) sensory neurons, and primarily function to convey information of environmental temperature to the central nervous system (CNS)[6]. The transient receptor potential cation channel subfamily M member 8 (TRPM8) is a proximate regulator of the cold-sensing cascade that culminates in the induction of BAT thermogenesis to defend body temperature in response to environmental cold[7]. TRPM8 can also be activated by chemical ligands such as menthol and the high-potency small molecule icilin[7,8]. Menthol-induced TRPM8 activation increases body temperature[9], BAT uncoupling protein 1 (UCP1) expression, and protects mice from diet-induced obesity[10], underlining the potential of developing TRPM8-based pharmacotherapies to treat obesity.

Because interventions that increase energy expenditure, including cold exposure, frequently elicit counter-regulatory induction of orexigenic feeding circuits[11,12], complementary anorexigenic actions are likely required to chronically reverse metabolic imbalances. Here, we hypothesized that the nicotinic acetylcholine receptor (nAChR) subtype α3β4 would be an ideal pharmacological partner to TRPM8 agonism by capitalizing on the well-described effects of smoking to suppress hunger. Pharmacological stimulation of hypothalamic α3β4 nAChRs suppresses appetite via the hypothalamic-melanocortin system[13]. Additionally, the nAChR α3β4 is the primary ganglionic nAChR that upon pharmacological stimulation depolarizes BAT and increases lipolysis[14–16], and somewhat paradoxically, nAChR activation also acts centrally to lower body temperature[17,18]. Therefore, we hypothesized that pharmacological stimulation of α3β4 will complement the thermogenic virtues of TRPM8 agonism while appropriately counter-balancing systemic hyperthermia and potential counter-regulatory hyperphagia. Thus, we demonstrate that dual nAChR α3β4 and TRPM8 agonism, which in essence biochemically mimics the two environmental stimuli known to improve systemic metabolism—cold exposure and cigarette smoking, evokes a cascade of physiological nodes that harmonize to reverse obesity and type 2 diabetes

We report that a potent TRPM8 agonist, icilin, enhances energy expenditure to lower body weight in diet-induced obese (DIO) mice. We discovered that combining icilin with a α3β4 nAChR agonist dimethylphenylpiperazinium (DMPP) elicits coordinated metabolic actions that synergize to lower body weight, correct glucose intolerance, and reduce hepatic steatosis. Mechanistically, we reveal that central melanocortin signaling as well as sympathetic nervous system-linked thermogenesis are indispensable for the orchestration of the complete metabolic benefits of this novel combination strategy.

Result

Icilin increases energy expenditure and lowers body weight. To test if the TRPM8 agonist icilin mimics the metabolic benefits of

cold exposure, we administered icilin to mice maintained on a high-fat, high sucrose diet (HFD). Chronic treatment with icilin for 14 days dose-dependently lowered body weight (Fig. 1a), reflected in a reduction in body fat (Supplementary Fig. 1a). This effect on body weight and fat mass was due to an increase in energy expenditure (Fig. 1b), while food intake (Fig. 1c) and locomotor activity were unaffected by icilin (Fig. 1d). In TRPM8 null mice, icilin had no effect on oxygen consumption rate (Fig. 1e, f) or weight loss (Supplementary Fig. 3d, f), underscoring that the ability of icilin to lower body weight by increasing energy expenditure requires functional TRPM8. In contrast to previous work[10,19], we did not detect meaningful expression of *Trpm8* in BAT of mice housed at 30 °C or at 5 °C suggesting that the icilin effect on BAT energy expenditure is not explained by direct effects of icilin on adipocytes (Supplementary Fig. 1b). In agreement, icilin did not increase *Ucp1* transcription or oxygen consumption in mouse (Supplementary Fig. 1c–d) or human (Supplementary Fig. 1e–f) primary brown adipocytes, suggesting indirect actions to increase thermogenesis, likely through induction of sympathetic tone.

DMPP improves diet-induced obesity and glucose intolerance. Although the ability of icilin to increase energy expenditure seems to be appropriately uncoupled from compensatory hyperphagia, we hypothesized that additional pharmacology concurrently targeting central satiety circuits would complement TRPM8-based pharmacology to achieve greater weight loss. We discovered that the nicotinic receptor α3β4 agonist DMPP dose-dependently lowered body weight in DIO mice (Fig. 2a). Similar to nicotine (Supplementary Fig. 2a, b), DMPP reduced body weight by suppressing food intake (Fig. 2b). However, in contrast to nicotine (Supplementary Fig. 2c, d), DMPP markedly improved diet-induced glucose intolerance, even at doses with negligible effect on body weight change (Fig. 2c, d).

Icilin and DMPP synergistically lower body weight. Following the results with icilin and DMPP monotherapy on energy expenditure and appetite, respectively, we tested icilin and DMPP in combination as a single formulation. Cotreatment with icilin (5 mg/kg) and DMPP (10 mg/kg) synergistically lowered body weight in DIO mice (Fig. 3a) coinciding with a robust reduction in food intake (Fig. 3b) and increased energy expenditure (Supplementary Fig. 3a). The synergistic weight-lowering effects of DMPP and icilin cotreatment were corroborated by chronic treatment studies (Fig. 5a, Supplementary Fig. 3b). To explore the central hypothalamic actions of the combination therapy, we assessed c-FOS immune reactivity as an indirect measure of neuronal activity. c-FOS staining in the paraventricular nucleus (PVN) was increased in mice treated with the combination of icilin and DMPP, but not in response to either monotherapy (Fig. 3c). The induction of c-FOS in the PVN following the combination therapy was absent in nAChR β4 KO mice (Fig. 3d), suggesting that α3β4 nAChRs are necessary for the anorexigenic effects of the treatment. In support, DIO nAChR β4 KO mice did not lose body weight in response to DMPP and icilin cotreatment (Supplementary Fig. 3h).

The notion that the satiety benefits of the combination treatment specifically implicate the PVN prompted us to investigate the role of the leptin–melanocortin system to the anorexigenic phenotype. We observed a complete loss-of-effect in DIO melanocortin-4 receptor (MC4R) KO mice following treatment with both the monotherapies and the combination of icilin and DMPP (Fig. 3e, f), underlining that the melanocortin pathway is indispensable for the weight-lowering benefits of the cotreatment.
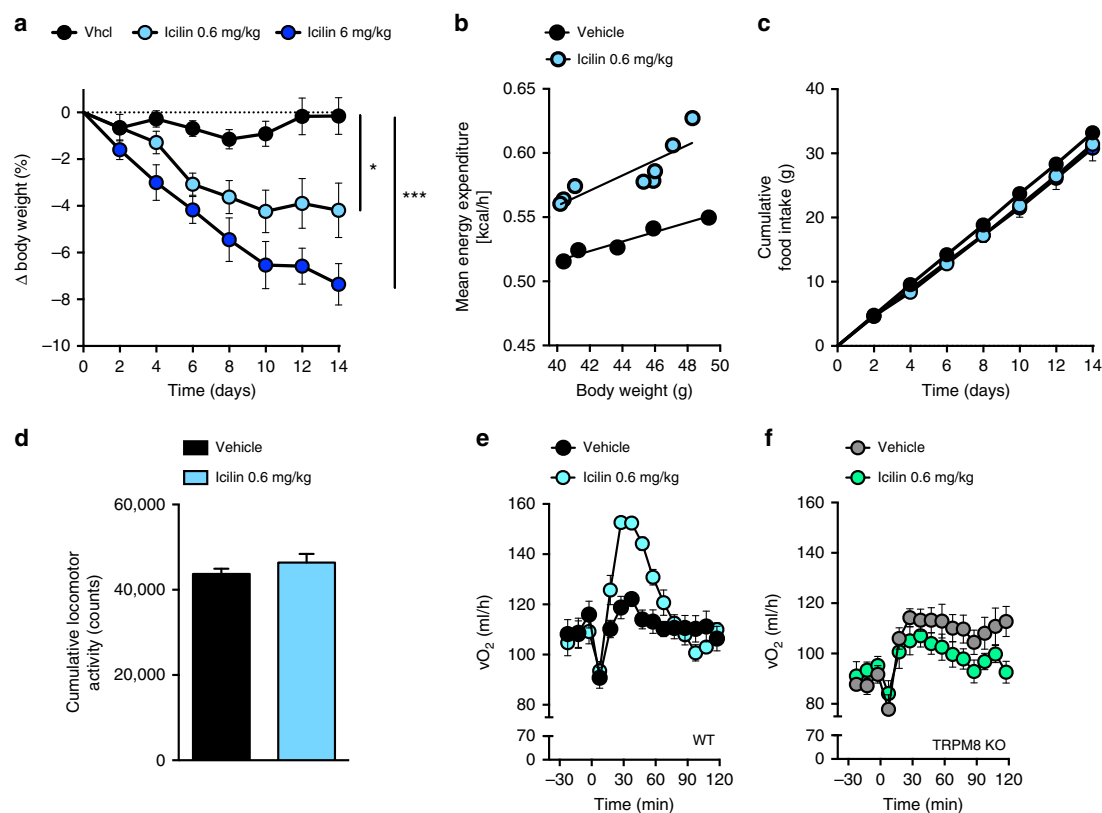
ARTICLE

Fig. 1 TRPM8 agonist icilin increases energy expenditure and lowers body weight in DIO mice. **a** Effects on body weight, **b** energy expenditure, **c** food intake, **d** locomotor activity following daily s.c. injections of vehicle (black, $n = 8$ for **a**, **c**; $n = 5$ for **b**, **d**), icilin 0.6 mg/kg (light blue, $n = 8$), and icilin 6 mg/kg (dark blue, $n = 6$) in DIO male C57Bl6j mice for 14 days. **e**, **f** Oxygen consumption following a single injection of vehicle (black/gray, $n = 8$) or icilin (blue/green, $n = 8$) to DIO male WT mice or DIO TRPM8 KO mice. *$p < 0.05$, ***$p < 0.001$ by two-way ANOVA (**a**, **c**) with Tukey post-hoc test and two-tailed Student's t-test (**d**). All data are presented as mean ± SEM

Icilin and DMPP stimulate thermogenic pathways. To gain insight into the mechanisms responsible for the energy expenditure induction downstream of the MC4R, we tested the ability of DMPP and icilin to reverse obesity in mice lacking β-adrenergic receptors (betaless mice). The weight loss following icilin and DMPP treatment was significantly blunted in the betaless mice (Fig. 4a), while food intake was suppressed (Fig. 4b), indicating the contribution of the adrenergic system to selectively mediate the effects on energy expenditure. Except for a subtle increase in brown fat *Pgc1a* mRNA in response to icilin and the cotreatment (Supplementary Fig. 5a), brown fat and inguinal white adipose tissue gene programs of thermogenesis, mitochondrial transport, creatine metabolism, and proteasomal activity were unaffected in treated betaless mice (Supplementary Fig. 5a–h). To assess the role of UCP1-mediated thermogenesis, we tested the combination of icilin and DMPP in UCP1 KO and WT mice. The body weight-lowering effect was blunted in UCP1 KO mice (Fig. 4c), while as observed in the betaless mice, food intake was still suppressed (Fig. 4d). We also confirmed the necessity of functional TRPM8 for DMPP and icilin-mediated reductions in body fat and weight (Supplementary Fig. 3b–g). Using Multi-Spectral Optoacoustic Tomography (MSOT) imaging of the BAT in vivo[20], we detected an increase in the optoacoustic signal intensity over the BAT region following both icilin and DMPP monotherapy. Coadministration of both molecules resulted in the largest increase (Fig. 4e). Only the combination of icilin and DMPP increased oxygen saturation of the

delivered blood to the BAT (Fig. 4f–g), emphasizing that the combination of icilin and DMPP is superior to the monotherapies in delivering oxygen for metabolic processes in the brown fat. Collectively, these data underscore that thermogenic pathways utilizing SNS-driven activation of β-ARs and UCP1 contribute substantially to the weight-lowering benefits of DMPP and icilin pharmacology.

Synergistic pharmacology is independent of temperature. Because mice housed at thermoneutral conditions may more accurately model drug-induced thermogenesis in humans[21,22], we tested DMPP and icilin cotreatment in DIO mice housed at 30 °C. Analogous to the effect at room temperature, we found that treatment of mice acclimated at 30 °C with the combination of DMPP and icilin synergistically lowered their body weight and fat mass in comparison with the monotherapies (Fig. 5a, c, d). Unlike the effect at room temperature, the weight loss of the mice housed at thermoneutrality was independent of a substantial reduction in food intake (Fig. 5b). DMPP and icilin monotherapies increased BAT multilocularity (Fig. 5e) and UCP1 protein (Fig. 5f, g), but not thermogenic gene programs in BAT (Fig. 5h) or inguinal white adipose tissue (iWAT) (Supplementary Fig. 6d). The combination of DMPP and icilin was superior in increasing BAT multilocularity (Fig. 5e), UCP1 protein levels (Fig. 5f, g), *Ucp1* mRNA, and genes involved in mitochondrial transport (Fig. 5h, i). DMPP monotherapy and its combination with icilin suppressed the expression of *Gamt*, an enzyme involved in creatine
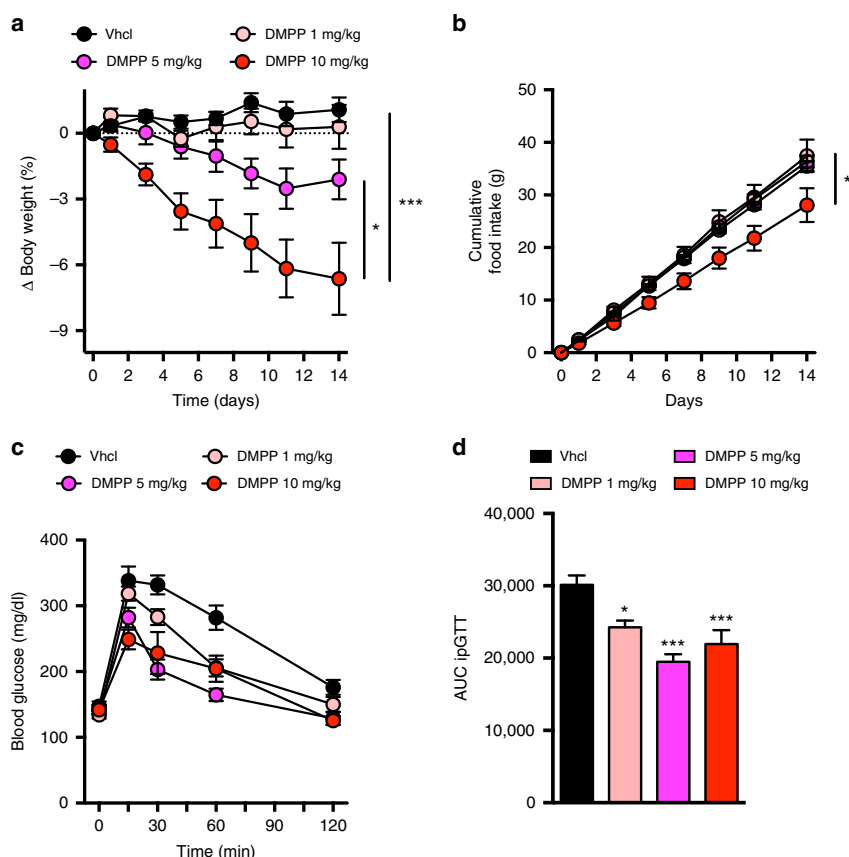
Fig. 2 The nicotinic receptor agonist DMPP lowers body weight and improves glucose tolerance in DIO mice. **a** Effects on body weight, **b** food intake, and **c**, **d** glucose tolerance following daily s.c. injections to DIO male C57Bl6j mice of vehicle (black, $n = 8$ for **a**, **b**; $n = 7$ for **c**, **d**), DMPP 1 mg/kg (light red, $n = 8$), DMPP 5 mg/kg (pink, $n = 7$ for **a**, **b**; $n = 8$ for **c**, **d**), and DMPP 10 mg/kg (dark red, $n = 7$) for 14 days. *$p < 0.05$, ***$p < 0.001$ by two-way ANOVA (**a**, **b**, **c**) and one-way ANOVA with Tukey post-hoc test (**d**). All data are presented as mean ± SEM

synthesis (Fig. 5j). No effects were observed on iWAT beiging (Supplementary Fig. 6b–c) or thermogenic gene programs in the iWAT of treated mice (Supplementary Fig. 6d–g). These findings underscore that the thermogenic complementary effects of dual TRPM8 and nAChR activation are preserved in DIO mice housed at thermoneutral conditions.

Icilin and DMPP improve glucose control and fatty liver disease. Whereas icilin monotherapy has negligible effects on glucose metabolism (Fig. 6a, b, Fig. 7a, Supplementary Fig. 8c), DMPP alone and in combination with icilin corrected diet-induced glucose intolerance following 1-weak of treatment (Fig. 6a, b). The insulin response during the glucose tolerance test (GTT) was lower following combination treatment relative to the monotherapies and vehicle control (Fig. 6c, d), implying enhanced insulin sensitivity. This notion was corroborated by HOMA-IR assessment (Fig. 6f) and by insulin tolerance tests (ITT) executed at both ambient room temperature (Fig. 6g) and at thermoneutral conditions (Fig. 6h) demonstrating superior effects of DMPP and icilin cotreatment relative to the monotherapies on insulin sensitivity. Notably, we observed opposing effects of icilin monotherapy on insulin sensitivity depending on the housing temperature. Hepatic glucose output was indirectly assessed by a pyruvate tolerance test (PTT). The glucose excursion during the PTT was substantially dampened by both icilin

and DMPP treatment relative to vehicle treated HFD mice (Fig. 6i, j). These long-term glycemic benefits were further improved when DMPP and icilin were coadministered (Fig. 6i, j). None of the treatments affected circulating lipoprotein fractions (Fig. 6k), but both DMPP and icilin monotherapies improved diet-induced hepatic steatosis (Fig. 6l) and diet-induced NAFLD-induced NASH at thermoneutral conditions (Fig. 6m, n). The combination of DMPP and icilin was superior to the monotherapies with respect to improving NAFLD and NASH. Several genes associated with cholesterol and triglyceride uptake, as well as bile acid metabolism, were altered by the treatments (Supplementary Fig. 7a, b). Notably, Cyp7b1 was highly induced by the combination of DMPP and icilin (Supplementary Fig. 7a). Plasma levels of alanine aminotransferase (ALT) and aspartate aminotransferase (AST) were unchanged (Supplementary Fig. 7c, d). Together, these data underscore that the combination of DMPP and icilin corrects multiple aspects of the metabolic syndrome inflicted by excess consumption of dietary fat and sugar.

Glycemic benefits are mediated by MC4R. The leptin–melanocortin system plays a key role in the central regulation of glucose metabolism[23]. To test if DMPP signals via the central leptin–melanocortin system to improve glycemia, we used MC4R KO mice. In the DIO MC4R KO mice, neither the monotherapies nor the combination of DMPP and icilin

ARTICLE
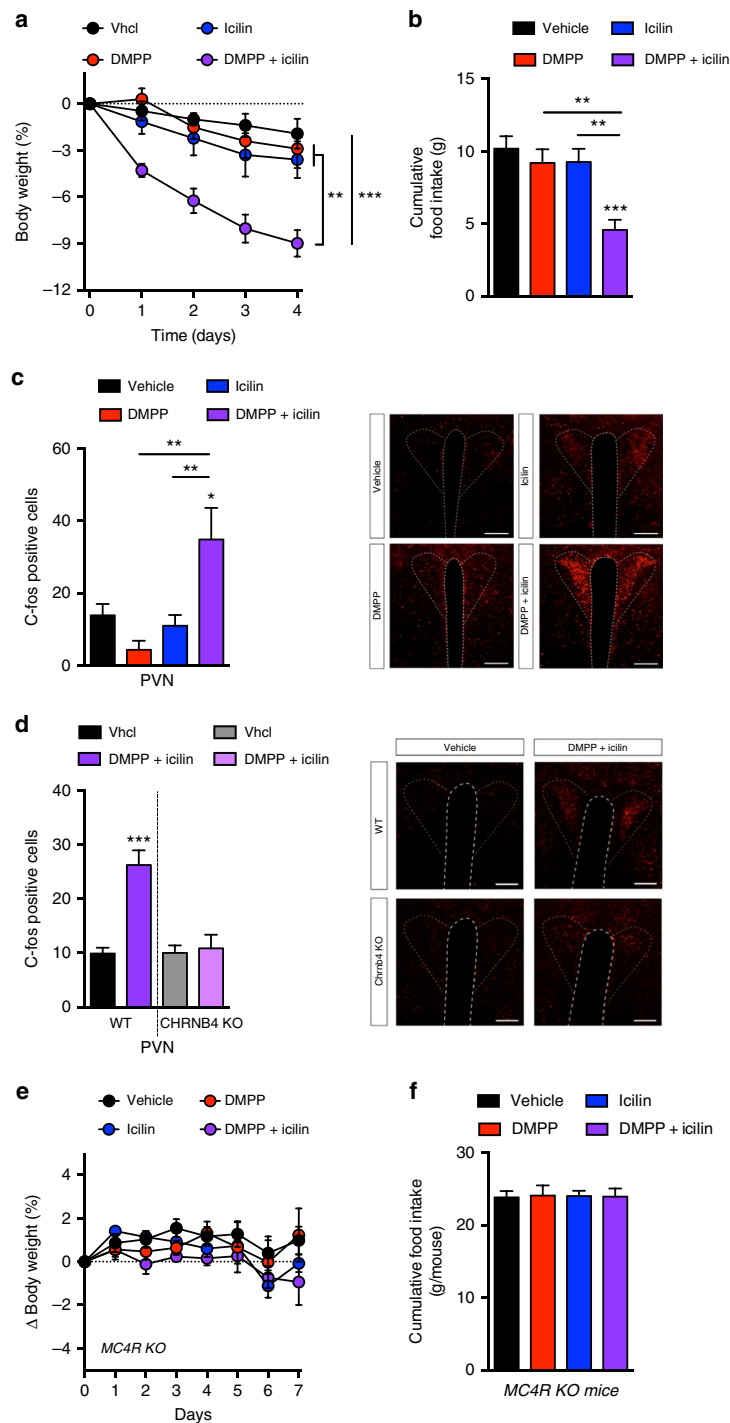
ameliorated glucose intolerance (Fig. 7c, d). UCP1 is required for sympathetic-induced BAT glucose utilization[24]. Here, we found that combination of DMPP and icilin improved diet-induced glucose intolerance equally in DIO WT and DIO UCP1 KO mice (Fig. 7e–h). The benefits of DMPP and icilin cotreatment on glucose tolerance were also preserved in

betaless mice (Supplementary Fig. 8a, b) and in TRPM8 KO mice (Supplementary Fig. 8d, e). Together, these data underline that both the glycemic and weight-lowering benefits linked to dual TRPM8 and nAChR α3β4 agonism are centrally mediated and require key signaling nodes in the leptin–melanocortin pathway.

ARTICLE

Fig. 3 Icilin and DMPP synergistically lower body weight in DIO mice via central mechanisms. **a** Effects on body weight, **b** cumulative food intake, and **c** cFOS positive neurons in the hypothalamus following daily s.c. injections to DIO male C57Bl6j mice of vehicle (black, n = 8 for **a**, **b**; n = 6 for **c**), DMPP 10 mg/kg (red, n = 8 for **a**, **b**; n = 6 for **c**), icilin 5 mg/kg (blue, n = 8 for **a**, **b**; n = 6 for **c**), or the combination of DMPP 10 mg/kg and icilin 5 mg/kg (purple, n = 7 for **a**, **b**; n = 8 for **c**) for 4 days (**a**, **b**) or 3 days (**c**), respectively. **d** cFOS positive neurons in the hypothalamus following daily s.c. injections to DIO male WT C57Bl6j mice or to DIO male CHRNB4 KO mice of vehicle (black, n = 5/gray, n = 4) or the combination of DMPP 10 mg/kg and icilin 5 mg/kg (purple, n = 5/light purple, n = 5) for 3 days. **e** Effects on body weight and **f** cumulative food intake following daily s.c. injections to HFD-fed male MC4R KO mice of vehicle (black, n = 8), DMPP 5 mg/kg (red, n = 8), icilin 5 mg/kg (blue, n = 8), or the combination of DMPP 5 mg/kg and icilin 5 mg/kg (purple, n = 7) for 7 days. All scale bars are 100 μm. *$p < 0.05$, **$p < 0.01$, ***$p < 0.001$ by two-way ANOVA (**a**, **e**) and one-way ANOVA with Tukey post-hoc test (**b**, **c**, **d**, **f**). All data are presented as mean ± SEM

Discussion

Inspired by the efficiency of two canonical environmental modulators of human energy metabolism—tobacco smoking and cold exposure—to suppress appetite and increase energy expenditure, respectively, we here explored a novel pharmacological strategy in which we aimed to simultaneously mimic the metabolic benefits of both phenomena through a "biochemical cigarette". We report that the small molecule icilin stimulates the cold receptor TRPM8 to elicit thermogenesis and lower body weight without influencing appetite. In parallel, we discovered that the nAChR α3β4 agonist DMPP suppresses appetite and reverses diet-induced glucose intolerance. Finally, we show that concerted treatment with icilin and DMPP elicits complementary metabolic benefits to reverse obesity, glucose intolerance, and hepatic steatosis in mouse models of obesity and glucose intolerance.

Targeting TRPM8 to increase energy expenditure as a means to combat obesity has previously been suggested[10,19,25–27]. Now, by revealing a potent anti-obesity potential of the TRPM8 agonist icilin, we add substantial support to this idea. In contrast to previous studies that report a cell autonomous effect of TRPM8 on adipocyte thermogenesis, we did not detect TRPM8 expression in adipocytes, nor did we observe any functional effect of icilin on BAT respiration or UCP1 induction. Conversely, our data propose that the ability of TRPM8 activity to increase energy expenditure is indirect—likely implicating sensory neurons and SNS-induced thermogenesis[28]. This is supported by the MSOT data showing a clear physiological phenomenon induced in BAT by the cotreatment, as well as by the data showing the blunted weight-lowering efficacy following cotreatment in the betaless mice. Importantly, the metabolic benefits of DMPP and icilin cotreatment were preserved under thermoneutral conditions. In contrast to previous work on pharmacological β-adrenergic stimulation[22], we observed that food intake was no longer suppressed following combination therapy at thermoneutrality. Instead, the synergistic weight loss induced by DMPP and icilin cotreatment at thermoneutrality was accompanied by a profound induction of brown fat UCP1 levels. Although it is still debated what rodent housing temperature most accurately mimics the human condition[29–31], the effectiveness of DMPP and icilin cotreatment to reverse the metabolic syndrome in DIO mice housed at both ambient room temperature and at thermoneutrality strengthens the translational value of this pharmacological approach.

The implication of hypothalamic α3β4 nAChR activation to elicit POMC activity and food intake suppression via the leptin–melanocortin system[13] encouraged us to investigate selective agonists for this receptor subtype in a potential combination therapy with TRPM8 agonists. DMPP is an agonist at the human α3β4[32] and is reported to act as a catecholamine and glucagon secretagogue through ganglionic nAChRs[33]. We identified a robust reduction in food intake following DMPP treatment, which was amplified by adjunctive icilin treatment. In agreement with previous findings showing that weight loss following activation of POMC expressed nAChRs is mediated

through MC4R signaling in the PVN[13], we discovered that the ability of DMPP and icilin cotreatment to lower body weight requires both functional α3β4 nAChRs and MC4Rs. Whereas the combination of DMPP and icilin likely converge to drive feeding via MC4R on PVN neurons, the MC4R-dependent increase in energy expenditure possibly implicates MC4Rs located elsewhere[34,35]. Our findings are thus in agreement with a reported divergence of melanocortin signaling in the control of food intake and energy expenditure[36]. The mechanism of how TRPM8 activation potentiates the anorexigenic mechanisms of α3β4 nAChR activation requires further study.

The ability of DMPP to lower HFD-linked hyperphagia and reverse obesity is comparable to that of other nAChR-agonists, including nicotine as shown here. However, the robust and weight-independent improvement in glycemic control following DMPP treatment might be a unique feature relative to other nAChR agonists. In fact, there is evidence that nicotine worsens glycemic control[37]. Recently, it was reported that UCP1 expression is required for β3-adrenergic receptor (AR)-mediated improvements in glucose metabolism[38]. Here, we find that the ability of DMPP and the combination of DMPP and icilin to reverse diet-induced glucose intolerance is independent of BAT UCP1 induction. Notably, while the effects on glucose tolerance appear to be predominantly driven by DMPP, the addition of icilin is required to maximize the benefits on insulin sensitivity. Supporting that mechanisms proximate to brown fat are driving the improvements in glucose metabolism, the potent glycemic benefits governed by DMPP pharmacology were completely lost in MC4R KO mice. However, mouse models of monogenetic obesity and diabetes exhibit a severe background phenotype, so the lack of pharmacological efficacy must be interpreted with caution. Thus, future studies are required to illuminate the molecular interplay between MC4R and α3β4 nAChR signaling in glucose control and for example if MC4Rs on cholinergic sympathetic preganglionic neurons are implicated in the glycemic benefits of α3β4 nAChR agonists[39].

It is well established that nicotine affects energy metabolism in humans[40]. However, behavioral and cardiovascular off-target effects compromise the utilization of nAChR-based anti-obesity pharmacotherapies. Insights into the tissue-specific and functional differences of distinct nicotinic receptor subtypes might provide important clues for future optimization of nAChR-targeting compounds. As of today, the study of TRP-channel pharmacology in relation to human energy expenditure has mostly focused on TRPV1[41–44] whereas the effects of potent TRPM8 targeting pharmacology on human energy expenditure are largely unexplored. One study suggested that a combined targeting of TRPM8 and TRPA1 might be required to relevantly increase human energy expenditure[45]. In parallel with assessing the translational value of co-targeting nAChRs and TRPM8, understanding the underlying mechanisms of actions are vital for the clinical progression of this strategy. A recent study found that cold-induced energy expenditure induction involves hepatic *Cyp7b1*-dependent bile acid synthesis, thereby suggesting a novel

ARTICLE
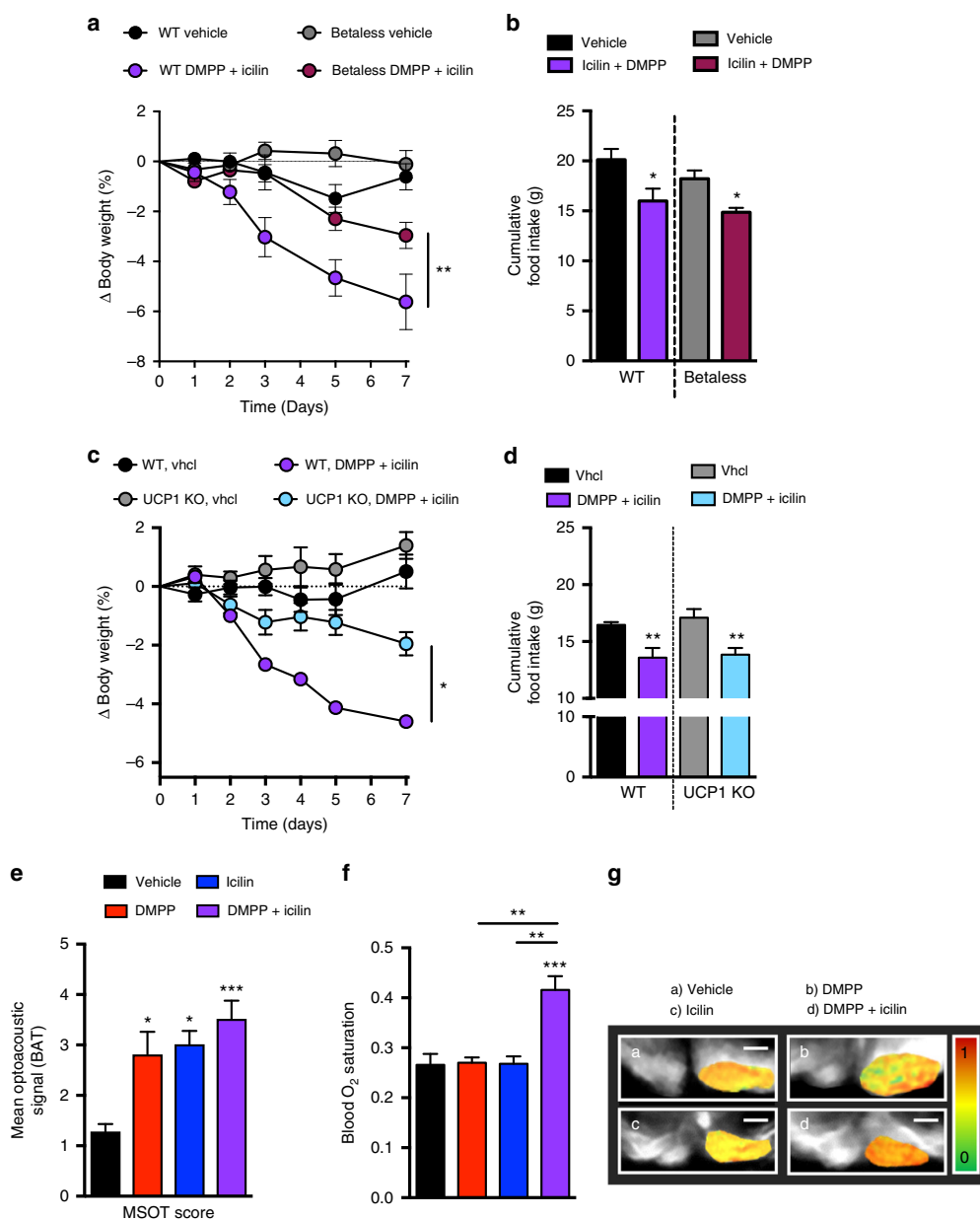
Fig. 4 Icilin and DMPP combination therapy increases sympathetic nervous system-linked BAT thermogenesis. **a** Effects on body weight and **b** cumulative food intake following daily s.c. injections to DIO male betaless mice or DIO male WT C57Bl6j mice of vehicle (black, $n = 8$/gray, $n = 8$) or the combination of DMPP 5 mg/kg and icilin 5 mg/kg (purple, $n = 8$/bordeaux, $n = 7$) for 7 days. **c** Effects on body weight and **d** cumulative food intake following daily s.c. injections to global UCP1 KO DIO male mice or DIO male C57Bl6j control mice of vehicle (black, $n = 7$/gray, $n = 7$) or the combination of DMPP 5 mg/kg and icilin 5 mg/kg (purple, $n = 7$/light blue, $n = 7$) for 7 days. **e** Mean optoacoustic signal intensity and **f** blood oxygen saturation (SO_2) measured by Multi-Spectral Optoacoustic Tomography (MSOT) in selected BAT regions of male C57Bl6j control mice of vehicle (black, $n = 6$), DMPP 10 mg/kg (red, $n = 6$), icilin 5 mg/kg (blue, $n = 6$), or the combination of DMPP 10 mg/kg and icilin 5 mg/kg (purple, $n = 6$). (**g–a** to **g–d**) MSOT image of BAT at 800 nm (gray scale) with overlaid of SO_2 (green-red scale) in: a control- (**g–a**), DMPP- (**g–b**), icilin- (**g–c**), and combination-injected mouse (g-d). All scale bars are 5 mm. *$p < 0.05$, **$p < 0.01$, ***$p < 0.001$ by two-way ANOVA (**a**, **c**), one-way ANOVA (**e**, **f**) with Tukey post-hoc test and two-tailed Student's t-test (within genotype) (**b**, **d**). All data are presented as mean ± SEM
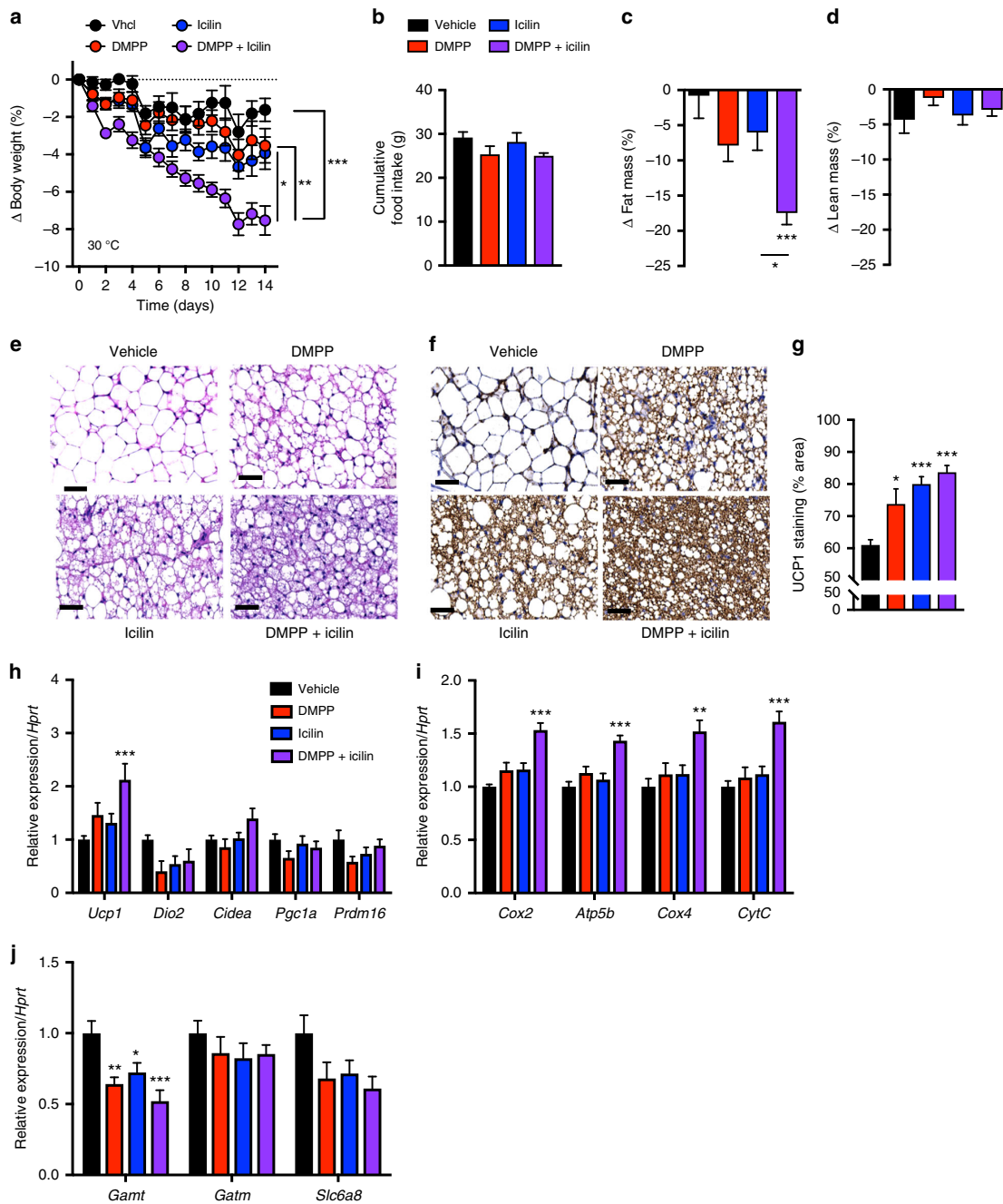
Fig. 5 Icilin and DMPP reverse obesity and increase BAT UCP1 at thermoneutral conditions. **a** Effects on body weight, **b** cumulative food intake, changes in **c** fat mass and **d** lean mass, **e** BAT H & E staining, and **f** UCP1 immunoreactivity staining in BAT with **g** quantification of UCP1 immunoreactivity staining (% area). BAT expression of genes involved in **h** thermogenesis, **i** mitochondrial transport, and **j** creatine signaling pathway following daily s.c. injections of vehicle (black or white, $n = 8$), DMPP 5 mg/kg (red, $n = 7$), icilin 5 mg/kg (blue, $n = 8$), or the combination of DMPP 5 mg/kg and icilin 5 mg/kg (purple, $n = 7$) to DIO male C57Bl6j chronically housed at 30 °C for 14 days. All scale bars are 50 μm. *$p < 0.05$, **$p < 0.01$, ***$p < 0.001$ by two-way ANOVA (**a**) and one-way ANOVA (**b**, **c**, **d**, **g**, **h**, **i**, **j**) with Tukey post-hoc test. All data are presented as mean ± SEM

ARTICLE

BAT-liver axis[46]. Notably, the combination of DMPP and icilin potently increases hepatic *Cyp7b1* expression, leaving the exciting opportunity that cold-mimicking effects on hepatic bile acid alterations contribute to the metabolic benefits of the combination therapy.

In summary, we report that stimulation of TRPM8 represents a novel strategy to pharmacologically mimic the benefits of cold exposure on energy metabolism. The ability of the potent TRPM8 agonist icilin to induce a negative energy state is substantially potentiated by coordinated activation of nAChRs by DMPP. The combination of DMPP and icilin engages central satiety circuits and increases BAT thermogenesis, which ultimately improves diet-induced obesity, glucose intolerance, and hepatic steatosis in mice. Conclusively, these data support the compelling potential in coordinated targeting of TRPM8 and α3β4-nAChRs for the treatment of the related epidemics of obesity, type 2 diabetes, and fatty liver disease.

ARTICLE
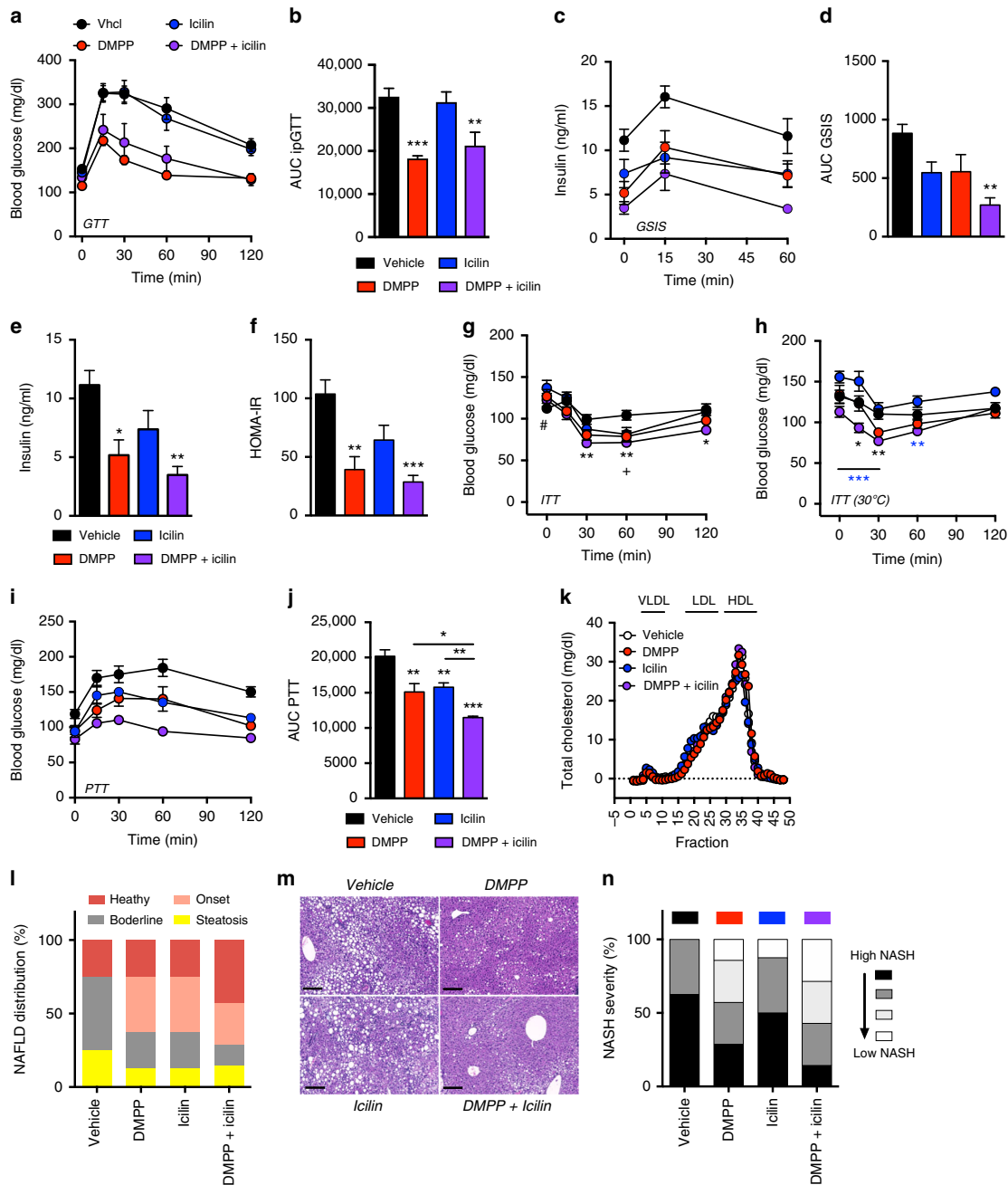
Fig. 6 Icilin and DMPP reverse diet-induced glucose intolerance, insulin resistance, and hepatic steatosis in DIO mice. **a**, **b** Effects on glucose tolerance and **c**, **d** glucose-stimulated insulin secretion following daily s.c. injections to DIO mice of vehicle (black, $n = 8$), DMPP 10 mg/kg (red, $n = 8$), icilin 5 mg/kg (blue, $n = 8$), or DMPP 10 mg/kg and icilin 5 mg/kg (purple, $n = 7$) for 7 days. **e** Effects on 6-h fasted insulin levels, **f** HOMA-IR score, and **g** insulin tolerance following daily s.c. injections to DIO mice of vehicle (black, $n = 8$), DMPP 10 mg/kg (red, $n = 8$), icilin 5 mg/kg (blue, $n = 8$), or DMPP 10 mg/kg and icilin 5 mg/kg (purple, $n = 7$) for 7 days at 23 °C. **h** Effect on insulin tolerance following 14 days of daily s.c. injections of vehicle (black, $n = 8$), DMPP 5 mg/kg (red, $n = 7$), icilin 5 mg/kg (blue, $n = 8$), or the combination of DMPP 5 mg/kg and icilin 5 mg/kg (purple, $n = 7$) in DIO mice housed at 30 °C. **i** and **j** Effect on pyruvate tolerance following daily s.c. injections to DIO mice of vehicle (black, $n = 7$), DMPP 5 mg/kg (red, $n = 7$), icilin 5 mg/kg (blue, $n = 7$), or DMPP 5 mg/kg and icilin 5 mg/kg (purple, $n = 7$) for 20 days. **k** Plasma lipoprotein fractions following daily s.c. injections to DIO mice of vehicle (black, $n = 7$), DMPP 5 mg/kg (red, $n = 7$), icilin 5 mg/kg (blue, $n = 7$), or DMPP 5 mg/kg and icilin 5 mg/kg (purple, $n = 7$) for 21 days. **l** Effect on hepatic steatosis score following daily s.c. injections to DIO mice housed at 23 °C of vehicle ($n = 8$), DMPP 10 mg/kg ($n = 8$), icilin 5 mg/kg ($n = 8$), or DMPP 10 mg/kg and icilin 5 mg/kg ($n = 7$) for 14 days. **m** Liver H & E stainings and **n** NASH severity (%) following daily s.c. injections to DIO mice housed at 30 °C of vehicle (black, $n = 8$), DMPP 5 mg/kg (red, $n = 7$), icilin 5 mg/kg (blue, $n = 8$), or DMPP 5 mg/kg and icilin 5 mg/kg (purple, $n = 7$) for 14 days. All scale bars are 200 μm. $*p < 0.05$, $**p < 0.01$, $***p < 0.001$ by two-way ANOVA (**a**, **c**, **g**, **h**, **i**) and one-way ANOVA (**b**, **d**, **e**, **f**, **j**) with Tukey post-hoc test. $^{\#}p < 0.05$ vehicle vs. icilin and $^{+}p < 0.05$ vehicle vs. DMPP (g). All data are presented as mean ± SEM
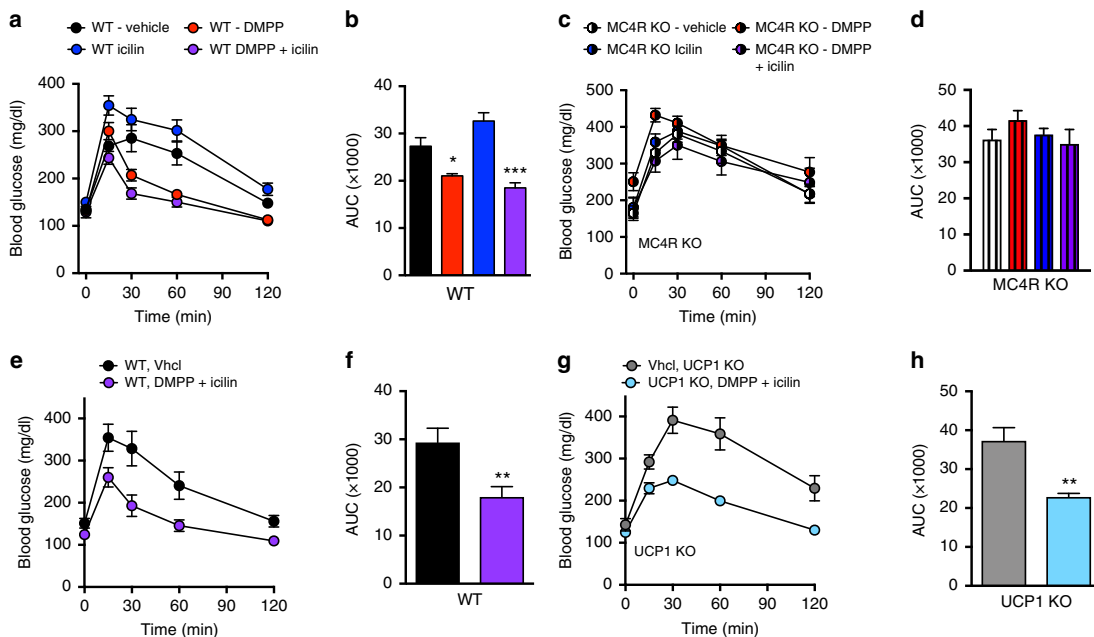
Fig. 7 The melanocortin system is indispensable for the glycemic benefits of icilin and DMPP combination therapy. **a** and **b** Effects on glucose tolerance following daily s.c. injections to DIO male C57Bl6j mice or **c**, **d** MC4R KO mice of vehicle (black, $n = 8$/striped white, $n = 8$), DMPP 5 mg/kg (red, $n = 8$/striped red, $n = 8$), icilin 5 mg/kg (blue, n = 8/striped blue, $n = 8$), or the combination of DMPP 5 mg/kg and icilin 5 mg/kg (purple, $n = 8$/striped purple, $n = 7$) for 7 days. **e** and **f** Effects on glucose tolerance following daily s.c. injections to DIO male C57Bl6j mice or **g**, **h** UCP1 KO mice of vehicle (black, $n = 7$/gray, $n = 7$) or the combination of DMPP 5 mg/kg and icilin 5 mg/kg (purple, $n = 7$/light blue, $n = 7$) for 7 days. $*p < 0.05$, $**p < 0.01$, $***p < 0.001$ by two-way ANOVA (**a**, **c**, **e**, **g**), one-way ANOVA wit Tukey post-hoc test (**b**, **d**), or two-tailed Student's t-test (**f**, **h**). All data are presented as mean ± SEM

Methods

Animals. For pharmacology studies, six- to eight-week-old male C57Bl6j mice were provided ad libitum access to a high-fat, high sucrose diet (D12331; Research Diets, New Brunswick, NJ, USA). The mice had free access to water and were maintained at 23 °C, with constant humidity and on a 12-h light–dark cycle. All mice were housed under specific-pathogen-free (SPF) conditions. Mice were maintained under these conditions for a minimum of 11 weeks before treatment initiation. For the thermoneutral study, mice were maintained at constant 30 °C ambient temperature for four to 7 weeks prior to study initiation. CHRNB4 KO mice were generated as described previously[47]. Homozygous mice were used to generate a colony of mice for pharmacological studies. UCP1 KO and MC4R KO were originally provided from Jackson Laboratory (strain names: B6.129-Ucp1tm1Kz/J; B6;129S4-Mc4rtm1Lowl/J, ME, USA). TRPM8 KO mice were generated as described[48] and provided from Jackson Laboratory (strain name: B6.129P2-$Trpm8^{\text{tm1Jul}}$/J). For pharmacological studies, homozygous WT and TRPM8 KO mice. Betaless mice were generated as described previously[49]. Homozygous mice were used to

generate a colony of mice for pharmacological studies. Mice were randomly assigned to pharmacological treatment groups based on body weight and body fat. The Animal studies were approved and conducted in accordance to the Danish Animal Experimentation Inspectorate and Animal Ethics Committee of the government of Upper Bavaria, Germany.

In vivo pharmacology and energy metabolism studies. Compounds were administered in a vehicle of 0.01 N NaOH and 1% Tween-80 and injected subcutaneously (s.c.) 0–2 h before the onset of the dark cycle at the indicated doses at a volume of 5 μl per g body weight. Coadministration of compounds was performed by single formulated injections. Researchers were not blinded to the treatment groups. Body composition (fat and lean mass) was analyzed using a magnetic resonance whole-body composition analyzer (Echo-MRI, Houston, TX, USA). Energy expenditure and home-cage locomotor activity were registered with a combined indirect calorimetry system (TSE PhenoMaster, TSE Systems, Bad Homburg, Germany). After 24 h of acclimatization, O_2 consumption and CO_2

ARTICLE

production were registered every 10 min for a total of 72 h to assess energy expenditure after daily s.c. administration of the indicated treatments. The multidimensional infrared light beam system determines home-cage locomotor activity with beams scanning the bottom and top levels of the cage resulting in activity expressed as beam breaks.

Glucose metabolism studies. Glucose tolerance, insulin sensitivity, and pyruvate tolerance were analyzed approximately 20 h after the last compound injections. For glucose and insulin tolerance tests, mice were fasted for 6 h and then challenged by an intraperitoneal injection of 1.5 g or 1.75 g glucose per kg body weight or 0.75 U insulin per kg body weight. Pyruvate tolerance was tested in overnight fasted mice at a dose of 1 g pyruvate per kg body weight. Glucose levels in all tolerance tests were measured in the blood sampled from the tail veins before (0 min) and at 15, 30, 60, and 120 min post injection using a handheld glucometer (Abbott, Wiesbaden, Germany). To measure glucose-stimulated insulin secretion, blood was collected from tail veins into EDTA-coated microvette tubes (Sarstedt, Nümbrecht, Germany) at time points 0, 15 and 60 min post glucose injection.

Blood parameters. Blood was immediately kept on ice, centrifuged at 3000 g and 4 °C, and plasma was stored at −80 °C. Commercially available kits were used to measure plasma levels of insulin (ALPCO Diagnostics, Salem, NH, USA), ALT, and AST (Thermo Fisher Scientific, Erlangen, Germany) according to the manufacturers' instructions. For fast performance liquid chromatography of cholesterol distribution in different lipoprotein fractions, plasma of the different treatment groups was pooled ($n = 7$) and measured on two Superose 6 columns connected in series[50].

Biochemical analysis. Mice were euthanized using CO_2 after a timed administration of compound and removal of food 2 h prior to the sacrifice. Tissue samples were collected and immediately snap-frozen in liquid nitrogen or kept on dry ice. For gene expression analysis, RNA was isolated using RNeasy Kit (Qiagen, Hilden, Germany) according to the manufacturers' instructions. Total RNA was reverse transcribed into cDNA using QuantiTect Reverse Transcription Kit (Qiagen, Hilden, Germany), which includes a gDNA elimination step. Gene expression in BAT, iWAT, and liver was profiled with quantitative real-time PCR using either TaqMan single probes or SYBR green (Thermo Fisher Scientific, Erlangen, Germany). The relative expression of the selected genes was normalized to the reference genes peptidylprolyl isomerase B (Ppib) or hypoxanthine-guanine phosphoribosyltransferase (Hprt). Data on gene expression were screened for singular statistically significant outliers using the maximum normed residual (Grubb's) test. Sequences of primers and TaqMan probes used are listed in alphabetical order in Supplementary tables 1, 2.

cFOS immunohistochemistry. For cFOS immunohistochemistry, DIO WT mice or DIO CHRNB4 KO mice were treated with compounds for 3 days. 2 h prior to perfusion, food was removed and mice received a final compound treatment. Mice were sacrificed with CO_2 and transcardially perfused with saline (0.9% NaCl) followed by 4% paraformaldehyde (PFA) in phosphate buffered saline (pH = 7.4). Brains were isolated and post-fixed in 4% PFA at 4 °C before being equilibrated for 48 h with 30% sucrose in Tris-buffered saline (TBS; pH 7.2). After sectioning into 30 μm coronal sections using a cryostat, brain slices were washed in TBS and incubated overnight at 4 °C with a primary antibody anti-cFOS (rabbit polyclonal SC-52, 1:1000, Santa Cruz Biotechnology, Inc, TX, USA) in a solution containing 0.25% gelatin and 0.5% TritonX-100 in TBS. After serial washes in TBS, sections were incubated with Alexa Fluor 568 donkey-anti-rabbit (1:1000, Molecular Probes, Life Technologies GmbH, Darmstadt, Germany) secondary antibody. Sections were serially washed with TBS, mounted on gelatin-pre-coated glass slides, and cover-slipped for image quantification. Quantification of cFOS immunoreactive (cFos+) cells was performed using ImageJ software. Images of single focal planes were captured at 20X magnification by a BZ-9000 fluorescence microscope (Keyence Corporation Itasca, IL, USA). The number of cFos+ nuclei within the PVN was determined according to the Allen mouse brain atlas. All morphometric analyses were performed without previous knowledge of the experimental group.

Histopathology. After chronic treatment mice were sacrificed with CO_2. Formalin fixed BAT, iWAT, and liver samples were embedded in paraffin using a vacuum infiltration processor TissueTEK VIP (Sakura, AV Alphen aan den Rijn, Netherlands). 3 μm thick slides were cut using a HMS35 (Zeiss, Jena, Germany) or HM340E (Thermo Fisher Scientific, Erlangen, Germany) rotatory microtome and H & E staining was performed. For H&E staining, rehydration was done in a decreasing ethanol series, rinsing with tapwater, 2 min Mayers acid Hemalum, bluing in tapwater followed by 1 min EosinY (both Sigma-Aldrich, MO, USA). Dehydration was performed in increasing ethanol series, mounting with Pertex® (Medite GmbH, Burgdorf, Germany) and coverslips (Carl Roth Chemicals, Karlsruhe, Germany). The slides were evaluated independently using a brightfield microscope (Axioplan; Zeiss, Jena, Germany). The hepatic steatosis score is defined as the unweighted sum of the three individual scores for steatosis, lobular inflammation, and ballooning degeneration. Steatosis is graded by the presence of fat vacuoles in liver cells according to the percentage of affected tissue (0: < 5%; 1:

5–33%; 2: 33–66%; 3: > 66%). Lobular inflammation is scored by overall assessment of inflammatory foci per 200x field (0: no foci; 1: < 2 foci; 2: 2–4 foci; 3: > 4 foci). The individual score for ballooning degeneration ranges from 0 (none), 1 (few cells) to 2 (many cells). Total scores range from 0 to 8 with scores < 2 considered non-steatosis, 3 considered as borderline steatosis, 4–5 considered onset of steatosis, and > 6 considered steatosis.

For UCP1 immunoreactivity, 3 μm sections of iWAT and BAT samples were stained on a Discovery XT automated stainer (Roche Diagnostics, Mannheim, Germany) employing rabbit anti-UCP1 antibody (1:1500; ab 10983, Abcam, Cambridge, UK). Signal detection was performed using biotinylated goat anti-rabbit (1:750, BA-1000, Vector Laboratories, Burlingame, CA, USA) as a secondary antibody and Dako detection kit (K5001; Agilent, Waldbronn, Germany). The stained tissue sections were scanned with an AxioScan.Z1 digital slide scanner (Zeiss, Jena, Germany) equipped with a 20x magnification objective.

Images were evaluated using the commercially available image analysis software Definiens Developer XD 2 (Definiens AG, Munich, Germany). A specific ruleset was developed in order to detect and quantify UCP1 stained tissue. The calculated parameter was the ratio of UCP1 stained tissue.

Isolation of primary brown adipocytes. Primary brown adipocytes were isolated from six- to eight-week-old male C57Bl6j mice. The brown adipose tissue was minced and digested at 37 °C for 40 min (1 mg/ml Collagenase II (Thermo Fisher Scientific, Erlangen, Germany), 3 U/ml Dispase II (Sigma-Aldrich, Munich, Germany), 0.01 mM $CaCl_2$ in PBS). The cell suspension was filtered using a 100 μm cell strainer, centrifuged and resuspended in growth medium (DMEM/F12 1:1 plus Glutamax (Thermo Fisher Scientific, Erlangen, Germany) containing 1% penicillin/streptomycin (Thermo Fisher Scientific, Erlangen, Germany) and 10% heat-inactivated FBS). After a second filtration step (40 μm cell strainer), pre-adipocytes were cultured to confluency in collagen-coated 12-well plates (VWR International GmbH, Darmstadt, Germany) (37 °C, 5% CO_2). Differentiation was induced by dexamethasone (5 μM), isobutyl-methylxanthine (0.5 mM), rosiglitazone (1 μM), indomethacin (125 μM), T3 (1 nM), and insulin (0.5 μg/ml) in growth medium. After 2 days of induction, adipocytes were cultured in growth medium containing rosiglitazone, T3, and insulin and at day 4 of differentiation, cells were grown in growth medium with T3 and insulin.

The study involving adipocytes derived from human BAT biopsies was reviewed and approved by the ethics committee of Maastricht University Medical Center (METC 10-3-012, NL31367.068.10, NCT03111719). Informed participant consent was obtained prior to surgery and all ethical regulations were followed. Human BAT cultures were generated similarly to previous work[51]. In short, the stromal vascular fraction was obtained from BAT from an individual undergoing deep neck surgery. Differentiation was initiated for 7 days via differentiation medium made up out of biotin (33 mM), pantothenate (17 mM), insulin (100 nM), dexamethasone (100 nM), IBMX (250 mM), rosiglitazone (5 mM), T3 (2 nM), and transferrin (10 mg/ml). Cells were transferred maintenance medium consisting of biotin (33 mM), pantothenate (17 mM), insulin (100 nM), dexamethasone (10 nM), T3 (2 nM), and transferrin (10 mg/ml) for another 5 days.

Primary brown adipocytes, gene expression. For gene expression analysis in differentiated primary brown adipocytes, cells were treated with isoproterenol (Sigma-Aldrich, Munich, Germany, 1 μM), icilin (1 and 10 μM) or control (0.1% DMSO) at day 6 of differentiation for 6 h in serum-free growth medium. Medium was removed and the cell plates were snap-frozen at −80 °C until RNA isolation.

Bioenergetics analysis. Primary brown adipocytes were cultured and differentiated on a XF96e-well plate. At day 5 of differentiation, cells were washed and incubated in DMEM XF Assay medium (Seahorse Bioscience, Santa Clara, CA, USA), supplemented with 25 mM glucose (Carl Roth, Karlsruhe, Germany) and 1.5% fatty acid free-BSA (Sigma-Aldrich, Munich, Germany) at 37 °C in a non-CO_2 incubator for 10 min. Tenfold higher concentrated compounds, dissolved in DMEM XF Assay medium without supplements, were loaded into the ports of a XF Assay Cartridge. Oxygen consumption rate (OCR) was measured using an extracellular flux analyzer (XF96, Seahorse Bioscience, Santa Clara, CA, USA). Basal OCR was recorded for 9 min, followed by measurement of OCR after injection of oligomycin (2 μg/ml, 23 min), norepinephrine (1 μM, 27 min), icilin (1 μM, 27 min) or control (0.1% DMSO, 27 min), carbonyl cyanide-p-trifluoromethoxyphenylhydrazone (FCCP) (1 μM, 14 min), rotenone (2.5 μM)/antimycin A (2.5 μM)/2-deoxyglucose (10 mM) (9 min). For normalization, the cell plate was fixed with 4% paraformaldehyde and subsequently co-stained with 4′,6-diamidino-2-phenylindole (Dapi) and Nile red. Using a PheraStar plate reader, the fluorescence signal was detected and the bioenergetics measurements were corrected for cell number and differentiation.

Multi-spectral Optoacoustic Tomography. Multi-spectral Optoacoustic Tomography (MSOT) measurements were conducted with a 256-channel real-time imaging MSOT scanner[52] (inVision 256-TF, iThera Medical GmbH, Munich, Germany) equipped with a tunable (wavelength range: 680–960 nm) pulsed (pulse duration: < 10 ns) optical parametric oscillator laser with a 10 Hz repetition rate. A fiber bundle was used for delivering homogeneous light along a line of illumination

11

50

ARTICLE

surrounding the animal body. Optoacoustic signals were acquired by a 256-element, cylindrically focused transducer array covering a solid angle of 270° around the imaged animal. The individual detector elements had a central frequency of 5 MHz. The system can acquire cross-sectional (transverse) images of oxygenated and deoxygenated hemoglobin over time. Processing of these images can yield maps of total blood volume, tissue oxygen saturation, and of their transients. A moving stage enables the imaging of different transverse planes, while the illumination and ultrasound detection components remain static.

Mouse MSOT measurements in vivo. C57Bl6j mice (Charles River Laboratories Inc, Charleston, USA) were anesthetized by i.p. injection of 139 mg/kg ketamine and 6.8 mg/kg xylazine and placed in the MSOT sample holder as described earlier[53]. In brief, each animal was placed onto a thin, polyethylene membrane and positioned in the water bath maintained at 34 °C. Temperature controlled water provided acoustic coupling and maintained animal temperature while imaging. For imaging brown adipose tissue, vehicle, DMPP, icilin or the combination of DMPP and icilin were injected i.p. 40 min before imaging. A total of six animals were used for the activation experiments. For each measurement, multiple images at 10 different wavelengths spanning 700 nm to 900 nm with 20-nm steps were recorded. Preliminary data processing was performed using the commercial suite provided by the manufacturing company (ViewMSOT, Xvue Ltd, Greece). Finally, a model-based image reconstruction method was applied on the raw optoacoustic signals, followed by a spectral unmixing step to calculate the saturation maps over selected regions of interest. Eigenspectra optoacoustic tomography achieves quantitative blood oxygenation imaging deep in tissues[54].

Statistics. Statistical analyses were performed on data distributed in a normal pattern using one- or two-way ANOVA followed by Tukey post-hoc analysis as appropriate or an unpaired two-tailed Student's t test. No statistical methods were used to predetermine sample size for in vivo pharmacology studies. Mean energy expenditure was analyzed using ANCOVA with body weight as covariate as previously suggested[55]. All results are presented as mean ± SEM, and $P < 0.05$ was considered significant.

Data availability
The authors declare that all data supporting the findings of this investigation are available within the article, its Supplementary Information, and from the corresponding authors upon reasonable request.

References
1. Heymsfield, S. B. & Wadden, T. A. Mechanisms, pathophysiology, and management of obesity. *N. Engl. J. Med.* **376**, 254–266 (2017).
2. Bray, G. A. & Greenway, F. L. Pharmacological approaches to treating the obese patient. *Clin. Endocrinol. Metab.* **5**, 455–479 (1976).
3. Virtanen, K. A. et al. Functional brown adipose tissue in healthy adults. *N. Engl. J. Med.* **360**, 1518–1525 (2009).
4. van Marken Lichtenbelt, W. D. et al. Cold-activated brown adipose tissue in healthy men. *N. Engl. J. Med.* **360**, 1500–1508 (2009).
5. Cypess, A. M. et al. Identification and importance of brown adipose tissue in adult humans. *N. Engl. J. Med.* **360**, 1509–1517 (2009).
6. Clapham, D. E. TRP channels as cellular sensors. *Nature* **426**, 517–524 (2003).
7. McKemy, D. D., Neuhausser, W. M. & Julius, D. Identification of a cold receptor reveals a general role for TRP channels in thermosensation. *Nature* **416**, 52–58 (2002).
8. Peier, A. M. et al. A TRP channel that senses cold stimuli and menthol. *Cell* **108**, 705–715 (2002).
9. Tajino, K. et al. Application of menthol to the skin of whole trunk in mice induces autonomic and behavioral heat-gain responses. *Am. J. Physiol. Regul. Integr. Comp. Physiol.* **293**, R2128–R2135 (2007).
10. Ma, S. et al. Activation of the cold-sensing TRPM8 channel triggers UCP1-dependent thermogenesis and prevents obesity. *J. Mol. Cell Biol.* **4**, 88–96 (2012).
11. Ravussin, Y., Xiao, C., Gavrilova, O. & Reitman, M. L. Effect of intermittent cold exposure on brown fat activation, obesity, and energy homeostasis in mice. *PLoS ONE* **9**, e85876 (2014).
12. Cottle, W. & Carlson, L. D. Adaptive changes in rats exposed to cold; caloric exchange. *Am. J. Physiol.* **178**, 305–308 (1954).
13. Mineur, Y. S. et al. Nicotine decreases food intake through activation of POMC neurons. *Science* **332**, 1330–1332 (2011).
14. Fink, S. A. & Williams, J. A. Adrenergic receptors mediating depolarization in brown adipose tissue. *Am. J. Physiol.* **231**, 700–706 (1976).
15. Batt, R. A. & Topping, D. L. Acute effects of nicotine on plasma free fatty acid concentrations and on the response to cold stress, in lean and obese (genotype ob/ob) mice. *Int. J. Obes.* **3**, 7–13 (1979).
16. Steiner, G. & Evans, S. Sympathetic ganglia in brown adipose tissue: a new tool to study ganglionic stimulants. *Am. J. Physiol.* **222**, 111–113 (1972).
17. Sack, R. et al. Lower core body temperature and attenuated nicotine-induced hypothermic response in mice lacking the beta4 neuronal nicotinic acetylcholine receptor subunit. *Brain Res. Bull.* **66**, 30–36 (2005).
18. Hall, G. H. & Myers, R. D. Hypothermia produced by nicotine perfused through the cerebral ventricles of the unanaesthetized monkey. *Neuropharmacology* **10**, 391–398 (1971).
19. Rossato, M. et al. Human white adipocytes express the cold receptor TRPM8 which activation induces UCP1 expression, mitochondrial activation and heat production. *Mol. Cell. Endocrinol.* **383**, 137–146 (2014).
20. Reber, J. et al. Non-invasive measurement of brown fat metabolism based on optoacoustic imaging of hemoglobin gradients. *Cell. Metab.* **27**, 689–701 (2018). e684.
21. Fischer, A. W., Cannon, B. & Nedergaard, J. Optimal housing temperatures for mice to mimic the thermal environment of humans: An experimental study. *Mol. Metab.* **7**, 161–170 (2018).
22. Xiao, C., Goldgof, M., Gavrilova, O. & Reitman, M. L. Anti-obesity and metabolic efficacy of the beta3-adrenergic agonist, CL316243, in mice at thermoneutrality compared to 22 degrees C. *Obes. (Silver Spring).* **23**, 1450–1459 (2015).
23. Morton, G. J. & Schwartz, M. W. Leptin and the central nervous system control of glucose metabolism. *Physiol. Rev.* **91**, 389–411 (2011).
24. Inokuma, K. et al. Uncoupling protein 1 is necessary for norepinephrine-induced glucose utilization in brown adipose tissue. *Diabetes* **54**, 1385–1391 (2005).
25. Moraes, M. N. et al. Cold-sensing TRPM8 channel participates in circadian control of the brown adipose tissue. *Biochim. Biophys. Acta* **1864**, 2415–2427 (2017).
26. Vizin, R. C. L. et al. Short-term menthol treatment promotes persistent thermogenesis without induction of compensatory food consumption in Wistar rats: implications for obesity control. *J. Appl. Physiol. (1985)* **124**, 672–683 (2018).
27. Jiang, C. et al. Dietary menthol-induced TRPM8 activation enhances WAT "browning" and ameliorates diet-induced obesity. *Oncotarget* **8**, 75114–75126 (2017).
28. Almeida, M. C. et al. Pharmacological blockade of the cold receptor TRPM8 attenuates autonomic and behavioral cold defenses and decreases deep body temperature. *J. Neurosci.* **32**, 2086–2099 (2012).
29. Speakman, J. R. & Keijer, J. Not so hot: optimal housing temperatures for mice to mimic the thermal environment of humans. *Mol. Metab.* **2**, 5–9 (2012).
30. Gaskill, B. N. & Garner, J. P. Letter-to-the-editor on "not so hot: optimal housing temperatures for mice to mimic the thermal environment of humans". *Mol. Metab.* **3**, 335–336 (2014).
31. Cannon, B. & Nedergaard, J. Nonshivering thermogenesis and its adequate measurement in metabolic studies. *J. Exp. Biol.* **214**, 242–253 (2011).
32. Chavez-Noriega, L. E. et al. Pharmacological characterization of recombinant human neuronal nicotinic acetylcholine receptors h alpha 2 beta 2, h alpha 2 beta 4, h alpha 3 beta 2, h alpha 3 beta 4, h alpha 4 beta 2, h alpha 4 beta 4 and h alpha 7 expressed in Xenopus oocytes. *J. Pharmacol. Exp. Ther.* **280**, 346–356 (1997).
33. Karlsson, S. & Ahren, B. Insulin and glucagon secretion by ganglionic nicotinic activation in adrenalectomized mice. *Eur. J. Pharmacol.* **342**, 291–295 (1998).
34. Mountjoy, K. G., Mortrud, M. T., Low, M. J., Simerly, R. B. & Cone, R. D. Localization of the melanocortin-4 receptor (MC4-R) in neuroendocrine and autonomic control circuits in the brain. *Mol. Endocrinol.* **8**, 1298–1308 (1994).
35. Kishi, T. et al. Expression of melanocortin 4 receptor mRNA in the central nervous system of the rat. *J. Comp. Neurol.* **457**, 213–235 (2003).
36. Balthasar, N. et al. Divergence of melanocortin pathways in the control of food intake and energy expenditure. *Cell* **123**, 493–505 (2005).
37. Wu, Y. et al. Activation of AMPKalpha2 in adipocytes is essential for nicotine-induced insulin resistance in vivo. *Nat. Med.* **21**, 373–382 (2015).
38. Olsen, J. M. et al. Beta3-adrenergically induced glucose uptake in brown adipose tissue is independent of UCP1 presence or activity: Mediation through the mTOR pathway. *Mol. Metab.* **6**, 611–619 (2017).
39. Rossi, J. et al. Melanocortin-4 receptors expressed by cholinergic neurons regulate energy balance and glucose homeostasis. *Cell. Metab.* **13**, 195–204 (2011).
40. Audrain-McGovern, J. & Benowitz, N. L. Cigarette smoking, nicotine, and body weight. *Clin. Pharmacol. Ther.* **90**, 164–168 (2011).
41. Yoneshiro, T., Aita, S., Kawai, Y., Iwanaga, T. & Saito, M. Nonpungent capsaicin analogs (capsinoids) increase energy expenditure through the activation of brown adipose tissue in humans. *Am. J. Clin. Nutr.* **95**, 845–850 (2012).

ARTICLE

42. Ang, Q. Y. et al. A new method of infrared thermography for quantification of brown adipose tissue activation in healthy adults (TACTICAL): a randomized trial. *J. Physiol. Sci.* **67**, 395–406 (2017).

43. Yoneshiro, T. et al. Recruited brown adipose tissue as an antiobesity agent in humans. *J. Clin. Invest.* **123**, 3404–3408 (2013).

44. Sun, L. et al. Capsinoids activate brown adipose tissue (BAT) with increased energy expenditure associated with subthreshold 18-fluorine fluorodeoxyglucose uptake in BAT-positive humans confirmed by positron emission tomography scan. *Am. J. Clin. Nutr.* **107**, 62–70 (2018).

45. Michlig, S. et al. Effects of TRP channel agonist ingestion on metabolism and autonomic nervous system in a randomized clinical trial of healthy subjects. *Sci. Rep.* **6**, 20795 (2016).

46. Worthmann, A. et al. Cold-induced conversion of cholesterol to bile acids in mice shapes the gut microbiome and promotes adaptive thermogenesis. *Nat. Med.* **23**, 839–849 (2017).

47. Xu, W. et al. Multiorgan autonomic dysfunction in mice lacking the beta2 and the beta4 subunits of neuronal nicotinic acetylcholine receptors. *J. Neurosci.* **19**, 9298–9305 (1999).

48. Bautista, D. M. et al. The menthol receptor TRPM8 is the principal detector of environmental cold. *Nature* **448**, 204–208 (2007).

49. Bachman, E. S. et al. betaAR signaling required for diet-induced thermogenesis and obesity resistance. *Science* **297**, 843–845 (2002).

50. Hofmann, S. M. et al. Defective lipid delivery modulates glucose tolerance and metabolic response to diet in apolipoprotein E-deficient mice. *Diabetes* **57**, 5–12 (2008).

51. Broeders, E. P. et al. The bile acid chenodeoxycholic acid increases human brown adipose tissue activity. *Cell. Metab.* **22**, 418–426 (2015).

52. Dima, A., Burton, N. C. & Ntziachristos, V. Multispectral optoacoustic tomography at 64, 128, and 256 channels. *J. Biomed. Opt.* **19**, 36021 (2014).

53. Razansky, D., Buehler, A. & Ntziachristos, V. Volumetric real-time multispectral optoacoustic tomography of biomarkers. *Nat. Protoc.* **6**, 1121–1129 (2011).

54. Tzoumas, S. et al. Eigenspectra optoacoustic tomography achieves quantitative blood oxygenation imaging deep in tissues. *Nat. Commun.* **7**, 12121 (2016).

55. Tschop, M. H. et al. A guide to analysis of mouse energy metabolism. *Nat. Methods* **9**, 57–63 (2011).

Acknowledgements

Author contributions

Additional information

Publisher's note: Springer Nature remains neutral with regard to jurisdictional claims in published maps and institutional affiliations.

Christoffer Clemmensen[1,2], Sigrid Jall[1,3], Maximilian Kleinert[1,4], Carmelo Quarta[1], Tim Gruber[1,3], Josefine Reber[5,6], Stephan Sachs[1,7], Katrin Fischer[1], Annette Feuchtinger[10], Angelos Karlas[5,6], Stephanie E. Simonds[11], Gerald Grandl[1], Daniela Loher[1], Eva Sanchez-Quant[1], Susanne Keipert[1], Martin Jastroch[1], Susanna M. Hofmann[7,8,9], Emmani B.M. Nascimento[12], Patrick Schrauwen[12], Vasilis Ntziachristos[5,6], Michael A. Cowley[11], Brian Finan[1], Timo D. Müller[1] & Matthias H. Tschöp[1,3]

[1]Institute of Diabetes and Regeneration Research, Helmholtz Zentrum Muenchen, German Research Center for Environmental Health (GmbH), Neuherberg, Germany. [2]Novo Nordisk Foundation Center for Basic Metabolic Research, Faculty of Health and Medical Sciences, University of Copenhagen, Copenhagen, Denmark. [3]Division of Metabolic Diseases, Department of Medicine, Technische Universität München, Munich, Germany. [4]Section for Molecular Physiology, Department of Nutrition, Exercise and Sports, Faculty of Science, University of Copenhagen, Copenhagen, Denmark. [5]Institute of Biological and Medical Imaging, Helmholtz Zentrum München, German Research Center for Environmental Health (GmbH), Neuherberg, Germany. [6]Chair for Biological Imaging, Technical University of Munich, Munich, Germany. [7]Institute of Diabetes and Regeneration Research, Helmholtz Zentrum Muenchen, German Research Center for Environmental Health (GmbH), Neuherberg, Germany. [8]German Center for Diabetes Research (DZD), Neuherberg, Germany. [9]Medizinische Klinik und Poliklinik IV, Klinikum der Ludwig Maximilian Universität (LMU), Munich, Germany. [10]Research Unit Analytical Pathology, Helmholtz Zentrum München, Neuherberg, Germany. [11]Department of Physiology, and Biomedicine Discovery Institute, Monash University, Clayton, Australia. [12]Department of Human Biology and Human Movement Sciences, NUTRIM School for Nutrition and Translational Research in Metabolism, Maastricht University Medical Center, Maastricht, Netherlands. These authors contributed equally: Christoffer Clemmensen, Sigrid Jall.

DOI: 10.1038/s41467-018-07479-1   **OPEN**

Publisher Correction: Coordinated targeting of cold and nicotinic receptors synergistically improves obesity and type 2 diabetes

Christoffer Clemmensen [1,2], Sigrid Jall[1,3], Maximilian Kleinert[1,4], Carmelo Quarta[1], Tim Gruber[1,3], Josefine Reber[5,6], Stephan Sachs[1,7], Katrin Fischer[1], Annette Feuchtinger[10], Angelos Karlas[5,6], Stephanie E. Simonds[11], Gerald Grandl[1], Daniela Loher[1], Eva Sanchez-Quant[1], Susanne Keipert[1], Martin Jastroch[1], Susanna M. Hofmann[7,8,9], Emmani B.M. Nascimento[12], Patrick Schrauwen[12], Vasilis Ntziachristos[5,6], Michael A. Cowley [11], Brian Finan [1], Timo D. Müller[1] & Matthias H. Tschöp[1,3]

Correction to: *Nature Communications* https://doi.org/10.1038/s41467-018-06769-y; published online 23 October 2018

In the original PDF version of this article, affiliation 1, 'Institute for Diabetes and Obesity, Helmholtz Diabetes Center (HDC), Helmholtz Zentrum Muenchen & German Center for Diabetes Research (DZD), Neuherberg, Germany', was incorrectly given as 'Institute of Diabetes and Regeneration Research, Helmholtz Zentrum Muenchen, German Research Center for Environmental Health (GmbH), Neuherberg, Germany '. This has now been corrected in the PDF version of the article; the HTML version was correct at the time of publication.

Published online: 20 November 2018

[1]Institute for Diabetes and Obesity, Helmholtz Diabetes Center (HDC), Helmholtz Zentrum Muenchen & German Center for Diabetes Research (DZD), Neuherberg, Germany. [2]Novo Nordisk Foundation Center for Basic Metabolic Research, Faculty of Health and Medical Sciences, University of Copenhagen, Copenhagen, Denmark. [3]Division of Metabolic Diseases, Department of Medicine, Technische Universität München, Munich, Germany. [4]Section for Molecular Physiology, Department of Nutrition, Exercise and Sports, Faculty of Science, University of Copenhagen, Copenhagen, Denmark. [5]Institute of Biological and Medical Imaging, Helmholtz Zentrum München, German Research Center for Environmental Health (GmbH), Neuherberg, Germany. [6]Chair for Biological Imaging, Technical University of Munich, Munich, Germany. [7]Institute of Diabetes and Regeneration Research, Helmholtz Zentrum Muenchen, German Research Center for Environmental Health (GmbH), Neuherberg, Germany. [8]German Center for Diabetes Research (DZD), Neuherberg, Germany. [9]Medizinische Klinik und Poliklinik IV, Klinikum der Ludwig Maximilian Universität (LMU), Munich, Germany. [10]Research Unit Analytical Pathology, Helmholtz Zentrum München, Neuherberg, Germany. [11]Department of Physiology, and Biomedicine Discovery Institute, Monash University, Clayton, Australia. [12]Department of Human Biology and Human Movement Sciences, NUTRIM School for Nutrition and Translational Research in Metabolism, Maastricht University Medical Center, Maastricht, Netherlands. These authors contributed equally: Christoffer Clemmensen, Sigrid Jall. Correspondence and requests for materials should be addressed to B.F. (email: brian.finan@helmholtz-muenchen.de)
or to T.D.Mül. (email: timo.mueller@helmholtz-muenchen.de) or to M.H.Töp. (email: matthias.tschoep@helmholtz-muenchen.de)

SUPPLEMENTAL MATERIAL

Coordinated Targeting of Cold and Nicotinic Receptors Synergistically Improves Obesity and Type 2 Diabetes

Christoffer Clemmensen, Sigrid Jall, Maximilian Kleinert, Carmelo Quarta, Tim Gruber, Josefine Reber, Stephan Sachs, Katrin Fischer, Annette Feuchtinger, Angelos Karlas, Stephanie E. Simonds, Gerald Grandl, Daniela Loher, Eva Sanchez-Quant, Susanne Keipert, Martin Jastroch, Susanna M. Hofmann, Emmani B.M. Nascimento, Patrick Schrauwen, Vasilis Ntziachristos, Michael A. Cowley, Brian Finan, Timo D. Müller and Matthias H. Tschöp

Supplemental Figure 1. TRPM8 is not expressed in murine brown adipocytes and icilin has no direct effect on brown fat thermogenesis in mouse or human primary adipocytes

(a) Effect on body lean and fat mass after daily s.c. administration to DIO male C57Bl6j mice of vehicle (black, n=8), icilin 0.6 mg/kg (light blue, n=8), or icilin 6 mg/kg (dark blue, n=6) for 14 days. (b) CT values of gene transcripts in BAT of female warm (30°C, n=8) and cold (5°C, n=7) acclimatized mice. (c) Effects of vehicle (black, n=3), icilin 1 μM (light blue, n=3), icilin 10 μM (dark blue, n=3), or isoproterenol (red, n=3) on UCP1 mRNA levels in primary brown adipocytes from C57Bl6j mice. (d) Effects of vehicle (black, n=22), icilin 1 μM (light blue, n=22), or norepinephrine 1 μM (red, n=24) on oxygen consumption rate (OCR) of primary brown adipocytes from C57Bl6j mice. (e) Effect of vehicle (black, n=3), icilin 1 μM (light blue, n=3), or icilin 10 μM (dark blue, n=3) on UCP1 mRNA expression in cultured adipocytes derived from human BAT. (f) Effects of vehicle (black, n=3) and icilin 1 μM (light blue, n=3) on OCR of primary adipocytes derived from human BAT. ***$p < 0.001$ by one-way ANOVA (a, c, e) with Tukey post-hoc test. All data are presented as mean ± SEM.

Supplemental Figure 2. Nicotine lowers body weight but has no impact on glucose tolerance in diet-induced obese mice

(a) Effects on body weight, (b) food intake, and (c-d) glucose tolerance following daily s.c. injections to DIO male C57Bl6j mice of vehicle (black, n=8), nicotine 1 mg/kg (green, n=8), and nicotine 2.5 mg/kg (turquoise, n=8) for 14 days. *p < 0.05, **p < 0.01, ***p < 0.001 by two-way ANOVA (a, b, c) and one-way ANOVA (d) with Tukey post-hoc test. All data are presented as mean ± SEM.

Clemmensen *et al.*, 2018, *Nature Communications* – Supplementary Material
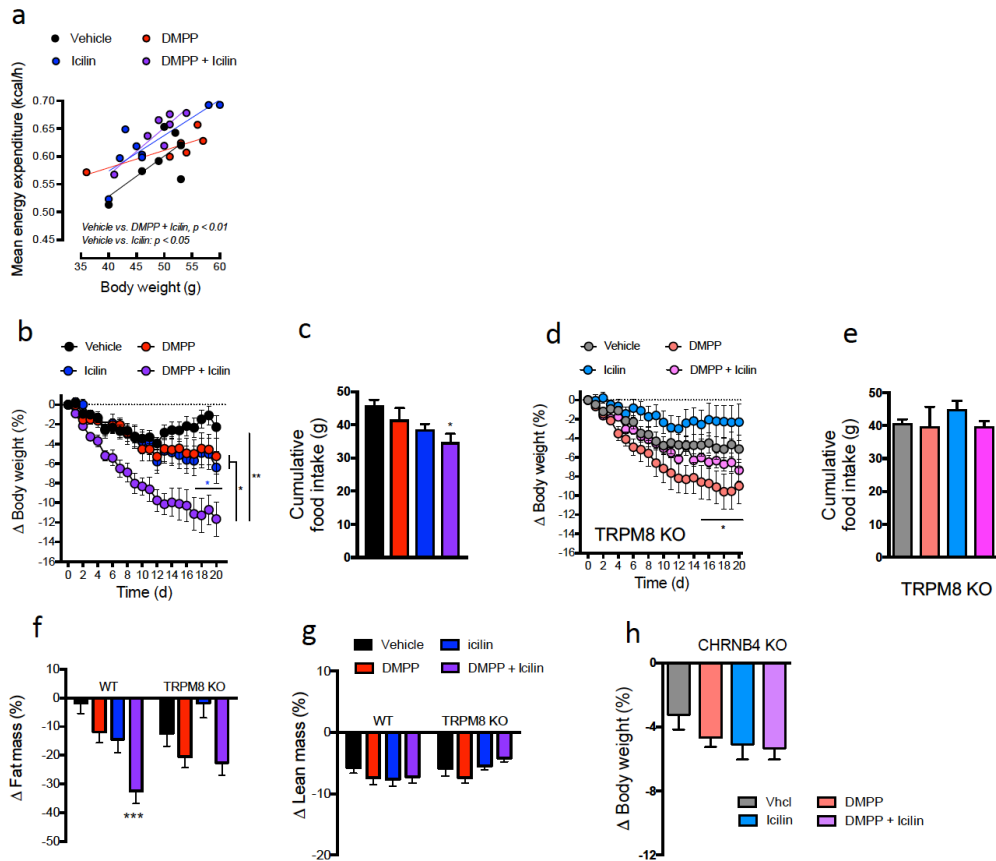
Supplemental Figure 3. Chronic DMPP and icilin co-administration increases energy expenditure by activating TRPM8 and CHRNB4

(a) Effect on mean energy expenditure with body weight as covariate following daily s.c. injections to DIO male C57Bl6j mice of vehicle (black, n=7), DMPP 5 mg/kg (red, n=6), icilin 5 mg/kg (blue, n=8), or the combination of DMPP 5 mg/kg and icilin 5 mg/kg (purple, n=7) for 3 days. (b) Effects on body weight and (c) cumulative food intake in DIO male WT mice compared to (d) effects on body weight and (e) cumulative food intake in DIO male TRPM8 KO mice. (f-g) Effects on fat and lean mass following daily s.c. injections to DIO WT and TRPM8 KO mice of vehicle (black, n=8/grey, n=8), DMPP 5 mg/kg (red, n=8/light red, n=8), icilin 5 mg/kg (blue, n=8/light blue, n=8), or the combination of DMPP 5 mg/kg and icilin 5 mg/kg (purple, n=8/pink, n=8) for 21 days. (h) Effects on body weight in DIO male CHRNB4 KO mice treated daily with s.c. injections of vehicle (grey, n=7), DMPP 5 mg/kg (light red, n=6), icilin 5 mg/kg (light blue, n=7), or the combination of DMPP 5 mg/kg and icilin 5 mg/kg (light purple, n=7) for 7 days. *p < 0.05, **p < 0.01, ***p < 0.001 by ANCOVA (vehicle vs. DMPP: p=0.52; vehicle vs. icilin: p=0.048, vehicle vs. DMPP/icilin: p=0.009), two-way ANOVA (b, d), and one-way ANOVA (c, e, f, g, h) with Tukey post-hoc test. All data are presented as mean ± SEM.

Supplemental Figure 4. Effects of sub-chronic administration of DMPP and icilin on thermogenic gene programs in DIO WT mice

Expression of genes in the BAT involved in (a) thermogenesis, (b) mitochondrial respiration chain, (c) creatine signaling pathway, and (d) proteasomal signaling in DIO male C57Bl6j mice. Expression of genes in the iWAT involved in (e) thermogenesis, (f) mitochondrial respiration chain, (g) creatine signaling pathway, and (h) proteasomal signaling in DIO male C57Bl6j mice. Tissues were analyzed following daily s.c. injections of vehicle (black, n=8), DMPP 5 mg/kg (red, n=8), icilin 5 mg/kg (blue, n=8), or the combination of DMPP 5 mg/kg and icilin 5 mg/kg (purple, n=8) for 7 days. *p < 0.05 by one-way ANOVA (a-h) with Tukey post-hoc test. All data are presented as mean ± SEM.

Supplemental Figure 5. Effects of sub-chronic administration of DMPP and icilin on thermogenic gene programs in betaless mice

Expression of genes in the BAT involved in (a) thermogenesis, (b) mitochondrial respiration chain, (c) creatine signaling pathway, and (d) proteasomal signaling in DIO male betaless mice. Expression of genes in the iWAT involved in (e) thermogenesis, (f) mitochondrial respiration chain, (g) creatine signaling pathway, and (h) proteasomal signaling in DIO male betaless mice. Tissues were analyzed following daily s.c. injections of vehicle (black, n=6), DMPP 5 mg/kg (orchid, n=6), icilin 5 mg/kg (ocean-blue, n=6), or the combination of DMPP 5 mg/kg and icilin 5 mg/kg (bordeaux, n=6) for 7 days. *p < 0.05 by one-way ANOVA with Tukey post-hoc test. All data are presented as mean ± SEM.
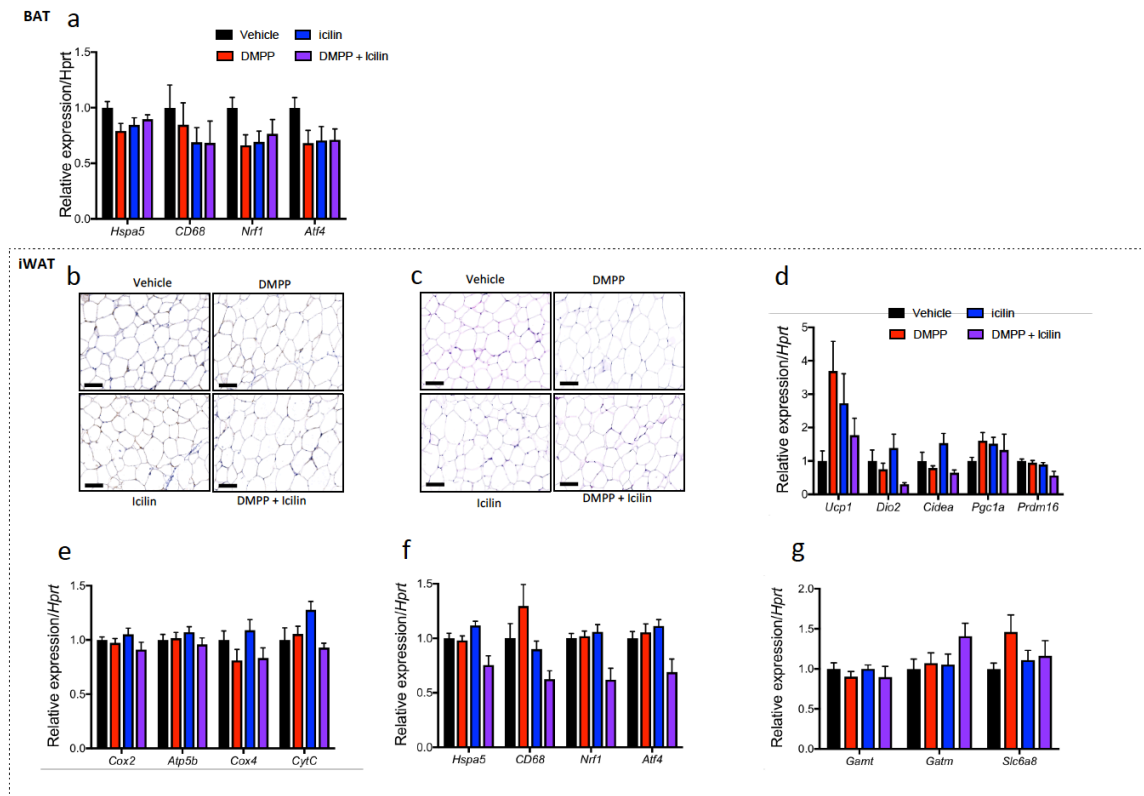
Supplemental Figure 6. Chronic administration of DMPP and icilin has no impact on iWAT thermogenic programs in DIO WT mice housed at thermoneutral conditions

(a) BAT expression of genes involved in proteasomal signaling following daily s.c. injections of vehicle (black, n=8), DMPP 5 mg/kg (red, n=7), icilin 5 mg/kg (blue, n=8), or the combination of DMPP 5 mg/kg and icilin 5 mg/kg (purple, n=7) to DIO male C57Bl6j chronically housed at 30ºC for 14 days. (b) UCP1 immunoreactivity staining in iWAT and (c) iWAT H & E staining. iWAT expression of genes involved in (d) thermogenesis, (e) mitochondrial respiration chain, (f) proteasomal signaling, and (g) creatine signaling pathway following daily s.c. injections of vehicle (black, n=8), DMPP 5 mg/kg (red, n=7), icilin 5 mg/kg (blue, n=8), or the combination of DMPP 5 mg/kg and icilin 5 mg/kg (purple, n=7) to DIO male C57Bl6j chronically housed at 30ºC for 14 days. All scale bars are 100μm. Data (a, d, e, f, g) were analyzed by one-way ANOVA with Tukey post-hoc test. All data are presented as mean ± SEM
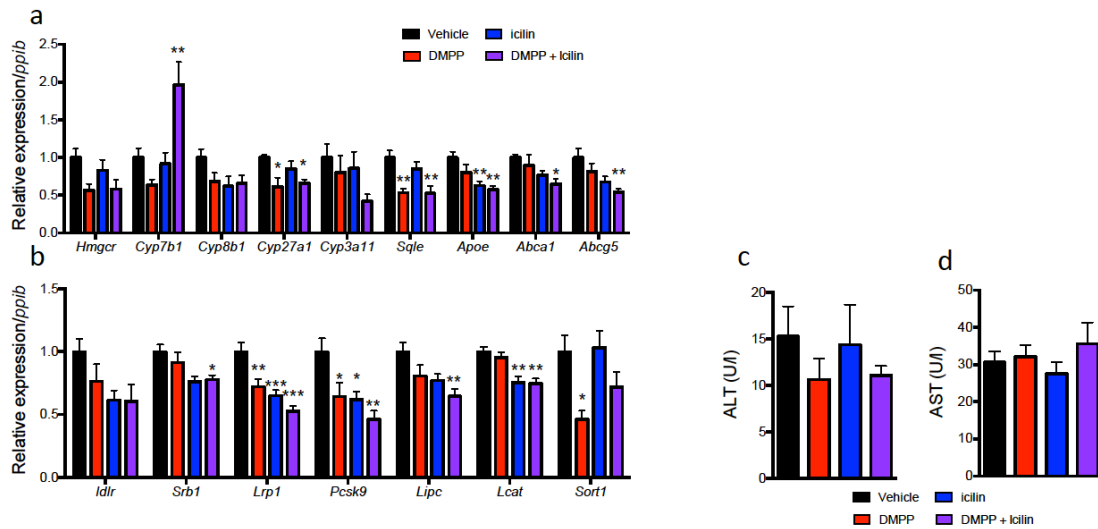
Supplemental Figure 7. Effects of sub-chronic administration of DMPP and icilin on hepatic gene expression, lipid content, and liver function

Hepatic expression of genes involved in (a) bile acid metabolism and (b) lipoprotein uptake following daily s.c. injections to DIO male C57Bl6j mice of vehicle (black, n=8), DMPP 5 mg/kg (red, n=8), icilin 5 mg/kg (blue, n=8), or the combination of DMPP 5 mg/kg and icilin 5 mg/kg (purple, n=8) for 7 days. Effects on plasma (c) ALT and (d) AST following daily s.c. injections to DIO male C57Bl6j mice of vehicle (black, n=7), DMPP 5 mg/kg (red, n=7), icilin 5 mg/kg (blue, n=6), or the combination of DMPP 5 mg/kg and icilin 5 mg/kg (purple, n=7) for 21 days *p < 0.05, **p < 0.01, ***p < 0.001 by one-way ANOVA (a-d) with Tukey post-hoc test. All data are presented as mean ± SEM.
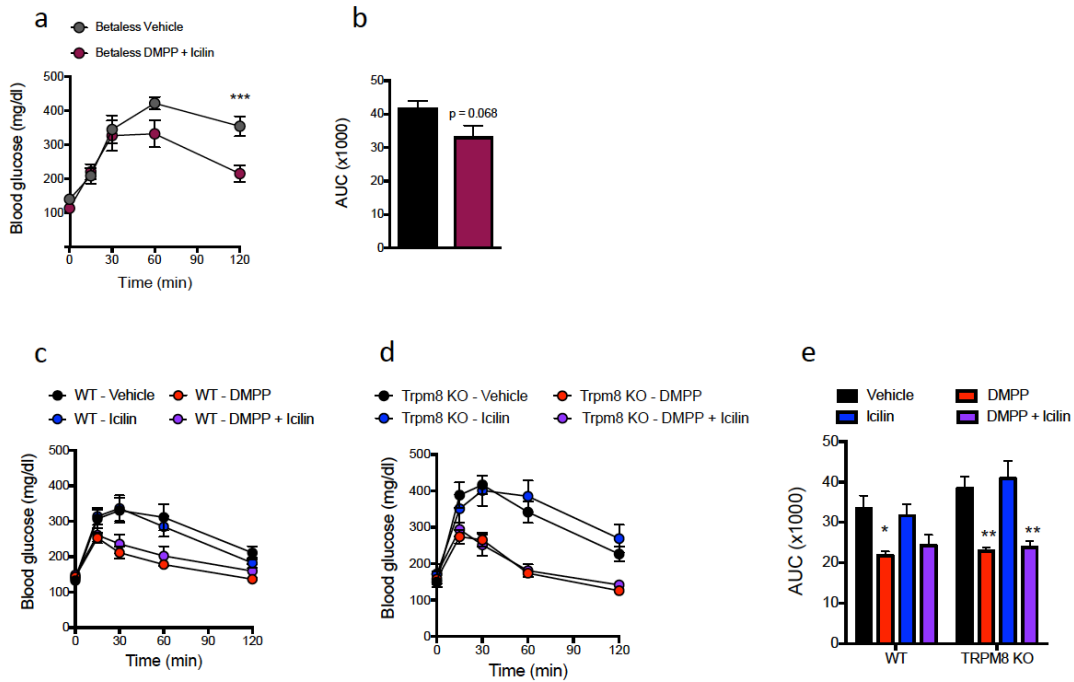
Supplemental Figure 8. Beta adrenergic receptors and TRPM8 receptors are dispensable for the glycemic benefits of DMPP and icilin co-administration

(a-b) Effects on glucose tolerance following daily s.c. injections to DIO male betaless mice of vehicle (black, n=6) or the combination of DMPP 5 mg/kg and icilin 5 mg/kg (bordeaux, n=6) for 7 days. (c-e) Effects on glucose tolerance following daily s.c. injections to DIO male TRPM8 WT and KO mice of vehicle (black, n=7 (WT) and n=8 (KO)), DMPP 5 mg/kg (red, n=8), icilin 5 mg/kg (blue, n=8), or the combination of DMPP 5 mg/kg and icilin 5 mg/kg (purple, n=8) for 21 days. *p < 0.05, **p < 0.01, ***p < 0.001 by two-way ANOVA (a, c, d), one-way ANOVA (e) with Tukey post-hoc test, or two-tailed Student's *t*-test (b). All data are presented as mean ± SEM.

Supplemental Table 1: List of primers

Gene name	Forward sequence (5' – 3')	Reverse sequence (3' – 5')
Abca1	AAAACCGCAGACATCCTTCAG	CATACCGAAACTCGTTCACCC
Abcg5	GTACATCGAGAGTGGCCAGA	CTGTGTATCGCAACGTCTCG
Apoe	GATCAGCTCGAGTGGCAAAG	TAGTGTCCTCCATCAGTGCC
Atf4	GATGAGCTTCCTGAACAGCG	GCCAAGCCATCATCCATAGC
Atp5b	CCGGGCAAGAAAGATACAGC	GTCCCACCATGTAGAAGGCT
Cd68	ACAAAACCAAGGTCCAGGGA	ATTCTGCGCCATGAATGTCC
Cidea	AATGGACACCGGGTAGTAAGT	CAGCCTGTATAGGTCGAAGGT
Cox2	GCCCTTCAAGCTCCTAGGTA	CTGGATCCTCTGCTTAGCGA
Cox4	CTAGAGGGACAGGGACACAC	TGGTTCATCTCTGCGAAGGT
Cyp3a11	CTCTCACTGGAAACCTGGGT	TCTGTGACAGCAAGGAGAGG
Cyp7b1	TCTGGGCCTCTCTAGCAAAC	GCACTTCTCGGATGATGCTG
Cyp8b1	CAGCGGACAAGAGTACCAGA	TGGATCTTCTTGCCCGACTT
Cyp27a1	CTTCATCGCACAAGGAGAGC	CCAAGGCAAGGTGGTAGAGA

CytC	GTTCAGAAGTGTGCCCAGTG	GTCTGCCCTTTCTCCCTTCT
Dio2	TGCCACCTTCTTGACTTTGC	GGTTCCGGTGCTTCTTAACC
Hmgcr	AGCTTGCCCGAATTGTATGTG	TGTGTTGTGAACCATGTGACTTC
Hprt	AAGCTTGCTGGTGAAAAGGA	TTGCGCTCATCTTAGGCTTT
Hspa5	GACTGCTGAGGCGTATTTGG	AGCATCTTTGGTTGCTTGTCG
Lcat	GTGCTCCACTTCTTACTGCG	GAACACATGGTCTTCAGGCC
Ldlr	TCAGACGAACAAGGCTGTCC	CCATCTAGGCAATCTCGGTCTC
Lipc	ATGTGGGGTTAGTGGACTGG	TTGTTCTTCCCGTCCATGGA
Lrp1	AACCTTATGAATCCACGCGC	TTCTTGGGGCCATCATCAGT
Nrf1	ACCCAAACTGAACACATGGC	GCAGTTACCTCATCAGCTGC
Pgc1a	AGCCGTGACCACTGACAACGAG	GCTGCATGGTTCTGAGTGCTAAG
Ppib	GCATCTATGGTGAGCGCTTC	CTCCACCTTCCGTACCACAT
Prdm16	CCGCTGTGATGAGTGTGATG	GGACGATCATGTGTTGCTCC
Sort1	ATCCCAGGAGACAAATGCCA	AACCTTCCGCCACAGACATA
Sqle	TGTTGCGGATGGACTCTTCT	GAGAACTGGACTGGGGTTGA

Supplemental Table 2: List of TaqMan probes

Gene name	Assay ID
Ckmt1	Mm00438221_m1
Ckmt2	Mm01285553_m1
Gamt	Mm00487473_m1
Gatm	Mm00491879_m1
Hprt	Mm01545399_m1
Ppib	Mm00478295_m1
Slc6a8	Mm0050623_m1
Trpm8	Mm01299593_m1
UCP1	Mm01244861_m1

Chapter 3 – *Role of downstream signaling molecule in body weight regulation, glucose metabolism, and cold receptor activation*

Manuscript in revision
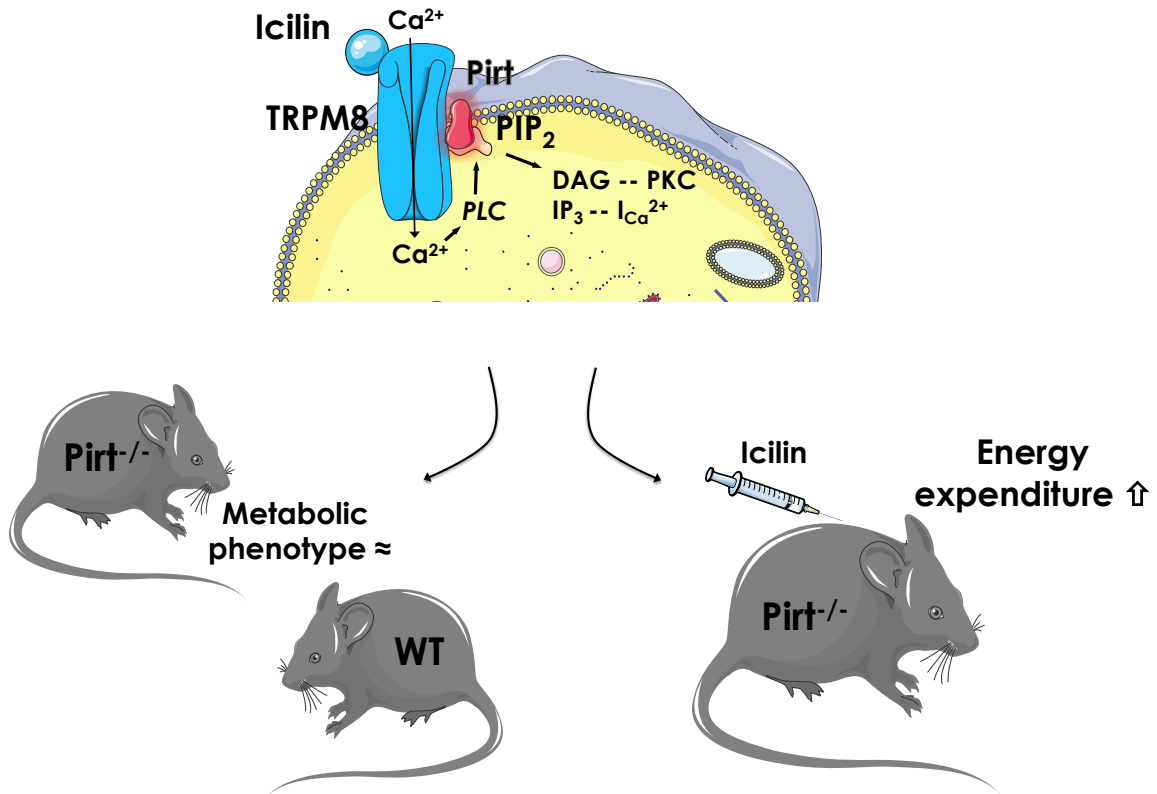
Figure 3. 3: Effect of the lack of Pirt (Pirt$^{-/-}$) on metabolism and icilin-mediated TRPM8 activation in mice *in vivo*. Suggested cellular model of Pirt involvement in TRPM8 signaling as modified from Yee N.S., 2016. Summary of metabolic consequence of genetic knockout of Pirt in male WT and Pirt$^{-/-}$ mice. In female Pirt$^{-/-}$ mice, body fat mass is significantly increased (not shown here). Lack of Pirt still leads to increase in energy expenditure upon icilin treatment in female mice. The figure was created using Sevier medical art and summarizes chapter III.

Pirt deficiency has subtle female-specific effects on energy and glucose metabolism in mice

Sigrid Jall[1,2,3], Brian Finan[1,3], Katrin Fischer[1,3], Gustav Collden[1,3], Xinzhong Dong[4], Matthias H. Tschöp[1,2,3], Timo D. Müller[1,3,*], Christoffer Clemmensen[1,3,5*]

[1]Institute for Diabetes and Obesity, Helmholtz Diabetes Center at Helmholtz Zentrum München, German Research Center for Environmental Health (GmbH), 85764 Neuherberg, Germany
[2]Division of Metabolic Diseases, Department of Medicine, Technische Universität München, 80333 Munich, Germany
[3]German Center for Diabetes Research (DZD), 85764 Neuherberg, Germany
[4]The Solomon H. Snyder Department of Neuroscience, Center for Sensory Biology, Johns Hopkins University School of Medicine, Baltimore, MD 21205, USA.
[5]Novo Nordisk Foundation Center for Basic Metabolic Research, Faculty of Health and Medical Sciences, University of Copenhagen, DK-2200 Copenhagen N, Denmark

*Co-corresponding authors:

Timo D. Müller; Phone: +49 89 3187-2106; Address: Institute for Diabetes and Obesity; Ingolstädter Landstraße 1, D-85764 Neuherberg; timo.mueller@helmholtz-muenchen.de

Christoffer Clemmensen; Phone: +45 22 91 63 33; Address: NNF Center for Basic Metabolic Research Nutrient and Metabolite Sensing; Blegdamsvej 3B, DK-2200 Copenhagen N; chc@sund.ku.dk

Manuscript in revision

Abstract

Objective: The contribution of brown adipose tissue (BAT) to adult human metabolic control is a topic of ongoing investigation. In context, understanding the cellular events leading to BAT uncoupling, heat production, and energy expenditure is anticipated to produce significant insight into this endeavor. The phosphoinositide interacting regulator of transient receptor potentials (Pirt) was recently put forward as a key protein regulating cold sensing downstream of the transient receptor potential melastatin 8 (TRPM8). Notably, TRPM8 has been identified as a non-canonical regulator of BAT thermogenesis. The aim of this investigation was to delineate the role of Pirt in energy homeostasis and glucose metabolism - and the possible involvement of Pirt in TRPM8-elicited energy expenditure.

Methods: To this end, we metabolically phenotyped male and female Pirt deficient (Pirt$^{-/-}$) mice exposed to a low-fat chow diet or to a high-fat, high-sugar (HFHS) diet.

Results: We identified that chow-fed female Pirt$^{-/-}$ mice have an increased susceptibility to develop obesity and glucose intolerance. This effect is abrogated when the mice are exposed to a HFHS diet. Conversely, Pirt$^{-/-}$ male mice display no metabolic phenotype on either diet relative to wild-type (WT) control mice. Finally, we observed that Pirt is dispensable for TRPM8-evoked energy expenditure.

Conclusion: We here report subtle metabolic abnormalities in female, but not male, Pirt$^{-/-}$ mice. Future studies are required to tease out if metabolic stressors beyond dietary interventions, e.g. temperature fluctuations, are interacting with Pirt-signaling and metabolic control in a sex-specific fashion.

Keywords
Signaling molecule; sex differences; body weight; energy metabolism; TRPM8; brown adipose tissue

Abbreviations
ARH: arcuate nucleus; BAT: brown adipose tissue; CT: cycle of threshold; DIO: diet-induced obese; eWAT: epididymal white adipose tissue; HFHS: high-fat, high-sugar; Hprt: hypoanthine-guanine phosphoribosyltransferase; hrs: hours; IHC: immunohistochemistry; i.p.: intraperitoneal; ipGTT: intraperitoneal glucose tolerance test; iWAT: inguinal white adipose tissue; ME: median eminence; NE: norepinephrine; PBS: phosphate-buffered saline; PFA: paraformaldehyde; PIP$_2$: phosphatidylinositol 4,5-bisphosphate; Pirt: phosphoinositide interacting regulator of transient receptor potentials; Pirt$^{-/-}$: Pirt deficient; Ppib: peptidylprolyl isomerase B; qPCR: quantitative real-time PCR; RER: respiratory exchange ratio; s.c.: subcutaneous; TBS: tris-buffered saline; TRPM8: transient receptor potential melastatin 8; TRPV1: TRP vanilloid 1; UCP1: uncoupling protein 1; VMH: ventromedial hypothalamic nucleus; WT: wild-type

1. Introduction

The ongoing global obesity epidemic is a consequence of a persistent positive energy balance emerging when food intake chronically exceeds energy expenditure [1]. Since the evidence of active brown adipose tissue (BAT) in humans, targeting of this metabolically active tissue has surfaced as a promising therapeutic intervention to keep energy balance and body weight in check [2-5]. Physiologically, BAT thermogenesis increases with prolonged exposure to cold, enabling mammals to maintain core body temperature upon fluctuations in environmental temperatures [6]. During this process of adaptive thermogenesis, norepinephrine (NE) released from sympathetic neurons activates β3-adrenoceptors on the cell surface of the brown adipocytes, which initiates a signaling cascade that results in activation of the uncoupling protein 1 (UCP1) and dissipation of heat at the expense of ATP production [6-9]. In contrast to the indirect activation of UCP1-dependent non-shivering thermogenesis upon cold temperatures, recent advances suggested the direct expression of a cold receptor, transient receptor potential melastatin 8 (TRPM8) on brown adipocytes [10].

TRPM8 channels are typically known to be expressed in dorsal root ganglia and they are activated upon temperatures below ~26ºC [11, 12]. The observation that TRPM8 channels can also be activated by exogenous ligands such as menthol or icilin ignited research interest in a potential role of TRPM8 in the pharmacological treatment of obesity [11, 12]. Of appreciable note, activation of TRPM8 channels with icilin acutely causes an increase in energy expenditure in mice, and long-term treatment with dietary menthol or subcutaneous injections of icilin prevents weight gain or lowers body weight in diet-induced obese (DIO) mice [10, 13]. Moreover, icilin treatment in mice housed at thermoneutrality, and in which BAT thermogenesis is at a minimum, leads to the re-expression of UCP1 protein in the BAT [13]. Controversies exist to date whether the effects of TRPM8 induction are mediated indirectly [13, 14] or directly [10], but together these findings suggest that pharmacological targeting of TRPM8 might be a viable anti-obesity strategy and thus underscore the imperative task of parsing out the molecular mechanisms connecting TRPM8 to energy expenditure and BAT thermogenesis. Phosphoinositide interacting regulator of TRPs (Pirt) was established as an endogenous regulator of TRP channels, including heat-sensing TRP vanilloid 1 (TRPV1) [15] and more recently cold-sensing TRPM8 [16, 17]. Pirt is a transmembrane protein predominantly expressed in dorsal root ganglia that increases sensitivity to exogenous TRPM8 stimulation in conjunction with the canonical cellular signal phosphatidylinositol 4,5-bisphosphate (PIP$_2$) [16, 18]. Pirt deficient (Pirt$^{-/-}$) mice have an impaired response to cold, indicating that the protein is involved in temperature sensation/regulation [16]. Moreover,

Pirt^{-/-} mice display a blunted behavioral response to icilin [16], suggesting that Pirt is required for both physiological and pharmacological TRPM8-based signaling.

Here we report that Pirt deficient female mice have an increased body weight and impaired glucose tolerance relative to wild-type (WT) mice. This increased susceptibility to develop obesity and glucose intolerance in Pirt^{-/-} is abrogated in the face of a high-fat, high-sugar (HFHS) diet as well as in male mice irrespective of the dietary regime. Finally, we reveal that Pirt is dispensable for TRPM8-induced BAT thermogenesis *in vivo*.

2. Material and Methods

2.1 Animal Housing and Phenotyping Conditions

The generation of the Pirt^{-/-} mouse is described elsewhere [15]. The cohorts were generated from homozygous breeding. Mice were maintained at 23 ± 1ºC, constant humidity, and on a 12 hour light-dark cycle with free access to food and water. Phenotypic analysis of Pirt^{-/-} mice and WT mice was initiated at the age of 8 weeks. A male and female cohort of eight WT and eight Pirt^{-/-} mice was phenotypically monitored on a standard chow diet. Another cohort of eight male and female WT and Pirt^{-/-} mice was switched from chow to HFHS diet (58% kcal from fat; D12331, Research Diets, New Brunswick, NJ, USA) at the age of 8 weeks. Body weight and food intake were assessed on a weekly basis until the age of 25 weeks. All procedures were approved by the Animal Use and Care Committee of Bavaria, Germany.

2.2 Glucose Tolerance Test

At 26 weeks of age, a glucose tolerance test was performed. Mice were fasted for 6 hours (hrs) and challenged with a bolus injection of glucose (5 µl/g body weight, intraperitoneal (i.p.)). Male mice on a chow and HFHS diet received 1.5 g glucose/kg body weight; female mice on a chow and HFHS diet were injected with 2.0 g glucose/kg body weight. Blood glucose was measured from the tail veins at the indicated timepoints with a handheld glucometer (Abbott GmbH & Co. KG, Wiesbaden, Germany).

2.3 Energy Metabolism Studies

Energy expenditure, respiratory exchange ratio (RER), and home-cage locomotor activity were assessed in 27-weeks old chow-fed female WT and Pirt^{-/-} using a combined indirect calorimetry system (TSE Systems, Bad Homburg, Germany). After a 24 hrs adaptation phase,

oxygen consumption and carbon dioxide production were measured every 10 minutes for up to 61 hrs.

2.4 Whole Body Composition

Whole-body composition (fat and lean mass) was measured using nuclear magnetic resonance technology (EchoMRI, Houston, TX, USA).

2.5 Acute Icilin Challenge

Female chow-fed WT and Pirt^{-/-} mice received a single injection of phosphate-buffered saline (PBS) or icilin (2 µmol/kg body weight; 5 µl/g body weight injection volume, subcutaneous (s.c.); Cat.No. 36945-98-9 (ROE01), Bicoll, Planegg, Germany), while oxygen consumption, carbon dioxide production, and locomotor activity were registered with indirect calorimetry.

2.6 Immunohistochemistry

WT and Pirt^{-/-} male mice were anesthetized with carbon dioxide and perfused by intracardiac puncture with saline and fixed with 4% paraformaldehyde (PFA) solution. Brains were harvested, kept in 4% PFA for 24 hrs at 4ºC, transferred to 30% sucrose, and sliced on a cryostat in the coronal plane at 30 µm. The slices were blocked in 0.25% gelatin and 0.5% Triton X-100 in tris-buffered saline (TBS) for 1 hour and incubated with Pirt (1:500, Biorbyt LLC, orb158159) antibody diluted in the blocking solution (TBS containing 0.25% gelatin and 0.5% Triton X-100) at 4ºC, overnight. Sections were washed 3 times in TBS and incubated with Alexa Fluor® 568 (1:500, Thermo Fisher Scientific, A-11011) diluted in the blocking solution for 1 hour at room temperature and stained with DAPI solution (1:3000, Thermo Fisher Scientific, 62248) for 3 minutes. Sections were washed in TBS, dried, and mounted with Slowfade Gold mounting medium (Thermo Fisher Scientific). Image stacks (30 µm thick) were collected through the z-axis at an interval of 2 µm using a Leica SP5 scanning confocal microscope equipped with a 20x objective and final images obtained by maximum intensity projection of the z-stack.

2.7 Gene expression analysis

For expression profiling of Pirt, tissues were collected from male C57Bl/6j WT and Pirt^{-/-} mice and immediately frozen on dry ice. RNA was extracted using QIAzol® Lysis Reagent (Qiagen, Hilden, Germany) and cDNA was synthesized using a QuantiTect Reverse Transcription Kit (Qiagen). Gene expression was profiled with quantitative real-time PCR

(qPCR) using SYBR® Green Real-Time PCR master mix (Life Technologies GmbH, Darmstadt, Germany). The relative expression of the Pirt gene (Forward primer 5´ACCACACCCAAAAGCAACTG´3; Reverse primer 5´GCCCTATCATCCTGAGCACT´3) was normalized to the reference genes hypoanthine-guanine phosphoribosyltransferase (Hprt) (Forward primer 5´AAGCTTGCTGGTGAAAAGGA´3; Reverse primer 5´TTGCGCTCATCTTAGGCTTT´3) and peptidylprolyl isomerase B (Ppib) (Forward primer 5´GCATCTATGGTGAGCGCTTC´3; Reverse primer 5´CTCCACCTTCCGTACCACAT´3). We used the threshold cycle method ($2^{-\Delta\Delta CT}$) of comparative PCR to analyze the results.

2.8 Statistical Analysis

Differences between genotypes or treatment were assessed by two-way ANOVA followed by Bonferroni`s post hoc analysis as appropriate or an unpaired two-tailed Student's t-test. All results are presented as mean ± s.e.m. *P* < 0.05 was considered statistically significant.

3. Results

3.1 Pirt expression

Pirt is reported to be highly expressed in dorsal root ganglia, enteric neurons, and sympathetic neurons [15]. Aiming to uncover a role for Pirt in energy metabolism, we here investigated Pirt expression in key metabolic tissues including adipose tissue and the hypothalamus. We report that Pirt is highly expressed in the cardiac muscle, the pituitary gland, and the hypothalamus (Fig 1a). Pirt is not detectable in BAT, suggesting that any involvement in energy expenditure is mediated indirectly, likely through the peripheral nervous system (Fig 1a). Conversely, the observation that Pirt is highly expressed in the hypothalamus prompted us to further parse the expression pattern in this region, using immunohistochemistry (IHC) on brain slices from WT and Pirt$^{-/-}$ mice (Fig. 1b). Therewith, we identify consistent Pirt protein expression in hypothalamic regions of the arcuate nucleus (ARH), the median eminence (ME), and part of the ventromedial hypothalamic nucleus (VMH). This expression pattern suggests that Pirt might play a role in the central control of energy metabolism. Knockout of the Pirt gene and the Pirt protein in the hypothalamus was confirmed by IHC and qPCR (Fig 1b,c).
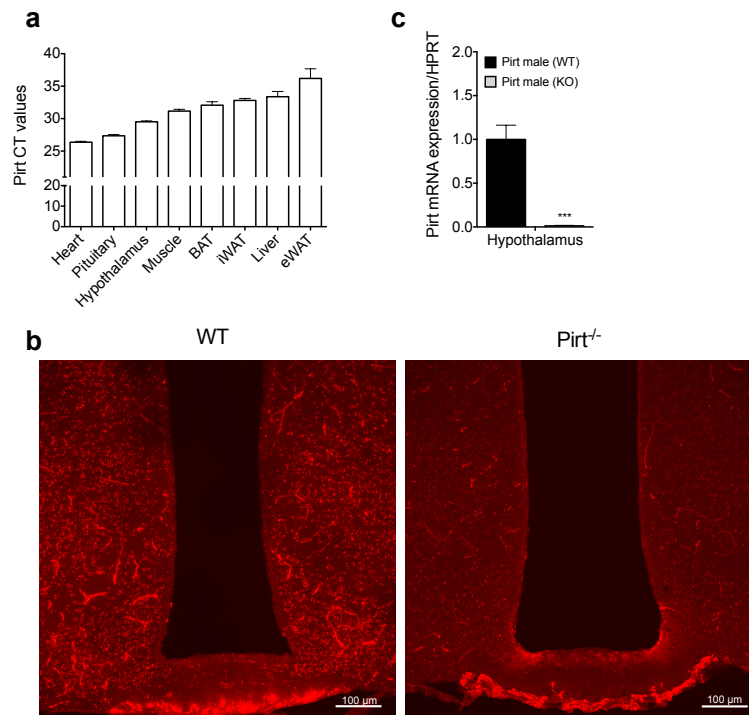
Figure 1: Pirt is expressed in hypothalamic nuclei. Relative gene expression of Pirt in the heart muscle, pituitary gland, hypothalamus, iWAT, quadriceps, eWAT, BAT, and liver of WT mice (n=6-8) (**a**). Immunohistochemistry of brain slices from WT and Pirt$^{-/-}$ mice (**b**). Pirt gene expression in the hypothalamus of WT mice compared to Pirt$^{-/-}$ mice (n=5 per genotype) (**c**). ***$P < 0.01$ determined by an unpaired two-tailed Student's t-test comparing WT with Pirt$^{-/-}$ mice.

3.2 Global ablation of Pirt has subtle effects on energy homeostasis in chow-fed female mice

To evaluate the role of Pirt in systemic control of energy metabolism, we exposed both male and female Pirt$^{-/-}$ mice and their WT controls to comprehensive metabolic phenotyping. We introduced a gene-environment metabolic stressor, by incorporation of a HFHS challenge in parallel cohorts of Pirt$^{-/-}$ and WT male and female mice. Pirt deficiency results in a marked increase in body weight in female mice maintained on a chow diet (Fig 2a) without differences in food intake (Fig 2l). Mirroring the difference in body weight, chow-fed female Pirt$^{-/-}$ mice exhibited a trend of more body fat relative to WT controls (Fig 2c, $p = 0.064$), while lean mass was comparable between genotypes (Fig 2d). Whereas ablation of Pirt amplifies body weight gain in female mice on a normal diet, this effect is annulled when mice are maintained on a HFHS diet (Fig 2b,c). Yet, body composition analysis revealed a significant reduction in lean mass in female Pirt$^{-/-}$ mice on a HFHS diet (Fig 2d; $p < 0.05$). Aiming to further understand the enhanced weight gain susceptibility in female Pirt$^{-/-}$ mice, we employed indirect calorimetry to analyze energy expenditure, substrate utilization, and locomotion. We did not observe differences in energy expenditure, RER, or locomotor activity between Pirt$^{-/-}$ and WT female mice (Fig 2i,j,k). Pirt knockout did not impact body

73

weight in male mice on a standard chow (Fig 2e) or on a HFHS diet (Fig 2f). Similarly, chow-fed and HFHS-fed male WT and Pirt^{-/-} mice did not differ with respect to food intake (data not shown) or body composition (Fig 2g,h).
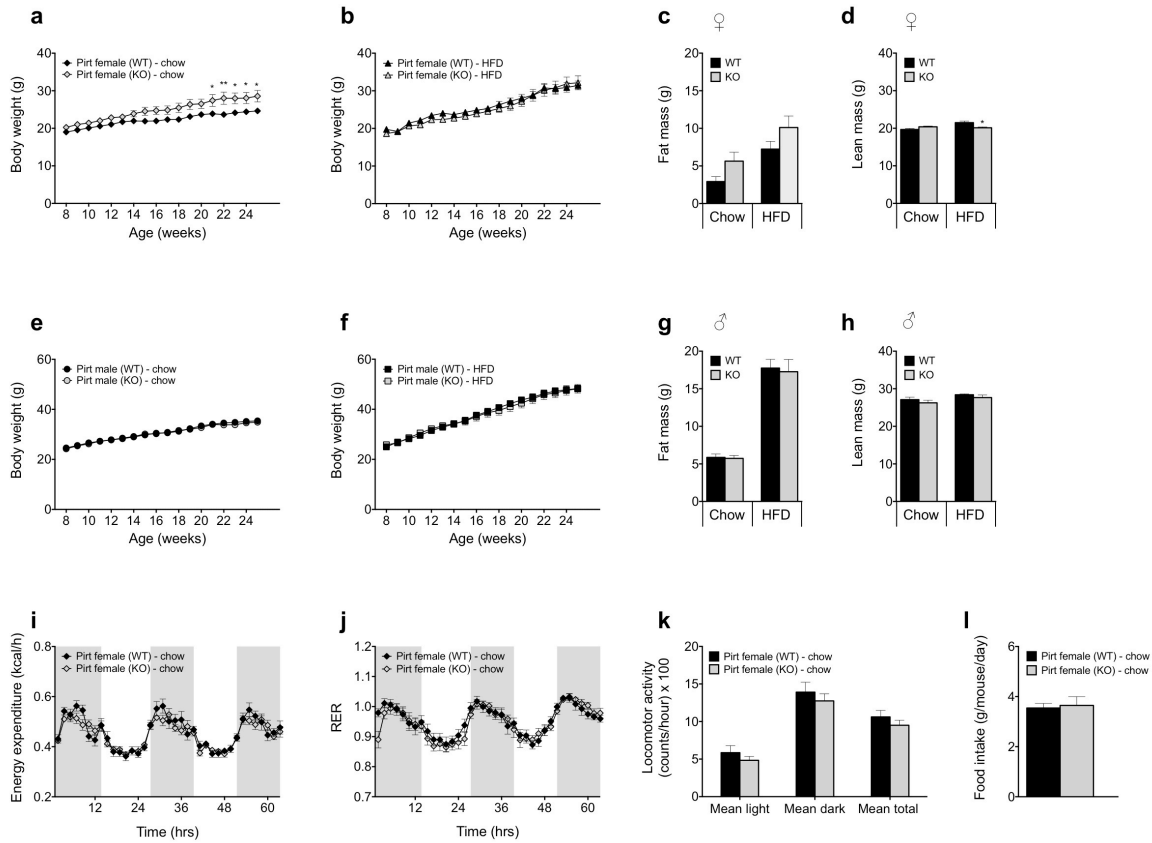
Figure 2: Sex- and diet-specific effects of Pirt deficiency on energy metabolism. Body weight progression of female WT and Pirt^{-/-} mice on a standard chow (**a**) and HFHS diet (**b**). Fat mass (**c**) and lean mass (**d**) of the female cohorts at 27 weeks of age. Body weight progression of male WT and Pirt^{-/-} mice on a standard chow (**e**) and HFHS diet (**f**). Fat mass (**g**) and lean mass (**h**) of the male cohorts at 27 weeks of age. Energy expenditure (**i**), respiratory exchange ratio (RER) (**j**) and cumulative locomotor activity (**k**) of female chow-fed WT and Pirt^{-/-} mice at 27 weeks of age. Average daily food intake in female WT and Pirt^{-/-} mice from week 8 - week 25 of age (**l**). Phenotyping cohorts with n=8 per sex, diet, and genotype. Data represent mean ± s.e.m. $^*P < 0.05$, $^{**}P < 0.01$ determined by two-way ANOVA or an unpaired two-tailed Student's t-test comparing WT with Pirt^{-/-} mice. ANOVA was followed by Tukey post hoc multiple comparison analysis to determine statistical significance.

3.3 Ablation of Pirt compromises glucose metabolism in female but not male mice

In order to determine the role of Pirt in glucose metabolism, we performed an intraperitoneal glucose tolerance test (ipGTT) in chow-fed and HFHS-fed (17 weeks of exposure) WT and Pirt^{-/-} mice of both sexes. Female Pirt^{-/-} mice maintained on a chow diet displayed an impaired glucose tolerance relative to WT control mice (Fig 3a,c; $p < 0.05$ and 0.01 resp.). Corroborating the weight phenotype, the impaired glucose tolerance observed in chow-fed female Pirt^{-/-} mice was abrogated when the female mice were exposed to a HFHS diet (Fig

3b,c). No difference in glucose tolerance between male, chow-fed and HFHS-fed WT and Pirt^{-/-} mice was observed (Fig 3d-f).
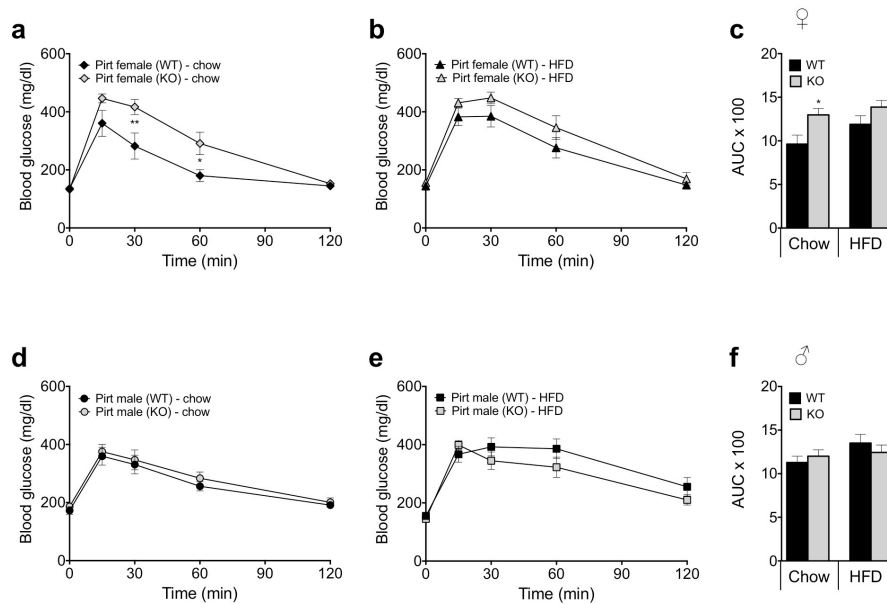
Figure 3: Female Pirt deficient mice have an impaired glucose tolerance. Blood glucose traces after an intraperitoneal glucose tolerance test in female chow-fed (**a**) and HFHS diet-fed (**b**) and male chow-fed (**d**) and HFHS diet-fed (**e**) WT and Pirt^{-/-} mice with the corresponding area under the curve (AUC) (**c,f**) at 26 weeks of age. Phenotyping cohorts with n=8 per sex, diet, and genotype. Data represent mean ± s.e.m. *$P < 0.05$, **$P < 0.01$ determined by two-way ANOVA or an unpaired two-tailed Student's t-test comparing WT with Pirt^{-/-} mice. ANOVA was followed by Tukey post hoc multiple comparison analysis to determine statistical significance.

3.4 TRPM8-linked amplification in energy expenditure is Pirt-independent

Since Pirt is a regulator of TRPM8 signaling [16], we next explored whether TRPM8-induced thermogenesis is compromised in mice lacking Pirt. A single s.c. injection of the TRPM8 super-agonist icilin (2 µmol/kg) significantly increased energy expenditure to a similar extent in WT and Pirt^{-/-} mice relative to saline-treated controls (Fig 4a-c). The amplification in energy expenditure following icilin treatment was independent of locomotor activity (Fig 4d). Thus, pharmacological activation of TRPM8 increases energy expenditure in a Pirt-independent fashion.
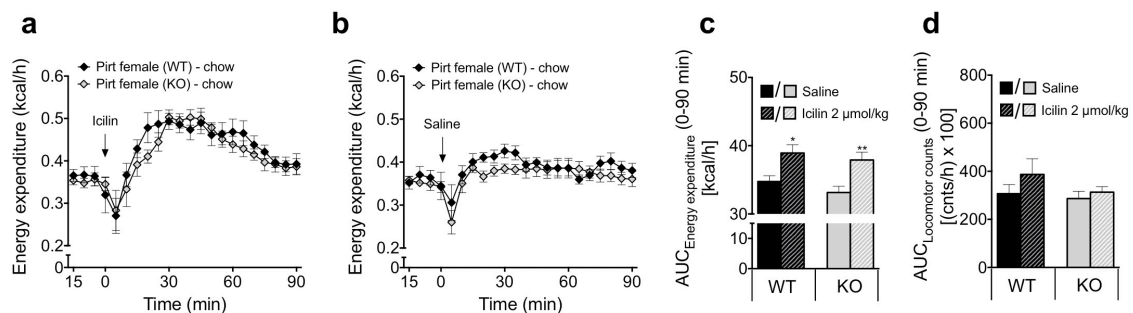
Figure 4: Pharmacological activation of TRPM8 with icilin induces energy expenditure in WT and Pirt^{-/-} mice. Energy expenditure of female chow-fed WT and Pirt^{-/-} mice after subcutaneous injections of icilin (2 µmol/kg) (**a**) or saline control (n=8 per genotype) (**b**), with respective area under the curve (AUC) after icilin and saline injections (0-90 minutes) (**c**) and AUC of locomotor activity in the same period (d). Data represent mean ± s.e.m. $^*P < 0.05$, $^{**}P < 0.01$ determined by an unpaired two-tailed Student's t-test comparing WT with Pirt^{-/-} mice.

4. Discussion

We here examined the impact of global Pirt gene ablation on energy and glucose metabolism in female and male mice fed either chow or high-fat diet. We identified a subtle increase in the susceptibility to develop obesity and glucose intolerance in Pirt^{-/-} female mice on a normal chow diet. This effect was absent when the animals were maintained on a HFHS diet. Male mice deficient for Pirt displayed no differences in glucose or energy metabolism relative to WT controls.

Recent reports describe a regulatory involvement of Pirt in the TRPM8 signaling pathway [16]. Because pharmacological TRPM8 activation induces UCP1-dependent thermogenesis in BAT [10, 13], we hypothesized that the lack of Pirt would impair energy homeostasis. In concordance with the proposed lack of TRPM8 expression in the BAT [13], we did not find Pirt expressed in the BAT. Thus, any effect of Pirt on BAT thermogenesis is most likely indirect through neuronal relays, which is in line with the suggested indirect effect of TRPM8 activation on BAT-dependent thermogenesis [13]. Interestingly, we identified, for the first time, a robust Pirt expression in several hypothalamic nuclei. The hypothalamus serves as the central hub for coordinating energy metabolic cues including sensory signals arising from the peripheral nervous system. Accordingly, the hypothalamic Pirt expression points to a possible central integrative function, which instigated us to continue our investigations on the role of Pirt in energy homeostatic control.

Because Pirt is involved in ambient temperature sensing [16], thermoneutral conditions may blunt the physiological role of Pirt. Consequently, we decided to execute the metabolic phenotyping at temperatures below the thermoneutral zone. Only female Pirt^{-/-} mice that were fed a standard chow diet, gained significantly more body weight compared to WT mice. Female C57Bl/6 mice are reported to have a higher core body temperature, which is associated with an increased metabolic rate [19, 20]. Pirt deficient mice exhibit defects in cold sensation [16]; the lack of Pirt in female mice on a standard chow diet could thus influence the capability to adjust metabolism to a mild cold stress. This is speculative, as is the ability of HFHS diet-induced thermogenesis to overwrite this susceptibility. Of note, although DIO female Pirt^{-/-} mice did not differ from WT mice with respect to body weight, they did have

significantly less lean mass, supporting the notion that Pirt deficiency results in subtle metabolic defects in females. Future studies are needed to tease out a possible interaction between Pirt in temperature regulation and Pirt in metabolic control. In context, a limitation of this study is that we did not investigate how Pirt deficient mice defend their body temperature at sub-ambient room temperatures and the potentially associated impact on body weight.

Out of the four cohorts of mice studied here, only the female chow-fed Pirt$^{-/-}$ mice had an impaired glucose metabolism compared to WT mice. Because of a tight relationship between obesity, glucose intolerance, and diabetes [21], we cannot rule out that the impaired glucose tolerance in Pirt$^{-/-}$ female mice is secondary to the increased body weight.

Pirt plays a regulatory role in altering the gating properties of TRPM8 following both cold temperature exposure and menthol application as demonstrated through *in vitro* experiments [16, 18]. We here investigated whether TRPM8 activity also requires Pirt *in vivo*. Thus, we pharmacologically activated TRPM8 receptors with icilin, a TRPM8 super-agonist, and monitored energy expenditure in female WT and Pirt$^{-/-}$ mice. Our results show that the icilin-evoked TRPM8-dependent energy expenditure induction is independent of Pirt. Consistent with this notion, divergent pathways downstream of TRPM8 have been reported [18], and more work is now needed to tease out TRPM8-Pirt signaling under diverse physiological challenges. Finally, since Pirt can regulate the function of other TRP channels, including TRPV1 and heat sensing [15], comprehensive investigations of metabolically relevant TRP channels – in particular those expressed in the hypothalamus – and their possible interconnectedness with Pirt are warranted.

5. Conclusion

In summary, we here report that Pirt contributes subtle, sex-specific effects on energy and glucose regulation. In contrast to emerging evidence based on *in vitro* studies [16, 18], Pirt does not appear to play a role for TRPM8-stimulated energy expenditure *in vivo*.

Author contributions

S.J. designed and performed the experiments, analyzed and interpreted data, and drafted the manuscript. K.F. and G.C. helped perform experiments. X.D. kindly provided the Pirt^{-/-} mouse. B.F., M.H.T., T.D.M. and C.C. co-conceptualized the project, analyzed, and interpreted data and co-wrote the manuscript with S.J.

Competing interests

M.H.T has served as SAB member of ERX Pharmaceuticals. The Institute for Diabetes and Obesity cooperates with Novo Nordisk and Sanofi-Aventis. B.F. is currently employee of Novo Nordisk.

References

[1]   Ng, M., Fleming, T., Robinson, M., Thomson, B., Graetz, N., Margono, C., et al., 2014. Global, regional, and national prevalence of overweight and obesity in children and adults during 1980-2013: a systematic analysis for the Global Burden of Disease Study 2013. Lancet 384: 766-781.

[2]   Tseng, Y.H., Kokkotou, E., Schulz, T.J., Huang, T.L., Winnay, J.N., Taniguchi, C.M., et al., 2008. New role of bone morphogenetic protein 7 in brown adipogenesis and energy expenditure. Nature 454: 1000-1004.

[3]   Cypess, A.M., Kahn, C.R., 2010. Brown fat as a therapy for obesity and diabetes. Curr Opin Endocrinol Diabetes Obes 17: 143-149.

[4]   Cypess, A.M., Lehman, S., Williams, G., Tal, I., Rodman, D., Goldfine, A.B., et al., 2009. Identification and importance of brown adipose tissue in adult humans. N Engl J Med 360: 1509-1517.

[5]   van Marken Lichtenbelt, W.D., Vanhommerig, J.W., Smulders, N.M., Drossaerts, J.M., Kemerink, G.J., Bouvy, N.D., et al., 2009. Cold-activated brown adipose tissue in healthy men. N Engl J Med 360: 1500-1508.

[6]   Cannon, B., Nedergaard, J., 2004. Brown adipose tissue: function and physiological significance. Physiol Rev 84: 277-359.

[7]   Rehnmark, S., Nechad, M., Herron, D., Cannon, B., Nedergaard, J., 1990. Alpha- and beta-adrenergic induction of the expression of the uncoupling protein thermogenin in brown adipocytes differentiated in culture. J Biol Chem 265: 16464-16471.

[8]   Ikeda, K., Maretich, P., Kajimura, S., 2018. The Common and Distinct Features of Brown and Beige Adipocytes. Trends Endocrinol Metab 29: 191-200.

[9]   Cao, W., Medvedev, A.V., Daniel, K.W., Collins, S., 2001. beta-Adrenergic activation of p38 MAP kinase in adipocytes: cAMP induction of the uncoupling protein 1 (UCP1) gene requires p38 MAP kinase. J Biol Chem 276: 27077-27082.

[10]   Ma, S., Yu, H., Zhao, Z., Luo, Z., Chen, J., Ni, Y., et al., 2012. Activation of the cold-sensing TRPM8 channel triggers UCP1-dependent thermogenesis and prevents obesity. J Mol Cell Biol 4: 88-96.

[11]   Peier, A.M., Moqrich, A., Hergarden, A.C., Reeve, A.J., Andersson, D.A., Story, G.M., et al., 2002. A TRP channel that senses cold stimuli and menthol. Cell 108: 705-715.

[12]   McKemy, D.D., Neuhausser, W.M., Julius, D., 2002. Identification of a cold receptor reveals a general role for TRP channels in thermosensation. Nature 416: 52-58.

[13]   Clemmensen, C., Jall, S., Kleinert, M., Quarta, C., Gruber, T., Reber, J., et al., 2018. Coordinated targeting of cold and nicotinic receptors synergistically improves obesity and type 2 diabetes. Nat Commun 9: 4304.

[14]   Ahern, G.P., 2013. Transient receptor potential channels and energy homeostasis. Trends Endocrinol Metab 24: 554-560.

[15]   Kim, A.Y., Tang, Z., Liu, Q., Patel, K.N., Maag, D., Geng, Y., et al., 2008. Pirt, a phosphoinositide-binding protein, functions as a regulatory subunit of TRPV1. Cell 133: 475-485.

[16]   Tang, Z., Kim, A., Masuch, T., Park, K., Weng, H., Wetzel, C., et al., 2013. Pirt functions as an endogenous regulator of TRPM8. Nat Commun 4: 2179.

[17]   Hilton, J.K., Salehpour, T., Sisco, N.J., Rath, P., Van Horn, W.D., 2018. Phosphoinositide-interacting regulator of TRP (PIRT) has opposing effects on human and mouse TRPM8 ion channels. J Biol Chem 293: 9423-9434.

[18]   Tang, M., Wu, G.Y., Dong, X.Z., Tang, Z.X., 2016. Phosphoinositide interacting regulator of TRP (Pirt) enhances TRPM8 channel activity in vitro via increasing channel conductance. Acta Pharmacol Sin 37: 98-104.

[19]   Sanchez-Alavez, M., Alboni, S., Conti, B., 2011. Sex- and age-specific differences in core body temperature of C57Bl/6 mice. Age (Dordr) 33: 89-99.

[20]   Yang, J.N., Tiselius, C., Dare, E., Johansson, B., Valen, G., Fredholm, B.B., 2007. Sex differences in mouse heart rate and body temperature and in their regulation by adenosine A1 receptors. Acta Physiol (Oxf) 190: 63-75.

[21]   Williams, L.M., Campbell, F.M., Drew, J.E., Koch, C., Hoggard, N., Rees, W.D., et al., 2014. The development of diet-induced obesity and glucose intolerance in C57BL/6 mice on a high-fat diet consists of distinct phases. PLoS One 9: e106159.

Chapter 4 – *Mechanistic evaluation of opposing acute and chronic effects of nicotine receptor activation on blood glucose*

Manuscript for submission
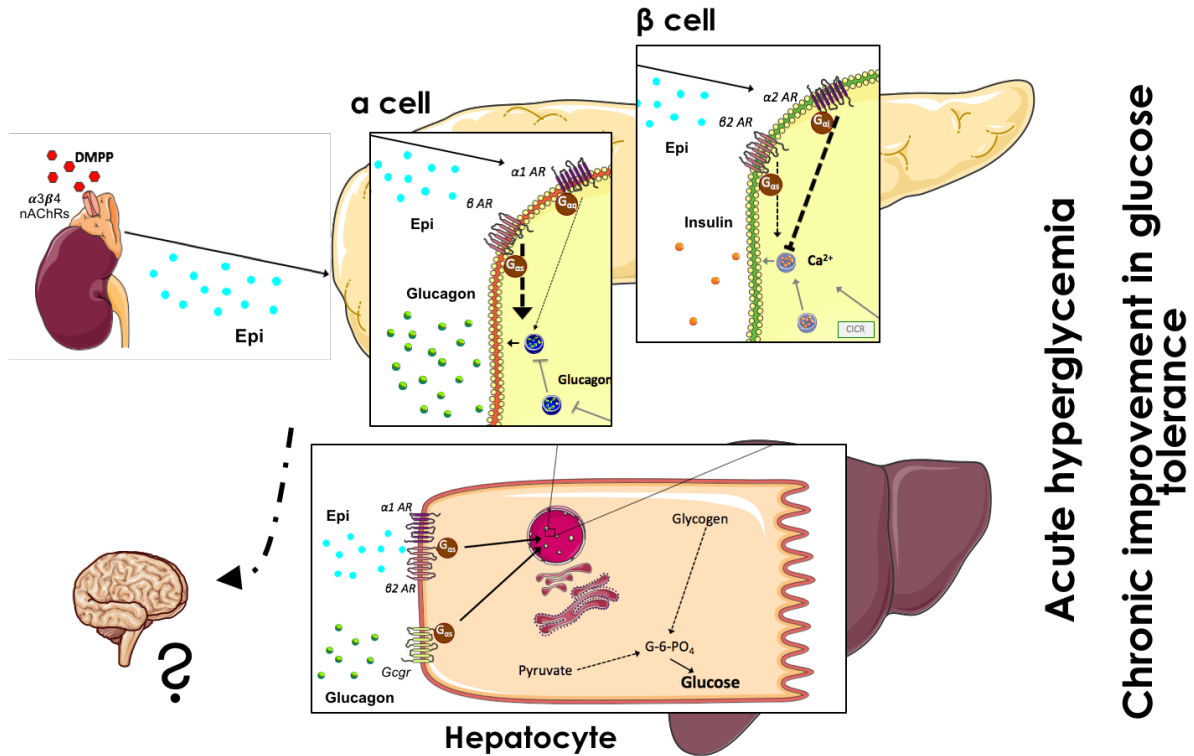
Figure 3. 4: Opposing effects of acute and chronic DMPP administration in DIO mice. Acutely, DMPP induces plasma epinephrine secretion from the adrenal medulla leading to increased glucagon release from pancreatic α-cells and decreased insulin secretion from pancreatic β-cells. Epinephrine and glucagon activate respective receptors on hepatocytes inducing glycogenolysis and gluconeogenesis, which leads to acute hyperglycemia. Chronic treatment with DMPP improves glucose tolerance via increased non-oxidative glucose disposal into the muscle, but potentially also via the central leptin-melanocortin pathway as suggested in chapter II (Clemmensen et al., 2018). The figure was created using Sevier medical art and summarizes chapter IV.

Pharmacological targeting of α3β4 nicotinic receptors improves peripheral insulin sensitivity in diet-induced obese mice

Sigrid Jall[1,2], Meri De Angelis[3], Anne-Marie Lundsgaard[4], Andreas M. Fritzen[4], Aaron Novikoff[1], Erik A. Richter[4], Bente Kiens[4], Karl-Werner Schramm[3,5], Matthias H. Tschöp[1,2], Christoffer Clemmensen#[1,6], Timo D. Müller#[1], Maximilian Kleinert#[1,4]

[1]Institute for Diabetes and Obesity, Helmholtz Diabetes Center (HDC) at Helmholtz Zentrum München & German Center for Diabetes Research (DZD), Ingolstädter Landstraße 1, 85764 Neuherberg, Germany.
[2]Division of Metabolic Diseases, Department of Medicine, Technische Universität München, 80333 Munich, Germany.
[3]Molecular EXposomics (MEX), Helmholtz Zentrum München - German Research Center for Environmental Health (GmbH), Ingolstädter Landstraße 1, 85764 Neuherberg, Germany.
[4]Department of Nutrition, Exercise and Sports, Section of Molecular Physiology, Faculty of Science, University of Copenhagen, Universitetsparken 13, DK-2100, Copenhagen, Denmark.
[5]Department für Biowissenschaftliche Grundlagen, TUM, Wissenschaftszentrum Weihenstephan für Ernährung, Landnutzung und Umwelt, Weihenstephaner Steig 23, 85350 Freising, Germany.
[6]Novo Nordisk Foundation Center for Basic Metabolic Research, Faculty of Health and Medical Sciences, University of Copenhagen, Blegdamsvej 3B, DK-2200 Copenhagen N, Denmark.

#Co-corresponding authors:

Christoffer Clemmensen; Phone: +45 22 91 63 33; Address: NNF Center for Basic Metabolic Research Nutrient and Metabolite Sensing; Blegdamsvej 3B, DK-2200 Copenhagen N; chc@sund.ku.dk

Timo D. Müller; Phone: +49 89 3187-2106; Address: Institute for Diabetes and Obesity; Ingolstädter Landstraße 1, D-85764 Neuherberg; timo.mueller@helmholtz-muenchen.de

Maximilian Kleinert; Phone: +49 89 3187-2110; Address: Institute for Diabetes and Obesity; Ingolstädter Landstraße 1, D-85764 Neuherberg; maximilian.kleinert@helmholtz-muenchen.de

Manuscript for submission

Abstract

Treatment with the α3β4 nicotinic acetylcholine receptor (nAChR) agonist, 1,1-Dimethyl-4-phenylpiperazinium iodide (DMPP), improves glucose tolerance in diet-induced obese (DIO) mice, but the physiological and molecular mechanisms behind DMPP-mediated glycemic improvements remain elusive. To further our understanding, we aimed to dissect the molecular underpinnings that manifest as glucose regulation by DMPP. In wild-type (WT) DIO mice, but not β4 nAChR knockout (KO) DIO mice, an acute single dose of DMPP was able to elevate blood glucose levels by ~200% at 150 minutes post-treatment, with a return to baseline after 300 minutes. This acute DMPP-mediated hyperglycemia was accompanied by an upregulation of hepatic gluconeogenic genes, a reduction in plasma insulin levels, and a transient increase in circulating epinephrine. When β-adrenergic receptor KO mice were pre-treated with the α2-adrenergic receptor antagonist yohimbine, the hyperglycemic effect of acute DMPP treatment was eliminated. In contrast to the detrimental effects of acute exposure, chronic DMPP treatment elicited glycemic benefits. An improvement in glucose tolerance was evident after just three consecutive days of DMPP treatment and chronic administration of DMPP increased *in vivo* glucose uptake into brown adipose tissue and skeletal muscle, despite a decrease in circulating insulin and unaltered canonical insulin signaling. Of interest, chronic treatment with DMPP did not recapitulate the increase in circulating epinephrine associated with a singular dose of DMPP.

Collectively, our data suggest that DMPP acutely triggers epinephrine-induced short-term hyperglycemia via stimulation of gluconeogenesis, while chronic DMPP-induced activation of α3β4 nAChRs improves glycemic control by improving peripheral insulin sensitivity in striated muscle and brown adipose tissue, notably via mechanisms independent of acute epinephrine release and signaling.

Introduction

Obesity and associated metabolic disorders, such as type 2 diabetes mellitus (T2DM), are major public health issues [1]. Considerable preclinical progress has been brought forward to tackle the obesity and T2DM pandemics, using different pharmacological strategies [2, 3]. Provocatively, the activation of central nicotine receptors has been suggested as a promising target to reduce food intake [4]. Mineur *et al* have shown that anorexigenic proopiomelanocortin (POMC) neurons express α3β4 nicotinic acetylcholine receptors (nAChRs) and pharmacological targeting of these receptors with nicotine can suppress food intake in mice [4]. Nicotine-dense tobacco smoke is associated with a lower body weight in humans, while smoking cessation is typically accompanied by body weight gain [5, 6]. Problematically, in humans, the broad nAChR-agonist nicotine is also associated with an increase in cancer risk [7], non-alcoholic fatty liver disease [8], and peripheral insulin resistance [9].

The nAChRs comprise several homo- or heteropentamers containing α subunits (*Chrna1-7* and *Chrna9-10*) and/or β subunits (*Chrnb1-4*) [10]. We have recently shown that selective targeting of the α3β4 nAChRs with 1,1-Dimethyl-4-phenylpiperazinium iodide (DMPP) reduces food intake in diet-induced obese (DIO) mice and robustly improves glucose tolerance independent of body weight loss [2, 11]. In contrast, the broad nAChR agonist nicotine has yielded inconsistent outcomes in rodents, resulting in detrimental effects [8, 12], no effects [2], or positive effects on glucose tolerance and insulin sensitivity [13-15]. The reasons for these discrepancies are not clear, but may be related to the use of different mouse strains, the selectivity of receptor subtype activation, or dosing paradigms. Notably, it is thought that nicotine-mediated improvements in glucose tolerance are mainly due to nicotine acting on α7 nAChRs [16]. Thus, the mechanisms underpinning the glycemic benefit of DMPP are likely distinct, especially since DMPP is a weak agonist a α7 nAChRs and most importantly fails to improve glucose tolerance in mice with disrupted leptin-melanocortin signaling [2].

Therefore, we strove to elucidate the mechanisms underpinning DMPP's robust glycemic benefit using insulin resistant DIO mice [17]. We first assessed the glucoregulatory effects of a single dose of DMPP in DIO mice, and observed a short-term hyperglycemic condition mediated by epinephrine's action on the pancreas and the liver. In contrast to the acute hyperglycemia associated with a single excursion of DMPP, chronic treatment with DMPP established an improvement in glucose tolerance without a concomitant enhancement of

epinephrine secretion after a consecutive seven day regimen. Chronic DMPP treatment enhanced peripheral insulin sensitivity and increased glucose uptake in the skeletal muscle, the heart, and the brown adipose tissue (BAT), while an effect in the less metabolically active white adipose tissues (WAT) was absent.

Material and Methods

Mice for pharmacological studies

For wild-type (WT) mouse studies, male C57Bl/6j mice were obtained from Janvier Labs. Lep[db] mice were provided from Jackson Laboratory (strain name: BKS.Cg-Dock7m +/+ Leprdb/J, Maine, USA). Other transgenic mice and their respective littermates were bred in-house. All mice were switched from a regular chow diet to a high-fat, high sucrose diet (HFD) (D12331; Research Diets, New Brunswick, NJ) at an age of eight weeks with *ad libitum* access to water and diet. Mice were maintained at 23ºC ambient temperature under specific-pathogen free conditions at constant humidity and on a 12-hours light-dark cycle. Cholinergic receptor nicotinic beta 4 subunit (Chrnb4) knockout (KO) mice were generated as described previously and homozygous mice were bred to generate a colony for *in vivo* studies [18]. Glucagon receptor (Gcgr) flox mice were bred with Alb cre to generate a colony of homozygous Gcgr flox x Alb cre mice. Fibroblast growth factor 21 (FGF21) KO mice were generated as described previously [19]. A colony of homozygous FGF21 KO mice was generated using het-het breeding. Betaless mice were homozygous for the triple KO of all beta-adrenergic receptors (β-AR) ($\beta_1\beta_2\beta_3$) and generated as described previously [20].

Pharmacological intervention studies

Interventions were performed in mice weighing $\geq$ 50 g. Mice were randomly assigned to pharmacological treatment groups based on body weight and *ad libitum* fed blood glucose. The executors were not blinded to the intervention groups. 1,1-Dimethyl-4-phenylpiperazinium iodide (D5891, Sigma-Aldrich, Munich, Germany) was administered in saline at 10 mg per kg body weight with the vehicle control group receiving 1% DMSO in saline. Yohimbine hydrochloride (Y3125-10G, Sigma-Aldrich, Munich, Germany) was administered in saline at 1 mg/kg body weight 60 minutes prior to DMPP injections. Compounds were administered subcutaneously at a volume of 5 µl per gram body weight. In the acute set-up, food was removed and *ad libitum* fed blood glucose levels were determined at 7 a.m. Blood glucose was measured mixed tail blood using hand-held glucometers (Abbott,

Wiesbaden, Germany). Blood for insulin measurements was collected at time points as indicated in the figures by bleeding mice from the tail vein into EDTA-coated microvette tubes (Sarstedt, Nümbrecht, Germany). In the chronic interventions, DMPP, if not stated otherwise, was injected daily before onset of the dark phase. For glucose tolerance tests, mice were fasted for 6 hours (starting at 7.30 a.m.) and received intraperitoneal (i.p.) injections of glucose at 1.75 g/kg body weight. In the chronic, 14 days studies, mice were fasted and timely injected with DMPP two hours prior to the sacrifice. All animal experimentations were approved and conducted in accordance to the Danish Animal Experimentation Inspectorate and Animal Ethics Committee of the government of Upper Bavaria, Germany.

Plasma parameters

The collected blood was immediately kept on ice and centrifuged ten minutes at 3000 g and 4ºC. Plasma was stored at -20ºC until further analysis. Insulin levels were analyzed using a commercially available ELISA kit (ALPCO Diagnostics, Salem, NH, USA) following the manufacturers' instructions. All plasma catecholamines were analyzed and detected with a high performance liquid chromatography (HPLC) system coupled with an electrochemical detector (EcD) as described previously [20]. The sample clean-up was performed according the protocol described by RECIPE (RECIPE, Munich, Germany). The Recipe ClinRep® complete kit contains all necessary chemicals and materials for the extraction. The limited amount of plasma per sample necessitated some modifications from the standard protocol. Therefore, 30 - 40 µl of plasma was diluted with 40 µl of water and 10 µl of internal standard was added. Upon vigorous mixing, the samples were charged on the sample preparation column. The column was shaken for 10 minutes and the solvent was removed on a vacuum manifold. The column was washed thrice with 1 mL washing solution to remove interfering components. After drying the column, the elution reagent was added (140 µL). The catecholamines were eluted from the extraction column via centrifugation and 20 µl of the eluate was injected as such into the HPLC-EcD system.

Biochemical analysis

For tissue collection, mice were either euthanized using CO_2 or killed by cervical dislocation. Tissues were extracted and immediately kept on dry ice or liquid nitrogen and stored at -80ºC until further analysis. For gene expression analysis, liver RNA was isolated using the TRIzol-based RNeasy Kit (Qiagen, Hilden, Germany) according to the manufacturers' instructions. cDNA was synthesized from total RNA using QuantiTect Reverse Transcription Kit (Qiagen,

Hilden, Germany). Gene expression profiles were assessed in the liver with the quantitative PCR (qPCR) technique using SYBR green (Thermo Fisher Scientific, Erlangen, Germany). Relative gene expression was normalized to the reference genes peptidylprolyl isomerase B (Ppib) or hypoxanthine-guanine phosphoribosyltransferase (Hprt). Sequences of primers used are listed in alphabetical order in supplemental table 1. Hepatic glycogen was measured using a commercially available kit (Biovision, Milpitas, CA, USA) following the manufacturers' instructions.

Western Blot Analyses

25 mg of quadriceps muscle was homogenized (Tissue Lyzer II, Qiagen, Germany) in ice-cold buffer as described previously [21]. Homogenates were rotated end-over-end for one hour and lysate supernatants were collected by centrifuging 20 minutes at 16000 g and 4 °C. Protein concentrations were determined in triplicates using the bicinchoninic acid (BCA) method (Pierce Biotechnology BCA, USA). Samples were heated (96 °C) in Laemmli buffer before subjected to SDS-PAGE and semi-dry blotting. The primary antibodies used were from Cell Signaling Technology, US (anti-Akt2 #3063, anti-Akt Thr308 #9275, anti-Akt Ser473 #9271, PAS #9611, TBC1D1 Thr596 #6927), Thermo Fisher Scientific, US (GLUT4 #PA1-1065), Upstate Biotechnology, US (TBC1D4 #07-741). Anti-TBC1D1 was kindly donated by Professor Grahame Hardie, University of Dundee, UK. Secondary antibodies were from Dako Cymation (Denmark). Membranes were probed with enhanced chemiluminescence (ECL$^+$; Amersham Biosciences, USA), and immune complexes were visualized using BioRad ChemiDoc™ MP Imaging System (Hercules, USA). Signals were quantified (Image Lab, Life Sciences, USA) and expressed as arbitrary units.

In vivo 2-deoxy-glucose uptake

For assessment of glucose clearance, glucose at 1.75 g/kg body weight glucose was injected at 10 µl per gram body weight together with ^{3}H-labelled 2-deoxy-glucose (^{3}H-2-DG) (60 µCi/ml) i.p. to mice treated daily with DMPP for eight days and fasted for six hours. Blood glucose was measured at the indicated time points using a handheld glucometer (Arseus Medical NV, Bornem, Belgium). For analysis of ^{3}H-2-DG clearance in indicated tissues, plasma ^{3}H activity was measured at 10, 20, and 40 minutes in 5 µl of blood by scintillation counting, and systemic ^{3}H-2-DG exposure estimated by the trapezoidal method. 25 mg of each tissue was used to determine the accumulation of phosphorylated ^{3}H-2-DG (^{3}H-2-DG-6-

P) by the precipitation method [22]. Glucose clearance was calculated by dividing tissue ^{3}H-2-DG-6-P counts by systemic ^{3}H-2-DG exposure.

Statistics

Data were analyzed in GraphPad Prism (version 6 and 8; GraphPad Software, San Diego, CA, USA). The types of statistical tests performed are outlined in the figure legends. P-values ≤ 0.05 were considered statistically significant. All results are presented as mean ± standard error of the mean (s.e.m.).

Results

DMPP has acute hyperglycemic effects in DIO mice, but exerts glycemic benefits after sub-chronic administration.

A single subcutaneous administration of DMPP (10 mg/kg) increased *ad libitum* fed blood glucose in DIO mice, with a peak at ~ 2 hours after treatment and return to baseline after 5 hours (Fig. 1A). Notably, this short-term hyperglycemic effect of DMPP was absent in mice that globally lack the β4 subunit of the α3β4 nAChRs (Chrnb4 KO) (Supplemental Fig. 1A). Despite its short-term hyperglycemic effect, a single treatment with DMPP did not affect glucose tolerance in DIO mice the following day (Fig. 1B). After two days of daily DMPP administration, DMPP lost its short-term hyperglycemic effect (Fig. 1C) and after day 3, improved glucose tolerance in DIO mice (Fig. 1D).
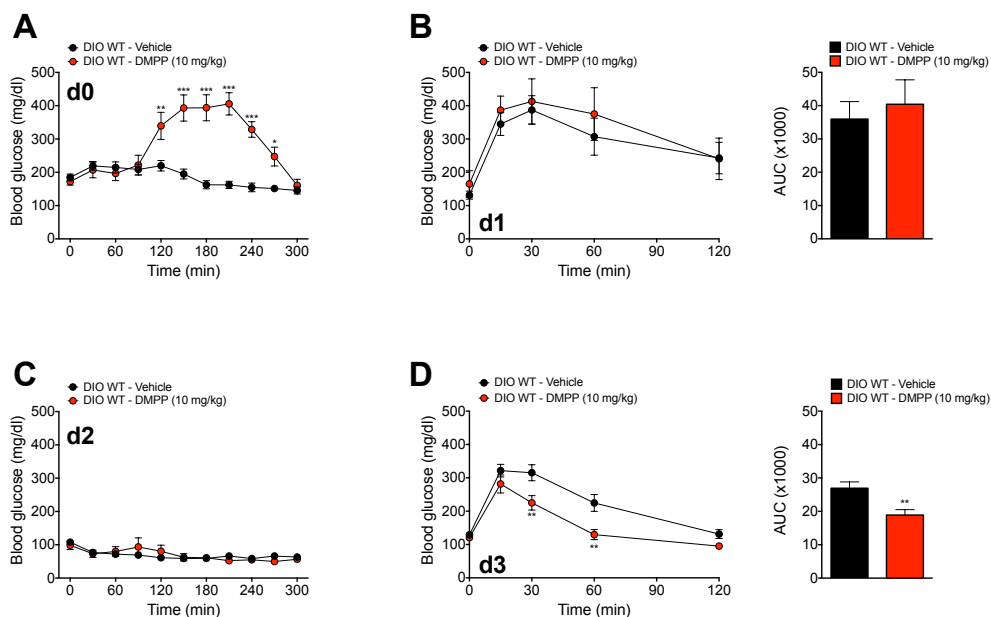
Figure 1 DMPP acutely elicits hyperglycemia, while chronically it improves glucose tolerance.
(**A**) Effect of first injection of 1,1-Dimethyl-4-phenylpiperazinium iodide (DMPP) (red) (10 mg/kg) or
vehicle (black) (injected at time point 0 minutes) on blood glucose in diet-induced obese (DIO) wild-
type (WT) mice on day 0. (**B**) Glucose tolerance with AUC determined 24 hours after the first
injection of DMPP or vehicle (i.e., on day 1 (d1)). (**C**) Effect of third injection of DMPP or vehicle
(injected at time point 0 minutes) on blood glucose on day 2. (**D**) Glucose tolerance with AUC
determined 18 hours after the third daily injection of DMPP or vehicle on day 3. All data are presented
as mean ± s.e.m (n = 7-8). Data in line graphs in (**A-D**) were assessed by two-way RM ANOVA (time
and drug as factors) with Bonferroni post-hoc tests when appropriate. Data in bar graphs in (AUCs in
B and **D**) were probed with two-tailed Student's t-tests, comparing the means of vehicle and DMPP.
*p < 0.05, **p < 0.01, ***p < 0.001 are effects of drug at indicated time point or, in bar graphs,
compared to vehicle.

DMPP-induced transient hyperglycemia is mediated via enhanced circulating epinephrine

The short-term hyperglycemia observed in DIO mice after a single DMPP injection was
associated with a trend towards reduced plasma insulin concentrations 150 minutes post-
treatment (p = 0.088 when assessed with a two-tailed Student's t-test) compared to saline-
treated control mice (Fig. 2A). In contrast, plasma insulin was not different between saline-
treated and DMPP-treated DIO Chrnb4 KO mice (Supplemental Fig. 1B). To gain insight into
whether the effects of DMPP on *ad libitum* fed blood glucose and insulin might be related to
circulating catecholamines, we assessed plasma epinephrine and norepinephrine
concentrations 80 minutes after DMPP injection, when glucose levels were still increasing.
DMPP stimulated a 6-fold increase in plasma epinephrine levels, but had no effect on
norepinephrine (Fig. 2B). Epinephrine is known to act on the pancreas to inhibit insulin
secretion, while enhancing glucagon secretion; and epinephrine also induces hepatic
gluconeogenesis and glycogenolysis [23, 24]. In agreement, hepatic glycogen content in
DMPP-treated mice was significantly reduced by 36% at 150 minutes after injection, an effect
that was subsequently restored 300 minutes after initial administration (Fig. 2C). An increase
in the expression of hepatic genes involved in gluconeogenesis was observed at 150 and 300
minutes following acute DMPP administration in DIO WT mice (Fig. 2D,E). However,
chronic treatment with DMPP over 14 days did not induce the gluconeogenic gene
upregulation seen during the singular administration (Fig. 2F).
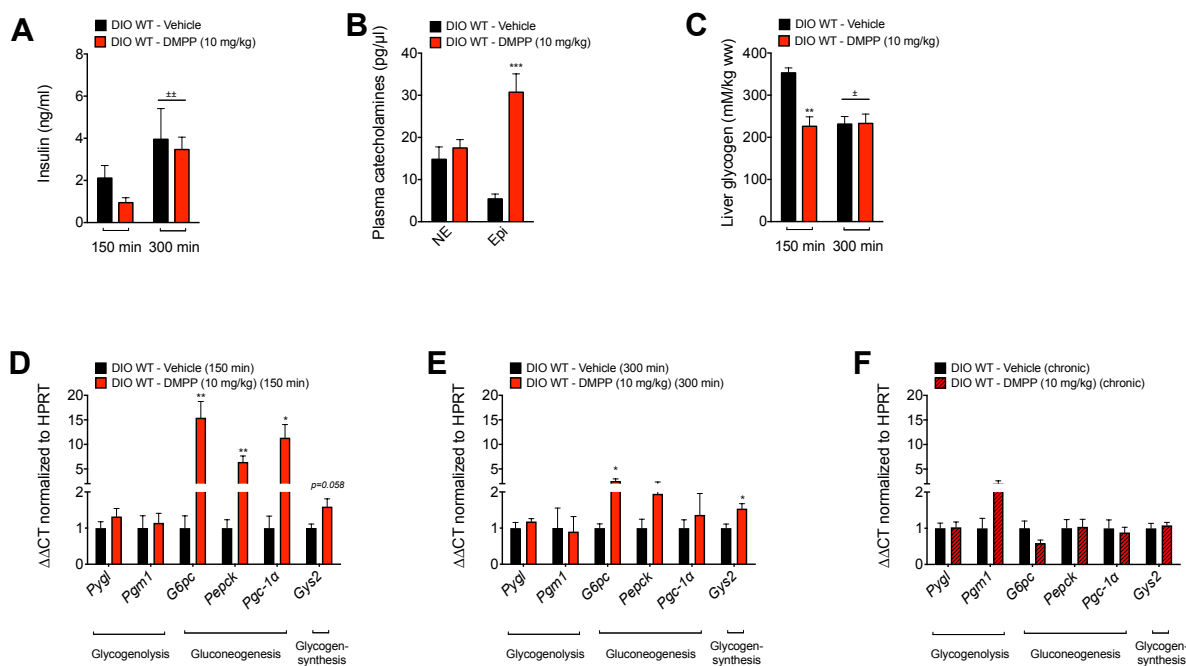
Figure 2 Acute DMPP elicits catecholamine-induced hyperglycemia. Effect of first injection of 1,1-Dimethyl-4-phenylpiperazinium iodide (DMPP) (10 mg/kg) or vehicle in diet-induced obese (DIO) wild-type (WT) mice on (**A**) plasma insulin concentrations at indicated time points (n = 3-5); on (**B**) plasma norepinephrine (NE) and epinephrine (Epi) concentrations determined in blood collected 80 minutes after DMPP was injected (n = 5-8); on (**C**) liver glycogen at indicated time points (n = 4-5); and on (**D, E**) expression of indicated genes in the liver at 150 minutes (D) and 300 minutes (E) (n = 4-5). (**F**) Effect of DMPP or vehicle injection on liver gene expression after 14 days of daily subcutaneous injections. DMPP or vehicle were injected 120 minutes prior to the cull of the mice (n = 7-8). All data are presented as mean ± s.e.m. Data in (**A** and **C**) were analyzed by two-way ANOVA (time and drug) with Tukey post-hoc test. Remaining data (**B**, **D-F**) were probed with two-tailed Student's t-tests, comparing the means of vehicle and DMPP. *$p < 0.05$, **$p < 0.01$, ***$p < 0.001$ effects of the drug, compared to vehicle. ±$p < 0.05$, ±±$p < 0.01$ main effects of time.
G6PC: Glucose-6-phosphatase; GYS2: Glycogen synthase 2 (Liver); PEPCK: Phosphoenolpyruvate carboxykinase; PGC1α: Peroxisome proliferator-activated receptor gamma, coactivator 1 alpha; PGM: Phosphoglucomutase 1; PYGL: Glycogen phosphorylase L

Glucagon induces the expression of gluconeogenic genes such as peroxisome proliferator-activated receptor gamma, coactivator 1-alpha (PGC-1α), phosphoenolpyruvate carboxykinase (PEPCK), and glucose-6-phosphatase (G6PC) all of which were increased upon a single, first injection of DMPP accompanied by an increase in blood glucose [25]. Therefore, we challenged DIO liver-specific glucagon receptor KO (Gcgr Li-KO) mice with a singular DMPP injection, which lead to a blunted hyperglycemic response, suggesting partial glucagon involvement and by profile an early glucagon-mediated spike in blood glucose (Fig. 3A). Glucagon action is known to trigger hepatic FGF21 release [26]. Single administration of DMPP, however, resulted in the same short-term hyperglycemia in global FGF21 KO mice as compared to DIO WT mice (Supplemental Fig. 2A), indicating that FGF21 does not mediate DMPP-induced hepatic glucose output. To further assess the contribution of

epinephrine on the observed short-term hyperglycemic effect of DMPP, we injected DIO mice globally lacking all β-AR with DMPP. Despite the absence of β-adrenergic receptor-mediated signaling in these mice, DMPP retained the capacity to increase blood glucose concentrations (Fig. 3B). Injection of betaless mice with DMPP significantly reduced plasma insulin concentrations at 150 minutes – an effect that was restored after 300 minutes (Fig. 3C). Liver glycogen content and gluconeogenic gene expression in DIO betaless mice were unaltered after 150 and 300 minutes following singular DMPP injection (Fig. 3D; Supplemental Fig. 2B,C). Pretreatment of betaless mice with an alpha2-AR (α_2-AR) antagonist, yohimbine (1 mg/kg), completely abolished the hyperglycemia induced by DMPP (Fig. 3E,F), suggesting epinephrine via actions on α_2- and β-adrenergic receptors to be the main mediator of DMPP's effects on glucose metabolism.
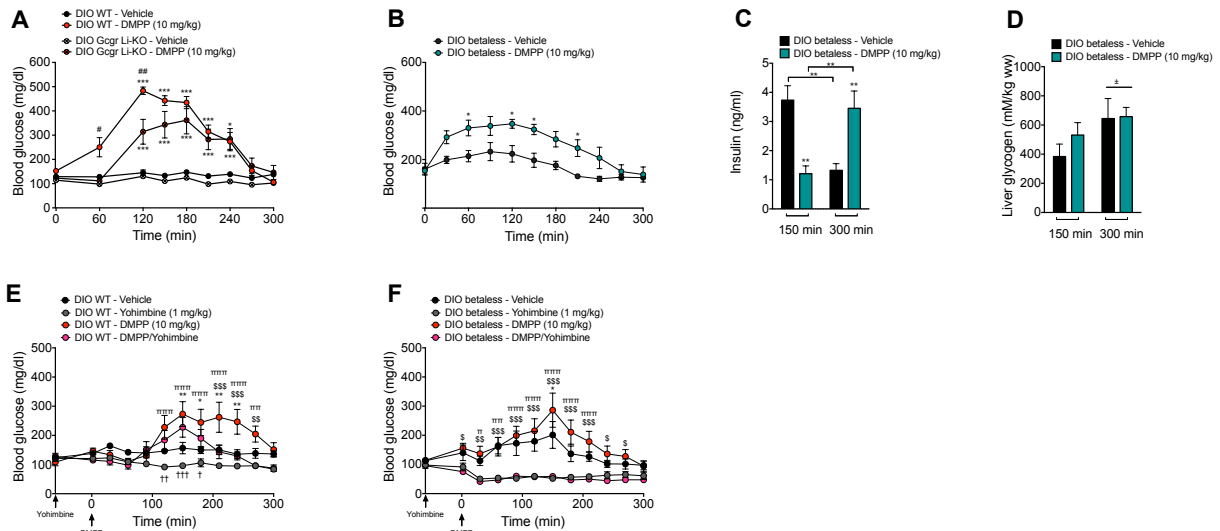
Figure 3 Acute DMPP elicits hyperglycemia via adrenergic signaling. Effect of first injection of 1,1-Dimethyl-4-phenylpiperazinium iodide (DMPP) (10 mg/kg) or vehicle (injected at time point 0 minutes) on blood glucose in (**A**) diet-induced obese (DIO) wild-type (WT) and liver-specific glucagon receptor knockout (KO) (Gcgr Li-KO) mice (n=7-8) and in (**B**) DIO betaless mice with effects of DMPP or vehicle on (**C**) plasma insulin and (**D**) liver glycogen at indicated time points (n = 6-7). Acute effects on blood glucose of a priming injection of vehicle or yohimbine (1 mg/kg) injected 60 minutes prior to DMPP or vehicle inection in DIO (**E**) WT and DIO (**F**) betaless mice (n = 4-6). All data are presented as mean ± s.e.m.. The data presented in the line graph in (**A**) were analyzed by three-way RM ANOVA with the three factors: time, genotype (WT vs. KO), and drug (DMPP vs. vehicle). The data presented in the line graph in (**B**) were analyzed by two-way RM ANOVA (time and drug); and data in the bar graphs (**C**, **D**) were analyzed by two-way ANOVA (time and drug). The data presented in line graphs in (**E**, **F**) were analyzed by two-way RM ANOVA with time as one factor and drug (vehicle, yohimbine, DMPP, DMPP+yohimbine) as the other factor. A Tukey post-hoc test was applied when appropriate. *p < 0.05, **p < 0.01, ***p < 0.001 effects of the drug compared to vehicle. #p < 0.05, ##p < 0.01, ###p < 0.001 effects of the intervention between genotypes. $p < 0.05, $$p < 0.01, $$$p < 0.001 difference between DMPP and DMPP+yohimbine. ππp < 0.01, πππp < 0.001 difference between DMPP and yohimbine. †p < 0.05, ††p < 0.01, †††p < 0.001 difference between yohimbine and DMPP+yohimbine.

Chronic DMPP selectively increases glucose uptake in the brown adipose tissue and the muscles.

Chronic administration of DMPP (10 mg/kg) in DIO mice potently improves glucose tolerance (Fig. 1D, Fig. 4A) [2], but whether this effect is secondary to an improvement in insulinotropic efficacy is unknown. Thus, we next assessed glucose tissue disposal with radioactively labeled 2-deoxy-glucose (^{3}H-2-DG). After daily treatment with DMPP over eight days, glucose-stimulated glucose disposal at day nine was increased into BAT, but not into inguinal or epididymal white adipose tissue (iWAT or eWAT) (Fig. 4B-D). DMPP also enhanced glucose disposal into both, the heart and skeletal muscle (Fig. 4E-G). Remarkably, this positive effect of DMPP on glucose disposal was evident despite lower insulin levels (Fig. 4H), together suggesting an improvement in peripheral insulin sensitivity. Interestingly, in contrast to its acute effect, an injection of DMPP after chronic treatment did not increase circulating catecholamines (Fig. 4I).
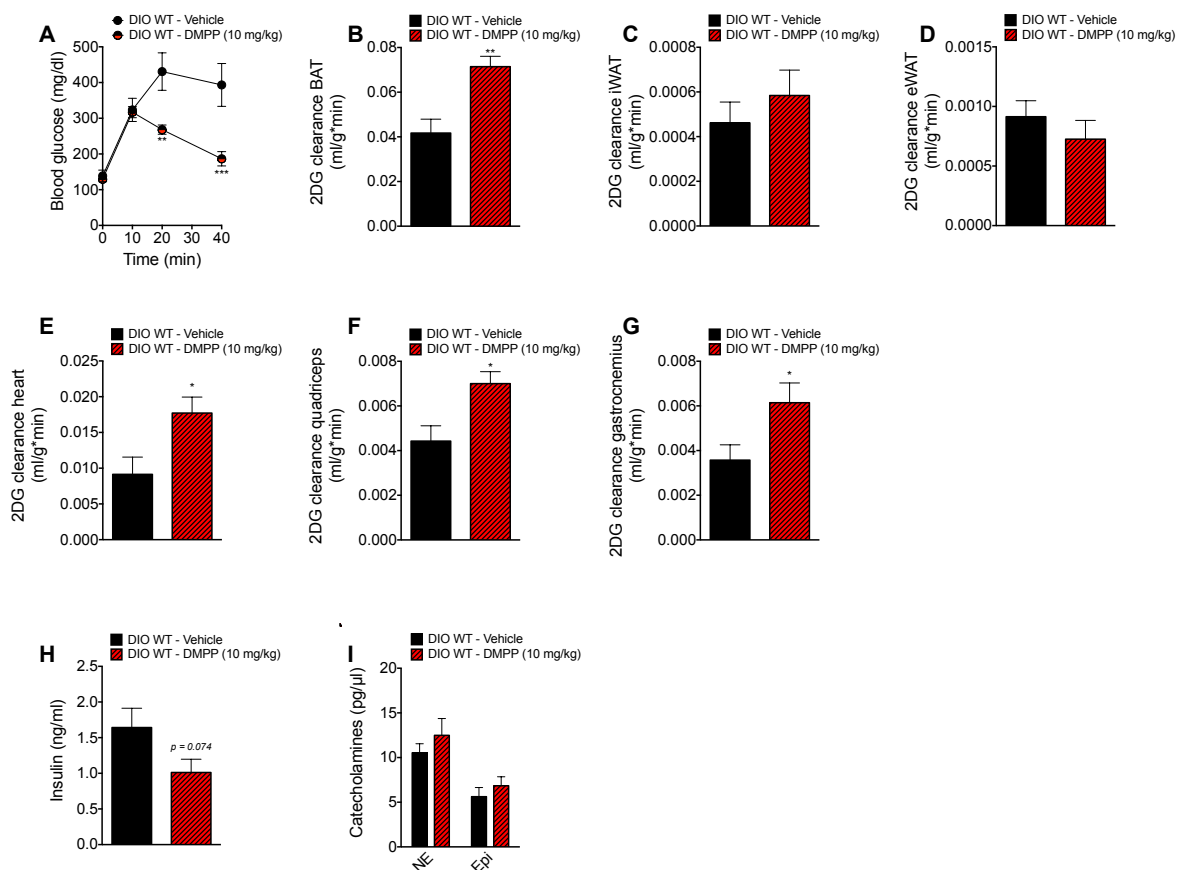
Figure 4 Chronic DMPP selectively increases glucose uptake into the BAT and the muscles. (**A**) Glucose tolerance 18 hours after eighth injection of daily 1,1-Dimethyl-4-phenylpiperazinium iodide (DMPP) (10 mg/kg) or vehicle in diet-induced obese (DIO) wild-type (WT) mice. 2-deoxy-glucose (^{3}H-2-DG) clearance in the (**B**) brown adipose tissue (BAT), (**C**) inguinal white adipose tissue (iWAT), (**D**) epididymal white adipose tissue (eWAT), (**E**) heart, (**F**) quadriceps, and (**G**) gastrocnemius. (**H**) Plasma insulin at 40 minutes post ^{3}H-2-DG injections. (**I**) Plasma catecholamines

in chronically treated DIO mice (day 7) 80 minutes after DMPP or vehicle injections. All data are presented as mean ± s.e.m (n = 6-8). Data in line graph in (**A**) were assessed by two-way RM ANOVA (time and drug) with a subsequent Bonferroni post-hoc test. Data in bar graphs in (**B-I**) were probed with two-tailed Student's t-tests, comparing the means of vehicle and DMPP. *$p < 0.05$, **$p < 0.01$, ***$p < 0.001$ effect of drug at indicated time point or, in bar graphs, compared to vehicle.

Given the quantitative importance of skeletal muscle in whole-body postprandial glucose disposal, we investigated canonical insulin signaling in muscle. Insulin-responsive signaling proteins Akt, TBC1D1 (TBC1 Domain Family Member 1), and TBC1D4 (TBC1 Domain Family Member 4) displayed similar phophosphorylation states across the DMPP- and vehicle-treated mice (Fig. 5A,B). A downstream target for these signaling proteins is the insulin-responsive glucose transporter GLUT4, however, the protein abundance of GLUT4 between DMPP- and vehicle-treated groups was also unaltered (Fig. 5A,B).
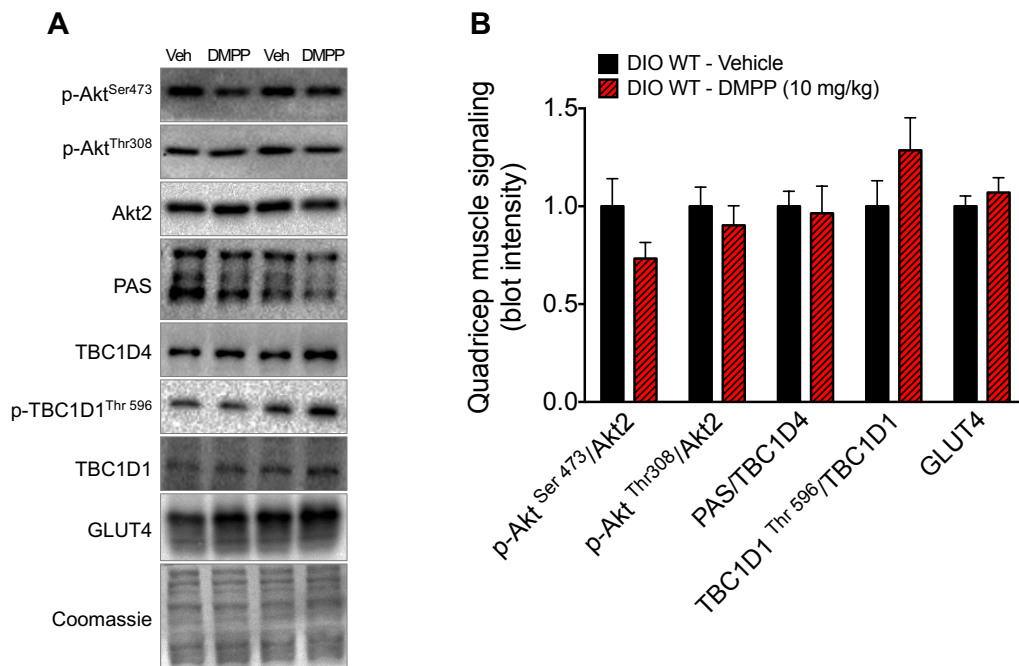
Figure 5 DMPP improves insulin sensitivity independent of canonical insulin signaling. Representative Western blots (**A**) and quantification (**B**) of phosphorylated Akt[Ser473], phosphorylated Akt[Thr308], Akt2, PAS, TBC1D4, phosphorylated TBC1D1[Thr596], TBC1D1, and GLUT4 protein content in quadriceps muscle from diet-induced obese (DIO) wild-type (WT) mice treated as described in Figure 4. Coomassie staining serves as a loading control. Western blot data are expressed as relative units compared to vehicle-treated mice. All data are presented as mean ± s.e.m. (n = 7). Differences were probed with two-tailed Student's t-tests, comparing the means of vehicle and DMPP for each protein (**B**).
GLUT4: Glucose transporter type 4; PAS: phospho Akt substrate; TBC1D4: TBC1 Domain Family Member 4; TBC1D1: TBC1 Domain Family Member 1

When taken together, the accrued data suggests chronic DMPP administration improves glucose tolerance via an epinephrine-independent mechanism that is capable of selectively

affecting glucose disposal capacity in the insulin-sensitive BAT and muscle tissues without impacting the status of insulin-associated signaling proteins or GLUT4 abundance. In agreement with previous work that implicates the CNS [2], we show that chronic DMPP fails to improve glucose tolerance in the leptin receptor deficient db/db mouse (Supplemental Fig. 2D). These data indicate that the peripheral improvement in insulin sensitivity might be mediated centrally.

Discussion

This research provides the first evidence that chronic treatment with the α3β4 nAChR agonist DMPP improves glycemia in DIO mice by enhancing peripheral insulin sensitivity. Specifically, we demonstrate that chronic DMPP treatment increases *in vivo* insulin-stimulated glucose uptake into BAT, skeletal muscle, and the heart. This pronounced glucose uptake into skeletal muscle was independent of insulin signaling and plasma insulin levels in DMPP-treated mice. A critical component to the beneficial effect of DMPP is a chronic treatment regimen. Three consecutive days of treatment with DMPP was sufficient to elicit a robust improvement in glucose tolerance, which is a surprising finding given that a single injection of DMPP into DIO mice elicited a rise in blood glucose that lasted approximately five hours. In order to investigate the paradoxical differences between the two treatment regimens, we used an array of genetic mouse models in combination with specific pharmacological tools to offer evidence that an increase in epinephrine secretion underpins the acute hyperglycemic effect observed in singular injections of DMPP.

The hyperglycemic episode following the first DMPP injection seems counterintuitive to the chronic glycemic benefit. However, there is precedence: Glucagon, for example, is a catabolic hormone that functions as a potent gluconeogenic agent acutely inducing hyperglycemia, yet, chronic treatment with glucagon in DIO mice can elicit glycemic benefits [25]. Our data strongly suggests that the acute hyperglycemic effect of DMPP is mediated through its involvement in β4 nAChRs-induced release of epinephrine. First to our reasoning, circulating epinephrine was increased following DMPP administration, suggesting that the epinephrine-releasing chromaffin cells of the adrenal medulla, which express α3β4 nAChRs, are directly triggered by DMPP stimulation [27]. Second, consistent with epinephrine's anti-insulinotropic effect at the α2-AR of the pancreatic β-cell [28, 29], acute DMPP treatment led towards a trend of lower insulin levels in DIO WT mice and decreased insulin levels in DIO betaless mice. Third, given epinephrine activates β-ARs of the pancreatic α-cell inducing

glucagon secretion [30], we found that the hyperglycemic effect of DMPP was blunted in Gcgr Li-KO mice. Moreover, hepatic genes related to gluconeogenesis were upregulated upon DMPP treatment, but failed to be induced in mice that are devoid of β_1-, β_2-, and β_3-ARs. Fourth, treatment of betaless mice with the α_2-AR antagonist yohimbine, to curtail epinephrine action at the pancreas and liver, eliminated the DMPP-induced hyperglycemia. Collectively, we suggest that epinephrine – eliciting the classic fight or flight metabolic response - accounts for the acute DMPP-induced hyperglycemia *in vivo*. It remains a possibility that DMPP can still directly act on nerves innervating pancreatic α- and β-cells to modulate insulin and glucagon secretion, as reported by Karlsson & Ahren [31]. In adrenalectomized mice, DMPP increased plasma insulin secretion two minutes upon intravenous injections. However, in our combined genetic and pharmacological model of yohimbine-treated betaless mice, insulin was not increased (*data not shown*), suggesting that DMPP does not exert direct effects on the pancreas, but that catecholamines are the main mediators of the short-term hyperglycemia *in vivo*. In agreement, Vu *et al.* previously observed similar hyperglycemic outcomes after treatment of lean mice with nicotine [15]. While DMPP exclusively elicited epinephrine secretion, nicotine increased both, plasma epinephrine and norepinephrine levels [15]. The latter could explain why acute nicotine treatment raised insulin levels [15], when we observed the opposite effect with DMPP.

In contrast to the acute hyperglycemic effect of DMPP, chronic DMPP improves glucose tolerance in DIO WT mice, consistent with our previous study [2]. By assessing glucose uptake *in vivo* with radioactive tracer, we now demonstrate for the first time that DMPP promoted peripheral insulin sensitivity while concomitantly plasma insulin trends to be decreased. Of note, among the fat depots, insulin-stimulated glucose uptake was increased into the BAT, but not into the iWAT or eWAT. This might be related to the previous observation that DMPP selectively induced protein expression of the uncoupling protein 1 (UCP1) in the BAT, but not in the iWAT in mice housed at thermoneutrality [2]. Moreover, DMPP treatment significantly enhanced insulin-stimulated glucose uptake into heart and skeletal muscle. The increase in muscle glucose uptake is of especial relevance given that skeletal muscle comprises ~40% of total body mass and is the key tissue for normal postprandial glucose disposal in humans [32]. Thus we aimed to understand whether DMPP affects key enzymes of insulin signaling. Phosphorylation of Akt and TBC1D1/4, however, were similar in vehicle- and DMPP-treated animals, indicating that DMPP did not alter the canonical insulin-signaling cascade. Similarly, the abundance of the insulin responsive GLUT4 protein was unaltered. Thus, the mechanisms underpinning the robust improvement

of *in vivo* glucose uptake upon chronic DMPP treatment remain to be elucidated. Intriguingly, after chronic treatment with DMPP, epinephrine was not increased in response to DMPP injection, suggesting that the chronic glycemic benefits of DMPP might not be solely a consequence of repeated epinephrine stimulation. In fact, we postulate the involvement of a hitherto unknown centrally mediated component since DMPP had no glycemic benefits in db/db mice lacking a functional leptin receptor. In agreement, it has been shown that DMPP also failed to improve glucose tolerance in melanocortin 4 receptor KO mice [2]. Together, this raises the intriguing hypothesis that the central leptin-melanocortin pathway is involved in the glycemic benefit of chronic DMPP. Of note, previous intracerebroventricular injections of leptin have been associated with an increased uptake of glucose into the BAT, but not the eWAT or retroperitoneal WAT, the heart, and the skeletal muscles, which strongly resembles our findings with DMPP [33]. This increase in glucose uptake was independent of a systemic release of catecholamines as the potency of leptin to increase glucose uptake in the tissues was retained upon adrenalectomization [34]. Since DMPP is implicated to activate $\alpha 3 \beta 4$ nAChRs expressed on POMC neurons [4], we thus postulate that chronic DMPP administration activates central leptin signaling pathways leading to an enhanced uptake of glucose in selective tissues.

In summary, we report a temporal dichotomy in the glycemic effects of DMPP. Acute hyperglycemic effects, mediated by a Chrnb4-dependent release of epinephrine are eclipsed by chronic glycemic benefits, which are driven by a robust improvement in peripheral insulin sensitivity. Deciphering the exact molecular mechanisms of DMPP in the future could reveal novel treatment strategies for diabetes.

Author contributions
S.J. designed and performed the experiments, analyzed and interpreted data, and wrote the manuscript. M. De A., A.M.L., and A.M.F. helped perform and analyze experiments. A.N. interpreted data and co-wrote the manuscript. B.K., E.A.R., K.W.S., and M.H.T. helped design and interpret experiments. C.C., T.D.M., and M.K. co-conceptualized the project, analyzed, and interpreted data and co-wrote the manuscript with S.J.

Competing interests
M.H.T has served as SAB member of ERX Pharmaceuticals. The Institute for Diabetes and Obesity cooperates with Novo Nordisk and Sanofi-Aventis.

References

[1]   Ng, M., Fleming, T., Robinson, M., Thomson, B., Graetz, N., Margono, C., et al., 2014. Global, regional, and national prevalence of overweight and obesity in children and adults during 1980-2013: a systematic analysis for the Global Burden of Disease Study 2013. Lancet 384: 766-781.

[2]   Clemmensen, C., Jall, S., Kleinert, M., Quarta, C., Gruber, T., Reber, J., et al., 2018. Coordinated targeting of cold and nicotinic receptors synergistically improves obesity and type 2 diabetes. Nat Commun 9: 4304.

[3]   Tschop, M.H., Finan, B., Clemmensen, C., Gelfanov, V., Perez-Tilve, D., Muller, T.D., et al., 2016. Unimolecular Polypharmacy for Treatment of Diabetes and Obesity. Cell Metab 24: 51-62.

[4]   Mineur, Y.S., Abizaid, A., Rao, Y., Salas, R., DiLeone, R.J., Gundisch, D., et al., 2011. Nicotine decreases food intake through activation of POMC neurons. Science 332: 1330-1332.

[5]   Williamson, D.F., Madans, J., Anda, R.F., Kleinman, J.C., Giovino, G.A., Byers, T., 1991. Smoking cessation and severity of weight gain in a national cohort. N Engl J Med 324: 739-745.

[6]   Audrain-McGovern, J., Benowitz, N.L., 2011. Cigarette smoking, nicotine, and body weight. Clin Pharmacol Ther 90: 164-168.

[7]   Walser, T., Cui, X., Yanagawa, J., Lee, J.M., Heinrich, E., Lee, G., et al., 2008. Smoking and lung cancer: the role of inflammation. Proc Am Thorac Soc 5: 811-815.

[8]   Sinha-Hikim, I., Friedman, T.C., Shin, C.S., Lee, D., Ivey, R., Sinha-Hikim, A.P., 2014. Nicotine in combination with a high-fat diet causes intramyocellular mitochondrial abnormalities in male mice. Endocrinology 155: 865-872.

[9]   Bergman, B.C., Perreault, L., Hunerdosse, D.M., Koehler, M.C., Samek, A.M., Eckel, R.H., 2009. Intramuscular lipid metabolism in the insulin resistance of smoking. Diabetes 58: 2220-2227.

[10]   McGehee, D.S., Role, L.W., 1995. Physiological diversity of nicotinic acetylcholine receptors expressed by vertebrate neurons. Annu Rev Physiol 57: 521-546.

[11]   Xiao, Y., Kellar, K.J., 2004. The comparative pharmacology and up-regulation of rat neuronal nicotinic receptor subtype binding sites stably expressed in transfected mammalian cells. J Pharmacol Exp Ther 310: 98-107.

[12]   Wu, Y., Song, P., Zhang, W., Liu, J., Dai, X., Liu, Z., et al., 2015. Activation of AMPKalpha2 in adipocytes is essential for nicotine-induced insulin resistance in vivo. Nat Med 21: 373-382.

[13]   Wang, X., Yang, Z., Xue, B., Shi, H., 2011. Activation of the cholinergic antiinflammatory pathway ameliorates obesity-induced inflammation and insulin resistance. Endocrinology 152: 836-846.

[14]   Borovikova, L.V., Ivanova, S., Zhang, M., Yang, H., Botchkina, G.I., Watkins, L.R., et al., 2000. Vagus nerve stimulation attenuates the systemic inflammatory response to endotoxin. Nature 405: 458-462.

[15]   Vu, C.U., Siddiqui, J.A., Wadensweiler, P., Gayen, J.R., Avolio, E., Bandyopadhyay, G.K., et al., 2014. Nicotinic acetylcholine receptors in glucose homeostasis: the acute hyperglycemic and chronic insulin-sensitive effects of nicotine suggest dual opposing roles of the receptors in male mice. Endocrinology 155: 3793-3805.

[16]   Marrero, M.B., Lucas, R., Salet, C., Hauser, T.A., Mazurov, A., Lippiello, P.M., et al., 2010. An alpha7 nicotinic acetylcholine receptor-selective agonist reduces weight gain and metabolic changes in a mouse model of diabetes. J Pharmacol Exp Ther 332: 173-180.

[17]   Kleinert, M., Clemmensen, C., Hofmann, S.M., Moore, M.C., Renner, S., Woods, S.C., et al., 2018. Animal models of obesity and diabetes mellitus. Nat Rev Endocrinol 14: 140-162.

[18]   Xu, W., Orr-Urtreger, A., Nigro, F., Gelber, S., Sutcliffe, C.B., Armstrong, D., et al., 1999. Multiorgan autonomic dysfunction in mice lacking the beta2 and the beta4 subunits of neuronal nicotinic acetylcholine receptors. J Neurosci 19: 9298-9305.

[19]   Hotta, Y., Nakamura, H., Konishi, M., Murata, Y., Takagi, H., Matsumura, S., et al., 2009. Fibroblast growth factor 21 regulates lipolysis in white adipose tissue but is not required for ketogenesis and triglyceride clearance in liver. Endocrinology 150: 4625-4633.

[20]   Bachman, E.S., Dhillon, H., Zhang, C.Y., Cinti, S., Bianco, A.C., Kobilka, B.K., et al., 2002. betaAR signaling required for diet-induced thermogenesis and obesity resistance. Science 297: 843-845.

[21]   Kleinert, M., Parker, B.L., Fritzen, A.M., Knudsen, J.R., Jensen, T.E., Kjobsted, R., et al., 2017. Mammalian target of rapamycin complex 2 regulates muscle glucose uptake during exercise in mice. J Physiol 595: 4845-4855.

[22]   Maarbjerg, S.J., Jorgensen, S.B., Rose, A.J., Jeppesen, J., Jensen, T.E., Treebak, J.T., et al., 2009. Genetic impairment of AMPKalpha2 signaling does not reduce muscle glucose uptake during treadmill exercise in mice. Am J Physiol Endocrinol Metab 297: E924-934.

[23]   Barth, E., Albuszies, G., Baumgart, K., Matejovic, M., Wachter, U., Vogt, J., et al., 2007. Glucose metabolism and catecholamines. Crit Care Med 35: S508-518.

[24]   De Marinis, Y.Z., Salehi, A., Ward, C.E., Zhang, Q., Abdulkader, F., Bengtsson, M., et al., 2010. GLP-1 inhibits and adrenaline stimulates glucagon release by differential modulation of N- and L-type Ca2+ channel-dependent exocytosis. Cell Metab 11: 543-553.

[25]   Muller, T.D., Finan, B., Clemmensen, C., DiMarchi, R.D., Tschop, M.H., 2017. The New Biology and Pharmacology of Glucagon. Physiol Rev 97: 721-766.

[26]   Cyphert, H.A., Alonge, K.M., Ippagunta, S.M., Hillgartner, F.B., 2014. Glucagon stimulates hepatic FGF21 secretion through a PKA- and EPAC-dependent posttranscriptional mechanism. PLoS One 9: e94996.

[27]   Sala, F., Nistri, A., Criado, M., 2008. Nicotinic acetylcholine receptors of adrenal chromaffin cells. Acta Physiol (Oxf) 192: 203-212.

[28]   Hsu, W.H., Xiang, H.D., Rajan, A.S., Boyd, A.E., 3rd, 1991. Activation of alpha 2-adrenergic receptors decreases Ca2+ influx to inhibit insulin secretion in a hamster beta-cell line: an action mediated by a guanosine triphosphate-binding protein. Endocrinology 128: 958-964.

[29]   Fagerholm, V., Haaparanta, M., Scheinin, M., 2011. alpha2-adrenoceptor regulation of blood glucose homeostasis. Basic Clin Pharmacol Toxicol 108: 365-370.

[30]   Hamilton, A., Zhang, Q., Salehi, A., Willems, M., Knudsen, J.G., Ringgaard, A.K., et al., 2018. Adrenaline Stimulates Glucagon Secretion by Tpc2-Dependent Ca(2+) Mobilization From Acidic Stores in Pancreatic alpha-Cells. Diabetes 67: 1128-1139.

[31]   Karlsson, S., Ahren, B., 1998. Insulin and glucagon secretion by ganglionic nicotinic activation in adrenalectomized mice. Eur J Pharmacol 342: 291-295.

[32]   DeFronzo, R.A., Jacot, E., Jequier, E., Maeder, E., Wahren, J., Felber, J.P., 1981. The effect of insulin on the disposal of intravenous glucose. Results from indirect calorimetry and hepatic and femoral venous catheterization. Diabetes 30: 1000-1007.

[33]   Minokoshi, Y., Haque, M.S., Shimazu, T., 1999. Microinjection of leptin into the ventromedial hypothalamus increases glucose uptake in peripheral tissues in rats. Diabetes 48: 287-291.

[34]   Haque, M.S., Minokoshi, Y., Hamai, M., Iwai, M., Horiuchi, M., Shimazu, T., 1999. Role of the sympathetic nervous system and insulin in enhancing glucose uptake in peripheral tissues after intrahypothalamic injection of leptin in rats. Diabetes 48: 1706-1712.

Supplemental table 1 Sequences of primers:

Gene	5' – 3' primer	5' – 3' primer
G6PC	CTGTCTGTCCCGGATCTACC	GCGCGAAACCAAACAAGAAG
GYS2	CGCTCCTTGTCGGTGACATC	CATCGGCTGTCGTTTTGGC
Hprt	AAGCTTGCTGGTGAAAAGGA	TTGCGCTCATCTTAGGCTTT
PEPCK	CTGCATAACGGTCTGGACTTC	CAGCAAACTCCCGTACTCC
PGC1α	AGCCGTGACCACTGACAACGAG	GCTGCATGGTTCTGAGTGCTAAG
PGM	CCAAAATCTTGCGGGCCATA	CCAGAACAAAGGGACAGCAC
Ppib	GCATCTATGGTGAGCGCTTC	CTCCACCTTCCGTACCACAT
PYGL	TACATTCAGGCTGTGCTGGA	AAGGCATCAAACACGGTTCC

Supplemental figures
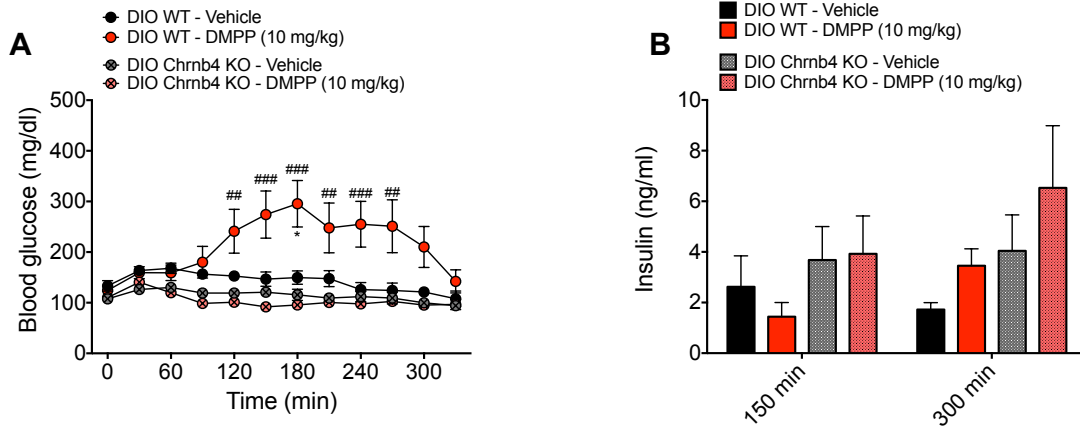
Supplemental figure 1 DMPP elicits hyperglycemia specifically via Chrnb4. (**A**) Effect of first injection of 1,1-Dimethyl-4-phenylpiperazinium iodide (DMPP) (10 mg/kg) or vehicle (injected at time point 0 minutes) on blood glucose in diet-induced obese (DIO) wild-type (WT) and Chrnb4 knockout (KO) mice (n = 6-8), (**B**) and plasma insulin at indicated time points (n = 4-8). All data are presented as mean ± s.e.m.. The data presented in the line graph in (**A**) and the bar graph in (**B**) were analyzed by three-way RM ANOVA with the three factors: time, genotype (WT vs. KO), and drug (DMPP vs. vehicle). A Tukey post-hoc test was applied. *$p < 0.05$, ***$p < 0.001$ effects of the drug, compared to vehicle. #$p < 0.05$, ##$p < 0.01$, ###$p < 0.001$ effect of intervention between genotypes.
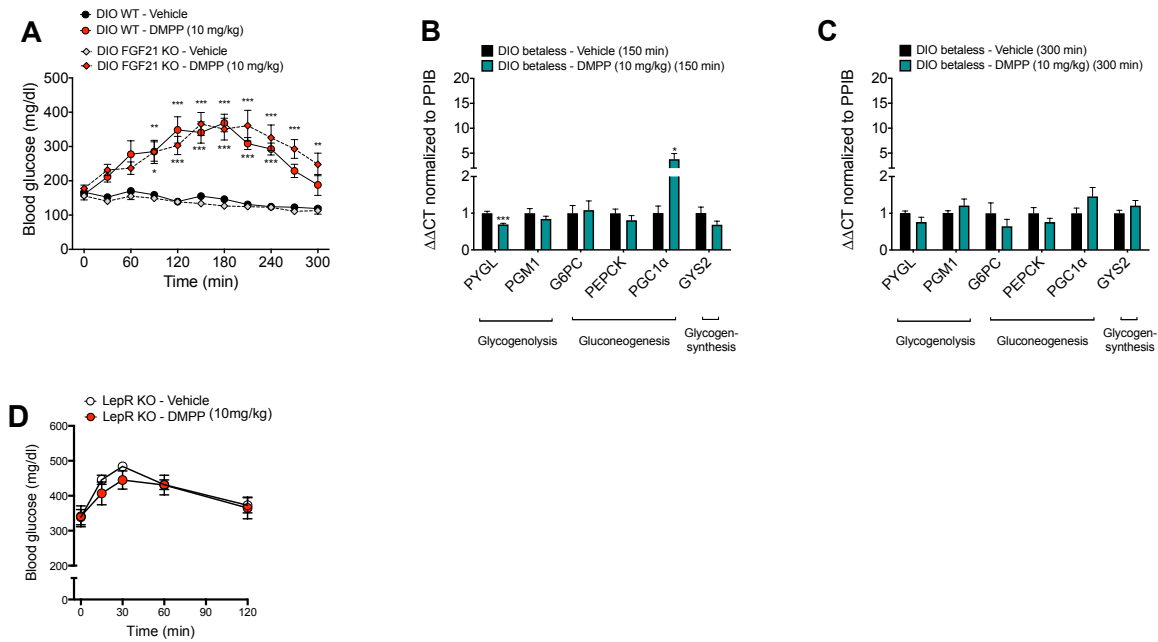
Supplemental figure 2 DMPP elicits hyperglycemia via epinephrine-mediated effects on the liver and chronically improves glucose tolerance involving the central leptin pathway. (**A**) Effect of first injection of 1,1-Dimethyl-4-phenylpiperazinium iodide (DMPP) (10 mg/kg) or vehicle (injected at time point 0 minutes) on blood glucose in diet-induced obese (DIO) wild-type (WT) and fibroblast growth factor 21 (FGF21) knockout (KO) mice (n = 8). (**B,C**) Effect of first injection of DMPP on liver gene expression in DIO betaless mice at 150 (**B**) and 300 minutes (**C**) (n = 6-7). (**D**) Glucose tolerance 18 hours after seventh injection of daily (DMPP) or vehicle in diet-induced obese (DIO) leptin receptor KO (db/db) mice (n = 7-10). All data are presented as mean ± s.e.m.. The data presented in the line graph in (**A**) were analyzed by three-way RM ANOVA with the three factors: time, genotype (WT vs. KO), and drug (DMPP vs. vehicle). The data presented in bar graphs (**B, C**) were probed with two-tailed Student's *t*-tests, comparing the means of vehicle and DMPP. The data presented in the line graph in (**D**) was analyzed by two-way ANOVA (time and drug). A Tukey post-hoc test was applied when appropriate. *$p < 0.05$, **$p < 0.01$, ***$p < 0.001$ effects of the drug, compared to vehicle.

Summary of Key Findings

The scope of the PhD thesis was to elucidate novel polypharmacological strategies to tackle the ever-growing obesity and diabetes pandemics across sexes. **Therefore, the first research aim was to assess the efficacy of the GLP-1/GIP/glucagon triagonist in DIO female mice**. Promising previous preclinical reports have established a potent body weight-lowering effect of the GLP-1/GIP/glucagon triagonist in DIO male mice that resembled bariatric surgery in its efficacy. **The second research aim was to assess the efficacy of a small molecule-based polypharmacological approach to target cold and nicotine receptors to improve metabolic disturbances in DIO male mice.** Icilin has been identified as super-agonist for cold receptors, TRPM8, and DMPP selectively activates α3β4 nAChRs.

Pirt has been proposed to act as an endogenous positive regulator of TRPM8 by enhancing TRPM8-mediated currents. **Thus**, **the third research aim was to assess the role of Pirt in energy and glucose metabolism and the necessity of Pirt in icilin-evoked activation of TRPM8-dependent energy expenditure.** Chronic DMPP potently improves glucose tolerance in DIO mice, but acutely DMPP elicits profound hyperglycemia. **The fourth research aim was to assess the opposing acute and chronic effects of DMPP on glycemia.**

Chapter I – Due to a sex bias in the evaluation of drugs and supported by an initiative of the NIH to also include female mice in preclinical studies, DIO female mice were chronically treated with the GLP-1/GIP/glucagon triagonist and the efficacy was compared to a fat mass-matched male cohort and HFD exposure-matched male cohort. Most importantly, the triagonist potently improved metabolic disturbances in fat mass-matched male and female mice to a comparable extent.

Chapter II – Concerted activation of TRPM8 cold receptors and α3β4 nAChRs synergistically improved body weight, hepatic steatosis, and glycemic control in DIO male mice. Icilin indirectly increased BAT-dependent energy expenditure, while DMPP suppressed food intake and potently improved glucose tolerance.

Chapter III – The global lack of Pirt only led to subtle female-specific metabolic dysfunctions in mice and Pirt was not relevant for the icilin-mediated increase in energy expenditure upon activation of TRPM8 receptors.

Chapter IV – The acute hyperglycemic effect of DMPP was associated with an increase in epinephrine secretion, which exerted classical "fight-or-flight" effects on the pancreatic α- and β-cells and the liver. Chronically, DMPP improved peripheral insulin sensitivity specifically in striated muscle, the heart, and the BAT, but not the white adipose tissue.

4 Discussion

Obesity and T2DM are a major public health problem. The first therapeutic approach to treat the metabolic disturbances is the modification of lifestyle, including nutrition counseling and exercise intervention (Wirth et al., 2014). Unfortunately, changing habits is difficult, consequently compliance and positive outcome rates are low. The availability of pharmacological treatment options is limited and differs geographically. Currently approved anti-obesity drugs in the USA include phentermine/topiramate, lorcaserine, liraglutide, naltrexone/bupropion, and orlistat, while only the latter three are approved in Europe. However, the body weight-lowering effect of pharmacotherapy is limited and bariatric surgery remains the best strategy to consistently treat morbid obesity. The invasive procedures, like vertical sleeve gastrectomy or Roux-en-Y gastric bypass are effective in lowering body weight and improving hyperglycemic complications in most patients (Schauer et al., 2017). Unfortunately, adverse effects, such as reoperations, pneumonia, and hernias can occur (Schauer et al., 2012). The procedures are expensive and only clinically indicated if patients are morbidly obese. Taken together, advancements in pharmacotherapy are urgently required to halt the rising prevalence of obesity and associated metabolic diseases.

4.1 Evolution of anti-obesity therapies - Lessons from history

In the early 20th century, the ideal beauty standard started to shift towards lower BMI and the pharmacological dieting industry became a multibillion-dollar business (Cohen et al., 2012). However, medical anti-obesity treatments failed to be effective and even turned out to be fatal in several cases (Cohen et al., 2012). In the 1950s, surgeons reported loss in body weight as common side effect upon surgical shortening of the small intestine for the treatment of ulcers (Celio and Pories, 2016, Henrikson, 1994). These observations ignited research interest in bariatric surgery for the therapy of obesity. In dogs, resections of parts of the intestine resulted in malabsorption and consequently body weight loss (Kremen et al., 1954). Although initial procedures were not as defined, patients were willing to undergo these massively invasive and irreversible interventions. Given the fact that jaw wiring represented the stand-alone therapy to that time, the inhibition level to accept surgeons resecting large parts of the intestine was probably lower than one would imagine nowadays (Rodgers et al., 1977). Initial bariatric surgeries were often associated with severe adverse effects, such as diarrhea, nausea, and bloating (Fobi, 2004), but procedures were refined over time and resulted in a loss of up to 27.5% of initial body weight 4 years after the surgery (Maciejewski et al., 2016). Interestingly, the incretin hormone GLP-1 was increased exclusively upon VSG and (Roux-

en-Y) gastric bypass, but not upon dieting-induced weight loss (Laferrere et al., 2008, Shankar et al., 2017, Tsoli et al., 2013), which put forward associations of an altered gut hormonal signaling upon successful bariatric surgery. However, persistent efficacy of VSG in GLP-1R KO mice suggested that GLP-1 acts in concert with other factors (Wilson-Perez et al., 2013). Thus, attempts to pharmacologically mimic bariatric surgery by targeting more than just one mechanism have evolved. The combinations of several distinct acting hormones or small molecules that are increased upon VSG or gastric bypass take the evolution of polypharmacology to the next level.

4.2 Polypharmacological mimicking of bariatric surgery – From bedside to bench

The simultaneous targeting of distinct mechanisms using polypharmacology has been proposed as early as in the 1940s, when the Clark & Clark's Clarkotabs (Camden, NJ, USA) were marketed as weight loss medication. In an attempt to personalize pharmacotherapy, Clarkotabs ("rainbow pills") came in different colors and prescribers were encouraged to give out different colored pills to the patients (Cohen et al., 2012). The composition of the rainbow pills changed over time, but usually combined *d*-amphetamine, chlorthalidone, and thyroid hormone for the induction of weight loss with digitalis, barbiturates, potassium, glandular extracts, and belladonna to counteract potential adverse effects (Cohen et al., 2012, Müller et al., 2018). Since all of these early attempts of polypharmacological anti-obesity therapy were devoid of thorough safety evaluations, at least 60 fatalities could be directly ascribed to the consumption of rainbow pills. In 1968, the FDA prohibited the distribution of anti-obesity medication, which combined thyroid hormones and amphetamines or other agents, in the USA (Cohen et al., 2012). The FDA announced them to be misbranded and confiscated 43 million pills from the companies (US Food and Drug Administration, 1968).

Learning lessons from human failures, polypharmacology has been further developed and refined. Today, the combination of naltrexone/bupropion is approved for the treatment of obesity. Confirmation studies report a total body weight loss of 6.1% with naltrexone/bupropion compared to 1.3% in the placebo group in combination with lifestyle modification therapy upon one year of administration (Greenway et al., 2010). In conjunction to intensive behavior modification, naltrexone/bupropion lowered body weight by 9.3% compared to 5.1% in the placebo group in the course of one year (Wadden et al., 2011). These studies promote naltrexone/bupropion as a promising medical therapy to treat obesity, but caution has to be used. Both studies were industry-sponsored, they were highly controlled efficacy studies, while real-life effectiveness studies are lacking, and the data were analyzed using the last observation carried forward strategy. Using this strategy, a bias is introduced, as

the last data obtained from dropouts are included in the analysis (Tek, 2016). As the one-year body weight-lowering efficacy of naltrexone/bupropion was remote to being comparable to Roux-en-Y gastric bypass (~ 30% loss in initial body weight compared to nonsurgical matches) (Maciejewski et al., 2016), novel polypharmacological strategies for the treatment of obesity were pursued. Encouraging preclinical results have been reported from the laboratories of Richard DiMarchi and Matthias Tschöp. One of their strategies involves the directed delivery of nuclear hormones to specific target cells. Chemical ligation of e.g. the thyroid hormone tri-iodothyronine (T3) to glucagon selectively transports T3 to cells that express GcgR (Finan et al., 2016). Singularly, T3 and glucagon promote body weight loss and ameliorate dyslipidemia (Danforth and Burger, 1984, Onur et al., 2005, Pucci et al., 2000). The selective activation of hepatic thyroid receptors (TR) β with T3 potently lowers cholesterol and lipoproteins (Cable et al., 2009, Erion et al., 2007) and activation of TR expressed in the adipose tissue induces energy expenditure and lipolysis (Oppenheimer et al., 1991). However, T3 treatment can be associated with severe adverse effects such as cardiac hypertrophy, bone deterioration, and muscle catabolism (Ishisaki et al., 2004, Kinugawa et al., 2005). Glucagon, as elaborated in 1.3.1, suppresses food intake and stimulates BAT-dependent thermogenesis (Billington et al., 1991, de Castro et al., 1978, Geary et al., 1992, Geary et al., 1993). As hypothesized, the glucagon/T3 co-agonist reversed diet-induced dyslipidemia and aspects of the metabolic syndrome in different mouse models of obesity (Finan et al., 2016). With a labeled version of the glucagon/T3 co-agonist, Finan *et al* proved specificity of the co-agonist as T3 accumulated in the liver and to a lesser extent in the pancreas, iWAT, and the heart, but not in tissues that did not express GcgR (Finan et al., 2016). Using genetically modified mouse lines, it was confirmed that the glucagon/T3 co-agonist depends on functional hepatic expression of GcgR as well as TRβ (Finan et al., 2016). The therapeutic significance of the glucagon/T3 co-agonist was further highlighted by its ability to potently decrease arterial plaque area in diseased LDL receptor KO mice and the ability to alleviate fibrosis in mice that already presented with an advanced fatty liver disease (Finan et al., 2016). Collectively, the preclinical evaluation of the glucagon/T3 co-agonist has been promising, but further assessments are required to decide whether the co-agonist proceeds to testing in higher mammals (Müller et al., 2018). The necessity of such investigations is highlighted by earlier attempts that specifically transported thyroid hormone to the liver. They successfully improved the lipoprotein profile (Baxter and Webb, 2009, Erion et al., 2007, Berkenstam et al., 2008), but chronic treatment of dogs was associated with cartilage damage and treatment of patients with familial hypercholesterolaemia in a phase III

study led to severe adverse hepatic effects, such as increases in ALT and AST (Sjouke et al., 2014), suggesting that chronically increased concentrations of T3 in the liver might be harmful.

Other approaches for peptide-mediated delivery of nuclear hormones included the combination of the incretin hormone GLP-1 with the steroid hormone estrogen. Based on beneficial cardiometabolic effects of estrogen replacement therapy in postmenopausal women, estrogen had been proposed as promising anti-obesity therapeutic (Mauvais-Jarvis et al., 2017). Estrogen acts centrally to reduce food intake and increases energy expenditure (Gao and Horvath, 2008). It is an insulinotropic hormone, suppresses hepatic gluconeogenesis, improves peripheral insulin sensitivity, and reduces cholesterol levels and visceral fat depots (Hodgin and Maeda, 2002, Wong et al., 2010, Yan et al., 2018, Nanda et al., 2003). However, sustained elevated endogenous estrogen as well as oral contraceptives containing ethinyl estrogen can promote breast cancer development at a significantly increased relative risk of 1.2 to 2.5 (Yue et al., 2013, Yager and Davidson, 2006, Yager, 2015, Key et al., 2002). With the specific transport of estrogen to GLP-1R expressing cells, DiMarchi and Tschöp developed a potent and safe drug that reversed diet-induced and genetic obesity in mice, improved glucose tolerance, and reduced plasma triglyceride and cholesterol levels (Finan et al., 2012).

In a further approach, dexamethasone was specifically delivered to GLP-1R expressing cells (Quarta et al., 2017). Excess body weight can trigger systemic inflammation, which might be causally involved in the progression of obesity-related comorbidities (see 1.1.1) (Lumeng and Saltiel, 2011, Hotamisligil, 2006). Glucocorticoids, such as dexamethasone, ameliorate inflammatory processes and act immunosuppressant, thus the GLP-1/dexamethasone co-agonist had been indicated as a drug to prevent the development of obesity-induced insulin resistance or NAFLD (Coutinho and Chapman, 2011). Paradoxically, glucocorticoid treatment in humans is associated with an increase in body weight, osteoporosis, and glucometabolic disturbances (Schacke et al., 2002). However, the targeted delivery of dexamethasone to GLP-1R expressing cells safely and synergistically reduced body weight and metabolic complications in DIO mice (Quarta et al., 2017).

The greatest efficacy of a polypharmacological drug to improve and reverse multiple nodes of metabolic disorders in animals has been achieved with the GLP-1/GIP/glucagon triagonist (Finan et al., 2015). The balanced agonist at all three hormonal receptors reversed adiposity in male DIO mice to a comparable extent as in mice that underwent Roux-en-Y gastric bypass or biliopancreatic diversion (Yin et al., 2011, Finan et al., 2015, Jall et al., 2017). In the scope of

this thesis, collaborators and I confirmed that the triagonist equally efficiently lowered body weight, body fat mass, and plasma cholesterol in DIO female mice compared to male mice that were matched in the body fat content (Jall et al., 2017). We assessed the effect of the triagonist across sexes due to an initiative of the NIH that specifically invoked to include female mice in preclinical research (Clayton and Collins, 2014). Generally, investigations on human and animal metabolism preferably study male subjects and mice. The "70-kg male" that is typically used as a standard model led to a bias in the reporting of biological research results (Clayton, 2016). Although in humans, the selection bias is less evident, preclinical metabolic studies mostly use male mice as female C57Bl/6j mice are somewhat protected against diet-induced obesity (Yang et al., 2014) and their obese state is associated with the development of only a moderate glucose intolerance (Pettersson et al., 2012, Gallou-Kabani et al., 2007, Riant et al., 2009). In a pharmacological study that aims at assessing the potency of drugs to reduce body weight and improve glucose tolerance, male mice are the preferred choice of model. In our study (Chapter I), female mice had to be maintained on a HFD for 30 weeks to match the fat mass content of males that were on the HFD for 6 weeks. In line with previous reports, obese C57Bl/6j female mice developed only mild glucose intolerance (Pettersson et al., 2012), whereas for the males, HFD feeding for 6 weeks was already sufficient to induce significant disturbances in the glucose metabolism (Jall et al., 2017). The underlying reasons for the discrepancies are thus far not completely understood, while the obvious differences between males and females are sex hormones. The two main female sex hormones are estrogen and progesterone and especially estrogen can protect against metabolic complications (Cignarella and Bolego, 2010). Upon ovariectomy, the lack of estrogen rendered female mice as susceptible to obesity as male mice (Hong et al., 2009). Moreover, ovariectomized mice developed glucose intolerance, which could be restored to normoglycemia upon external application of estrogen (Riant et al., 2009). In humans, whole-body insulin sensitivity was 41% greater in premenopausal women compared to men (Nuutila et al., 1995) and estrogen replacement therapy in postmenopausal women with coronary heart disease lowered the incidence of T2DM by 35% (Kanaya et al., 2003). Conflicting data exist on the role of estrogens in inflammatory pathways, with some researchers reporting pro- and some describing anti-inflammatory actions of estrogen (Straub, 2007). In order to test the impact of the sex hormones on the efficacy of the GLP-1/GIP/glucagon triagonist, future studies are warranted comparing male, female, and ovariectomized female mice. Finally, to exclude any impact of the duration of HFD exposure on the outcome of the triagonist treatment, a male cohort was included that was maintained on the HFD for 30 weeks. These

mice had significantly more body fat and consequently, the triagonist was more effective in lowering body weight in these mice compared to the female mice (Jall et al., 2017).

4.3 Polypharmacological activation of cold and nicotine receptors – Lessons from nature

As human metabolic diseases are diverse, I aimed to further expand the toolbox for personalized medicines. Based on the preclinical success of the different polypharmacological co- and triagonists, collaborators and I strove to develop a novel small molecule-based strategy to tackle the obesity and diabetes pandemics by modulating both aspects of energy metabolism – energy intake and expenditure. Learning from nature, we aimed to target two major canonical environmental modulators of human metabolism, namely smoking and cold, in a two-pronged approach.

Temperatures below ~ 26°C activate the cold receptor TRPM8 that is predominantly expressed in afferent dorsal root or trigeminal ganglia neurons (McKemy, 2007, Peier et al., 2002). Some controversies exist on the expression pattern of TRPM8, as few reports suggest expression of TRPM8 in the BAT (Ma et al., 2012) and WAT (Jiang et al., 2017) of mice or the WAT of humans (Rossato et al., 2014). These studies report a cell autonomous effect of menthol-evoked TRPM8 activation to induce UCP1-dependent thermogenesis (Ma et al., 2012, Jiang et al., 2017). As opposed to these studies, collaborators and I did not detect (functional) TRPM8 expression in the BAT or WAT of mice (Clemmensen et al., 2018). The results shown in chapter II of the PhD thesis strongly point to an indirect, sympathetic nervous system-driven, effect of icilin-induced TRPM8 activation on energy expenditure (Clemmensen et al., 2018), which is consistent with a previous publication (Ahern, 2013). In accordance, the MSOT data showed an increase in BAT blood flow upon treatment with icilin and DMPP, which resembles physiological adaptations to cold-induced activation of BAT thermogenesis (Reber et al., 2018). Moreover, icilin and DMPP led to an attenuated body weight loss in mice without β_1-, β_2- and β_3-ARs and maintained the potency to reverse the metabolic syndrome in DIO mice housed at thermoneutral conditions (Clemmensen et al., 2018). These results highlight the translational value of icilin, which potently reduced body weight by activating energy expenditure mechanisms specifically via TRPM8 receptors (Clemmensen et al., 2018).

To counteract a potential compensatory hyperphagia upon icilin-induced increases in energy expenditure (Ravussin et al., 2014, Cottle and Carlson, 1954), we identified the nicotinic $\alpha3\beta4$ nAChRs as promising conjunctive drug target. The small molecule DMPP is relatively

specific for α3β4 nAChRs (Xiao and Kellar, 2004) and chronic treatment with DMPP had robust anorectic effects, which were amplified by simultaneous icilin administration (Clemmensen et al., 2018). Accordingly, the two-pronged strategy of icilin and DMPP co-administration potently reduced body weight in DIO mice. Mechanistically, we identified that the combination of DMPP and icilin required both, functional α3β4 nAChRs and MC4Rs, to lower body weight (Clemmensen et al., 2018). These observations are in line with previous reports demonstrating the involvement of MC4R signaling in the body weight-lowering effect of hypothalamic nAChR activation (Mineur et al., 2011). While DMPP as well as icilin synergistically activate central MC4R on PVN neurons to explain the amplified reduction in food intake, the MC4R-dependent increase in energy expenditure most likely is mediated by MC4Rs expressed elsewhere (Mountjoy et al., 1994, Kishi et al., 2003), supporting the proposed divergent regulation of food intake and energy expenditure by the melanocortin pathway (Balthasar et al., 2005). The dose-dependent body weight-lowering effect of DMPP has been achieved with other nAChRs agonists (Mangubat et al., 2012, Mineur et al., 2011, Marrero et al., 2010). However, the robust and weight-independent improvements in diet-induced glucose intolerance were unique to DMPP (Clemmensen et al., 2018). In stark contrast, nicotine administration has been shown to have deleterious effects on glucose metabolism in mice and humans (Wu et al., 2015, Bergman et al., 2009). The glycemic improvements with DMPP were specifically mediated via α3β4 nAChRs as DMPP did not reduce body weight and improve glucose tolerance (*data not shown*) in Chrnb4 KO mice. We used mice that globally lack the β4 (gene name: Chrnb4) nAChR subunit as a model for the global lack of α3β4 nAChRs. I confirmed, with an elaborate tissue screen comparing WT and Chrnb4 KO mice, that a knockdown of β4 nAChR subunits was accompanied by a downregulation of α3 nAChR subunits (*unpublished data*), which is in line with previous reports (Kedmi et al., 2004). Most notably, an intact leptin-melanocortin system was necessary for the glycemic benefits of DMPP (Clemmensen et al., 2018). These surprising findings warrant further studies which investigate the molecular interdependency between MC4Rs and α3β4 nAChRs signaling in glucose handling and illuminate whether MC4Rs on cholinergic sympathetic preganglionic neurons are involved in the glycemic benefits of the α3β4 nAChRs agonist DMPP (Rossi et al., 2011). Together, the results presented in chapter II of the PhD thesis put forward a novel polypharmacological strategy to combat obesity by targeting TRPM8 and α3β4 nAChRs (Clemmensen et al., 2018). As of today, several reports suggest promising effects of transient receptor potential vanilloid 1 (TRPV1) pharmacology in the field of human energy expenditure (Yoneshiro et al., 2012, Ang et al., 2017, Sun et al.,

2018), albeit only one study highlights the potential TRPM8 and TRPA1 co-activation could hold in the activation of human energy expenditure (Michlig et al., 2016). For the design of future studies that aim to manipulate human energy metabolism, it is of uttermost importance to acquire more *in depth* understanding of the molecular regulation of TRP-channels. Therefore, in chapter III of the PhD thesis, collaborators and I investigated a downstream signaling molecule, Pirt, which acts as a positive endogenous regulator of TRPV1 and TRPM8 (Tang et al., 2013, Kim et al., 2008). It has been shown that Pirt enhances menthol- and cold-evoked TRPM8-mediated currents by calcium imaging studies using Fura 2-AM-loaded HEK 293 that either expressed TRPM8 alone or TRPM8 together with Pirt. The latter showed an increased Ca^{2+} influx at warmer temperatures compared to TRPM8 expressing cells. Additionally, the amplitude in Ca^{2+} influx was greater in TRPM8/Pirt expressing cells upon decreases in temperature (Tang et al., 2013). The application of menthol to the cells significantly increased Ca^{2+} influx in TRPM8/Pirt expressing cells at 32ºC with a half maximal effective concentration (EC_{50}) of ~ 200 μM menthol compared to ~ 600 μM for TRPM8, suggesting that Pirt increases the menthol affinity of TRPM8 channels at warm temperatures (Tang et al., 2013). Moreover, in whole-cell voltage-clamp the corrected current density, at varying concentrations of menthol, was higher in TRPM8 and Pirt co-expressing cells compared to cells expressing TRPM8 alone, with an EC_{50} value of ~ 90 μM menthol for TRPM8/Pirt and ~ 150 μM for TRPM8 (Tang et al., 2013). Pirt is predominantly expressed in dorsal root ganglia (DRG) and trigeminal neurons and has been previously identified to enhance TRPV1 and TRPM8-mediated currents in synergy with PIP_2 (Kim et al., 2008, Tang et al., 2016). Mice globally lacking Pirt (Pirt^{-/-}) presented with an increased latency to withdraw tails from a hot water bath and to respond to a hot plate with shaking or licking of the hindpaw (Kim et al., 2008), suggesting that Pirt^{-/-} affects behavioral responses to noxious heat. In support for a role of Pirt in cold sensing, Pirt^{-/-} mice had an increased latency to withdraw paws from a cold (-1ºC) plate (Tang et al., 2013). In the scope of this PhD thesis (chapter III), collaborators and I investigated whether the lack of Pirt in mice leads to a metabolically relevant phenotype. Cohorts of male and female Pirt^{-/-} and WT mice on a standard chow or HFD did not differ with respect to body weight, food intake, or glucose metabolism, except for the female Pirt^{-/-} mice on a chow diet, which gained significantly more body weight without differences in the food consumption, energy expenditure, or locomotor activity. The phenotypic analysis has been performed at room temperature and since Pirt^{-/-} mice exhibit an impaired behavioral response to cold temperatures (Tang et al., 2013), female mice might have failed to adapt their whole body energy metabolism to the mild cold stress

(23ºC). In general, female C57Bl/6 mice have higher core body temperatures, locomotor activity, and heart rate (*unpublished data*) (Sanchez-Alavez et al., 2011, Yang et al., 2007). The importance of the body temperature in energy metabolism has been shown as early as 1867 and recently, scientists highlighted the necessity to account for differences in this parameter (Landsberg et al., 2009, Tschöp et al., 2011, Speakman, 2013, Sanders-Ezn, 1867). Already in the early 20th century, an increase of body temperature by 1ºC has been associated with a 10%-13% rise in oxygen consumption in men (Du Bois, 1921). Female WT mice may have further increased their metabolic rate due to the mild cold stress, while female Pirt$^{-/-}$ mice did not, which potentially led to an increased body weight in female Pirt$^{-/-}$ mice. The ability of a HFD to overwrite the metabolic dysfunction is speculative, but although HFD-fed female Pirt$^{-/-}$ mice were not heavier than WT mice, they did have a significantly decreased lean mass and overall (irrespective of diet regime) the genotype had a main effect on fat mass, which was higher in the female Pirt$^{-/-}$ mice. Importantly, collaborators and I addressed a potential impaired adaptation in energy expenditure as underlying reason for the genotypic body weight difference by indirect calorimetry, but failed to detect differences. However, insignificant trends towards lower locomotor activity and nocturnal energy expenditure in Pirt$^{-/-}$ mice could suggest that the mild cold stress of 23ºC was not sufficient to induce pronounced differences in metabolic adaptations. Future studies are necessary to investigate whether a chronic cold stress of 4ºC leads to a significant body weight difference in chow- and HFD-fed female WT and Pirt$^{-/-}$ mice. In addition to behavioral deficits to respond to cold and hot temperatures, Pirt$^{-/-}$ mice have an impaired response to icilin-evoked activation of TRPM8 (Tang et al., 2013). More specifically, WT and Pirt$^{-/-}$ mice were exposed to a cold (0ºC) plate and icilin was injected in the hindpaw. Pirt$^{-/-}$ mice had higher latency time to withdraw their paws from the plate, indicating that the lack of Pirt affects icilin-mediated activation of TRPM8 receptors (Tang et al., 2013). Collaborators and I were interested, whether Pirt is necessary in the icilin-evoked activation of TRPM8-dependent energy expenditure. We reported in chapter III that icilin still induced energy expenditure in Pirt$^{-/-}$ mice, suggesting that Pirt is not required for the TRPM8-mediated increase in energy metabolism. Taken together, the lack of Pirt is associated with a subtle female-specific increase in body weight and body fat mass. Although Pirt acts as endogenous positive regulator of TRPM8, it is not necessary for the icilin-mediated activation of TRPM8, which induces energy expenditure.

Puzzled by the glycemic benefits of DMPP in DIO mice (chapter II), collaborators and I aimed to investigate the underlying mechanism in chapter IV of the presented PhD thesis. We

assessed the time-course of DMPP's effects on blood glucose and identified that the first DMPP injection acutely led to a rise in *ad libitum* fed blood glucose, which we hypothesized was mediated through a β4 nAChRs-induced release of epinephrine. We underpinned this hypothesis by measuring circulating plasma epinephrine, which was 6-fold increased 80 minutes upon DMPP injections. α3β4 nAChRs are expressed on chromaffin cells of the adrenal medulla (Sala et al., 2008) and DMPP is known to act as catecholamine and glucagon secretagogue (Karlsson and Ahren, 1998). Moreover, epinephrine inhibits insulin secretion via the $α_2$-AR of the pancreatic β-cell (Hsu et al., 1991, Fagerholm et al., 2011) and consequently, first injections of DMPP led towards a trend of lower insulin in DIO WT mice and significantly decreased insulin in DIO betaless mice. On the pancreatic α-cell, epinephrine binds β-ARs, which leads to secretion of glucagon (Hamilton et al., 2018). In agreement, the hyperglycemic effect of DMPP was blunted in liver-specific GcgR KO (GcgR Li-KO) mice. Most importantly, yohimbine treatment in betaless mice eliminated the DMPP-induced acute hyperglycemia, strongly suggesting that the rise in blood glucose was mediated via catecholamines (chapter IV). With these results we do not exclude that DMPP could directly act on nerves innervating pancreatic α- and β-cells to modulate insulin and glucagon secretion (Karlsson and Ahren, 1998), however we would have expected to detect an increase in insulin secretion in yohimbine-pretreated DMPP-injected betaless mice, which we failed to observe (*data not shown*). We therefore conclude that DMPP exerts its short-term hyperglycemic effects solely via an increase in catecholamines. In agreement, nicotine treatment in lean mice had similar acute hyperglycemic effects, which were associated with an increase in both, epinephrine as well as norepinephrine (Vu et al., 2014). The increase of norepinephrine could explain why acute nicotine treatment induced insulin levels (Vu et al., 2014), when DMPP did the opposite. Chronic treatment with DMPP, however, improved glucose tolerance in DIO mice (Clemmensen et al., 2018). Collaborators and I demonstrated in chapter IV that chronic treatment of DIO mice with DMPP promoted peripheral insulin sensitivity, while concomitantly plasma insulin trended to be decreased. Using radioactively labeled glucose, we found a selective increase in uptake of glucose in the striated muscle, the heart, and the BAT, but not the epididymal white adipose tissue (eWAT) and iWAT following chronic DMPP treatment. In agreement, we established in chapter II that DMPP monotherapy induced UCP1 protein expression selectively in the BAT, but not the iWAT of mice housed at thermoneutrality (Clemmensen et al., 2018). The increased glucose uptake in the muscle is specifically relevant as skeletal muscle makes up ~ 40% of the total body mass and is the most important tissue for postprandial glucose disposal in humans (DeFronzo et al.,

1981). Intriguingly, we did not find key enzymes of insulin signaling affected by DMPP, indicating that it did not change the canonical insulin signaling pathway. The mechanisms of the chronic glycemic benefits of DMPP remain to be clarified, but our data suggest that it is independent of repeated secretions of epinephrine. In fact, we have reported in chapters II and IV that the glycemic benefits depend on an intact leptin-melanocortin signaling (Clemmensen et al., 2018), therefore we postulate the possibility of a so far undescribed central mediation of the improvements in glucose tolerance upon DMPP treatment.

4.4 Outlook

In the presented PhD thesis, I have contributed to the preclinical evaluation of novel polypharmacological options for the treatment of obesity and associated diseases by assessing the efficacy of peptide-based and small molecule-based approaches in DIO mice. In the face of rising concerns about the global obesity endemic, novel pharmacological interventions are urgently needed. A special interest centers on different approaches, which lead to a reduction in food intake and/or an increase in energy expenditure, with the goal to further the development of personalized medicine. A metabolically healthy, obese person does not require drug therapy, which improves glucose and liver metabolism, but instead is in need for a medication targeting the adipose tissue inducing body fat loss. In turn, a normal weight subject who suffers from type 2 diabetes seeks efficient treatment with a drug that specifically improves glucose metabolism without inducing excess body weight loss. Thus, the preclinical evaluation of different strategies to reverse obesity and multiple aspects of the metabolic syndrome is of uttermost importance in the progression of novel treatment options to fight overweight and associated complications.

In chapter I, collaborators and I assessed the efficacy of the GLP-1/GIP/glucagon triagonist to reduce body weight and improve metabolic disturbances in diet-induced obese female mice. The triagonist reduced body weight to a comparable extent in female and fat-mass matched male mice. However, female C57Bl/6j mice were protected from diet-induced glucose intolerance (Jall et al., 2017). Consequently, the triagonist did not induce further improvements in glucose metabolism, which differentiates the efficacy of the triagonist between sexes. We thus postulate that the GLP-1/GIP/glucagon triagonist should be tested in male, female, and ovariectomized female mice to rule out the influences of the sex hormones on the efficacy of the pharmacotherapy to improve glucose metabolism.

For chapter II, collaborators and I demonstrated that pharmacological stimulation of TRPM8 induced energy expenditure mechanisms. By coordinately activating α3β4 nAChRs with DMPP, the beneficial effects on metabolism were potentiated resulting in the improvement of diet-induced obesity, glucose intolerance, and hepatic steatosis in mice (Clemmensen et al., 2018). To decipher the underlying mechanisms, further studies are warranted using transgenic mouse lines that specifically lack TRPM8 and Chrnb4 in the DRG or POMC neurons. It is of great interest, whether the ablation of TRPM8 in the DRG and trigeminal neurons completely abolishes the effect of icilin on energy expenditure in mice. As hypothesized in this thesis, the effect of icilin on energy expenditure is mediated via activation of TRPM8 expressed on sensory efferent neurons. Crossing TRPM8 flox mice with NaV1.8 cre mice would lead to the

selective loss of TRPM8 in DRG and trigeminal neurons. If icilin did not increase energy expenditure in these mice, we would be able to make more comprehensive conclusions on the mechanism of TRPM8's effect on metabolism. Selective ablation of nicotinic α3β4 AChRs in POMC neurons, by crossing Chrnb4 flox mice with POMC cre mice, could give insights to the mode of action of DMPP on food intake and glucose metabolism chronically (chapter II) and acutely (chapter IV).

In chapter III, collaborators and I reported subtle female-specific effects of Pirt deficiency on energy and glucose metabolism. Moreover, Pirt was not required for icilin-induced activation of TRPM8-dependent energy expenditure. Future studies are needed that investigate the possible interaction between Pirt in temperature regulation and Pirt in metabolic control. A limitation of the presented data is that we did not expose female WT and Pirt$^{-/-}$ mice to a chronic cold stress to assess the impact of this metabolic challenge on body weight. Moreover, further insight in the involvement of Pirt in body weight homeostasis could be obtained, if the metabolic phenotype of Pirt$^{-/-}$ mice housed chronically at thermoneutrality was assessed. At thermoneutrality, Pirt signaling is not active and it would be of interest whether body weight between female WT and Pirt$^{-/-}$ mice was indistinguishable to strengthen the proposed impact of Pirt on body weight in female chow-fed mice.

In chapter IV, collaborators and I presented a temporal dichotomy in the effects of DMPP on blood glucose. The acute hyperglycemia was associated with an increased epinephrine secretion, whereas chronic DMPP treatment induced glycemic benefits characterized by enhanced peripheral insulin sensitivity. It is currently unknown whether the glycemic benefits of DMPP are mediated via the moderate loss in body weight. Consequently, it will be of interest to perform a pair-feeding study, where vehicle-treated mice would be pair-fed to DMPP-treated mice. Depending on the loss of body weight in the pair-fed mice, we could draw conclusions on whether glycemic benefits are secondary to or independent of the body weight lowering effect of DMPP. Moreover, we have recently described that the benefits of chronic DMPP treatment on glucose tolerance depend on an intact leptin-melanocortin pathway (Clemmensen et al., 2018). To unravel an interconnectedness of the opposing acute and chronic effects of DMPP on glucose metabolism, it will be necessary to assess the glycemic consequence of a single injection of DMPP in db/db or MC4R KO mice.

5 References

2004. *Weight Management: State of the Science and Opportunities for Military Programs*. Washington (DC).

ABD EL AZIZ, M. S., KAHLE, M., MEIER, J. J. & NAUCK, M. A. 2017. A meta-analysis comparing clinical effects of short- or long-acting GLP-1 receptor agonists versus insulin treatment from head-to-head studies in type 2 diabetic patients. *Diabetes Obes Metab,* 19**,** 216-227.

AHERN, G. P. 2013. Transient receptor potential channels and energy homeostasis. *Trends Endocrinol Metab,* 24**,** 554-60.

ALLISON, D. B., HESHKA, S., NEALE, M. C. & HEYMSFIELD, S. B. 1994. Race effects in the genetics of adolescents' body mass index. *Int J Obes Relat Metab Disord,* 18**,** 363-8.

AMERICAN DIABETES, A. 2014. Diagnosis and classification of diabetes mellitus. *Diabetes Care,* 37 Suppl 1**,** S81-90.

AMERICAN DIABETES, A. 2015. (7) Approaches to glycemic treatment. *Diabetes Care,* 38 Suppl**,** S41-8.

ANDERSON, J. W., BRINKMAN, V. L. & HAMILTON, C. C. 1992. Weight loss and 2-y follow-up for 80 morbidly obese patients treated with intensive very-low-calorie diet and an education program. *Am J Clin Nutr,* 56**,** 244S-246S.

ANG, Q. Y., GOH, H. J., CAO, Y., LI, Y., CHAN, S. P., SWAIN, J. L., HENRY, C. J. & LEOW, M. K. 2017. A new method of infrared thermography for quantification of brown adipose tissue activation in healthy adults (TACTICAL): a randomized trial. *J Physiol Sci,* 67**,** 395-406.

APFELBAUM, M., FRICKER, J. & IGOIN-APFELBAUM, L. 1987. Low- and very-low-calorie diets. *Am J Clin Nutr,* 45**,** 1126-34.

ARAGHI, M. H., CHEN, Y. F., JAGIELSKI, A., CHOUDHURY, S., BANERJEE, D., HUSSAIN, S., THOMAS, G. N. & TAHERI, S. 2013. Effectiveness of lifestyle interventions on obstructive sleep apnea (OSA): systematic review and meta-analysis. *Sleep,* 36**,** 1553-62, 1562A-1562E.

ASHCROFT, F. M. 1996. Mechanisms of the glycaemic effects of sulfonylureas. *Horm Metab Res,* 28**,** 456-63.

ATKINSON, R. L. 1989. Low and very low calorie diets. *Med Clin North Am,* 73**,** 203-15.

AUDRAIN-MCGOVERN, J. & BENOWITZ, N. L. 2011. Cigarette smoking, nicotine, and body weight. *Clin Pharmacol Ther,* 90**,** 164-8.

AUTHIER, F. & DESBUQUOIS, B. 2008. Glucagon receptors. *Cell Mol Life Sci,* 65**,** 1880-99.

BACHMAN, E. S., DHILLON, H., ZHANG, C. Y., CINTI, S., BIANCO, A. C., KOBILKA, B. K. & LOWELL, B. B. 2002. betaAR signaling required for diet-induced thermogenesis and obesity resistance. *Science,* 297**,** 843-5.

BAKER, M. T. 2011. The history and evolution of bariatric surgical procedures. *Surg Clin North Am,* 91**,** 1181-201, viii.

BALSIGER, B. M., POGGIO, J. L., MAI, J., KELLY, K. A. & SARR, M. G. 2000. Ten and more years after vertical banded gastroplasty as primary operation for morbid obesity. *J Gastrointest Surg,* 4**,** 598-605.

BALTHASAR, N., COPPARI, R., MCMINN, J., LIU, S. M., LEE, C. E., TANG, V., KENNY, C. D., MCGOVERN, R. A., CHUA, S. C., JR., ELMQUIST, J. K. & LOWELL, B. B. 2004. Leptin receptor signaling in POMC neurons is required for normal body weight homeostasis. *Neuron,* 42**,** 983-91.

BALTHASAR, N., DALGAARD, L. T., LEE, C. E., YU, J., FUNAHASHI, H., WILLIAMS, T., FERREIRA, M., TANG, V., MCGOVERN, R. A., KENNY, C. D., CHRISTIANSEN, L. M., EDELSTEIN, E., CHOI, B., BOSS, O., ASCHKENASI, C., ZHANG, C. Y., MOUNTJOY, K., KISHI, T., ELMQUIST, J. K. & LOWELL, B. B. 2005. Divergence of melanocortin pathways in the control of food intake and energy expenditure. *Cell,* 123**,** 493-505.

BAUTISTA, D. M., SIEMENS, J., GLAZER, J. M., TSURUDA, P. R., BASBAUM, A. I., STUCKY, C. L., JORDT, S. E. & JULIUS, D. 2007. The menthol receptor TRPM8 is the principal detector of environmental cold. *Nature,* 448**,** 204-8.

BAXTER, J. D. & WEBB, P. 2009. Thyroid hormone mimetics: potential applications in atherosclerosis, obesity and type 2 diabetes. *Nat Rev Drug Discov,* 8**,** 308-20.

BELANGER, A. J. C., L.A.; D'AGOSTINO, R.B. 1988. Means at each examination and inter-examination consistency of specified characteristics: Framingham Heart Study, 30-year followup. *In:* GOVERNMENT PRINTING OFFICE (ed.). Washington, D.C.

BELLO, N. T., KEMM, M. H., OFELDT, E. M. & MORAN, T. H. 2010. Dose combinations of exendin-4 and salmon calcitonin produce additive and synergistic reductions in food intake in nonhuman primates. *Am J Physiol Regul Integr Comp Physiol,* 299**,** R945-52.

BERGMAN, B. C., PERREAULT, L., HUNERDOSSE, D. M., KOEHLER, M. C., SAMEK, A. M. & ECKEL, R. H. 2009. Intramuscular lipid metabolism in the insulin resistance of smoking. *Diabetes,* 58**,** 2220-7.

BERKENSTAM, A., KRISTENSEN, J., MELLSTROM, K., CARLSSON, B., MALM, J., REHNMARK, S., GARG, N., ANDERSSON, C. M., RUDLING, M., SJOBERG, F., ANGELIN, B. & BAXTER, J. D. 2008. The thyroid hormone mimetic compound KB2115 lowers plasma LDL cholesterol and stimulates bile acid synthesis without cardiac effects in humans. *Proc Natl Acad Sci U S A,* 105**,** 663-7.

BETTGE, K., KAHLE, M., ABD EL AZIZ, M. S., MEIER, J. J. & NAUCK, M. A. 2017. Occurrence of nausea, vomiting and diarrhoea reported as adverse events in clinical trials studying glucagon-like peptide-1 receptor agonists: A systematic analysis of published clinical trials. *Diabetes Obes Metab,* 19**,** 336-347.

BIERTHO, L., STEFFEN, R., BRANSON, R., POTOCZNA, N., RICKLIN, T., PIEC, G. & HORBER, F. F. 2005. Management of failed adjustable gastric banding. *Surgery,* 137**,** 33-41.

BILLINGTON, C. J., BRIGGS, J. E., LINK, J. G. & LEVINE, A. S. 1991. Glucagon in physiological concentrations stimulates brown fat thermogenesis in vivo. *Am J Physiol,* 261**,** R501-7.

BJORNDAL, B., BURRI, L., STAALESEN, V., SKORVE, J. & BERGE, R. K. 2011. Different adipose depots: their role in the development of metabolic syndrome and mitochondrial response to hypolipidemic agents. *J Obes,* 2011**,** 490650.

BOGARDUS, C., LILLIOJA, S., RAVUSSIN, E., ABBOTT, W., ZAWADZKI, J. K., YOUNG, A., KNOWLER, W. C., JACOBOWITZ, R. & MOLL, P. P. 1986. Familial dependence of the resting metabolic rate. *N Engl J Med,* 315**,** 96-100.

BOUCHARD, C., TREMBLAY, A., DESPRES, J. P., NADEAU, A., LUPIEN, P. J., THERIAULT, G., DUSSAULT, J., MOORJANI, S., PINAULT, S. & FOURNIER, G. 1990. The response to long-term overfeeding in identical twins. *N Engl J Med,* 322**,** 1477-82.

BOUCHARD, C., TREMBLAY, A., DESPRES, J. P., THERIAULT, G., NADEAU, A., LUPIEN, P. J., MOORJANI, S., PRUDHOMME, D. & FOURNIER, G. 1994. The response to exercise with constant energy intake in identical twins. *Obes Res,* 2**,** 400-10.

BRAY, G. A. & GREENWAY, F. L. 1976. Pharmacological approaches to treating the obese patient. *Clinics in Endocrinology and Metabolism,* 5**,** 455-479.

BRAY, M. S., LOOS, R. J., MCCAFFERY, J. M., LING, C., FRANKS, P. W., WEINSTOCK, G. M., SNYDER, M. P., VASSY, J. L., AGURS-COLLINS, T. & CONFERENCE WORKING, G. 2016. NIH working group report-using genomic information to guide weight management: From universal to precision treatment. *Obesity (Silver Spring),* 24**,** 14-22.

BREHM, B. J. & D'ALESSIO, D. A. 2000. Environmental Factors Influencing Obesity. *In:* DE GROOT, L. J., CHROUSOS, G., DUNGAN, K., FEINGOLD, K. R., GROSSMAN, A., HERSHMAN, J. M., KOCH, C., KORBONITS, M., MCLACHLAN, R., NEW, M., PURNELL, J., REBAR, R., SINGER, F. & VINIK, A. (eds.) *Endotext.* South Dartmouth (MA).

BROEDERS, E. P., NASCIMENTO, E. B., HAVEKES, B., BRANS, B., ROUMANS, K. H., TAILLEUX, A., SCHAART, G., KOUACH, M., CHARTON, J., DEPREZ, B., BOUVY, N. D., MOTTAGHY, F., STAELS, B., VAN MARKEN LICHTENBELT, W. D. & SCHRAUWEN, P. 2015. The Bile Acid Chenodeoxycholic Acid Increases Human Brown Adipose Tissue Activity. *Cell Metab,* 22**,** 418-26.

BUCHAN, A. M., POLAK, J. M., CAPELLA, C., SOLCIA, E. & PEARSE, A. G. 1978. Electronimmunocytochemical evidence for the K cell localization of gastric inhibitory polypeptide (GIP) in man. *Histochemistry,* 56**,** 37-44.

BUCHWALD, H., AVIDOR, Y., BRAUNWALD, E., JENSEN, M. D., PORIES, W., FAHRBACH, K. & SCHOELLES, K. 2004. Bariatric surgery: a systematic review and meta-analysis. *JAMA,* 292**,** 1724-37.

BUCHWALD, H. & RUCKER, R. D. 1987. *The rise and fall of jejunoileal bypass. In Nelson RL, Nyhus LM (eds): Surgery of the Small Intestine*, Norwalk, Conn., Appleton Century Crofts.

BUFFA, R., POLAK, J. M., PEARSE, A. G., SOLCIA, E., GRIMELIUS, L. & CAPELLA, C. 1975. Identification of the intestinal cell storing gastric inhibitory peptide. *Histochemistry,* 43**,** 249-55.

BUTEAU, J., FOISY, S., JOLY, E. & PRENTKI, M. 2003. Glucagon-like peptide 1 induces pancreatic beta-cell proliferation via transactivation of the epidermal growth factor receptor. *Diabetes,* 52**,** 124-32.

BUTLER, A. E., JANSON, J., BONNER-WEIR, S., RITZEL, R., RIZZA, R. A. & BUTLER, P. C. 2003. Beta-cell deficit and increased beta-cell apoptosis in humans with type 2 diabetes. *Diabetes,* 52**,** 102-10.

CABLE, E. E., FINN, P. D., STEBBINS, J. W., HOU, J., ITO, B. R., VAN POELJE, P. D., LINEMEYER, D. L. & ERION, M. D. 2009. Reduction of hepatic steatosis in rats and mice after treatment with a liver-targeted thyroid hormone receptor agonist. *Hepatology,* 49**,** 407-17.

CAMPBELL, J. E. & DRUCKER, D. J. 2013. Pharmacology, physiology, and mechanisms of incretin hormone action. *Cell Metab,* 17**,** 819-37.

CANNON, B. & NEDERGAARD, J. 2004. Brown adipose tissue: function and physiological significance. *Physiol Rev,* 84**,** 277-359.

CAO, J., MENG, S., CHANG, E., BECKWITH-FICKAS, K., XIONG, L., COLE, R. N., RADOVICK, S., WONDISFORD, F. E. & HE, L. 2014. Low concentrations of metformin suppress glucose production in hepatocytes through AMP-activated protein kinase (AMPK). *J Biol Chem,* 289**,** 20435-46.

CARLSON, M. G., SNEAD, W. L. & CAMPBELL, P. J. 1993. Regulation of free fatty acid metabolism by glucagon. *J Clin Endocrinol Metab,* 77**,** 11-5.

CEGLA, J., TROKE, R. C., JONES, B., THARAKAN, G., KENKRE, J., MCCULLOUGH, K. A., LIM, C. T., PARVIZI, N., HUSSEIN, M., CHAMBERS, E. S., MINNION, J., CUENCO, J., GHATEI, M. A.,

MEERAN, K., TAN, T. M. & BLOOM, S. R. 2014. Coinfusion of low-dose GLP-1 and glucagon in man results in a reduction in food intake. *Diabetes,* 63**,** 3711-20.

CELIO, A. C. & PORIES, W. J. 2016. A History of Bariatric Surgery: The Maturation of a Medical Discipline. *Surg Clin North Am,* 96**,** 655-67.

CERF, M. E. 2013. Beta cell dysfunction and insulin resistance. *Front Endocrinol (Lausanne),* 4**,** 37.

CHAGNON, Y. C., PERUSSE, L. & BOUCHARD, C. 1997. Familial aggregation of obesity, candidate genes and quantitative trait loci. *Curr Opin Lipidol,* 8**,** 205-11.

CHAMBERS, A. P., KIRCHNER, H., WILSON-PEREZ, H. E., WILLENCY, J. A., HALE, J. E., GAYLINN, B. D., THORNER, M. O., PFLUGER, P. T., GUTIERREZ, J. A., TSCHOP, M. H., SANDOVAL, D. A. & SEELEY, R. J. 2013. The effects of vertical sleeve gastrectomy in rodents are ghrelin independent. *Gastroenterology,* 144**,** 50-52 e5.

CHEN, S. S., ZHANG, Y., SANTOMANGO, T. S., WILLIAMS, P. E., LACY, D. B. & MCGUINNESS, O. P. 2007. Glucagon chronically impairs hepatic and muscle glucose disposal. *Am J Physiol Endocrinol Metab,* 292**,** E928-35.

CHENG, V. & KASHYAP, S. R. 2011. Weight considerations in pharmacotherapy for type 2 diabetes. *J Obes,* 2011.

CHO, N. H., SHAW, J. E., KARURANGA, S., HUANG, Y., DA ROCHA FERNANDES, J. D., OHLROGGE, A. W. & MALANDA, B. 2018. IDF Diabetes Atlas: Global estimates of diabetes prevalence for 2017 and projections for 2045. *Diabetes Res Clin Pract,* 138**,** 271-281.

CHRISTENSEN, M., VEDTOFTE, L., HOLST, J. J., VILSBOLL, T. & KNOP, F. K. 2011. Glucose-dependent insulinotropic polypeptide: a bifunctional glucose-dependent regulator of glucagon and insulin secretion in humans. *Diabetes,* 60**,** 3103-9.

CHUA, S. C., JR., CHUNG, W. K., WU-PENG, X. S., ZHANG, Y., LIU, S. M., TARTAGLIA, L. & LEIBEL, R. L. 1996. Phenotypes of mouse diabetes and rat fatty due to mutations in the OB (leptin) receptor. *Science,* 271**,** 994-6.

CHUNG, W. K. 2012. An overview of mongenic and syndromic obesities in humans. *Pediatr Blood Cancer,* 58**,** 122-8.

CIGNARELLA, A. & BOLEGO, C. 2010. Mechanisms of estrogen protection in diabetes and metabolic disease. *Horm Mol Biol Clin Investig,* 4**,** 575-80.

CLAYTON, J. A. 2016. Studying both sexes: a guiding principle for biomedicine. *FASEB J,* 30**,** 519-24.

CLAYTON, J. A. & COLLINS, F. S. 2014. Policy: NIH to balance sex in cell and animal studies. *Nature,* 509**,** 282-3.

CLEMMENSEN, C., CHABENNE, J., FINAN, B., SULLIVAN, L., FISCHER, K., KUCHLER, D., SEHRER, L., OGRAJSEK, T., HOFMANN, S. M., SCHRIEVER, S. C., PFLUGER, P. T., PINKSTAFF, J., TSCHOP, M. H., DIMARCHI, R. & MULLER, T. D. 2014. GLP-1/glucagon coagonism restores leptin responsiveness in obese mice chronically maintained on an obesogenic diet. *Diabetes,* 63**,** 1422-7.

CLEMMENSEN, C., FINAN, B., FISCHER, K., TOM, R. Z., LEGUTKO, B., SEHRER, L., HEINE, D., GRASSL, N., MEYER, C. W., HENDERSON, B., HOFMANN, S. M., TSCHOP, M. H., VAN DER PLOEG, L. H. & MULLER, T. D. 2015. Dual melanocortin-4 receptor and GLP-1 receptor agonism amplifies metabolic benefits in diet-induced obese mice. *EMBO Mol Med,* 7**,** 288-98.

CLEMMENSEN, C., JALL, S., KLEINERT, M., QUARTA, C., GRUBER, T., REBER, J., SACHS, S., FISCHER, K., FEUCHTINGER, A., KARLAS, A., SIMONDS, S. E., GRANDL, G., LOHER, D., SANCHEZ-QUANT, E., KEIPERT, S., JASTROCH, M., HOFMANN, S. M., NASCIMENTO, E. B. M., SCHRAUWEN, P., NTZIACHRISTOS, V., COWLEY, M. A., FINAN, B., MULLER, T. D. & TSCHOP, M. H. 2018. Coordinated targeting of cold and nicotinic receptors synergistically improves obesity and type 2 diabetes. *Nat Commun,* 9**,** 4304.

CLEMMENSEN, C., MULLER, T. D., WOODS, S. C., BERTHOUD, H. R., SEELEY, R. J. & TSCHOP, M. H. 2017. Gut-Brain Cross-Talk in Metabolic Control. *Cell,* 168**,** 758-774.

COHEN, P. A., GODAY, A. & SWANN, J. P. 2012. The return of rainbow diet pills. *Am J Public Health,* 102**,** 1676-86.

COLMAN, E. 2005. Anorectics on trial: a half century of federal regulation of prescription appetite suppressants. *Ann Intern Med,* 143**,** 380-5.

COLQUITT, J. L., PICKETT, K., LOVEMAN, E. & FRAMPTON, G. K. 2014. Surgery for weight loss in adults. *Cochrane Database Syst Rev***,** CD003641.

COMMINS, S. P., WATSON, P. M., LEVIN, N., BEILER, R. J. & GETTYS, T. W. 2000. Central leptin regulates the UCP1 and ob genes in brown and white adipose tissue via different beta-adrenoceptor subtypes. *J Biol Chem,* 275**,** 33059-67.

CONSIDINE, R. V., SINHA, M. K., HEIMAN, M. L., KRIAUCIUNAS, A., STEPHENS, T. W., NYCE, M. R., OHANNESIAN, J. P., MARCO, C. C., MCKEE, L. J., BAUER, T. L. & ET AL. 1996. Serum immunoreactive-leptin concentrations in normal-weight and obese humans. *N Engl J Med,* 334**,** 292-5.

COTTLE, W. & CARLSON, L. D. 1954. Adaptive changes in rats exposed to cold; caloric exchange. *Am J Physiol,* 178**,** 305-8.

COUTINHO, A. E. & CHAPMAN, K. E. 2011. The anti-inflammatory and immunosuppressive effects of glucocorticoids, recent developments and mechanistic insights. *Mol Cell Endocrinol,* 335**,** 2-13.

COWLEY, M. A., CONE, R., ENRIORI, P., LOUISELLE, I., WILLIAMS, S. M. & EVANS, A. E. 2003. Electrophysiological actions of peripheral hormones on melanocortin neurons. *Ann N Y Acad Sci,* 994**,** 175-86.

COWLEY, M. A., SMART, J. L., RUBINSTEIN, M., CERDAN, M. G., DIANO, S., HORVATH, T. L., CONE, R. D. & LOW, M. J. 2001. Leptin activates anorexigenic POMC neurons through a neural network in the arcuate nucleus. *Nature,* 411**,** 480-4.

CUTTING, W. C., MEHRTENS, H. G. & TAINTER, M. L. 1933. Actions and uses of dinitrophenol: Promising metabolic applications. *Journal of the American Medical Association,* 101**,** 193.

CYPESS, A. M., WEINER, L. S., ROBERTS-TOLER, C., FRANQUET ELIA, E., KESSLER, S. H., KAHN, P. A., ENGLISH, J., CHATMAN, K., TRAUGER, S. A., DORIA, A. & KOLODNY, G. M. 2015. Activation of human brown adipose tissue by a beta3-adrenergic receptor agonist. *Cell Metab,* 21**,** 33-8.

DALTON, M., CAMERON, A. J., ZIMMET, P. Z., SHAW, J. E., JOLLEY, D., DUNSTAN, D. W., WELBORN, T. A. & AUSDIAB STEERING, C. 2003. Waist circumference, waist-hip ratio and body mass index and their correlation with cardiovascular disease risk factors in Australian adults. *J Intern Med,* 254**,** 555-63.

DANFORTH, E., JR. & BURGER, A. 1984. The role of thyroid hormones in the control of energy expenditure. *Clin Endocrinol Metab,* 13**,** 581-95.

DAY, J. W., OTTAWAY, N., PATTERSON, J. T., GELFANOV, V., SMILEY, D., GIDDA, J., FINDEISEN, H., BRUEMMER, D., DRUCKER, D. J., CHAUDHARY, N., HOLLAND, J., HEMBREE, J., ABPLANALP, W., GRANT, E., RUEHL, J., WILSON, H., KIRCHNER, H., LOCKIE, S. H., HOFMANN, S., WOODS, S. C., NOGUEIRAS, R., PFLUGER, P. T., PEREZ-TILVE, D., DIMARCHI, R. & TSCHOP, M. H. 2009. A new glucagon and GLP-1 co-agonist eliminates obesity in rodents. *Nat Chem Biol,* 5**,** 749-57.

DE CASTRO, J. M., PAULLIN, S. K. & DELUGAS, G. M. 1978. Insulin and glucagon as determinants of body weight set point and microregulation in rats. *J Comp Physiol Psychol,* 92**,** 571-9.

DE MARINIS, Y. Z., SALEHI, A., WARD, C. E., ZHANG, Q., ABDULKADER, F., BENGTSSON, M., BRAHA, O., BRAUN, M., RAMRACHEYA, R., AMISTEN, S., HABIB, A. M., MORITOH, Y., ZHANG, E., REIMANN, F., ROSENGREN, A., SHIBASAKI, T., GRIBBLE, F., RENSTROM, E., SEINO, S., ELIASSON, L. & RORSMAN, P. 2010. GLP-1 inhibits and adrenaline stimulates glucagon release by differential modulation of N- and L-type Ca2+ channel-dependent exocytosis. *Cell Metab,* 11**,** 543-553.

DE SILVA, A., SALEM, V., LONG, C. J., MAKWANA, A., NEWBOULD, R. D., RABINER, E. A., GHATEI, M. A., BLOOM, S. R., MATTHEWS, P. M., BEAVER, J. D. & DHILLO, W. S. 2011. The gut hormones PYY 3-36 and GLP-1 7-36 amide reduce food intake and modulate brain activity in appetite centers in humans. *Cell Metab,* 14**,** 700-6.

DEACON, C. F. 2004. Circulation and degradation of GIP and GLP-1. *Horm Metab Res,* 36**,** 761-5.

DEFRONZO, R. A., JACOT, E., JEQUIER, E., MAEDER, E., WAHREN, J. & FELBER, J. P. 1981. The effect of insulin on the disposal of intravenous glucose. Results from indirect calorimetry and hepatic and femoral venous catheterization. *Diabetes,* 30**,** 1000-7.

DESPRES, J. P., LEMIEUX, I. & PRUD'HOMME, D. 2001. Treatment of obesity: need to focus on high risk abdominally obese patients. *BMJ,* 322**,** 716-20.

DEUTSCHE ADIPOSITAS GESELLSCHAFT. 2014. *Interdisziplinäre Leitlinie der Qualität S3 zur „Prävention und Therapie der Adipositas"* [Online]. Available: http://www.adipositas-gesellschaft.de/fileadmin/PDF/Leitlinien/S3_Adipositas_Praevention_Therapie_2014.pdf [Accessed December 28 2017].

DIMA, A., BURTON, N. C. & NTZIACHRISTOS, V. 2014. Multispectral optoacoustic tomography at 64, 128, and 256 channels. *J Biomed Opt,* 19**,** 36021.

DRENT, M. L., LARSSON, I., WILLIAM-OLSSON, T., QUAADE, F., CZUBAYKO, F., VON BERGMANN, K., STROBEL, W., SJOSTROM, L. & VAN DER VEEN, E. A. 1995. Orlistat (Ro 18-0647), a lipase inhibitor, in the treatment of human obesity: a multiple dose study. *Int J Obes Relat Metab Disord,* 19**,** 221-6.

DRUCKER, D. J., PHILIPPE, J., MOJSOV, S., CHICK, W. L. & HABENER, J. F. 1987. Glucagon-like peptide I stimulates insulin gene expression and increases cyclic AMP levels in a rat islet cell line. *Proc Natl Acad Sci U S A,* 84**,** 3434-8.

DU BOIS, E. F. 1921. The basal metabolism in fever. *Journal of the American Medical Association,* 77**,** 352-5.

EBERT, R., NAUCK, M. & CREUTZFELDT, W. 1991. Effect of exogenous or endogenous gastric inhibitory polypeptide (GIP) on plasma triglyceride responses in rats. *Horm Metab Res,* 23**,** 517-21.

ECKEL, R. H., FUJIMOTO, W. Y. & BRUNZELL, J. D. 1979. Gastric inhibitory polypeptide enhanced lipoprotein lipase activity in cultured preadipocytes. *Diabetes,* 28**,** 1141-2.

EFFERTZ, T., ENGEL, S., VERHEYEN, F. & LINDER, R. 2016. The costs and consequences of obesity in Germany: a new approach from a prevalence and life-cycle perspective. *Eur J Health Econ,* 17**,** 1141-1158.

EISENSTEIN, A. B. & STRACK, I. 1968. Effects of glucagon on carbohydrate synthesis and enzyme activity in rat liver. *Endocrinology,* 83**,** 1337-48.

EL-MIR, M. Y., NOGUEIRA, V., FONTAINE, E., AVERET, N., RIGOULET, M. & LEVERVE, X. 2000. Dimethylbiguanide inhibits cell respiration via an indirect effect targeted on the respiratory chain complex I. *J Biol Chem,* 275**,** 223-8.

ELVERT, R., HERLING, A. W., BOSSART, M., WEISS, T., ZHANG, B., WENSKI, P., WANDSCHNEIDER, J., KLEUTSCH, S., BUTTY, U., KANNT, A., WAGNER, M., HAACK, T., EVERS, A., DUDDA, A., LORENZ, M., KEIL, S. & LARSEN, P. J. 2018. Running on mixed fuel-dual agonistic approach of GLP-1 and GCG receptors leads to beneficial impact on body weight and blood glucose control: A comparative study between mice and non-human primates. *Diabetes Obes Metab,* 20**,** 1836-1851.

EMA. 2012a. *Assessement report for Xenical* [Online]. Available: https://www.ema.europa.eu/documents/variation-report/xenical-h-c-000154-20-0057-epar-assessment-report_en.pdf [Accessed October 31 2018].

EMA. 2012b. *Assessment report - Byetta* [Online]. Available: https://www.ema.europa.eu/documents/variation-report/byetta-h-c-698-ii-0029-epar-assessment-report-variation_en.pdf [Accessed October 31 2018].

EMA. 2012c. *Assessment report - Lyxumia* [Online]. Available: https://www.ema.europa.eu/documents/assessment-report/lyxumia-epar-public-assessment-report_en.pdf [Accessed October 31 2018].

EMA. 2014a. *Assessment report - Eperzan* [Online]. Available: https://www.ema.europa.eu/documents/assessment-report/eperzan-epar-public-assessment-report_en.pdf [Accessed October 31 2018].

EMA. 2014b. *Assessment report - Trulicity* [Online]. Available: https://www.ema.europa.eu/documents/assessment-report/trulicity-epar-public-assessment-report_en.pdf [Accessed October 31 2018].

EMA. 2014c. *Mysimba - Assessment report for an initial marketing authorisation application* [Online]. Available: https://www.ema.europa.eu/documents/assessment-report/mysimba-epar-public-assessment-report_en.pdf [Accessed October 31 2018].

EMA. 2015. *Assessment report - Saxenda* [Online]. Available: https://www.ema.europa.eu/documents/assessment-report/saxenda-epar-public-assessment-report_en.pdf [Accessed October 31 2018].

EMA. 2016. *Assessment report - Metformin containing medicinal products* [Online]. Available: https://www.ema.europa.eu/documents/referral/metformin-article-31-referral-chmp-assessment-report_en.pdf [Accessed October 31 2018].

EMA. 2017a. *Assessment report - Ozempic* [Online]. Available: https://www.ema.europa.eu/documents/assessment-report/ozempic-epar-public-assessment-report_en.pdf [Accessed October 31 2018].

EMA. 2017b. *Assessment report - Victoza* [Online]. Available: https://www.ema.europa.eu/documents/variation-report/victoza-h-c-1026-ii-0042-epar-assessment-report-variation_en.pdf [Accessed October 31 2018].

ERION, M. D., CABLE, E. E., ITO, B. R., JIANG, H., FUJITAKI, J. M., FINN, P. D., ZHANG, B. H., HOU, J., BOYER, S. H., VAN POELJE, P. D. & LINEMEYER, D. L. 2007. Targeting thyroid hormone receptor-beta agonists to the liver reduces cholesterol and triglycerides and improves the therapeutic index. *Proc Natl Acad Sci U S A,* 104**,** 15490-5.

FAGERHOLM, V., HAAPARANTA, M. & SCHEININ, M. 2011. alpha2-adrenoceptor regulation of blood glucose homeostasis. *Basic Clin Pharmacol Toxicol,* 108**,** 365-70.

FARAG, Y. M. & GABALLA, M. R. 2011. Diabesity: an overview of a rising epidemic. *Nephrol Dial Transplant,* 26**,** 28-35.

FIELDING, G. A. & REN, C. J. 2005. Laparoscopic adjustable gastric band. *Surg Clin North Am,* 85**,** 129-40, x.

FINAN, B., CLEMMENSEN, C., ZHU, Z., STEMMER, K., GAUTHIER, K., MULLER, L., DE ANGELIS, M., MORETH, K., NEFF, F., PEREZ-TILVE, D., FISCHER, K., LUTTER, D., SANCHEZ-GARRIDO, M. A., LIU, P., TUCKERMANN, J., MALEHMIR, M., HEALY, M. E., WEBER, A., HEIKENWALDER, M., JASTROCH, M., KLEINERT, M., JALL, S., BRANDT, S., FLAMANT, F., SCHRAMM, K. W., BIEBERMANN, H., DORING, Y., WEBER, C., HABEGGER, K. M., KEUPER, M., GELFANOV, V., LIU, F., KOHRLE, J., ROZMAN, J., FUCHS, H., GAILUS-DURNER, V., HRABE DE ANGELIS, M., HOFMANN, S. M., YANG, B., TSCHOP, M. H., DIMARCHI, R. & MULLER, T. D. 2016. Chemical Hybridization of Glucagon and Thyroid Hormone Optimizes Therapeutic Impact for Metabolic Disease. *Cell,* 167**,** 843-857 e14.

FINAN, B., MA, T., OTTAWAY, N., MÜLLER, T. D., HABEGGER, K. M., HEPPNER, K. M., KIRCHNER, H., HOLLAND, J., HEMBREE, J., RAVER, C., LOCKIE, S. H., SMILEY, D. L., GELFANOV, V., YANG, B., HOFMANN, S., BRUEMMER, D., DRUCKER, D. J., PFLUGER, P. T., PEREZ-TILVE, D., GIDDA, J., VIGNATI, L., ZHANG, L., HAUPTMAN, J. B., LAU, M., BRECHEISEN, M., UHLES, S., RIBOULET, W., HAINAUT, E., SEBOKOVA, E., CONDE-KNAPE, K., KONKAR, A., DIMARCHI, R. D. & TSCHÖP, M. H. 2013. Unimolecular dual incretins maximize metabolic benefits in rodents, monkeys, and humans. *Sci Transl Med,* 5**,** 209ra151.

FINAN, B., YANG, B., OTTAWAY, N., SMILEY, D. L., MA, T., CLEMMENSEN, C., CHABENNE, J., ZHANG, L., HABEGGER, K. M., FISCHER, K., CAMPBELL, J. E., SANDOVAL, D., SEELEY, R. J., BLEICHER, K., UHLES, S., RIBOULET, W., FUNK, J., HERTEL, C., BELLI, S., SEBOKOVA, E., CONDE-KNAPE, K., KONKAR, A., DRUCKER, D. J., GELFANOV, V., PFLUGER, P. T., MULLER, T. D., PEREZ-TILVE, D., DIMARCHI, R. D. & TSCHOP, M. H. 2015. A rationally designed monomeric peptide triagonist corrects obesity and diabetes in rodents. *Nat Med,* 21**,** 27-36.

FINAN, B., YANG, B., OTTAWAY, N., STEMMER, K., MÜLLER, T. D., YI, C. X., HABEGGER, K., SCHRIEVER, S. C., GARCIA-CACERES, C., KABRA, D. G., HEMBREE, J., HOLLAND, J., RAVER, C., SEELEY, R. J., HANS, W., IRMLER, M., BECKERS, J., DE ANGELIS, M. H., TIANO, J. P., MAUVAIS-JARVIS, F., PEREZ-TILVE, D., PFLUGER, P., ZHANG, L., GELFANOV, V., DIMARCHI, R. D. & TSCHÖP, M. H. 2012. Targeted estrogen delivery reverses the metabolic syndrome. *Nat Med,* 18**,** 1847-56.

FOBI, M. A. 2004. Surgical treatment of obesity: a review. *J Natl Med Assoc,* 96**,** 61-75.

FRIED, S. K., BUNKIN, D. A. & GREENBERG, A. S. 1998. Omental and subcutaneous adipose tissues of obese subjects release interleukin-6: depot difference and regulation by glucocorticoid. *J Clin Endocrinol Metab,* 83**,** 847-50.

FROHLICH, J., SCHOLLMEYER, P. & GEROK, W. 1978. Carbohydrate metabolism in renal failure. *Am J Clin Nutr,* 31**,** 1541-6.

GALLOU-KABANI, C., VIGE, A., GROSS, M. S., RABES, J. P., BOILEAU, C., LARUE-ACHAGIOTIS, C., TOME, D., JAIS, J. P. & JUNIEN, C. 2007. C57BL/6J and A/J mice fed a high-fat diet delineate components of metabolic syndrome. *Obesity (Silver Spring),* 15**,** 1996-2005.

GAO, Q. & HORVATH, T. L. 2008. Cross-talk between estrogen and leptin signaling in the hypothalamus. *Am J Physiol Endocrinol Metab,* 294**,** E817-26.

GARBER, A. J., DONOVAN, D. S., JR., DANDONA, P., BRUCE, S. & PARK, J. S. 2003. Efficacy of glyburide/metformin tablets compared with initial monotherapy in type 2 diabetes. *J Clin Endocrinol Metab,* 88**,** 3598-604.

GEARY, N., KISSILEFF, H. R., PI-SUNYER, F. X. & HINTON, V. 1992. Individual, but not simultaneous, glucagon and cholecystokinin infusions inhibit feeding in men. *Am J Physiol,* 262**,** R975-80.

GEARY, N., LE SAUTER, J. & NOH, U. 1993. Glucagon acts in the liver to control spontaneous meal size in rats. *Am J Physiol,* 264**,** R116-22.

GORAN, M. I. 1997. Genetic influences on human energy expenditure and substrate utilization. *Behav Genet,* 27**,** 389-99.

GÖTZ, A., JALL, S., TSCHÖP, M.H., MÜLLER T.D., 2017. Inkretinbasierte Medikamente zur Diabetes- und Adipositastherapie. *Diabetologe,* 13**,** 9.

GREENWAY, F. L., FUJIOKA, K., PLODKOWSKI, R. A., MUDALIAR, S., GUTTADAURIA, M., ERICKSON, J., KIM, D. D., DUNAYEVICH, E. & GROUP, C.-I. S. 2010. Effect of naltrexone plus bupropion on weight loss in overweight and obese adults (COR-I): a multicentre, randomised, double-blind, placebo-controlled, phase 3 trial. *Lancet,* 376**,** 595-605.

GRIFFEN, W. O., JR., YOUNG, V. L. & STEVENSON, C. C. 1977. A prospective comparison of gastric and jejunoileal bypass procedures for morbid obesity. *Ann Surg,* 186**,** 500-9.

GRUNDLINGH, J., DARGAN, P. I., EL-ZANFALY, M. & WOOD, D. M. 2011. 2,4-dinitrophenol (DNP): a weight loss agent with significant acute toxicity and risk of death. *J Med Toxicol,* 7**,** 205-12.

GUSTAFSON, A., KING, C. & REY, J. A. 2013. Lorcaserin (Belviq): A Selective Serotonin 5-HT2C Agonist In the Treatment of Obesity. *P T,* 38**,** 525-34.

GUTZWILLER, J. P., DREWE, J., GOKE, B., SCHMIDT, H., ROHRER, B., LAREIDA, J. & BEGLINGER, C. 1999. Glucagon-like peptide-1 promotes satiety and reduces food intake in patients with diabetes mellitus type 2. *Am J Physiol*, 276, R1541-4.

HAMILTON, A., ZHANG, Q., SALEHI, A., WILLEMS, M., KNUDSEN, J. G., RINGGAARD, A. K., CHAPMAN, C. E., GONZALEZ-ALVAREZ, A., SURDO, N. C., ZACCOLO, M., BASCO, D., JOHNSON, P. R. V., RAMRACHEYA, R., RUTTER, G. A., GALIONE, A., RORSMAN, P. & TARASOV, A. I. 2018. Adrenaline Stimulates Glucagon Secretion by Tpc2-Dependent Ca(2+) Mobilization From Acidic Stores in Pancreatic alpha-Cells. *Diabetes*, 67, 1128-1139.

HANLEY, A. J., ZINMAN, B., SHERIDAN, P., YUSUF, S., GERSTEIN, H. C., DIABETES REDUCTION ASSESSMENT WITH, R. & ROSIGLITAZONE MEDICATION, I. 2010. Effect of Rosiglitazone and Ramipril on {beta}-cell function in people with impaired glucose tolerance or impaired fasting glucose: the DREAM trial. *Diabetes Care*, 33, 608-13.

HARDIE, D. G., ROSS, F. A. & HAWLEY, S. A. 2012. AMPK: a nutrient and energy sensor that maintains energy homeostasis. *Nat Rev Mol Cell Biol*, 13, 251-62.

HARRIS, R. B. 1990. Role of set-point theory in regulation of body weight. *FASEB J*, 4, 3310-8.

HEAL, D. J., SMITH, S. L., GOSDEN, J. & NUTT, D. J. 2013. Amphetamine, past and present--a pharmacological and clinical perspective. *J Psychopharmacol*, 27, 479-96.

HENDERSON, S. J., KONKAR, A., HORNIGOLD, D. C., TREVASKIS, J. L., JACKSON, R., FRITSCH FREDIN, M., JANSSON-LOFMARK, R., NAYLOR, J., ROSSI, A., BEDNAREK, M. A., BHAGROO, N., SALARI, H., WILL, S., OLDHAM, S., HANSEN, G., FEIGH, M., KLEIN, T., GRIMSBY, J., MAGUIRE, S., JERMUTUS, L., RONDINONE, C. M. & COGHLAN, M. P. 2016. Robust anti-obesity and metabolic effects of a dual GLP-1/glucagon receptor peptide agonist in rodents and non-human primates. *Diabetes Obes Metab*, 18, 1176-1190.

HENRIKSON, V. 1994. Can small bowel resection be defended as therapy for obesity? *Obesity Surgery*, 4, 54-55.

HERRERA, B. M. & LINDGREN, C. M. 2010. The genetics of obesity. *Curr Diab Rep*, 10, 498-505.

HESS, D. S. & HESS, D. W. 1998. Biliopancreatic diversion with a duodenal switch. *Obes Surg*, 8, 267-82.

HODGIN, J. B. & MAEDA, N. 2002. Minireview: estrogen and mouse models of atherosclerosis. *Endocrinology*, 143, 4495-501.

HOFMANN, S. M., PEREZ-TILVE, D., GREER, T. M., COBURN, B. A., GRANT, E., BASFORD, J. E., TSCHOP, M. H. & HUI, D. Y. 2008. Defective lipid delivery modulates glucose tolerance and metabolic response to diet in apolipoprotein E-deficient mice. *Diabetes*, 57, 5-12.

HONG, J., STUBBINS, R. E., SMITH, R. R., HARVEY, A. E. & NUNEZ, N. P. 2009. Differential susceptibility to obesity between male, female and ovariectomized female mice. *Nutr J*, 8, 11.

HOTAMISLIGIL, G. S. 2006. Inflammation and metabolic disorders. *Nature*, 444, 860-7.

HOTTA, Y., NAKAMURA, H., KONISHI, M., MURATA, Y., TAKAGI, H., MATSUMURA, S., INOUE, K., FUSHIKI, T. & ITOH, N. 2009. Fibroblast growth factor 21 regulates lipolysis in white adipose tissue but is not required for ketogenesis and triglyceride clearance in liver. *Endocrinology*, 150, 4625-33.

HSU, W. H., XIANG, H. D., RAJAN, A. S. & BOYD, A. E., 3RD 1991. Activation of alpha 2-adrenergic receptors decreases Ca2+ influx to inhibit insulin secretion in a hamster beta-cell line: an action mediated by a guanosine triphosphate-binding protein. *Endocrinology*, 128, 958-64.

HUNDAL, R. S., KRSSAK, M., DUFOUR, S., LAURENT, D., LEBON, V., CHANDRAMOULI, V., INZUCCHI, S. E., SCHUMANN, W. C., PETERSEN, K. F., LANDAU, B. R. & SHULMAN, G. I. 2000. Mechanism by which metformin reduces glucose production in type 2 diabetes. *Diabetes*, 49, 2063-9.

IKEDA, K., MARETICH, P. & KAJIMURA, S. 2018. The Common and Distinct Features of Brown and Beige Adipocytes. *Trends Endocrinol Metab*, 29, 191-200.

IP, W., SHAO, W., CHIANG, Y. T. & JIN, T. 2013. GLP-1-derived nonapeptide GLP-1(28-36)amide represses hepatic gluconeogenic gene expression and improves pyruvate tolerance in high-fat diet-fed mice. *Am J Physiol Endocrinol Metab*, 305, E1348-58.

ISHISAKI, A., TOKUDA, H., YOSHIDA, M., HIRADE, K., KUNIEDA, K., HATAKEYAMA, D., SHIBATA, T. & KOZAWA, O. 2004. Activation of p38 mitogen-activated protein kinase mediates thyroid hormone-stimulated osteocalcin synthesis in osteoblasts. *Mol Cell Endocrinol*, 214, 189-95.

JALL, S., SACHS, S., CLEMMENSEN, C., FINAN, B., NEFF, F., DIMARCHI, R. D., TSCHOP, M. H., MULLER, T. D. & HOFMANN, S. M. 2017. Monomeric GLP-1/GIP/glucagon triagonism corrects obesity, hepatosteatosis, and dyslipidemia in female mice. *Mol Metab*, 6, 440-446.

JIANG, C., ZHAI, M., YAN, D., LI, D., LI, C., ZHANG, Y., XIAO, L., XIONG, D., DENG, Q. & SUN, W. 2017. Dietary menthol-induced TRPM8 activation enhances WAT "browning" and ameliorates diet-induced obesity. *Oncotarget*, 8, 75114-75126.

JOHNSTON, D., DACHTLER, J., SUE-LING, H. M., KING, R. F. & MARTIN L, G. 2003. The Magenstrasse and Mill operation for morbid obesity. *Obes Surg*, 13, 10-6.

KAHN, S. E., HAFFNER, S. M., HEISE, M. A., HERMAN, W. H., HOLMAN, R. R., JONES, N. P., KRAVITZ, B. G., LACHIN, J. M., O'NEILL, M. C., ZINMAN, B., VIBERTI, G. & GROUP, A. S. 2006a. Glycemic durability of rosiglitazone, metformin, or glyburide monotherapy. *N Engl J Med*, 355**,** 2427-43.

KAHN, S. E., HULL, R. L. & UTZSCHNEIDER, K. M. 2006b. Mechanisms linking obesity to insulin resistance and type 2 diabetes. *Nature*, 444**,** 840-6.

KAMINSKI, R. M., BANERJEE, M. & ROGAWSKI, M. A. 2004. Topiramate selectively protects against seizures induced by ATPA, a GluR5 kainate receptor agonist. *Neuropharmacology*, 46**,** 1097-104.

KANAYA, A. M., HERRINGTON, D., VITTINGHOFF, E., LIN, F., GRADY, D., BITTNER, V., CAULEY, J. A., BARRETT-CONNOR, E., HEART & ESTROGEN/PROGESTIN REPLACEMENT, S. 2003. Glycemic effects of postmenopausal hormone therapy: the Heart and Estrogen/progestin Replacement Study. A randomized, double-blind, placebo-controlled trial. *Ann Intern Med*, 138**,** 1-9.

KARAGIANNIS, T., PASCHOS, P., PALETAS, K., MATTHEWS, D. R. & TSAPAS, A. 2012. Dipeptidyl peptidase-4 inhibitors for treatment of type 2 diabetes mellitus in the clinical setting: systematic review and meta-analysis. *BMJ*, 344**,** e1369.

KARLSSON, S. & AHREN, B. 1998. Insulin and glucagon secretion by ganglionic nicotinic activation in adrenalectomized mice. *Eur J Pharmacol*, 342**,** 291-5.

KEDMI, M., BEAUDET, A. L. & ORR-URTREGER, A. 2004. Mice lacking neuronal nicotinic acetylcholine receptor beta4-subunit and mice lacking both alpha5- and beta4-subunits are highly resistant to nicotine-induced seizures. *Physiol Genomics*, 17**,** 221-9.

KEY, T., APPLEBY, P., BARNES, I., REEVES, G., ENDOGENOUS, H. & BREAST CANCER COLLABORATIVE, G. 2002. Endogenous sex hormones and breast cancer in postmenopausal women: reanalysis of nine prospective studies. *J Natl Cancer Inst*, 94**,** 606-16.

KIM, A. Y., TANG, Z., LIU, Q., PATEL, K. N., MAAG, D., GENG, Y. & DONG, X. 2008. Pirt, a phosphoinositide-binding protein, functions as a regulatory subunit of TRPV1. *Cell*, 133**,** 475-85.

KIM, W. D., LEE, Y. H., KIM, M. H., JUNG, S. Y., SON, W. C., YOON, S. J. & LEE, B. W. 2012. Human monoclonal antibodies against glucagon receptor improve glucose homeostasis by suppression of hepatic glucose output in diet-induced obese mice. *PLoS One*, 7**,** e50954.

KINUGAWA, K., JEONG, M. Y., BRISTOW, M. R. & LONG, C. S. 2005. Thyroid hormone induces cardiac myocyte hypertrophy in a thyroid hormone receptor alpha1-specific manner that requires TAK1 and p38 mitogen-activated protein kinase. *Mol Endocrinol*, 19**,** 1618-28.

KISHI, T., ASCHKENASI, C. J., LEE, C. E., MOUNTJOY, K. G., SAPER, C. B. & ELMQUIST, J. K. 2003. Expression of melanocortin 4 receptor mRNA in the central nervous system of the rat. *J Comp Neurol*, 457**,** 213-35.

KLEINER, D. E., BRUNT, E. M., VAN NATTA, M., BEHLING, C., CONTOS, M. J., CUMMINGS, O. W., FERRELL, L. D., LIU, Y. C., TORBENSON, M. S., UNALP-ARIDA, A., YEH, M., MCCULLOUGH, A. J., SANYAL, A. J. & NONALCOHOLIC STEATOHEPATITIS CLINICAL RESEARCH, N. 2005. Design and validation of a histological scoring system for nonalcoholic fatty liver disease. *Hepatology*, 41**,** 1313-21.

KLEINERT, M., PARKER, B. L., FRITZEN, A. M., KNUDSEN, J. R., JENSEN, T. E., KJOBSTED, R., SYLOW, L., RUEGG, M., JAMES, D. E. & RICHTER, E. A. 2017. Mammalian target of rapamycin complex 2 regulates muscle glucose uptake during exercise in mice. *J Physiol*, 595**,** 4845-4855.

KOOY, A., DE JAGER, J., LEHERT, P., BETS, D., WULFFELE, M. G., DONKER, A. J. & STEHOUWER, C. D. 2009. Long-term effects of metformin on metabolism and microvascular and macrovascular disease in patients with type 2 diabetes mellitus. *Arch Intern Med*, 169**,** 616-25.

KORNER, J., BESSLER, M., INABNET, W., TAVERAS, C. & HOLST, J. J. 2007. Exaggerated glucagon-like peptide-1 and blunted glucose-dependent insulinotropic peptide secretion are associated with Roux-en-Y gastric bypass but not adjustable gastric banding. *Surg Obes Relat Dis*, 3**,** 597-601.

KREMEN, A. J., LINNER, J. H. & NELSON, C. H. 1954. An experimental evaluation of the nutritional importance of proximal and distal small intestine. *Ann Surg*, 140**,** 439-48.

LAFERRERE, B., HESHKA, S., WANG, K., KHAN, Y., MCGINTY, J., TEIXEIRA, J., HART, A. B. & OLIVAN, B. 2007. Incretin levels and effect are markedly enhanced 1 month after Roux-en-Y gastric bypass surgery in obese patients with type 2 diabetes. *Diabetes Care*, 30**,** 1709-16.

LAFERRERE, B., TEIXEIRA, J., MCGINTY, J., TRAN, H., EGGER, J. R., COLARUSSO, A., KOVACK, B., BAWA, B., KOSHY, N., LEE, H., YAPP, K. & OLIVAN, B. 2008. Effect of weight loss by gastric bypass surgery versus hypocaloric diet on glucose and incretin levels in patients with type 2 diabetes. *J Clin Endocrinol Metab*, 93**,** 2479-85.

LAFONTAN, M. & LANGIN, D. 2009. Lipolysis and lipid mobilization in human adipose tissue. *Prog Lipid Res*, 48**,** 275-97.

LANDSBERG, L., YOUNG, J. B., LEONARD, W. R., LINSENMEIER, R. A. & TUREK, F. W. 2009. Do the obese have lower body temperatures? A new look at a forgotten variable in energy balance. *Trans Am Clin Climatol Assoc,* 120**,** 287-95.

LE ROUX, C. W. & BUETER, M. 2014. The physiology of altered eating behaviour after Roux-en-Y gastric bypass. *Exp Physiol,* 99**,** 1128-32.

LEIBEL, R. L. 1990. Is obesity due to a heritable difference in 'set point' for adiposity? *West J Med,* 153**,** 429-31.

LEIBEL, R. L., ROSENBAUM, M. & HIRSCH, J. 1995. Changes in energy expenditure resulting from altered body weight. *N Engl J Med,* 332**,** 621-8.

LEV-RAN, A. 2001. Human obesity: an evolutionary approach to understanding our bulging waistline. *Diabetes Metab Res Rev,* 17**,** 347-62.

LILLIOJA, S., MOTT, D. M., SPRAUL, M., FERRARO, R., FOLEY, J. E., RAVUSSIN, E., KNOWLER, W. C., BENNETT, P. H. & BOGARDUS, C. 1993. Insulin resistance and insulin secretory dysfunction as precursors of non-insulin-dependent diabetes mellitus. Prospective studies of Pima Indians. *N Engl J Med,* 329**,** 1988-92.

LIM, G. E. & BRUBAKER, P. L. 2006. Glucagon-Like Peptide 1 Secretion by the L-Cell. *The View From Within,* 55**,** S70-S77.

LISSNER, L., ODELL, P. M., D'AGOSTINO, R. B., STOKES, J., 3RD, KREGER, B. E., BELANGER, A. J. & BROWNELL, K. D. 1991. Variability of body weight and health outcomes in the Framingham population. *N Engl J Med,* 324**,** 1839-44.

LONNEMAN, D. J., JR., REY, J. A. & MCKEE, B. D. 2013. Phentermine/Topiramate extended-release capsules (qsymia) for weight loss. *P T,* 38**,** 446-52.

LOOK, A. R. G. & WING, R. R. 2010. Long-term effects of a lifestyle intervention on weight and cardiovascular risk factors in individuals with type 2 diabetes mellitus: four-year results of the Look AHEAD trial. *Arch Intern Med,* 170**,** 1566-75.

LUMENG, C. N. & SALTIEL, A. R. 2011. Inflammatory links between obesity and metabolic disease. *J Clin Invest,* 121**,** 2111-7.

MA, S., YU, H., ZHAO, Z., LUO, Z., CHEN, J., NI, Y., JIN, R., MA, L., WANG, P., ZHU, Z., LI, L., ZHONG, J., LIU, D., NILIUS, B. & ZHU, Z. 2012. Activation of the cold-sensing TRPM8 channel triggers UCP1-dependent thermogenesis and prevents obesity. *J Mol Cell Biol,* 4**,** 88-96.

MAARBJERG, S. J., JORGENSEN, S. B., ROSE, A. J., JEPPESEN, J., JENSEN, T. E., TREEBAK, J. T., BIRK, J. B., SCHJERLING, P., WOJTASZEWSKI, J. F. & RICHTER, E. A. 2009. Genetic impairment of AMPKalpha2 signaling does not reduce muscle glucose uptake during treadmill exercise in mice. *Am J Physiol Endocrinol Metab,* 297**,** E924-34.

MACIEJEWSKI, M. L., ARTERBURN, D. E., VAN SCOYOC, L., SMITH, V. A., YANCY, W. S., JR., WEIDENBACHER, H. J., LIVINGSTON, E. H. & OLSEN, M. K. 2016. Bariatric Surgery and Long-term Durability of Weight Loss. *JAMA Surg,* 151**,** 1046-1055.

MAFFEI, M., HALAAS, J., RAVUSSIN, E., PRATLEY, R. E., LEE, G. H., ZHANG, Y., FEI, H., KIM, S., LALLONE, R., RANGANATHAN, S. & ET AL. 1995. Leptin levels in human and rodent: measurement of plasma leptin and ob RNA in obese and weight-reduced subjects. *Nat Med,* 1**,** 1155-61.

MAKARONIDIS, J. M. & BATTERHAM, R. L. 2016. Potential Mechanisms Mediating Sustained Weight Loss Following Roux-en-Y Gastric Bypass and Sleeve Gastrectomy. *Endocrinol Metab Clin North Am,* 45**,** 539-52.

MANGUBAT, M., LUTFY, K., LEE, M. L., PULIDO, L., STOUT, D., DAVIS, R., SHIN, C. S., SHAHBAZIAN, M., SEASHOLTZ, S., SINHA-HIKIM, A., SINHA-HIKIM, I., O'DELL, L. E., LYZLOV, A., LIU, Y. & FRIEDMAN, T. C. 2012. Effect of nicotine on body composition in mice. *J Endocrinol,* 212**,** 317-26.

MARRERO, M. B., LUCAS, R., SALET, C., HAUSER, T. A., MAZUROV, A., LIPPIELLO, P. M. & BENCHERIF, M. 2010. An alpha7 nicotinic acetylcholine receptor-selective agonist reduces weight gain and metabolic changes in a mouse model of diabetes. *J Pharmacol Exp Ther,* 332**,** 173-80.

MATTHEWS, D. R., HOSKER, J. P., RUDENSKI, A. S., NAYLOR, B. A., TREACHER, D. F. & TURNER, R. C. 1985. Homeostasis model assessment: insulin resistance and beta-cell function from fasting plasma glucose and insulin concentrations in man. *Diabetologia,* 28**,** 412-9.

MAUVAIS-JARVIS, F., MANSON, J. E., STEVENSON, J. C. & FONSECA, V. A. 2017. Menopausal Hormone Therapy and Type 2 Diabetes Prevention: Evidence, Mechanisms, and Clinical Implications. *Endocr Rev,* 38**,** 173-188.

MCKEMY, D. D. 2007. TRPM8: The Cold and Menthol Receptor. *In:* LIEDTKE, W. B. & HELLER, S. (eds.) *TRP Ion Channel Function in Sensory Transduction and Cellular Signaling Cascades.* Boca Raton (FL).

MCKEMY, D. D., NEUHAUSSER, W. M. & JULIUS, D. 2002. Identification of a cold receptor reveals a general role for TRP channels in thermosensation. *Nature,* 416**,** 52-8.

MEHTA, T., SMITH, D. L., JR., MUHAMMAD, J. & CASAZZA, K. 2014. Impact of weight cycling on risk of morbidity and mortality. *Obes Rev,* 15**,** 870-81.

MEISTER, B., GOMUC, B., SUAREZ, E., ISHII, Y., DURR, K. & GILLBERG, L. 2006. Hypothalamic proopiomelanocortin (POMC) neurons have a cholinergic phenotype. *Eur J Neurosci,* 24**,** 2731-40.

MELDRUM, D. R., MORRIS, M. A. & GAMBONE, J. C. 2017. Obesity pandemic: causes, consequences, and solutions-but do we have the will? *Fertil Steril,* 107**,** 833-839.

MENTLEIN, R., GALLWITZ, B. & SCHMIDT, W. E. 1993. Dipeptidyl-peptidase IV hydrolyses gastric inhibitory polypeptide, glucagon-like peptide-1(7-36)amide, peptide histidine methionine and is responsible for their degradation in human serum. *Eur J Biochem,* 214**,** 829-35.

MICHLIG, S., MERLINI, J. M., BEAUMONT, M., LEDDA, M., TAVENARD, A., MUKHERJEE, R., CAMACHO, S. & LE COUTRE, J. 2016. Effects of TRP channel agonist ingestion on metabolism and autonomic nervous system in a randomized clinical trial of healthy subjects. *Sci Rep,* 6**,** 20795.

MIDDLETON, K. R., ANTON, S. D. & PERRI, M. G. 2013. Long-Term Adherence to Health Behavior Change. *Am J Lifestyle Med,* 7**,** 395-404.

MINEUR, Y. S., ABIZAID, A., RAO, Y., SALAS, R., DILEONE, R. J., GUNDISCH, D., DIANO, S., DE BIASI, M., HORVATH, T. L., GAO, X. B. & PICCIOTTO, M. R. 2011. Nicotine decreases food intake through activation of POMC neurons. *Science,* 332**,** 1330-2.

MIYAZAKI, Y., MAHANKALI, A., MATSUDA, M., GLASS, L., MAHANKALI, S., FERRANNINI, E., CUSI, K., MANDARINO, L. J. & DEFRONZO, R. A. 2001. Improved glycemic control and enhanced insulin sensitivity in type 2 diabetic subjects treated with pioglitazone. *Diabetes Care,* 24**,** 710-9.

MORIGNY, P., HOUSSIER, M., MOUISEL, E. & LANGIN, D. 2016. Adipocyte lipolysis and insulin resistance. *Biochimie,* 125**,** 259-66.

MORRISON, S. F., MADDEN, C. J. & TUPONE, D. 2014. Central neural regulation of brown adipose tissue thermogenesis and energy expenditure. *Cell Metab,* 19**,** 741-756.

MOUNTJOY, K. G., MORTRUD, M. T., LOW, M. J., SIMERLY, R. B. & CONE, R. D. 1994. Localization of the melanocortin-4 receptor (MC4-R) in neuroendocrine and autonomic control circuits in the brain. *Mol Endocrinol,* 8**,** 1298-308.

MU, J., JIANG, G., BRADY, E., DALLAS-YANG, Q., LIU, F., WOODS, J., ZYCBAND, E., WRIGHT, M., LI, Z., LU, K., ZHU, L., SHEN, X., SINHAROY, R., CANDELORE, M. L., QURESHI, S. A., SHEN, D. M., ZHANG, F., PARMEE, E. R. & ZHANG, B. B. 2011. Chronic treatment with a glucagon receptor antagonist lowers glucose and moderately raises circulating glucagon and glucagon-like peptide 1 without severe alpha cell hypertrophy in diet-induced obese mice. *Diabetologia,* 54**,** 2381-91.

MÜLLER, T. D., CLEMMENSEN, C., FINAN, B., DIMARCHI, R. D. & TSCHÖP, M. H. 2018. Anti-Obesity Therapy: from Rainbow Pills to Polyagonists. *Pharmacol Rev,* 70**,** 712-746.

NAGLER, J., SCHRIEVER, S. C., DE ANGELIS, M., PFLUGER, P. T. & SCHRAMM, K. W. 2018. Comprehensive analysis of nine monoamines and metabolites in small amounts of peripheral murine (C57Bl/6 J) tissues. *Biomed Chromatogr,* 32.

NANDA, S., GUPTA, N., MEHTA, H. C. & SANGWAN, K. 2003. Effect of oestrogen replacement therapy on serum lipid profile. *Aust N Z J Obstet Gynaecol,* 43**,** 213-6.

NATIONAL INSTITUTES OF HEALTH. 2017. *NIH Clinical Research Trials And You* [Online]. Available: https://www.nih.gov/health-information/nih-clinical-research-trials-you/basics [Accessed January 2 2019].

NEARY, N. M., SMALL, C. J., DRUCE, M. R., PARK, A. J., ELLIS, S. M., SEMJONOUS, N. M., DAKIN, C. L., FILIPSSON, K., WANG, F., KENT, A. S., FROST, G. S., GHATEI, M. A. & BLOOM, S. R. 2005. Peptide YY3-36 and glucagon-like peptide-17-36 inhibit food intake additively. *Endocrinology,* 146**,** 5120-7.

NOSSO, G., GRIFFO, E., COTUGNO, M., SALDALAMACCHIA, G., LUPOLI, R., PACINI, G., RICCARDI, G., ANGRISANI, L. & CAPALDO, B. 2016. Comparative Effects of Roux-en-Y Gastric Bypass and Sleeve Gastrectomy on Glucose Homeostasis and Incretin Hormones in Obese Type 2 Diabetic Patients: A One-Year Prospective Study. *Horm Metab Res,* 48**,** 312-7.

NOYAN-ASHRAF, M. H., MOMEN, M. A., BAN, K., SADI, A. M., ZHOU, Y. Q., RIAZI, A. M., BAGGIO, L. L., HENKELMAN, R. M., HUSAIN, M. & DRUCKER, D. J. 2009. GLP-1R agonist liraglutide activates cytoprotective pathways and improves outcomes after experimental myocardial infarction in mice. *Diabetes,* 58**,** 975-83.

NUTTALL, F. Q. 2015. Body Mass Index: Obesity, BMI, and Health: A Critical Review. *Nutr Today,* 50**,** 117-128.

NUUTILA, P., KNUUTI, M. J., MAKI, M., LAINE, H., RUOTSALAINEN, U., TERAS, M., HAAPARANTA, M., SOLIN, O. & YKI-JARVINEN, H. 1995. Gender and insulin sensitivity in the heart and in skeletal muscles. Studies using positron emission tomography. *Diabetes,* 44**,** 31-6.

OBEN, J., MORGAN, L., FLETCHER, J. & MARKS, V. 1991. Effect of the entero-pancreatic hormones, gastric inhibitory polypeptide and glucagon-like polypeptide-1(7-36) amide, on fatty acid synthesis in explants of rat adipose tissue. *J Endocrinol,* 130**,** 267-72.

OKAMOTO, H., KIM, J., AGLIONE, J., LEE, J., CAVINO, K., NA, E., RAFIQUE, A., KIM, J. H., HARP, J., VALENZUELA, D. M., YANCOPOULOS, G. D., MURPHY, A. J. & GROMADA, J. 2015. Glucagon Receptor Blockade With a Human Antibody Normalizes Blood Glucose in Diabetic Mice and Monkeys. *Endocrinology,* 156**,** 2781-94.

ONUR, S., HAAS, V., BOSY-WESTPHAL, A., HAUER, M., PAUL, T., NUTZINGER, D., KLEIN, H. & MULLER, M. J. 2005. L-tri-iodothyronine is a major determinant of resting energy expenditure in underweight patients with anorexia nervosa and during weight gain. *Eur J Endocrinol,* 152**,** 179-84.

OPPENHEIMER, J. H., SCHWARTZ, H. L., LANE, J. T. & THOMPSON, M. P. 1991. Functional relationship of thyroid hormone-induced lipogenesis, lipolysis, and thermogenesis in the rat. *J Clin Invest,* 87**,** 125-32.

PALOYAN, E. & HARPER, P. V., JR. 1961. Glucagon as a regulating factor of plasma lipids. *Metabolism,* 10**,** 315-23.

PATEL, D. D., ANTONI, C., FREEDMAN, S. J., LEVESQUE, M. C. & SUNDY, J. S. 2017. Phase 2 to phase 3 clinical trial transitions: Reasons for success and failure in immunologic diseases. *J Allergy Clin Immunol,* 140**,** 685-687.

PATTI, M. E., HOUTEN, S. M., BIANCO, A. C., BERNIER, R., LARSEN, P. R., HOLST, J. J., BADMAN, M. K., MARATOS-FLIER, E., MUN, E. C., PIHLAJAMAKI, J., AUWERX, J. & GOLDFINE, A. B. 2009. Serum bile acids are higher in humans with prior gastric bypass: potential contribution to improved glucose and lipid metabolism. *Obesity (Silver Spring),* 17**,** 1671-7.

PEDERSON, R. A. & BROWN, J. C. 1978. Interaction of gastric inhibitory polypeptide, glucose, and arginine on insulin and glucagon secretion from the perfused rat pancreas. *Endocrinology,* 103**,** 610-5.

PEIER, A. M., MOQRICH, A., HERGARDEN, A. C., REEVE, A. J., ANDERSSON, D. A., STORY, G. M., EARLEY, T. J., DRAGONI, I., MCINTYRE, P., BEVAN, S. & PATAPOUTIAN, A. 2002. A TRP channel that senses cold stimuli and menthol. *Cell,* 108**,** 705-15.

PERKINS, R. G. 1919. A Study of the Munitions Intoxications in France.

PETERLI, R., STEINERT, R. E., WOELNERHANSSEN, B., PETERS, T., CHRISTOFFEL-COURTIN, C., GASS, M., KERN, B., VON FLUEE, M. & BEGLINGER, C. 2012. Metabolic and hormonal changes after laparoscopic Roux-en-Y gastric bypass and sleeve gastrectomy: a randomized, prospective trial. *Obes Surg,* 22**,** 740-8.

PETTERSSON, U. S., WALDEN, T. B., CARLSSON, P. O., JANSSON, L. & PHILLIPSON, M. 2012. Female mice are protected against high-fat diet induced metabolic syndrome and increase the regulatory T cell population in adipose tissue. *PLoS One,* 7**,** e46057.

PICCIOTTO, M. R., ZOLI, M., LENA, C., BESSIS, A., LALLEMAND, Y., LE NOVERE, N., VINCENT, P., PICH, E. M., BRULET, P. & CHANGEUX, J. P. 1995. Abnormal avoidance learning in mice lacking functional high-affinity nicotine receptor in the brain. *Nature,* 374**,** 65-7.

POIRIER, P., GILES, T. D., BRAY, G. A., HONG, Y., STERN, J. S., PI-SUNYER, F. X. & ECKEL, R. H. 2006. Obesity and cardiovascular disease: pathophysiology, evaluation, and effect of weight loss. *Arterioscler Thromb Vasc Biol,* 26**,** 968-76.

PRADHAN, G., SAMSON, S. L. & SUN, Y. 2013. Ghrelin: much more than a hunger hormone. *Curr Opin Clin Nutr Metab Care,* 16**,** 619-24.

PRENTICE, A. M. & JEBB, S. A. 2001. Beyond body mass index. *Obes Rev,* 2**,** 141-7.

PUCCI, E., CHIOVATO, L. & PINCHERA, A. 2000. Thyroid and lipid metabolism. *Int J Obes Relat Metab Disord,* 24 Suppl 2**,** S109-12.

QUARTA, C., CLEMMENSEN, C., ZHU, Z., YANG, B., JOSEPH, S. S., LUTTER, D., YI, C. X., GRAF, E., GARCIA-CACERES, C., LEGUTKO, B., FISCHER, K., BROMMAGE, R., ZIZZARI, P., FRANKLIN, B. S., KRUEGER, M., KOCH, M., VETTORAZZI, S., LI, P., HOFMANN, S. M., BAKHTI, M., BASTIDAS-PONCE, A., LICKERT, H., STROM, T. M., GAILUS-DURNER, V., BECHMANN, I., PEREZ-TILVE, D., TUCKERMANN, J., HRABE DE ANGELIS, M., SANDOVAL, D., COTA, D., LATZ, E., SEELEY, R. J., MULLER, T. D., DIMARCHI, R. D., FINAN, B. & TSCHOP, M. H. 2017. Molecular Integration of Incretin and Glucocorticoid Action Reverses Immunometabolic Dysfunction and Obesity. *Cell Metab,* 26**,** 620-632 e6.

QUETELET A 1968. *A treatise on man and the development of his faculties*.

RASK, E., OLSSON, T., SODERBERG, S., JOHNSON, O., SECKL, J., HOLST, J. J., AHREN, B., NORTHERN SWEDEN MONITORING OF, T. & DETERMINANTS IN CARDIOVASCULAR, D. 2001. Impaired incretin response after a mixed meal is associated with insulin resistance in nondiabetic men. *Diabetes Care,* 24**,** 1640-5.

RAVUSSIN, Y., XIAO, C., GAVRILOVA, O. & REITMAN, M. L. 2014. Effect of intermittent cold exposure on brown fat activation, obesity, and energy homeostasis in mice. *PLoS One,* 9**,** e85876.

RAZANSKY, D., BUEHLER, A. & NTZIACHRISTOS, V. 2011. Volumetric real-time multispectral optoacoustic tomography of biomarkers. *Nat Protoc,* 6**,** 1121-9.

REAVEN, G. M. 1988. Banting lecture 1988. Role of insulin resistance in human disease. *Diabetes,* 37**,** 1595-607.

REBER, J., WILLERSHAUSER, M., KARLAS, A., PAUL-YUAN, K., DIOT, G., FRANZ, D., FROMME, T., OVSEPIAN, S. V., BEZIERE, N., DUBIKOVSKAYA, E., KARAMPINOS, D. C., HOLZAPFEL, C., HAUNER, H., KLINGENSPOR, M. & NTZIACHRISTOS, V. 2018. Non-invasive Measurement of Brown Fat Metabolism Based on Optoacoustic Imaging of Hemoglobin Gradients. *Cell Metab,* 27**,** 689-701 e4.

REHNMARK, S., NECHAD, M., HERRON, D., CANNON, B. & NEDERGAARD, J. 1990. Alpha- and beta-adrenergic induction of the expression of the uncoupling protein thermogenin in brown adipocytes differentiated in culture. *J Biol Chem,* 265**,** 16464-71.

RIANT, E., WAGET, A., COGO, H., ARNAL, J. F., BURCELIN, R. & GOURDY, P. 2009. Estrogens protect against high-fat diet-induced insulin resistance and glucose intolerance in mice. *Endocrinology,* 150**,** 2109-17.

RICHTER, B., BANDEIRA-ECHTLER, E., BERGERHOFF, K. & LERCH, C. L. 2008. Dipeptidyl peptidase-4 (DPP-4) inhibitors for type 2 diabetes mellitus. *Cochrane Database Syst Rev***,** CD006739.

RODGERS, S., BURNET, R., GOSS, A., PHILLIPS, P., GOLDNEY, R., KIMBER, C., THOMAS, D., HARDING, P. & WISE, P. 1977. Jaw wiring in treatment of obesity. *Lancet,* 1**,** 1221-2.

ROH, E. & KIM, M. S. 2016. Brain Regulation of Energy Metabolism. *Endocrinol Metab (Seoul),* 31**,** 519-524.

ROJAS, L. B. & GOMES, M. B. 2013. Metformin: an old but still the best treatment for type 2 diabetes. *Diabetol Metab Syndr,* 5**,** 6.

ROSENSTOCK, J., DAVIES, M., HOME, P. D., LARSEN, J., KOENEN, C. & SCHERNTHANER, G. 2008. A randomised, 52-week, treat-to-target trial comparing insulin detemir with insulin glargine when administered as add-on to glucose-lowering drugs in insulin-naive people with type 2 diabetes. *Diabetologia,* 51**,** 408-16.

ROSSATO, M., GRANZOTTO, M., MACCHI, V., PORZIONATO, A., PETRELLI, L., CALCAGNO, A., VENCATO, J., DE STEFANI, D., SILVESTRIN, V., RIZZUTO, R., BASSETTO, F., DE CARO, R. & VETTOR, R. 2014. Human white adipocytes express the cold receptor TRPM8 which activation induces UCP1 expression, mitochondrial activation and heat production. *Mol Cell Endocrinol,* 383**,** 137-46.

ROSSI, J., BALTHASAR, N., OLSON, D., SCOTT, M., BERGLUND, E., LEE, C. E., CHOI, M. J., LAUZON, D., LOWELL, B. B. & ELMQUIST, J. K. 2011. Melanocortin-4 receptors expressed by cholinergic neurons regulate energy balance and glucose homeostasis. *Cell Metab,* 13**,** 195-204.

RUBIN, R. R., WADDEN, T. A., BAHNSON, J. L., BLACKBURN, G. L., BRANCATI, F. L., BRAY, G. A., CODAY, M., CROW, S. J., CURTIS, J. M., DUTTON, G., EGAN, C., EVANS, M., EWING, L., FAULCONBRIDGE, L., FOREYT, J., GAUSSOIN, S. A., GREGG, E. W., HAZUDA, H. P., HILL, J. O., HORTON, E. S., HUBBARD, V. S., JAKICIC, J. M., JEFFERY, R. W., JOHNSON, K. C., KAHN, S. E., KNOWLER, W. C., LANG, W., LEWIS, C. E., MONTEZ, M. G., MURILLO, A., NATHAN, D. M., PATRICIO, J., PETERS, A., PI-SUNYER, X., POWNALL, H., REJESKI, W. J., ROSENTHAL, R. H., RUELAS, V., TOLEDO, K., VAN DORSTEN, B., VITOLINS, M., WILLIAMSON, D., WING, R. R., YANOVSKI, S. Z., ZHANG, P. & LOOK, A. R. G. 2014. Impact of intensive lifestyle intervention on depression and health-related quality of life in type 2 diabetes: the Look AHEAD Trial. *Diabetes Care,* 37**,** 1544-53.

SAHOO, K., SAHOO, B., CHOUDHURY, A. K., SOFI, N. Y., KUMAR, R. & BHADORIA, A. S. 2015. Childhood obesity: causes and consequences. *J Family Med Prim Care,* 4**,** 187-92.

SALA, F., NISTRI, A. & CRIADO, M. 2008. Nicotinic acetylcholine receptors of adrenal chromaffin cells. *Acta Physiol (Oxf),* 192**,** 203-12.

SALTER, J. M. 1960. Metabolic Effects of Glucagon in the Wistar Rat. *The American Journal of Clinical Nutrition,* 8.

SAMAD, F., YAMAMOTO, K., PANDEY, M. & LOSKUTOFF, D. J. 1997. Elevated expression of transforming growth factor-beta in adipose tissue from obese mice. *Mol Med,* 3**,** 37-48.

SANCHEZ-ALAVEZ, M., ALBONI, S. & CONTI, B. 2011. Sex- and age-specific differences in core body temperature of C57Bl/6 mice. *Age (Dordr),* 33**,** 89-99.

SANDERS-EZN, H. 1867. Der respiratorische Gasanstausch bei grossen Temperaturveränderungen. *Berichte der Kön. sichs. Gesellschaft der Wissensch.***,** 58.

SCHACKE, H., DOCKE, W. D. & ASADULLAH, K. 2002. Mechanisms involved in the side effects of glucocorticoids. *Pharmacol Ther,* 96**,** 23-43.

SCHAUER, P. R., BHATT, D. L. & KASHYAP, S. R. 2017. Bariatric Surgery or Intensive Medical Therapy for Diabetes after 5 Years. *N Engl J Med,* 376**,** 1997.

SCHAUER, P. R., KASHYAP, S. R., WOLSKI, K., BRETHAUER, S. A., KIRWAN, J. P., POTHIER, C. E., THOMAS, S., ABOOD, B., NISSEN, S. E. & BHATT, D. L. 2012. Bariatric surgery versus intensive medical therapy in obese patients with diabetes. *N Engl J Med,* 366**,** 1567-76.

SCHUSTER, D. P. 2010. Obesity and the development of type 2 diabetes: the effects of fatty tissue inflammation. *Diabetes Metab Syndr Obes,* 3**,** 253-62.

SCHWARTZ, M. W., WOODS, S. C., PORTE, D., JR., SEELEY, R. J. & BASKIN, D. G. 2000. Central nervous system control of food intake. *Nature,* 404**,** 661-71.

SCOPINARO, N., GIANETTA, E., ADAMI, G. F., FRIEDMAN, D., TRAVERSO, E., MARINARI, G. M., CUNEO, S., VITALE, B., BALLARI, F., COLOMBINI, M., BASCHIERI, G. & BACHI, V. 1996. Biliopancreatic diversion for obesity at eighteen years. *Surgery,* 119**,** 261-8.

SHANKAR, S. S., MIXSON, L. A., CHAKRAVARTHY, M., CHISHOLM, R., ACTON, A. J., JONES, R., MATTAR, S. G., MILLER, D. L., PETRY, L., BEALS, C. R., STOCH, S. A., KELLEY, D. E. & CONSIDINE, R. V. 2017. Metabolic improvements following Roux-en-Y surgery assessed by solid meal test in subjects with short duration type 2 diabetes. *BMC Obes,* 4**,** 10.

SHAW, R. J., LAMIA, K. A., VASQUEZ, D., KOO, S. H., BARDEESY, N., DEPINHO, R. A., MONTMINY, M. & CANTLEY, L. C. 2005. The kinase LKB1 mediates glucose homeostasis in liver and therapeutic effects of metformin. *Science,* 310**,** 1642-6.

SHERMAN, M. M., UNGUREANU, S. & REY, J. A. 2016. Naltrexone/Bupropion ER (Contrave): Newly Approved Treatment Option for Chronic Weight Management in Obese Adults. *P T,* 41**,** 164-72.

SILECCHIA, G., BORU, C., PECCHIA, A., RIZZELLO, M., CASELLA, G., LEONETTI, F. & BASSO, N. 2006. Effectiveness of laparoscopic sleeve gastrectomy (first stage of biliopancreatic diversion with duodenal switch) on co-morbidities in super-obese high-risk patients. *Obes Surg,* 16**,** 1138-44.

SINHA-HIKIM, I., FRIEDMAN, T. C., SHIN, C. S., LEE, D., IVEY, R. & SINHA-HIKIM, A. P. 2014. Nicotine in combination with a high-fat diet causes intramyocellular mitochondrial abnormalities in male mice. *Endocrinology,* 155**,** 865-72.

SJOSTROM, L., RISSANEN, A., ANDERSEN, T., BOLDRIN, M., GOLAY, A., KOPPESCHAAR, H. P. & KREMPF, M. 1998. Randomised placebo-controlled trial of orlistat for weight loss and prevention of weight regain in obese patients. European Multicentre Orlistat Study Group. *Lancet,* 352**,** 167-72.

SJOUKE, B., LANGSLET, G., CESKA, R., NICHOLLS, S. J., NISSEN, S. E., OHLANDER, M., LADENSON, P. W., OLSSON, A. G., HOVINGH, G. K. & KASTELEIN, J. J. 2014. Eprotirome in patients with familial hypercholesterolaemia (the AKKA trial): a randomised, double-blind, placebo-controlled phase 3 study. *Lancet Diabetes Endocrinol,* 2**,** 455-63.

SNIDERMAN, A. D., BHOPAL, R., PRABHAKARAN, D., SARRAFZADEGAN, N. & TCHERNOF, A. 2007. Why might South Asians be so susceptible to central obesity and its atherogenic consequences? The adipose tissue overflow hypothesis. *Int J Epidemiol,* 36**,** 220-5.

SPARKS, L. M. 2017. Exercise training response heterogeneity: physiological and molecular insights. *Diabetologia,* 60**,** 2329-2336.

SPEAKMAN, J. R. 2013. Measuring energy metabolism in the mouse - theoretical, practical, and analytical considerations. *Front Physiol,* 4**,** 34.

STANLEY, B. G., HA, L. H., SPEARS, L. C. & DEE, M. G., 2ND 1993. Lateral hypothalamic injections of glutamate, kainic acid, D,L-alpha-amino-3-hydroxy-5-methyl-isoxazole propionic acid or N-methyl-D-aspartic acid rapidly elicit intense transient eating in rats. *Brain Res,* 613**,** 88-95.

STEFATER, M. A., PEREZ-TILVE, D., CHAMBERS, A. P., WILSON-PEREZ, H. E., SANDOVAL, D. A., BERGER, J., TOURE, M., TSCHOP, M., WOODS, S. C. & SEELEY, R. J. 2010. Sleeve gastrectomy induces loss of weight and fat mass in obese rats, but does not affect leptin sensitivity. *Gastroenterology,* 138**,** 2426-36, 2436 e1-3.

STERNE, J. 1957. Du nouveau dans les antidiabétiques, le N N diméthyl-diguanide. *Maroc med,* 36**,** 1295-1296.

STEVENSON, R. W., STEINER, K. E., DAVIS, M. A., HENDRICK, G. K., WILLIAMS, P. E., LACY, W. W., BROWN, L., DONAHUE, P., LACY, D. B. & CHERRINGTON, A. D. 1987. Similar dose responsiveness of hepatic glycogenolysis and gluconeogenesis to glucagon in vivo. *Diabetes,* 36**,** 382-9.

STRAUB, R. H. 2007. The complex role of estrogens in inflammation. *Endocr Rev,* 28**,** 521-74.

SUN, L., CAMPS, S. G., GOH, H. J., GOVINDHARAJULU, P., SCHAEFFERKOETTER, J. D., TOWNSEND, D. W., VERMA, S. K., VELAN, S. S., SUN, L., SZE, S. K., LIM, S. C., BOEHM, B. O., HENRY, C. J. & LEOW, M. K. 2018. Capsinoids activate brown adipose tissue (BAT) with increased energy expenditure associated with subthreshold 18-fluorine fluorodeoxyglucose uptake in BAT-positive humans confirmed by positron emission tomography scan. *Am J Clin Nutr,* 107**,** 62-70.

SUSULIC, V. S., FREDERICH, R. C., LAWITTS, J., TOZZO, E., KAHN, B. B., HARPER, M. E., HIMMS-HAGEN, J., FLIER, J. S. & LOWELL, B. B. 1995. Targeted disruption of the beta 3-adrenergic receptor gene. *J Biol Chem,* 270**,** 29483-92.

SVANE, M. S., BOJSEN-MOLLER, K. N., NIELSEN, S., JORGENSEN, N. B., DIRKSEN, C., BENDTSEN, F., KRISTIANSEN, V. B., HARTMANN, B., HOLST, J. J. & MADSBAD, S. 2016. Effects of

endogenous GLP-1 and GIP on glucose tolerance after Roux-en-Y gastric bypass surgery. *Am J Physiol Endocrinol Metab,* 310**,** E505-14.

SWINNEN, S. G., HOEKSTRA, J. B. & DEVRIES, J. H. 2009. Insulin therapy for type 2 diabetes. *Diabetes Care,* 32 Suppl 2**,** S253-9.

TAINTER, M. L., CUTTING, W. C. & STOCKTON, A. B. 1934. Use of Dinitrophenol in Nutritional Disorders : A Critical Survey of Clinical Results. *Am J Public Health Nations Health,* 24**,** 1045-53.

TALCHAI, C., XUAN, S., LIN, H. V., SUSSEL, L. & ACCILI, D. 2012. Pancreatic beta cell dedifferentiation as a mechanism of diabetic beta cell failure. *Cell,* 150**,** 1223-34.

TAN, T. M., FIELD, B. C., MCCULLOUGH, K. A., TROKE, R. C., CHAMBERS, E. S., SALEM, V., GONZALEZ MAFFE, J., BAYNES, K. C., DE SILVA, A., VIARDOT, A., ALSAFI, A., FROST, G. S., GHATEI, M. A. & BLOOM, S. R. 2013. Coadministration of glucagon-like peptide-1 during glucagon infusion in humans results in increased energy expenditure and amelioration of hyperglycemia. *Diabetes,* 62**,** 1131-8.

TANG, M., WU, G. Y., DONG, X. Z. & TANG, Z. X. 2016. Phosphoinositide interacting regulator of TRP (Pirt) enhances TRPM8 channel activity in vitro via increasing channel conductance. *Acta Pharmacol Sin,* 37**,** 98-104.

TANG, Z., KIM, A., MASUCH, T., PARK, K., WENG, H., WETZEL, C. & DONG, X. 2013. Pirt functions as an endogenous regulator of TRPM8. *Nat Commun,* 4**,** 2179.

TEK, C. 2016. Naltrexone HCI/bupropion HCI for chronic weight management in obese adults: patient selection and perspectives. *Patient Prefer Adherence,* 10**,** 751-9.

TORGERSEN, Z., OSMOLAK, A. & FORSE, R. A. 2014. Sleeve gastrectomy and Roux En Y gastric bypass: current state of metabolic surgery. *Curr Opin Endocrinol Diabetes Obes,* 21**,** 352-7.

TORNEHAVE, D., KRISTENSEN, P., ROMER, J., KNUDSEN, L. B. & HELLER, R. S. 2008. Expression of the GLP-1 receptor in mouse, rat, and human pancreas. *J Histochem Cytochem,* 56**,** 841-51.

TREVASKIS, J. L., SUN, C., ATHANACIO, J., D'SOUZA, L., SAMANT, M., TATARKIEWICZ, K., GRIFFIN, P. S., WITTMER, C., WANG, Y., TENG, C. H., FOROOD, B., PARKES, D. G. & ROTH, J. D. 2015. Synergistic metabolic benefits of an exenatide analogue and cholecystokinin in diet-induced obese and leptin-deficient rodents. *Diabetes Obes Metab,* 17**,** 61-73.

TSCHÖP, M. H., FINAN, B., CLEMMENSEN, C., GELFANOV, V., PEREZ-TILVE, D., MULLER, T. D. & DIMARCHI, R. D. 2016. Unimolecular Polypharmacy for Treatment of Diabetes and Obesity. *Cell Metab,* 24**,** 51-62.

TSCHÖP, M. H., SPEAKMAN, J. R., ARCH, J. R., AUWERX, J., BRUNING, J. C., CHAN, L., ECKEL, R. H., FARESE, R. V., JR., GALGANI, J. E., HAMBLY, C., HERMAN, M. A., HORVATH, T. L., KAHN, B. B., KOZMA, S. C., MARATOS-FLIER, E., MULLER, T. D., MUNZBERG, H., PFLUGER, P. T., PLUM, L., REITMAN, M. L., RAHMOUNI, K., SHULMAN, G. I., THOMAS, G., KAHN, C. R. & RAVUSSIN, E. 2011. A guide to analysis of mouse energy metabolism. *Nat Methods,* 9**,** 57-63.

TSOLI, M., CHRONAIOU, A., KEHAGIAS, I., KALFARENTZOS, F. & ALEXANDRIDES, T. K. 2013. Hormone changes and diabetes resolution after biliopancreatic diversion and laparoscopic sleeve gastrectomy: a comparative prospective study. *Surg Obes Relat Dis,* 9**,** 667-77.

TZOUMAS, S., NUNES, A., OLEFIR, I., STANGL, S., SYMVOULIDIS, P., GLASL, S., BAYER, C., MULTHOFF, G. & NTZIACHRISTOS, V. 2016. Eigenspectra optoacoustic tomography achieves quantitative blood oxygenation imaging deep in tissues. *Nat Commun,* 7**,** 12121.

U.S. FOOD & DRUG. 2018. *The Drug Development Process* [Online]. Available: https://www.fda.gov/ForPatients/Approvals/Drugs/default.htm [Accessed October 30 2018].

U.S. NATIONAL INSTITUTES OF HEALTH. 2018. *A Phase 1, Single Dose Study to Evaluate the Safety and Pharmacokinetics of MEDI0382 in Healthy Volunteers* [Online]. Available: https://clinicaltrials.gov/ct2/results?term=MEDI0382&pg=1 [Accessed November 5 2018].

UKKOLA, O., KESANIEMI, Y. A., TREMBLAY, A. & BOUCHARD, C. 2004. Two variants in the resistin gene and the response to long-term overfeeding. *Eur J Clin Nutr,* 58**,** 654-9.

UNICK, J. L., BEAVERS, D., BOND, D. S., CLARK, J. M., JAKICIC, J. M., KITABCHI, A. E., KNOWLER, W. C., WADDEN, T. A., WAGENKNECHT, L. E., WING, R. R. & LOOK, A. R. G. 2013. The long-term effectiveness of a lifestyle intervention in severely obese individuals. *Am J Med,* 126**,** 236-42, 242 e1-2.

US FOOD AND DRUG ADMINISTRATION 1968. press release.

VAGE, V., SOLHAUG, J. H., BERSTAD, A., SVANES, K. & VISTE, A. 2002. Jejunoileal bypass in the treatment of morbid obesity: a 25-year follow-up study of 36 patients. *Obes Surg,* 12**,** 312-8.

VAN DAMMEN, L., WEKKER, V., DE ROOIJ, S. R., GROEN, H., HOEK, A. & ROSEBOOM, T. J. 2018. A systematic review and meta-analysis of lifestyle interventions in women of reproductive age with overweight or obesity: the effects on symptoms of depression and anxiety. *Obes Rev,* 19**,** 1679-1687.

VAN DER GROEP, P., BOUTER, A., VAN DER ZANDEN, R., SICCAMA, I., MENKO, F. H., GILLE, J. J., VAN KALKEN, C., VAN DER WALL, E., VERHEIJEN, R. H. & VAN DIEST, P. J. 2006. Distinction between hereditary and sporadic breast cancer on the basis of clinicopathological data. *J Clin Pathol,* 59**,** 611-7.

VAN MARKEN LICHTENBELT, W. D., VANHOMMERIG, J. W., SMULDERS, N. M., DROSSAERTS, J. M., KEMERINK, G. J., BOUVY, N. D., SCHRAUWEN, P. & TEULE, G. J. 2009. Cold-activated brown adipose tissue in healthy men. *N Engl J Med,* 360**,** 1500-8.

VARELA, L. & HORVATH, T. L. 2012. Leptin and insulin pathways in POMC and AgRP neurons that modulate energy balance and glucose homeostasis. *EMBO Rep,* 13**,** 1079-86.

VU, C. U., SIDDIQUI, J. A., WADENSWEILER, P., GAYEN, J. R., AVOLIO, E., BANDYOPADHYAY, G. K., BISWAS, N., CHI, N. W., O'CONNOR, D. T. & MAHATA, S. K. 2014. Nicotinic acetylcholine receptors in glucose homeostasis: the acute hyperglycemic and chronic insulin-sensitive effects of nicotine suggest dual opposing roles of the receptors in male mice. *Endocrinology,* 155**,** 3793-805.

WADDEN, T. A. 1995. *Very-low-calorie diets: Appraisal and recommendations,* New York: Guilford Press.

WADDEN, T. A., FOREYT, J. P., FOSTER, G. D., HILL, J. O., KLEIN, S., O'NEIL, P. M., PERRI, M. G., PI-SUNYER, F. X., ROCK, C. L., ERICKSON, J. S., MAIER, H. N., KIM, D. D. & DUNAYEVICH, E. 2011. Weight loss with naltrexone SR/bupropion SR combination therapy as an adjunct to behavior modification: the COR-BMOD trial. *Obesity (Silver Spring),* 19**,** 110-20.

WALSER, T., CUI, X., YANAGAWA, J., LEE, J. M., HEINRICH, E., LEE, G., SHARMA, S. & DUBINETT, S. M. 2008. Smoking and lung cancer: the role of inflammation. *Proc Am Thorac Soc,* 5**,** 811-5.

WANG, X., CAHILL, C. M., PINEYRO, M. A., ZHOU, J., DOYLE, M. E. & EGAN, J. M. 1999. Glucagon-like peptide-1 regulates the beta cell transcription factor, PDX-1, in insulinoma cells. *Endocrinology,* 140**,** 4904-7.

WASADA, T., MCCORKLE, K., HARRIS, V., KAWAI, K., HOWARD, B. & UNGER, R. H. 1981. Effect of gastric inhibitory polypeptide on plasma levels of chylomicron triglycerides in dogs. *J Clin Invest,* 68**,** 1106-7.

WEATHERFORD, S. C. & RITTER, S. 1988. Lesion of vagal afferent terminals impairs glucagon-induced suppression of food intake. *Physiol Behav,* 43**,** 645-50.

WEISBERG, S. P., MCCANN, D., DESAI, M., ROSENBAUM, M., LEIBEL, R. L. & FERRANTE, A. W., JR. 2003. Obesity is associated with macrophage accumulation in adipose tissue. *J Clin Invest,* 112**,** 1796-808.

WEISS, R. & CAPRIO, S. 2005. The metabolic consequences of childhood obesity. *Best Pract Res Clin Endocrinol Metab,* 19**,** 405-19.

WHO. 2016. *Global Report on Diabetes* [Online]. Available: http://apps.who.int/iris/bitstream/10665/204871/1/9789241565257_eng.pdf?u [Accessed May 24 2017].

WHO. 2018a. *Diabetes* [Online]. Available: http://www.who.int/news-room/fact-sheets/detail/diabetes [Accessed November 21 2018].

WHO. 2018b. *Obesity and overweight* [Online]. Available: http://www.who.int/news-room/fact-sheets/detail/obesity-and-overweight [Accessed November 21 2018].

WILKINSON, L. H. & PELOSO, O. A. 1981. Gastric (reservoir) reduction for morbid obesity. *Arch Surg,* 116**,** 602-5.

WILSON-PEREZ, H. E., CHAMBERS, A. P., RYAN, K. K., LI, B., SANDOVAL, D. A., STOFFERS, D., DRUCKER, D. J., PEREZ-TILVE, D. & SEELEY, R. J. 2013. Vertical sleeve gastrectomy is effective in two genetic mouse models of glucagon-like Peptide 1 receptor deficiency. *Diabetes,* 62**,** 2380-5.

WIRTH, A., WABITSCH, M. & HAUNER, H. 2014. Prävention und Therapie der Adipositas. *Dtsch Arztebl International,* 111**,** 9.

WONG, W. P., TIANO, J. P., LIU, S., HEWITT, S. C., LE MAY, C., DALLE, S., KATZENELLENBOGEN, J. A., KATZENELLENBOGEN, B. S., KORACH, K. S. & MAUVAIS-JARVIS, F. 2010. Extranuclear estrogen receptor-alpha stimulates NeuroD1 binding to the insulin promoter and favors insulin synthesis. *Proc Natl Acad Sci U S A,* 107**,** 13057-62.

WU, Q., XIAO, Z., CHENG, Z. & TIAN, H. 2013. Changes of blood glucose and gastrointestinal hormones 4 months after Roux-en-Y gastric bypass surgery in Chinese obese type 2 diabetes patients with lower body mass index. *J Diabetes Investig,* 4**,** 214-21.

WU, Y., SONG, P., ZHANG, W., LIU, J., DAI, X., LIU, Z., LU, Q., OUYANG, C., XIE, Z., ZHAO, Z., ZHUO, X., VIOLLET, B., FORETZ, M., WU, J., YUAN, Z. & ZOU, M. H. 2015. Activation of AMPKalpha2 in adipocytes is essential for nicotine-induced insulin resistance in vivo. *Nat Med*, 21**,** 373-82.

XIAO, Y. & KELLAR, K. J. 2004. The comparative pharmacology and up-regulation of rat neuronal nicotinic receptor subtype binding sites stably expressed in transfected mammalian cells. *J Pharmacol Exp Ther*, 310**,** 98-107.

XU, W., ORR-URTREGER, A., NIGRO, F., GELBER, S., SUTCLIFFE, C. B., ARMSTRONG, D., PATRICK, J. W., ROLE, L. W., BEAUDET, A. L. & DE BIASI, M. 1999. Multiorgan autonomic dysfunction in mice lacking the beta2 and the beta4 subunits of neuronal nicotinic acetylcholine receptors. *J Neurosci*, 19**,** 9298-305.

YAGER, J. D. 2015. Mechanisms of estrogen carcinogenesis: The role of E2/E1-quinone metabolites suggests new approaches to preventive intervention--A review. *Steroids,* 99**,** 56-60.

YAGER, J. D. & DAVIDSON, N. E. 2006. Estrogen carcinogenesis in breast cancer. *N Engl J Med*, 354**,** 270-82.

YAN, H., YANG, W., ZHOU, F., LI, X., PAN, Q., SHEN, Z., HAN, G., NEWELL-FUGATE, A., TIAN, Y., MAJETI, R., LIU, W., XU, Y., WU, C., ALLRED, K., ALLRED, C., SUN, Y. & GUO, S. 2018. Estrogen Improves Insulin Sensitivity and Suppresses Gluconeogenesis via the Transcription Factor Foxo1. *Diabetes*.

YANG, J. N., TISELIUS, C., DARE, E., JOHANSSON, B., VALEN, G. & FREDHOLM, B. B. 2007. Sex differences in mouse heart rate and body temperature and in their regulation by adenosine A1 receptors. *Acta Physiol (Oxf),* 190**,** 63-75.

YANG, Y., SMITH, D. L., JR., KEATING, K. D., ALLISON, D. B. & NAGY, T. R. 2014. Variations in body weight, food intake and body composition after long-term high-fat diet feeding in C57BL/6J mice. *Obesity (Silver Spring)*, 22**,** 2147-55.

YE, J. 2009. Emerging role of adipose tissue hypoxia in obesity and insulin resistance. *Int J Obes (Lond)*, 33**,** 54-66.

YEE, N.S. 2016. TRPM8 ion channels as potential cancer biomarker and target in pancreatic cancer. *Adv Protein Chem Sruct Biol*, 104:127-155.

YIN, D. P., GAO, Q., MA, L. L., YAN, W., WILLIAMS, P. E., MCGUINNESS, O. P., WASSERMAN, D. H. & ABUMRAD, N. N. 2011. Assessment of different bariatric surgeries in the treatment of obesity and insulin resistance in mice. *Ann Surg*, 254**,** 73-82.

YONESHIRO, T., AITA, S., KAWAI, Y., IWANAGA, T. & SAITO, M. 2012. Nonpungent capsaicin analogs (capsinoids) increase energy expenditure through the activation of brown adipose tissue in humans. *Am J Clin Nutr*, 95**,** 845-50.

YUE, W., YAGER, J. D., WANG, J. P., JUPE, E. R. & SANTEN, R. J. 2013. Estrogen receptor-dependent and independent mechanisms of breast cancer carcinogenesis. *Steroids,* 78**,** 161-70.

ZANDER, M., MADSBAD, S., MADSEN, J. L. & HOLST, J. J. 2002. Effect of 6-week course of glucagon-like peptide 1 on glycaemic control, insulin sensitivity, and beta-cell function in type 2 diabetes: a parallel-group study. *Lancet*, 359**,** 824-30.

ZHANG, M., HU, T., ZHANG, S. & ZHOU, L. 2015. Associations of Different Adipose Tissue Depots with Insulin Resistance: A Systematic Review and Meta-analysis of Observational Studies. *Sci Rep*, 5**,** 18495.

ZHANG, Y., PROENCA, R., MAFFEI, M., BARONE, M., LEOPOLD, L. & FRIEDMAN, J. M. 1994. Positional cloning of the mouse obese gene and its human homologue. *Nature*, 372**,** 425-32.

131

6 Appendix

6.1 Mouse models

6.1.1 Genetically modified mouse lines

UCP1 KO, Lep^{db} mice, and MC4R KO were provided from Jackson Laboratory (strain names: B6.129-Ucp1tm1Kz/J; BKS.Cg-Dock7m +/+ Leprdb/J; B6;129S4-Mc4rtm1Lowl/J, Maine, USA). The generation of the betaless mice is described elsewhere (Bachman et al., 2002). In short, homozygous $\beta_1\beta_2$-AR knockout mice (Ardb1,2tm1Bkk (beta 1,2 knockout)) were bred with homozygous β_3-AR knockout mice (Ardb3tm1Lowl (beta 3 knockout)), resulting in homozygous $\beta_1\beta_2\beta_3$-AR KO (betaless) mice. Breeding pairs of the betaless mice were kindly provided by Prof. Dr. Françoise Rohner-Jeanrenaud and Prof. Dr. Brad Lowell. For pharmacological studies a colony of homozygous triple $\beta_1\beta_2\beta_3$-AR knockout mice were bred.

Breeding pairs of the Chrnb4 KO mice were kindly provided by Dr. Uwe Maskos and generated as described previously (Xu et al., 1999). Briefly, exon 5 of the Chrnb4 gene was replaced with a puromycin resistance gene, loxP site, and exons 3-9 of the Hprt gene and electroporated into AB2.2 embryonic stem cells (ESC), which were injected into blastocysts and transmitted into the germline.

FGF21 KO mice were kindly provided by Nobuyuki Itoh and generated as described previously (Hotta et al., 2009). Briefly, the targeting vector consisted of FGF21 gene fragments, 5' and 3' homology recombination arms, a fragment for an IRES-LacZ-polyA/PGK-neo cassette, and a diphtheria toxin A expression cassette. Exons 2 and 3 and part of exon 1 of the FGF21 gene were replaced by the IRES-LacZ-polyA/PGK-neo cassette. Following linearization of the targeting vector, it was electroporated into C57Bl/6 ESC to produce germ-line chimeras with FGF21-disrupted ESC (+/-) and morulae from 129 Sv mice (Hotta et al., 2009).

Pirt$^{-/-}$ mice were generated as described previously and kindly provided by Xinzhong Dong (Kim et al., 2008). To obtain a global knockout of the *Pirt* gene, the open reading frame of *Pirt* was substituted by an axonal tracer farnesylated enhanced green fluorescent protein (EGFPf). The EGFPf is under control of the Pirt promoter (Kim et al., 2008).

TRPM8 KO mice were generated as described previously (Bautista et al., 2007) by homologous recombination in E14Tg2A.4 ESC and injection of positive clones into C57Bl/6 blastocysts. We obtained TRPM8 KO mice from Jackson Laboratory (strain name: B6.129P2-*Trpm8*^{tm1Jul}/J) and bred a colony of WT and KO mice.

6.1.2 Genotyping protocols of genetically modified mouse lines

Mice were weaned at the age of three to four weeks. DNA was isolated from ear clips using a genomic DNA isolation kit (Favorgen). Genotypes of mutant mice were evaluated by performing a polymerase chain reaction (PCR). All PCR reactions were separated in a 2-3% agarose gel (Biozym Scientific GmbH) or the QIAxcel Advanced system (Qiagen). For gels, the powdered agarose was dissolved in a tris-acetate-EDTA (TAE) buffer, which contained 5 µl PeqGREEN dye (VWR) per 100 ml of buffer.

6.1.2.1 Gradient PCR

Each mouse line, for which the PCR has not been established, was evaluated by performing a gradient PCR. To this end, a DNA pool containing presumably WT as well as genetically modified mice was mixed with the PCR buffer (**Table 6. 1**) and run at the following PCR conditions (**Table 6. 2**). The condition that yielded the clearest band was applied to all further PCR analysis.

Table 6. 1 PCR protocol for one reaction – Gradient PCR

Substance	Volume (µl)
5x Buffer	2.5
Betaine	2.5
$MgCl_2$	**0.5 / 1 / 1.5 / 2**
dNTP (10 mM)	0.25
Primer 1 (20 µM)	0.3
Primer 2 (20 µM)	0.3
Primer 3 (20 µM)	0.3
GoTaq Polymerase	0.15
Nuclease-free water	**3.9 / 3.4 / 2.9 / 2.4**
DNA	2
Total	**12.7**

Table 6. 2 PCR program for gradient PCR

Step	Temperature (ºC)	Time (s)	Cycles
Initial denaturation	95	300	
Denaturation	95	45	
Annealing	**55-65**	45	35
Elongation	72	45	
Final elongation	72	600	
Hold	4	∞	

6.1.2.2 Genotyping protocol of Chrnb4 KO mice

In order to assess the genotypes of homozygous and heterozygous Chrnb4 KO mice and Chrnb4 WT mice, DNA from the Chrnb4 KO mouse line was assessed according to the Chrnb4 KO PCR protocol (**Table 6. 3**) applying the Chrnb4 KO PCR program (**Table 6. 4**).

Table 6. 3 Chrnb4 KO PCR protocol for one reaction

Substance	Volume (µl)
5x Buffer	2.5
Betaine	2.5
$MgCl_2$	1.5
dNTP (10 mM)	0.25
Primer 1 (20 µM)	0.3
Primer 2 (20 µM)	0.3
Primer 3 (20 µM)	0.3
GoTaq Polymerase	0.15
Nuclease-free water	2.9
DNA	2
Total	**12.7**

Table 6. 4 PCR program for Chrnb4 KO PCR

Step	Temperature (ºC)	Time (s)	Cycles
Initial denaturation	95	300	
Denaturation	95	45	
Annealing	63	45	35
Elongation	72	75	
Final elongation	72	600	
Hold	4	∞	
Primer 1	*5'- TGTAGAGCGAGCATCCGAACA -3'*		
Primer 2	*5'- TCTCTACTTAGGCTGCCTGTCT -3'*		
Primer 3	*5'- AGTACCTTCTGAGGCGGAAAGA -3'*		

The wild-type band appears at 273 bp and Chrnb4 KO band at 150 bp.

6.1.2.3 Genotyping protocol of FGF21 KO mice

In order to assess the genotypes of homozygous and heterozygous FGF21 KO mice and FGF21 WT mice, DNA from the FGF21 KO mouse line was assessed according to the FGF21 KO PCR protocol (**Table 6. 5**) applying the FGF21 KO PCR program (**Table 6. 6**).

Table 6. 5 FGF21 KO PCR protocol for one reaction

Substance	Volume (µl)
5x Buffer	2.5
Betaine	2.5
$MgCl_2$	2
dNTP (10 mM)	0.25
Primer 1 (20 µM)	0.5
Primer 2 (20 µM)	0.5
Primer 3 (20 µM)	0.5
GoTaq Polymerase	0.15
Nuclease-free water	3.1
DNA	2
Total	**14**

Table 6. 6 PCR program for FGF21 KO PCR

Step	Temperature (ºC)	Time (s)	Cycles
Initial denaturation	95	120	
Denaturation	95	30	
Annealing	58	42	35
Elongation	72	60	
Final elongation	72	300	
Hold	4	∞	
Primer 1	*5'- GACTGTTCAGTCAGGGATTG-3'*		
Primer 2	*5'- CCCGTGATATTGCTGAAGAG -3'*		
Primer 3	*5'- ACAGGGTCTCAGGTTCAAAG -3'*		

The wild-type band appears at 541 bp and FGF21 KO band at 243 bp.

6.1.2.4 Genotyping protocol of GcgR flx x Alb cre mice

In order to evaluate genotypes of GcgR Li-KO mice, Alb cre positive or negative mice were assessed using the Alb cre PCR protocol (**Table 6. 7**) applying Alb cre specific PCR conditions (**Table 6. 8**).

Table 6. 7 Alb cre PCR protocol for one reaction

Substance	Volume (μl)
5x Buffer	5
Betaine	5
MgCl$_2$	1
dNTP (10 mM)	0.5
Primer 1 (20 μM)	0.6
Primer 2 (20 μM)	0.6
Primer 3 (20 μM)	0.6
Primer 4 (20 μM)	0.6
GoTaq Polymerase	0.3
Nuclease-free water	8.8
DNA	2
Total	**25**

Table 6. 8 PCR program for Alb cre PCR

Step	Temperature (ºC)	Time (s)	Cycles
Initial denaturation	94	180	
Denaturation	94	45	
Annealing	60	45	36
Elongation	72	60	
Final elongation	72	120	
Hold	4	∞	
Primer 1	*5'- CTAGGCCACAGAATTGAAAGATC -3'*		
Primer 2	*5'- GTAGGTGGAAATTCTAGCATCAT -3'*		
Primer 3	*5'- GCGGTCTGGCAGTAAAAACTATC -3'*		
Primer 4	*5'- GTGAAACAGCATTGCTGTCACTT -3'*		

The control band appears at 324 bp and cre band at 100 bp.

In addition to the Alb cre PCR, the GcgR flx PCR was performed on the DNA of these mice (**Table 6. 9** and **Table 6. 10**). Alb cre positive, homozygous GcgR flx mice were used for *in vivo* studies. Alb cre negative, homozygous GcgR flx mice served as control mice.

Table 6. 9 GcgR flox PCR protocol for one reaction

Substance	Volume (µl)
5x Buffer	5
Betaine	5
$MgCl_2$	3.5
dNTP (10 mM)	0.5
Primer 1 (20 µM)	1
Primer 2 (20 µM)	1
GoTaq Polymerase	0.3
Nuclease-free water	6.7
DNA	2
Total	**25**

Table 6. 10 PCR program for GcgR flx PCR

Step	Temperature (ºC)	Time (s)	Cycles
Initial denaturation	94	120	
Denaturation	94	30	
Annealing	61.5	35	35
Elongation	72	60	
Final elongation	72	180	
Hold	4	∞	
Primer 1	*5'- TCACTCAGGAGGATGTACATGC -3'*		
Primer 2	*5'- AGCCTGAGAACTTCCTATGTCC -3'*		

The wild-type band appears at 162 bp and GcgR flox band at 205 bp.

6.1.2.5 Genotyping protocol of Pirt$^{-/-}$ mice

In order to assess the genotypes of homozygous and heterozygous Pirt$^{-/-}$ mice and Pirt WT mice, DNA from the Pirt$^{-/-}$ mouse line was assessed according to the Pirt$^{-/-}$ PCR protocol (**Table 6. 11**) applying the Pirt$^{-/-}$ PCR program (**Table 6. 12**).

Table 6. 11 Pirt$^{-/-}$ PCR protocol for one reaction

Substance	Volume (µl)
5x Buffer	5
Betaine	6.55
$MgCl_2$	2
dNTP (10 mM)	0.5
Primer 1 (20 µM)	0.1
Primer 2 (20 µM)	0.5
Primer 3 (20 µM)	0.5
GoTaq Polymerase	0.4
Nuclease-free water	6.55
DNA	2
Total	**25**

Table 6. 12 PCR program for Pirt$^{-/-}$ PCR

Step	Temperature (ºC)	Time (s)	Cycles
Initial denaturation	94	120	
Denaturation	94	15	
Annealing	56	30	35
Elongation	72	30	
Final elongation	72	420	
Hold	4	∞	
Primer 1	*5'- ATCTTACAGGTCACATCTGTGG -3'*		
Primer 2	*5'- TGGTTTCCATAGCTGTGGATG -3'*		
Primer 3	*5'- GGAGAAACAGCTAAAGTGCG -3'*		

The wild-type band appears at 657 bp and Pirt$^{-/-}$ band at 500 bp.

6.1.2.6 Genotyping protocol of TRPM8 KO mice

In order to assess the genotypes of homozygous and heterozygous TRPM8 KO mice and TRPM8 WT mice, DNA from the TRPM8 mouse line was assessed according to the TRPM8 KO PCR protocol (**Table 6. 13**) applying the TRPM8 KO PCR program (**Table 6. 14**).

Table 6. 13 TRPM8 KO PCR protocol for one reaction

Substance	Volume (μl)
5x Buffer	2.4
MgCl$_2$	0.96
dNTP (10 mM)	0.24
Primer 1 (20 μM)	0.3
Primer 2 (20 μM)	0.6
Primer 3 (20 μM)	0.6
GoTaq Polymerase	0.12
Nuclease-free water	3.76
DNA	2
Total	**10.98**

Table 6. 14 PCR program for TRPM8 KO PCR

Step	Temperature (ºC)	Time (s)	Cycles
Initial denaturation	94	180	
Denaturation	94	30	
Annealing	67	60	35
Elongation	72	60	
Final elongation	72	120	
Hold	4	∞	
Primer 1	*5'- CCTTGGCTGCTGGATTCACACAGC -3'*		
Primer 2	*5'- CAGGCTGAGCATGAAATGCTGATCTG -3'*		
Primer 3	*5'- GCTTGCTGGCCCCCAAGGGT -3'*		

The wild-type band appears at 426 bp and TRPM8 KO band at 500 bp.

6.1.2.7 Genotyping protocol of UCP1 KO mice

In order to assess the genotypes of homozygous and heterozygous UCP1 KO mice and UCP1 WT mice, DNA from the UCP1 mouse line was assessed according to the UCP1 KO PCR protocol (**Table 6. 15**) applying the UCP1 KO PCR program (**Table 6. 16**).

Table 6. 15 UCP1 KO PCR protocol for one reaction

Substance	Volume (µl)
5x Buffer	2.5
Betaine	2.5
$MgCl_2$	1
dNTP (10 mM)	0.5
Primer 1 (20 µM)	0.5
Primer 2 (20 µM)	0.5
Primer 3 (20 µM)	0.5
GoTaq Polymerase	0.15
Nuclease-free water	2.9
DNA	2
Total	**13.05**

Table 6. 16 PCR program for UCP1 KO PCR

Step	Temperature (ºC)	Time (s)	Cycles
Initial denaturation	94	240	
Denaturation	94	20	
Annealing	55	20	30
Elongation	72	60	
Final elongation	72	120	
Hold	4	∞	
Primer 1	*5'- GGGGTAGTATGCAAGAGAGGTG -3'*		
Primer 2	*5'- CCTTTATACCTAATGGTACTGGAAGC -3'*		
Primer 3	*5'- CCTACCCGCTTCCATTGCTCA -3'*		

The wild-type band appears at 211 bp and UCP1 KO band at 500 bp.

6.2 Materials

6.2.1 Research diets

Table 6. 17 Research diets

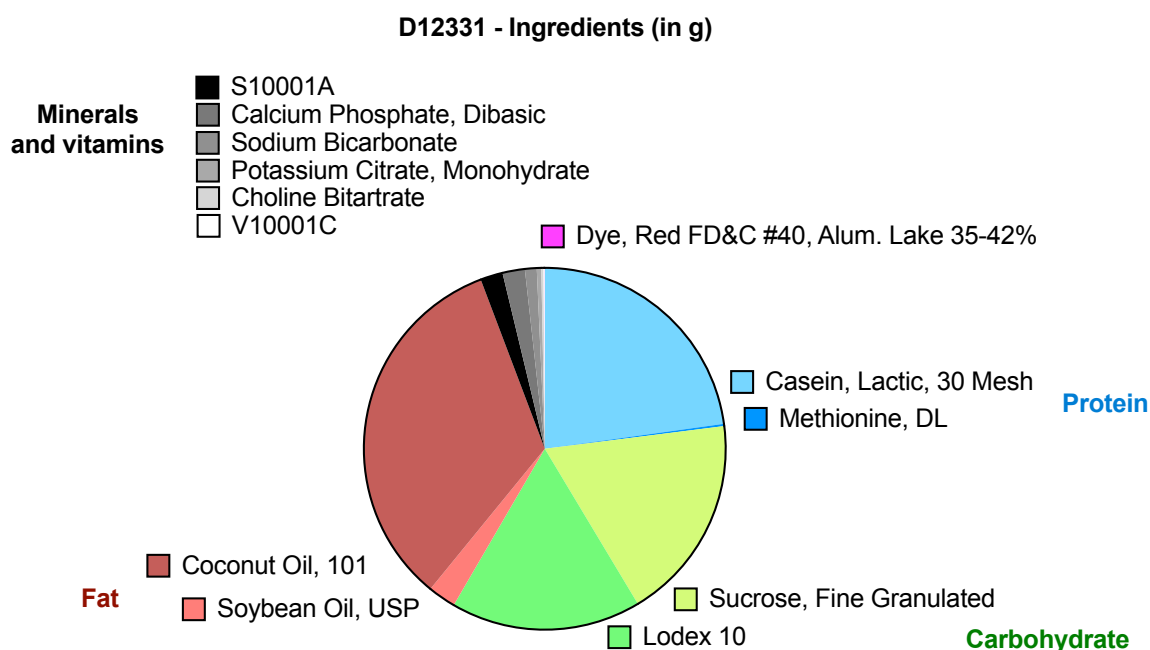| Name	Product code	Provider
Rodent Diet with 58 kcal% Fat and Sucrose (**Figure 6. 1**)	D12331i	Research Diets, Inc., New Brunswick, USA

D12331 - Ingredients (in g)

Figure 6. 1 Ingredients of D12331 diet in grams

6.2.2 Chemicals

Table 6. 18 List of chemicals in alphabetical order

Name	Product code	Provider
Agarose	840004	Biozym Scientific GmbH, Hessisch Oldendorf, Germany
Antimycin A from *Streptomyces sp.*	A8674-25MG	Sigma-Aldrich Chemie GmbH, Taufkirchen, Germany
BaOH	B-4059-500ml	Sigma-Aldrich Chemie GmbH, Taufkirchen, Germany
Betaine (5 M), PCR reagent	B0300	Sigma-Aldrich Chemie GmbH, Taufkirchen, Germany
Bovine Serum Albumin (BSA)	A3803	Sigma-Aldrich Chemie GmbH, Taufkirchen, Germany
$CaCl_2$	CN93.2	Carl Roth GmbH + Co. KG, Karlsruhe, Germany
Carbonyl cyanide-p-trifluoromethoxyphenylhydrazone (FCCP)	C2920	Sigma-Aldrich Chemie GmbH, Taufkirchen, Germany
Chloroform	C2432-500ML	Sigma-Aldrich Chemie GmbH,

		Taufkirchen, Germany
Collagen A	L7220	VWR International GmbH, Darmstadt, Germany
Collagenase II	17101015	Sigma-Aldrich Chemie GmbH, Taufkirchen, Germany
DAPI solution	62248	Thermo Fisher Scientific Inc., Waltham, USA
Dexamethasone	D-4902	Sigma-Aldrich Chemie GmbH, Taufkirchen, Germany
Dispase II (neutral protease, grade II)	04942078001	Sigma-Aldrich Chemie GmbH, Taufkirchen, Germany
DMEM/F-12, GlutaMAX supplement	10565018	Thermo Fisher Scientific Inc., Waltham, USA
DMEM XF Assay medium	102365-100	Agilent, Waldbronn, Germany
DMPP	D5891	Sigma-Aldrich Chemie GmbH, Taufkirchen, Germany
DMSO	A994.2	Carl Roth GmbH + Co. KG, Karlsruhe, Germany
DNA/RNA-Farbstoff, peqGREEN	732-2960	VWR International GmbH, Darmstadt, Germany
Deoxynucleotide-triphosphate (dNTP) Solution Mix	N0447 L	New England Biolabs GmbH, Frankfurt, Germany
D-(+)-Glucose	HN06.4	Carl Roth GmbH + Co. KG, Karlsruhe, Germany
Enhanced chemiluminescence (ECL$^+$)	RPN2232	Amersham Biosciences, Piscataway, NJ, USA
EosinY	230251	Sigma-Aldrich Chemie GmbH, Taufkirchen, Germany
Ethanol	1.00983.2500	Th. Geyer GmbH & Co. KG, Renningen, Germany
Fetal bovine serum (FBS)	10270106	Thermo Fisher Scientific Inc., Waltham, USA
Gelatin from porcine skin	SAFSG1890	VWR International GmbH, Darmstadt, Germany
Glycogen	G-8876	Sigma-Aldrich Chemie GmbH, Taufkirchen, Germany
Hydrochloric acid (HCl 0.1 N)	31955.293	VWR International GmbH, Darmstadt, Germany
Icilin	10137	Cayman Chemical, Michigan, USA
	36945-98-9 (ROE01)	Bicoll, Planegg, Germany
Indomethacine	I-7378	Sigma-Aldrich Chemie GmbH, Taufkirchen, Germany
Insulin (injections)	00175165	Sanofi-Aventis Deutschland GmbH, Frankfurt, Germany
Insulin solution, human (cellculture)	I9278	Sigma-Aldrich Chemie GmbH, Taufkirchen, Germany
Isobutylmethylxanthine (IBMX)	I-7018	Sigma-Aldrich Chemie GmbH, Taufkirchen, Germany
(−)-Isoproterenol hydrochloride	I6504	Sigma-Aldrich Chemie GmbH, Taufkirchen, Germany

140

Mayers acid Hemalum	51275	Sigma-Aldrich Chemie GmbH, Taufkirchen, Germany
Mercaptoethanol	M6250-10ML	Sigma-Aldrich Chemie GmbH, Taufkirchen, Germany
NaCl (Spüllösung) 0,9%	BRAU3570160	B. Braun Melsungen AG, Hessen, Germany
Nuclease-free water	T143.5	Carl Roth GmbH + Co. KG, Karlsruhe, Germany
(±)-Norepinephrine (+)-bitartrate salt	SAFSA0937-1G	VWR International GmbH, Darmstadt, Germany
Oligomycin	O4876-5MG	Sigma-Aldrich Chemie GmbH, Taufkirchen, Germany
Paraformaldehyde	0335.3	Carl Roth GmbH + Co. KG, Karlsruhe, Germany
PBS (1X), liquid; pH:7.4	10010056	Thermo Fisher Scientific Inc., Waltham, USA
Perchloric acid, 70%	311421	Sigma-Aldrich Chemie GmbH, Taufkirchen, Germany
Penicillin-Streptomycin (10,000 U/mL)	15140122	Thermo Fisher Scientific Inc., Waltham, USA
peq Gold 50bp Ladder	25-2000	VWR International GmbH, Darmstadt, Germany
Pertex®	41-4010-00	Medite GmbH, Burgdorf, Germany
Primers		Thermo Fisher Scientific Inc., Waltham, USA
QIAzol Lysis Reagent	79306	QIAGEN GmbH, Hilden, Germany
Rosiglitazone	71740	Cayman Chemical, Michigan, USA
Rotenone	R8875	Sigma-Aldrich Chemie GmbH, Taufkirchen, Germany
SlowFade Gold Antifade Mountant with DAPI	S36938	Thermo Fisher Scientific Inc., Waltham, USA
Sodium hydroxide concentrate (0.1 M NaOH)	319481-1L	VWR International GmbH, Darmstadt, Germany
Sodium Pyruvate (100 mM)	11360070	Thermo Fisher Scientific Inc., Waltham, USA
TaqMan Gene Expression Assay		Thermo Fisher Scientific Inc., Waltham, USA
Tri-iodothyronine	T-6397	Sigma-Aldrich Chemie GmbH, Taufkirchen, Germany
Triton™ X-100	X100	Sigma-Aldrich Chemie GmbH, Taufkirchen, Germany
TWEEN® 80	P1754	Sigma-Aldrich Chemie GmbH, Taufkirchen, Germany
Versene® (EDTA), 0.02%	LONZ17-711E	Lonza Group Ltd., Basel, Switzerland
$ZnSO_4$	Z-2876-500ml	Sigma-Aldrich Chemie GmbH, Taufkirchen, Germany

6.2.3 Instruments and equipment

Table 6. 19 List of instruments and equipment in alphabetical order

Item	Name	Provider
Automated Home Cage Phenotyping	PhenoMaster	TSE Systems
Balance	Ranger® 3000	Ohaus Corporation, Parsippany, USA
Body Composition Analyzer for Live Small Animals (Mice), Organs, and Biopsies	EchoMRI™ 3-in-1	Echo-MRI, Houston, USA
ChemiDoc™ MP Imaging System		Bio-Rad Laboratories, Inc. Hercules, USA
Cell strainer	40 µM (FALC352340), 100µM (FALC352360)	Corning B.V. Life Sciences, Amsterdam, The Netherlands
Centrifuges	Perfect Spin Mini	VWR International GmbH, Darmstadt, Germany
	Microcentrifuge for PCR plates (521-1648)	VWR International GmbH, Darmstadt, Germany
	MIKRO 200 MIKRO 220 R	Andreas Hettich GmbH & Co.KG, Tuttlingen, Germany
Collagen-precoated cell culture plates	Corning™ BioCoat™ Collagen (10412311)	Thermo Fisher Scientific Inc., Waltham, USA
Coverslips		Carl Roth GmbH + Co. KG, Karlsruhe, Germany
Cryostat	Leica CM3050 S Research Cryostat	Leica Mikrosysteme Vertrieb GmbH, Wetzlar, Germany
Electrophorese chamber	PerfectBlue™ Gel System	VWR International GmbH, Darmstadt, Germany
Extracellular flux analyzer	Seahorse XFe96 Analyzer	Agilent, Waldbronn, Germany
Genotyping instrument	QIAxcel Advanced	QIAGEN GmbH, Hilden, Germany
Glucometer and glucose strips	FreeStyle Freedom Lite Glucometer and strips (7081470)	Abbott Laboratories GmbH, Hannover, Germany
Glucometer and glucose strips	Contour XT glucometer kit (1517080)	Arseus Medical NV, Bornem, Belgium
Heparin-coated tubes	Microvette (CB300K2E)	Sarstedt, Nürnberg, Germany
Incubators with Stainless-Steel Chamber	Heracell™ 150i CO_2	Thermo Fisher Scientific Inc., Waltham, USA
Liquid Scintillation Spectrometers	Tri-Carb 2900TR	Perkin-Elmer, Boston, USA
Microplate reader	HTS Microplate Reader – PHERAstar FS	BMG LABTECH GmbH, Ortenberg, Germany
Microscope	BZ-9000 fluorescence microscope,	Keyence Coporation Itasca, USA,
	Leica SP5,	Leica Mikrosysteme GmbH, Wetzlar, Germany,
	Axioplan	Zeiss, Jena, Germany

Mobile phase HPLC	ClinRep® Nr. 1210	RECIPE Chemicals + Instruments GmbH, Munich, Germany
MSOT scanner	256-channel real-time imaging MSOT scanner	inVision 256-TF, iThera Medical GmbH, Munich, Germany
Pipets	PIPETGIRL (155021),	INTEGRA Biosciences AG, Zizers, Switzerland
	Pipet-LiteMehrkanalL8-10XLS+ (17013802), Pipet-Lite Mehrkanal L8-200XLS+ (17013805)	Mettler-Toledo GmbH, Gießen, Germany
Pipet tips	768 Fine Point Tips 1200ul, LTS (RT-L1200F), Tips 250µl, SS-L250 (17005875), TIPS 20µl, SS-L10 (17005873)	Mettler-Toledo GmbH, Gießen, Germany
Power supply	PEQ Power 300V	VWR International GmbH, Darmstadt, Germany
qPCR cycler	QuantStudio	Thermo Fisher Scientific Inc., Waltham, USA
Reaction tubes	PP-tube 50ml (62.547.254), PP-tube 15ml (62.554.502), SafeSeal tube 2ml PP (72695500), SafeSeal tube 1,5ml (72.706),	Sarstedt, Nürnberg, Germany
	PCR 8er-softstrips 0,2ml (711038)	Biozym Scientific GmbH, Hessisch Oldendorf, Germany
Rotatory microtome	HMS35	Zeiss, Jena, Germany
	HM340E	Thermo Fisher Scientific Inc., Waltham, USA
Scanner	AxioScan.Z1 digital slide scanner	Zeiss, Oberkochen, Germany
Serological pipets	25ml (86.1685.001), 10 ml (861254001)	Sarstedt, Nürnberg, Germany
Syringes	9161502	B. Braun Melsungen AG, Hessen, Germany
Thermal PCR cycler	Mastercycler® nexus	Eppendorf AG, Hamburg, Germany
Tissue lyser	TissueLyser II	QIAGEN GmbH, Hilden, Germany
Vacuum infiltration processor	TissueTEK VIP	Sakura, AV Alphen aan den Rijn, Netherland

6.2.4 Antibodies

Table 6. 20 List of antibodies in alphabetical order

Target	MW (kDa)	Host	Dilution factor	Product code	Company
Primary antibodies					
Akt2	60	rabbit	1:1000	3063	Cell Signaling Technology (CST), Danvers, USA
Akt Ser473	60	rabbit	1:1000	9271	CST, Danvers, USA
Akt Thr308	60	rabbit	1:1000	9275	CST, Danvers, USA
cFOS	62	rabbit	1:1000	SC-52	Santa Cruz Biotechnology, Inc, USA
GLUT4	46	rabbit	1:1000	PA1-1065	Thermo Fisher Scientific Inc., Waltham, USA
PAS		rabbit	1:500	9611	CST, Danvers, USA
Pirt	15	rabbit	1:500	orb158159	Biorbyt LLC, San Francisco, USA
TBC1D1 Thr596	160	rabbit	1:1000	6927	CST, Danvers, USA
TBC1D4	160	rabbit	1:1000	07-741	Upstate Biotechnology Inc., Lake Placid, USA
UCP1	32	rabbit	1:1500	ab 10983	Abcam, Cambridge, UK
Secondary antibodies					
Rabbit IgG		donkey	1:1000	A10042	Thermo Fisher Scientific Inc., Waltham, USA
Rabbit IgG		goat	1:500	A-11011	Thermo Fisher Scientific Inc., Waltham, USA
Rabbit IgG		goat	1:750	BA-1000	Vector Laboratories, Burlingame, USA

Akt (Protein kinase B); Akt2 (Protein kinase Akt-2); GLUT4 (Glucose transporter type 4); PAS (Phospho Akt substrate); Pirt (Phosphoinositide interacting regulator of TRPs); TBC1D1 (TBC1 Domain Family Member 1); TBC1D4 (TBC1 Domain Family Member 4); UCP1 (Uncoupling protein 1)

6.2.5 Taqman probes

Table 6. 21 List of taqman probes in alphabetical order

Gene name	Abbreviation	Reference sequence
Creatine Kinase, Mitochondrial 1B	**Ckmt1**	Mm00438221_m1
Creatine Kinase, Mitochondrial 2	**Ckmt2**	Mm01285553_m1
Guanidinoacetate N-Methyltransferase	**Gamt**	Mm00487473_m1
Glycine Amidinotransferase	**Gatm**	Mm00491879_m1
Hypoxanthine Phosphoribosyltransferase	**Hprt**	Mm01545399_m1
Peptidylprolyl Isomerase B	**Ppib**	Mm00478295_m1
Solute Carrier Family 6 Member 8	**Slc6a8**	Mm0050623_m1
Transient receptor potential melastatin 8	**Trpm8**	Mm01299593_m1
Uncoupling protein 1	**UCP1**	Mm01244861_m1

6.2.6 Primer sequences

Table 6. 22 List of primers (mouse) in alphabetical order

Abbreviation	Forward primer (5' – 3')	Reverse primer (5' – 3')
Abca1	AAAACCGCAGACATCCTTCAG	CATACCGAAACTCGTTCACCC
Abcg5	GTACATCGAGAGTGGCCAGA	CTGTGTATCGCAACGTCTCG
Apoe	GATCAGCTCGAGTGGCAAAG	TAGTGTCCTCCATCAGTGCC
Atf4	GATGAGCTTCCTGAACAGCG	GCCAAGCCATCATCCATAGC
Atp5b	CCGGGCAAGAAAGATACAGC	GTCCCACCATGTAGAAGGCT
Cd68	ACAAAACCAAGGTCCAGGGA	ATTCTGCGCCATGAATGTCC
Cidea	AATGGACACCGGGTAGTAAGT	CAGCCTGTATAGGTCGAAGGT
Cox2	GCCCTTCAAGCTCCTAGGTA	CTGGATCCTCTGCTTAGCGA
Cox4	CTAGAGGGACAGGGACACAC	TGGTTCATCTCTGCGAAGGT
Cyp3a11	CTCTCACTGGAAACCTGGGT	TCTGTGACAGCAAGGAGAGG
Cyp7b1	TCTGGGCCTCTCTAGCAAAC	GCACTTCTCGGATGATGCTG
Cyp8b1	CAGCGGACAAGAGTACCAGA	TGGATCTTCTTGCCCGACTT
Cyp27a1	CTTCATCGCACAAGGAGAGC	CCAAGGCAAGGTGGTAGAGA
CytC	GTTCAGAAGTGTGCCCAGTG	GTCTGCCCTTTCTCCCTTCT
Dio2	TGCCACCTTCTTGACTTTGC	GGTTCCGGTGCTTCTTAACC
G6PC	CTGTCTGTCCCGGATCTACC	GCGCGAAACCAAACAAGAAG
GYS2	CGCTCCTTGTCGGTGACATC	CATCGGCTGTCGTTTTGGC
Hmgcr	AGCTTGCCCGAATTGTATGTG	TGTGTTGTGAACCA TGTGACTTC
Hprt	AAGCTTGCTGGTGAAAAGGA	TTGCGCTCATCTTAGGCTTT
Hspa5	GACTGCTGAGGCGTATTTGG	AGCA TCTTTGGTTGCTTGTCG
Lcat	GTGCTCCACTTCTTACTGCG	GAACACA TGGTCTTCAGGCC
Ldlr	TCAGACGAACAAGGCTGTCC	CCATCTAGGCAATCTCGGTCTC
Lipc	ATGTGGGGTTAGTGGACTGG	TTGTTCTTCCCGTCCATGGA
Lrp1	AACCTTATGAATCCACGCGC	TTCTTGGGGCCATCATCAGT
Nrf1	ACCCAAACTGAACACA TGGC	GCAGTTACCTCATCAGCTGC
PEPCK	CTGCATAACGGTCTGGACTTC	CAGCAAACTCCCGTACTCC
Pgc1α	AGCCGTGACCACTGACAACGAG	GCTGCATGGTTCTGAGTGCTAAG
PGM	CCAAAATCTTGCGGGCCATA	CCAGAACAAAGGGACAGCAC
Pirt	ACCACACCCAAAAGCAACTG	GCCCTATCATCCTGAGCACT
Ppib	GCATCTATGGTGAGCGCTTC	CTCCACCTTCCGTACCACAT
Prdm16	CCGCTGTGA TGAGTGTGATG	GGACGA TCATGTGTTGCTCC
PYGL	TACATTCAGGCTGTGCTGGA	AAGGCATCAAACACGGTTCC
Sort1	ATCCCAGGAGACAAATGCCA	AACCTTCCGCCACAGACATA
Sqle	TGTTGCGGATGGACTCTTCT	GAGAACTGGACTGGGGTTGA

Abca1 (ATP binding cassette subfamily A member 1); Abcg5 (ATP binding cassette subfamily G member 5); Apoe (Apolipoprotein E); Atf4 (Activating transcription factor 4); Atp5b (ATP synthase F1 subunit beta); Cd68 (CD68 molecule); Cidea (Cell death-inducing DFFA-like effector A); Cox2 (Mitochondrially encoded cytochrome C oxidase II); Cox4 (Cytochrome C oxidase subunit 4I1); Cyp3a11 (Cytochrome P450, family 3, subfamily a, polypeptide 11); Cyp7b1 (Cytochrome P450 family 7 subfamily B member 1); Cyp8b1 (Cytochrome P450 family 8 subfamily B member 1); Cyp27a1 (Cytochrome P450 family 27 subfamily A member 1); CytC (Cytochrome C); Dio2 (Iodothyronine deiodinase 2); G6pc (Glucose-6-phosphatase); GYS2 (Glycogen synthase 2 (Liver)); Hmgcr (3-Hydroxy-3-methylglutaryl-CoA reductase); Hprt (Hypoxanthine-guanine phosphoribosyltransferase);

Hspa5 (Heat shock protein family A (Hsp70) member 5); Lcat (Lecithin-cholesterol acyltransferase); Ldlr (Low density lipoprotein receptor); Lipc (Lipase C, hepatic type); Lrp1 (LDL receptor related protein 1); Nrf1 (Nuclear respiratory factor 1); PEPCK (Phosphoenolpyruvate carboxykinase); Pgc1α (Peroxisome proliferator-activated receptor gamma, coactivator 1 alpha); PGM (Phosphoglucomutase 1); Pirt (Phosphoinositide interacting regulator of TRPs); PPIB (Peptidylprolyl isomerase B); Prdm16 (PR/SET domain 16); PYGL (Glycogen phosphorylase L); Sort1 (Sortilin 1); Sqle (Squalene epoxidase)

6.2.7 Kits

Table 6. 23 List of kits in alphabetical order

Name	Catalogue number	Provider
ClinRep® Complete Kit		RECIPE Chemicals + Instruments GmbH, Munich, Germany
Dako detection kit	K5001	Agilent, Waldbronn, Germany
FavorPrep™ Tissue Genomic DNA Extraction Mini Kit	FATGK 001-2	Favorgen Biotech Corporation, Ping, Taiwan
FGF21 ELISA	EZRMFGF21-26K	Merck Millipore, Darmstadt, Germany
Glycogen Colorimetric/Fluorometric Assay Kit	K646-100	Biovision Inc., Milpitas, USA
GoTaq® G2 Flexi DNA Polymerase	M7808	Promega GmbH, Mannheim, Germany
Infinity™ ALT (GPT) Liquid Stable Reagent	TR71121	Thermo Fisher Scientific Inc., Waltham, USA
Infinity™ AST (GOT) Liquid Stable Reagent	TR70121	Thermo Fisher Scientific Inc., Waltham, USA
Infinity Total Cholesterol	TR13421	Thermo Fisher Scientific Inc., Waltham, USA
LabAssay™ Triglyceride	290-63701	Wako, Neuss, Germany
Mouse / Rat Leptin ELISA	22-LEPMS-E01	Alpco Diagnostics, Salem, USA
Mouse Ultrasensitive Insulin ELISA	80-INSMSU-E10	Alpco Diagnostics, Salem, USA
NEFA-HR(2) R1 Set	434-91795	Wako, Neuss, Germany
NEFA-HR(2) R2 Set	436-91995	Wako, Neuss, Germany
NEFA Standard	270-77000	Wako, Neuss, Germany
Pierce™ BCA Protein Assay Kit	23225	Thermo Fisher Scientific Inc., Waltham, USA
QuantiTect Reverse Transcription Kit	205313	QIAGEN GmbH, Hilden, Germany
RNeasy Mini Kit	74106	QIAGEN GmbH, Hilden, Germany
SYBR® Green PCR master mix	4364344	Thermo Fisher Scientific Inc., Waltham, USA
TaqMan Universal Master Mix II, no UNG	4440047	Thermo Fisher Scientific Inc., Waltham, USA

6.2.8 Software

Table 6. 24 List of software

Name	Version	Provider
Definiens Developer	XD 2	Definiens AG, Munich, Germany
GraphPad PRISM	6, 8	GraphPad Software, Inc. La Jolla, USA
Image Processing and Analysis in Java		ImageJ
Microsoft® Office for Mac	14.5.5	Microsoft Corporation, Redmond, USA
Seahorse XF96 Software		Seahorse Bioscience, USA
ViewMSOT	Xvue Ltd	iThera Medical GmbH, Munich, Germany

6.3 Protocol extracellular flux analyzer

Table 6. 25 Bioenergetic profiling of primary brown adipocytes

Protocol steps			
Start protocol			
	Command	**Time (minutes)**	**Port (Substance)**
	Calibrate		
	Mix	2	
	Measure	2	
	Mix	2	
	Measure	2	
	Mix	2	
	Measure	2	
	Inject		**A (Oligomycin)**
	Mix	2	
	Measure	2	
	Mix	2	
	Measure	2	
	Mix	2	
	Measure	2	
	Mix	2	
	Measure	2	
	Mix	2	
	Measure	2	
	Mix	2	
	Measure	2	
	Inject		**B (Vehicle, Isoproterenol, Icilin)**
	Mix	2	
	Measure	2	
	Mix	2	
	Measure	2	
	Mix	2	
	Measure	2	
	Mix	2	
	Measure	2	

147

Mix	2	
Measure	2	
Mix	2	
Measure	2	
Mix	2	
Measure	2	
Inject		**C (FCCP)**
Mix	2	
Measure	2	
Mix	2	
Measure	2	
Mix	2	
Measure	2	
Mix	2	
Measure	2	
Inject		**D (Rotenone/Antimycin A/2-DG)**
Mix	2	
Measure	2	
Mix	2	
Measure	2	
Mix	2	
Measure	2	
Mix	2	
Measure	2	

End protocol

6.4 Letters of approval

6.4.1 Letter of approval - Molecular Metabolism, 2017 Mar 1; 6(5):440-446

From: "Molecular Metabolism, ELS" <molmet@elsevier.com>
To: "Sigrid Hedwig Jall" <sigrid.jall@helmholtz-muenchen.de>
Sent: Tuesday, November 13, 2018 1:03:05 PM
Subject: Re: Permission inquiry [181102-008477] [181113-005960]

Dear Dr Jall,
This is always allowed, as long as you give the proper citation.
Kind regards
Margriet ten Napel
Journal Manager
Global Journals Production

ELSEVIER
Radarweg 29, Amsterdam, 1043 NX, Netherlands

We equip communities with the knowledge that drives critical decision-making and innovation to tackle challenges of greatest importance to humanity, science and the planet. Find out how we work with partnerships to drive sustainable development.

For assistance, please visit our Customer Support site where you can search for solutions on a range of topics and find answers to frequently asked questions.

From: Sigrid Jall
Date: 02/11/2018 02.25 PM

Dear Ladies and Gentlemen,

I am the author of the following paper published by Elsevier:
Jall S., Sachs S., Clemmensen C., Finan B., Neff F., DiMarchi R.D., Tschöp M.H., Müller T.D., Hofmann S.M. (2017) Monomeric GLP-1/GIP/glucagon triagonism corrects obesity, hepatosteatosis, and dyslipidemia in female mice. Molecular Metabolism, 6(5), 440-446. DOI: 10.1016/j.molmet.2017.02.002

This work is based on my PhD thesis. I wish to include this work within the electronic and printed version of my thesis, which I am required to deposit in the Technische Universität München's online repository, mediaTUM (https://mediatum.ub.tum.de).

Thank you very much for your advice whether this is acceptable.

Yours sincerely,
Sigrid Jall

6.4.2 Letter of approval – Nature Communications, 2018 Oct 23; 9(1):4304-4316

RE: Permission inquiry   November 5, 2018 3:41 PM

From: "Journalpermissions" <journalpermissions@springernature.com>

To: "Sigrid Hedwig Jall" <sigrid.jall@helmholtz-muenchen.de>

Dear Sigrid,

Thank you for your email. This work is licensed under a Creative Commons Attribution 4.0 International License, which permits unrestricted use, distribution, and reproduction in any medium, provided you give appropriate credit to the original author(s) and the source, provide a link to the Creative Commons license, and indicate if changes were made. **You are not required to obtain permission to reuse this article.** The images or other third party material in this article are included in the article's Creative Commons license, unless indicated otherwise in the credit line; if the material is not included under the Creative Commons license, users will need to obtain permission from the license holder to reproduce the material. To view a copy of this license, visit http://creativecommons.org/licenses/by/4.0/.

Best wishes,
Oda

Oda Siqveland
Permissions Assistant

SpringerNature
The Campus, 4 Crinan Street, London N1 9XW,
United Kingdom
T +44 (0) 207 014 6851

http://www.nature.com
http://www.springer.com
http://www.palgrave.com

From: Jall, Sigrid [mailto:sigrid.jall@helmholtz-muenchen.de]
Sent: 02 November 2018 14:39
To: Journalpermissions
Subject: Permission inquiry

Dear Ladies and Gentlemen,

I am the author of the following paper published by Springer Nature:

Christoffer Clemmensen[*], Sigrid Jall[*], et al (2018) Coordinated targeting of cold and nicotinic receptors synergistically improves obesity and type 2 diabetes. **Nature Communications, 9(1):4304.** DOI 10.1038/s41467-018-06769-y

This work is based on my PhD thesis. I wish to include this work within the electronic and printed version of my thesis, which I am required to deposit in the Technische Universität München's online repository, mediaTUM (https://mediatum.ub.tum.de).

Thank you very much for your advice whether this is acceptable.

7 Acknowledgments

8 Curriculum vitae

9 List of Publications

Christoffer Clemmensen*, **Jall S***, et al (2018). Coordinated Targeting of Cold and Nicotinic Receptors Synergistically Improves Obesity and Type 2 Diabetes. *Nat Commun* **9(1)**:4304-4316

Jall S, et al (2018). Polypharmakologie als ein neuer Ansatz zur Präzisionsmedizin in der Adipositas- und Diabetestherapie. *Adipositas* **12(02)**:76-83

Götz A., et al (2017). Inkretinbasierte Medikamente zur Diabetes- und Adipositastherapie: Entwicklungsperspektiven. *Der Diabetologe* **13(07)**:505-513

Duncan L, et al (2017). Significant Locus and Metabolic Genetic Correlations Revealed in Genome-Wide Association Study of Anorexia Nervosa. *Am J Psychiatry* **174(9):**850-858

Jall S, et al (2017). Monomeric GLP-1/GIP/glucagon triagonism corrects obesity, hepatosteatosis, and dyslipidemia in female mice. *Mol Metab* **6(5)**:440-446

Finan B*, Clemmensen C*, et al (2016). Chemical Hybridization of Glucagon and Thyroid Hormone Optimizes Therapeutic Impact for Metabolic Disease. *Cell* **167(3):**843-857

Mueller KM, et al (2016). Adipocyte Glucocorticoid Receptor Deficiency Attenuates Aging- and HFD-Induced Obesity and Impairs the Feeding-Fasting Transition. *Diabetes* **66(2):**272-286

Hinney A, et al (2016). Evidence for three genetic loci involved in both anorexia nervosa risk and variation of body mass index. *Mol Psychiatry* **22(2):**192-201

BIBLIOMETRICS

ORCID: 0000-0001-8716-4523

Peer reviewed articles: 8 (+1 in revision)

Number of first author papers: 2 + 1 German review

Total citations: 128 (Google Scholar)

H-index: 4 (Google Scholar)

PRESENTATIONS

19/04/2018 - 20/04/2018

2nd German French Conference on Diabetes Research | Berlin, Germany
"*Coordinated targeting of cold and nicotinic receptors synergistically reverses metabolic diseases*" (Poster presentation)

22/02/2018

SAB Meeting | Homburg, Germany
"*The role of TRPM8 in the systemic regulation of energy metabolism*" (Poster presentation)

11/12/2017 - 12/12/2017

    DZD SAB Meeting | Hohenkammer, Germany

    "*Coordinated targeting of cold and nicotinic receptors synergistically improves diet-induced obesity and diabetes in mice*" (Poster presentation)

20/11/2017

    GEnCoDe Topic 2 | Neuherberg, Germany

    "*Coordinated targeting of cold and nicotinic receptors synergistically reverses metabolic diseases*" (Oral presentation)

09/05/2017 - 13/05/2017

    Keystone Conference | Copenhagen, Denmark

    "*GLP-1 mediated delivery of thyroid hormone T3 reverses diet-induced obesity and glucose intolerance in mice*" (Poster presentation)

22/11/2016

    GEnCoDe Topic 2 | Neuherberg, Germany
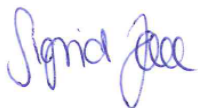
    "*GLP-1/GIP/glucagon triagonism corrects obesity in male and female mice equally*" (Poster presentation)

24/09/2015 - 26/09/2015

    3rd Eyes Meeting | Modena, Italy

    "*Inflammatory phenotype of type 2 diabetes associated macrophages characterized by the potassium channel Kv1.3 and the purinergic receptor P2x7*" (Oral presentation)

Dirlewang, January 14th, 2019

Sigrid Jall

Sigrid Jall

10 Declaration of Authorship

Ich erkläre an Eides statt, dass ich die bei der Fakultät für Medizin der TUM zur Promotionsprüfung vorgelegte Arbeit mit dem Titel:

„Polypharmacological strategies to reverse obesity and improve multiple aspects of the metabolic syndrome in mice"

am Institut für Diabetes und Adipositas (Helmholtz Zentrum München) unter der Anleitung und Betreuung durch Prof. Dr. Matthias Tschöp ohne sonstige Hilfe erstellt und bei der Abfassung nur die gemäß § 6 Abs. 6 und 7 Satz 2 angegebenen Hilfsmittel benutzt habe.

Ich habe keine Organisation eingeschaltet, die gegen Entgelt Betreuerinnen und Betreuer für die Anfertigung von Dissertationen sucht, oder die mir obliegenden Pflichten hinsichtlich der Prüfungsleistungen für mich ganz oder teilweise erledigt.

Ich habe die Dissertation in dieser oder ähnlicher Form in keinem anderen Prüfungsverfahren als Prüfungsleistung vorgelegt.
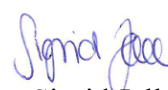
Die vollständige Dissertation wurde noch nicht veröffentlicht.

Ich habe den angestrebten Doktorgrad noch nicht erworben und bin nicht in einem früheren Promotionsverfahren für den angestrebten Doktorgrad endgültig gescheitert.

Die öffentlich zugängliche Promotionsordnung der TUM ist mir bekannt, insbesondere habe ich die Bedeutung von § 28 (Nichtigkeit der Promotion) und § 29 (Entzug des Doktorgrades) zur Kenntnis genommen. Ich bin mir der Konsequenzen einer falschen Eidesstattlichen Erklärung bewusst.

Mit der Aufnahme meiner personenbezogenen Daten in die Alumni-Datei bei der TUM bin ich einverstanden.

Dirlewang, den 14.01.2019   Sigrid Jall

156